

**Role of c-di-GMP in determining sessile or motile lifestyle in
Aeromonas caviae Sch3N**

Manal Almahmeed

(BSc, MSc)

A thesis submitted for the degree of Doctor of Philosophy



Department of Infection and Immunity

The Medical School

The University of Sheffield

June 2014

Summary

The bacterial second messenger c-di-GMP has been recently found to be implicated in controlling many cellular processes in bacteria, one of them is the switch between motility and sessility. When in a sessile lifestyle (such as in a biofilm), bacteria are known to be more resistant to immune defences and to antibiotics. Mesophilic *Aeromonas* species are known to constitutively express a single polar flagellum which allows the bacteria to swim in liquid environments. They as well are able to express many peritrichous lateral flagella which allow them to move as a group (swarm). The multiple lateral flagella although are needed for swarming, they are, however, also required for biofilm formation. This study investigates the relationship between different components within the c-di-GMP network and the lateral flagella (*laf*) genes expression.

Diguanylate cyclases containing GGDEF domains are responsible for c-di-GMP synthesis and phosphodiesterases containing EAL domains are known to breakdown the second messenger. Thirteen GGDEF-EAL domains encoding genes present in *A. caviae* Sch3N were mutated by plasmid insertion mutagenesis after which the effects of these mutations were studied phenotypically and by transcriptional fusions. We have found differences among the mutants in their ability to form a biofilm and on the activities of the lateral flagellin promoters *lafA1p* and *lafA2p*. C-di-GMP is known to bind to the PilZ domain and to RNA domains (riboswitches) to exert its function. We have mutated the *pilZ* gene present in the lateral flagella gene cluster by insertion of a kanamycin cassette and also we have deleted the *lafK* riboswitch by Spliced Overlap Extension PCR. Performance of phenotypic and β -galactosidase assays following these mutations allowed us to conclude that the *lafK* c-di-GMP type I riboswitch seems to act as a c-di-GMP modulator in *A. caviae*. In addition, the *lafK* riboswitch acts as an “OFF switch” which prevents the expression of LafK, the major regulator of the *laf* operon.

Table of Contents

List of Figures	VII
List of Tables	XIV
Abbreviations	XV
Acknowledgment	XVII
Chapter 1: Introduction	2
1.1. The genus <i>Aeromonas</i>	2
1.1.1. Taxonomy	2
1.1.2. Morphology, physiology, and biochemistry	6
1.1.3. Ecology	6
1.2. <i>Aeromonas</i> pathogenesis	7
1.2.1. <i>Aeromonas</i> infections in fish	7
1.2.1.1. Fish infections caused by the psychrophilic aeromonads	8
1.2.1.2. Fish infections caused by the mesophilic aeromonads	8
1.2.2. <i>Aeromonas</i> infections in animals	8
1.2.3. <i>Aeromonas</i> infections in humans	8
1.2.3.1. Epidemiology of human infections caused by <i>Aeromonas</i> species	9
1.2.3.2. Role of <i>Aeromonas</i> in gastroenteritis	10
1.2.4. Virulence factors of <i>Aeromonas</i> spp.	14
1.2.4.1. Resistance to antibiotics	14
1.2.4.2. Capsule	15
1.2.4.3. Lipopolysaccharide (LPS)	16
1.2.4.4. Alpha-glucan	16
1.2.4.5. The S-layer	16
1.2.4.6. Iron-binding mechanisms	16
1.2.4.7. Exotoxins	17
1.2.4.8. Extracellular enzymes	19
1.2.4.9. Type II, III and VI protein secretion systems	19
1.2.4.10. Pili	23
1.2.4.11. Flagella	23
1.2.4.11.1. Types of flagella possessed by <i>Aeromonas</i> species	23
1.2.4.11.2. Evidence for the possession of two distinct flagellar systems by mesophilic <i>Aeromonas</i> species	24
1.2.4.11.3. Other bacteria which possess two flagellar systems	25
1.2.4.11.4. <i>Aeromonas</i> polar flagellar system	25

1.2.4.11.5. <i>Aeromonas</i> lateral flagellar system	32
1.2.4.11.6. Pathogenicity of <i>Aeromonas</i> during motility and sessility and the roles played by flagella in each setting	40
1.3. Cyclic dimeric guanosine monophosphate (c-di-GMP).....	47
1.3.1. Discovery of and roles played by c-di-GMP.....	47
1.3.2. c-di-GMP turnover.....	48
1.3.2.1. Synthesis of c-di-GMP.....	48
1.3.2.1.1. Mechanisms of DGC activation/ inactivation	49
1.3.2.1.1.1. Phosphorylation-dependent regulation.....	49
1.3.2.1.1.2. Product feed back inhibition	49
1.3.2.1.1.3. Environmental signals-based regulation	50
1.3.2.1.1.4. Competitive inhibition of DGCs	51
1.3.2.2. Hydrolysis of c-di-GMP.....	53
1.3.3. Presence of GGDEF and EAL domains in bacterial genomes.....	55
1.3.4. Sensory domains linked to GGDEF and EAL domains.....	56
1.3.5. Tandemly arranged domains (composite proteins) and their functions	58
1.3.6. Receptors (effectors) for c-di-GMP	61
1.3.6.1. PilZ domain.....	61
1.3.6.2. Enzymatically inactive GGDEF and EAL domains.....	65
1.3.6.3. Transcription factors	65
1.3.6.4. Polynucleotide phosphorylase (PNPase).....	71
1.3.6.5. Riboswitches	72
1.3.7. Targets of c-di-GMP	75
1.3.8. The c-di-GMP signalling network in <i>Aeromonas</i> species.....	76
1.3.8.1. Role of c-di-GMP in controlling the switch between motility and sessility in <i>Aeromonas</i> species.....	77
1.3.8.2. Interrelation between c-di-GMP signalling system and quorum sensing (QS) system in <i>Aeromonas</i> species.....	78
1.4. Hypothesis of this study	82
1.5. Objectives of this study.....	82
Chapter 2: Materials and methods	84
2.1. Bacterial strains and plasmids.....	84
2.2. Bacterial growth and maintenance conditions	84
2.2.1. Liquid media	84
2.2.2. Incubation of broth cultures	84
2.2.3. Solid media	84

2.2.4. Incubation and storage of agar-based cultures	85
2.2.5. Sterilization of bacteriological media	93
2.2.6. Antibiotics.....	93
2.2.7. Other media supplements.....	94
2.3. Conventional tests.....	94
2.3.1. Oxidase test.....	94
2.4. DNA and RNA techniques.....	94
2.4.1. Extraction of bacterial chromosomal DNA.....	94
2.4.2. Plasmid extraction (miniprep).....	95
2.4.3. DNA purification	96
2.4.4. DNA Restriction digestion.....	97
2.4.5. DNA ligation.....	97
2.4.6. Polymerase chain reaction (PCR)	97
2.4.6.1. Primer design	97
2.4.6.2. PCR amplification using GoTaq® DNA polymerase	98
2.4.6.3. Colony PCR screening using GoTaq DNA polymerase	99
2.4.6.4. PCR amplification using KOD Hot Start DNA Polymerase.....	99
2.4.6.5. PCR amplification using Platinum <i>Pfx</i> DNA Polymerase	100
2.4.7. RNA extraction	101
2.4.8. Reverse Transcriptase Polymerase Chain Reaction (RT-PCR)	102
2.4.9. Agarose gel electrophoresis	104
2.4.9.1. Extraction of DNA fragment from agarose gel.....	105
2.5. Introduction of genetic material into bacterial cells.....	105
2.5.1. Transformation by heat shock.....	106
2.5.1.1. Preparation of competent cells for heat shock transformation.....	107
2.5.2. Bacterial conjugation	108
2.5.3. Bacterial triparental conjugation.....	108
2.6. The β -galactosidase assay	108
2.7. Biofilm assay	111
2.8. Western blot analysis	111
2.8.1. Preparation of swimming bacteria for SDS-PAGE.....	112
2.8.2. Preparation of swarming bacteria for SDS-PAGE.....	112
2.8.3. Sodium Dodecyl Sulphate Polyacrylamide Gel Electrophoresis (SDS-PAGE)	113
2.8.4. Performing Western blotting.....	114
2.9. Statistics	115

Chapter 3: Role played by <i>A. caviae</i> GGDEF-EAL domains in motility, biofilm formation, and lateral flagellar genes expression	117
3.1. Introduction.....	117
3.2. Overexpression of the genes <i>AHA1208</i> , <i>AHA0382</i> , and <i>mshH</i> in <i>A. caviae</i> Sch3N	118
3.2.1. About the genes <i>AHA1208</i> , <i>AHA0382</i> , and <i>mshH</i>	118
3.2.2. Cloning of the genes <i>AHA1208</i> and <i>AHA0382</i> in <i>E. coli</i> DH5 α	126
3.2.3. Introducing multiple copies of <i>AHA1208</i> and <i>mshH</i> into <i>A. caviae</i> Sch3N by bacterial conjugation	130
3.2.4. Effects of overexpression of <i>AHA1208</i> on <i>A. caviae</i> phenotype	130
3.2.5. Effects of overexpression of <i>mshH</i> on <i>A. caviae</i> phenotype.....	134
3.3. Phenotypic and molecular effects of mutating each of the thirteen GGDEF-EAL encoding genes in <i>A. caviae</i>	138
3.3.1. Creating mutations in <i>A. caviae</i> Sch3N GGDEF-EAL encoding genes	138
3.3.2. Effects of mutations on <i>A. caviae</i> Sch3N motility and its ability to form a biofilm	145
3.3.2.1. Motility assays	145
3.3.2.2. Biofilm formation	147
3.3.2.3. Growth of <i>A. caviae</i> mutants on Congo Red (CR) agar.....	149
3.3.3. Transcriptional analysis of <i>lafA1</i> , <i>lafA2</i> , and <i>lafK</i> genes expression in the background of <i>A. caviae</i> mutants	150
3.3.3.1. Construction of plasmids containing promoters of the <i>A. caviae</i> genes <i>lafA1</i> , <i>lafA2</i> , and <i>lafK</i>	150
3.3.3.2. β -galactosidase assay	155
3.3.4. Complementation and over expression of the <i>A. caviae</i> genes <i>AHA2484</i> , <i>AHA3342</i> , and <i>AHA2698</i>	159
3.3.4.1. Construction of plasmids containing the <i>A. caviae</i> genes <i>AHA2484</i> , <i>AHA3342</i> , and <i>AHA2698</i> for complementation and overexpression.....	161
3.3.4.2. Transfer of plasmids containing each of the genes <i>AHA2484</i> , <i>AHA3342</i> , and <i>AHA2698</i> to <i>A. caviae</i> wild type strain and <i>A. caviae</i> mutant strains MA2, MA10, and MA12 by conjugation	161
3.3.4.3. Phenotypic effects of complementation and overexpression of the <i>A. caviae</i> gene <i>AHA2484</i>	164
3.3.4.4. Phenotypic effects of complementation and overexpression of the gene <i>AHA3342</i>	169
3.3.4.5. Phenotypic effects of complementation and overexpression of the gene <i>AHA2698</i>	173
Table 3.1. Summary of the results obtained following mutation, complementation, and.....	177
3.4. Discussion.....	178
3.4.1. Hypothesis testing	178
3.4.1.1. Overexpression of <i>AHA1208</i>	178

3.4.1.2. Overexpression of <i>AHA0382</i>	181
3.4.1.3. Overexpression of <i>MshH</i>	181
3.4.2. Mutations in <i>A. caviae</i> GGDEF-EAL encoding genes	182
3.4.2.1. Complementation and overexpression of <i>AHA2484</i> , <i>AHA3342</i> , and <i>AHA2698</i>	183
3.4.3. Reliability and reproducibility of biofilm assay and growth on CR agar	185
Chapter 4: The effect of <i>pilZ</i> gene knockout on <i>A. caviae</i> Sch3N lifestyle	188
4.1. Introduction.....	188
4.2. Testing the expression of <i>pilZ</i> gene during swarming	189
4.3. <i>pilZ</i> gene knockout.....	193
4.3.1. Phenotypic studies of MA124.....	204
4.3.1.1. Motility assay	204
4.3.1.2. Biofilm assay	204
4.3.1.3. Growth on Congo Red agar	204
4.3.2. Transcriptional fusions.....	208
4.4. Discussion	210
4.4.1. PilZ expression during swarming of <i>A. caviae</i>	210
4.4.2. Phenotypic effects of <i>A. caviae pilZ</i> gene knockout	212
4.4.2.1. Effects of <i>pilZ</i> gene knockout on <i>A. caviae</i> motility.....	212
4.4.2.2. Effects of <i>pilZ</i> gene knockout on the ability of <i>A. caviae</i> to form a biofilm.....	213
4.4.3. Effects of <i>A. caviae pilZ</i> gene knockout on the promoters activities of the genes <i>lafA1</i> , <i>lafA2</i> , and <i>lafK</i>	214
Chapter 5: The role of <i>lafK</i> riboswitch as a c-di-GMP receptor	216
5.1. Introduction.....	216
5.2. Bioinformatic analysis of <i>A. caviae lafK</i> gene.....	217
5.2.1. <i>A. caviae lafK</i> gene promoter location prediction using computational analysis	217
5.2.2. Prediction of <i>lafK</i> GEMM riboswitch location and architecture	217
5.2.3. Computational analysis of <i>lafK</i> open reading frames and conserved domains	222
5.3. Effect of <i>A. caviae lafK</i> riboswitch deletion on lateral flagellar genes expression.....	223
5.3.1. <i>lafK</i> riboswitch deletion using the Spliced Overlap Extension (SOE) PCR technique	223
5.3.2. Quantitative determination of the effect of <i>A. caviae lafK</i> riboswitch deletion on the lateral flagellar genes expression using β -galactosidase assay	226
5.3.2.1. Fusion of <i>lafKp</i> and <i>lafKp</i> Δ riboswitch to the promoter-less plasmid vector pKAGb2(-).....	226
5.3.2.2. β -Galactosidase assay results	231

5.4. Effect of deleting the P1 and P2 hairpins of the <i>lafK</i> riboswitch on <i>A. caviae</i> lateral flagellar genes expression	232
5.4.1. P1 and P2 hairpins deletion using the Spliced Overlap Extension (SOE) PCR technique	232
5.4.2. Quantitative determination of the effect of P1 and P2 hairpins deletion on the lateral flagellar genes expression using β -galactosidase assay	233
5.4.2.1. Fusion of <i>lafKp</i> Δ P1 and <i>lafKp</i> Δ P2 to the promoter-less plasmid vector pKAGb2(-)	233
5.4.2.2. β -Galactosidase assay results	234
5.5. Effect of creating mutations within the stems of the P1 and P2 hairpins on the <i>A. caviae</i> lateral flagellar genes expression	241
5.5.1. Creating mutations within the stems of P1 and P2 loops using the Spliced Overlap Extension (SOE) PCR technique	241
5.5.2. Quantitative determination of the effect of creating a mutation within the stem of P1 domain on the <i>A. caviae</i> lateral flagellar genes expression using the β -galactosidase assay	242
5.5.2.1. Fusion of <i>lafKp</i> with a mutation in the stem of P1 domain to the promoter-less plasmid vector pKAGb2(-)	242
5.5.2.2. β -Galactosidase assay results	243
5.6. Complementation of <i>lafK</i> gene with <i>lafK</i> Δ riboswitch	248
5.6.1. Deletion of <i>lafK</i> riboswitch and introducing <i>lafK</i> Δ riboswitch into CM100	248
5.6.2. Testing the complemented strain using the motility assay	252
5.6.3. Testing the ability of the complemented strain to produce the lateral flagellin protein when grown in liquid medium	254
5.7. Discussion	257
Chapter 6: Final conclusions	266
Appendix: Primers used in this study	270
I- Primers used to mutate GGDEF-EAL-encoding genes	270
II- Primers used for complementing GGDEF-EAL encoding genes	271
III- Primers used to overexpress GGDEF-EAL encoding genes	272
IV- Primers used for <i>lafA1</i> , <i>lafA2</i> , and <i>lafK</i> promoters fusions	273
V- Primers used to knockout <i>pilZ</i> gene	274
VI- Primers used in RT-PCR	275
VII- Primers used for <i>lafK</i> riboswitch deletion, disscetion and complementation	276
VIII- Primers used for DNA sequencing and clone screening	278
References	280

List of Figures

Chapter 1: Introduction

Figure 1.1. The five chromosomal regions containing the polar flagellar genes of <i>A. caviae</i> Sch3N	28
Figure 1.2. The lateral flagellar operon of <i>Aeromonas caviae</i> Sch3N	35
Figure 1.3. A diagram showing the structure of a lateral flagellum in <i>A. caviae</i> Sch3N	36
Figure 1.4. A diagram showing the ability of a mesophilic <i>Aeromonas</i> cell to switch between its polar and lateral flagellar systems	42
Figure 1.5. A diagram summarizes the cycle of swimming motility, swarming motility, and biofilm formation in human gastroenteritis caused by <i>A. caviae</i>	46
Figure 1.6. The chemical structure of c-di-GMP	47
Figure 1.7. Effects of c-di-GMP on certain cellular processes	48
Figure 1.8. Chemical formula for the formation of c-di-GMP	49
Figure 1.9. Phosphorylation-dependent mechanism of DGC activation	51
Figure 1.10. Regulation of DGC activity by non-competitive feedback inhibition	52
Figure 1.11. Mechanism of regulation of the DGC protein YfiN in <i>P. aeruginosa</i>	53
Figure 1.12. Chemical formula for the hydrolysis of c-di-GMP	55
Figure 1.13. The protein-protein interaction mechanism of regulation proposed for the <i>E. coli</i> PilZ domain containing protein YcgR	64
Figure 1.14. Activation of Type 3 fimbriae genes expression by PilZ protein MrkH in <i>K. pneumonia</i>	64
Figure 1.15. The proposed model for the regulation of <i>P. aeruginosa</i> polar flagellar genes expression mediated by the transcription factor FleQ	68
Figure 1.16. First model of <i>pel</i> promoter regulation by FleQ transcription factor	69
Figure 1.17. The second suggested model of repression and derepression of <i>pel</i> genes transcription in <i>P. aeruginosa</i> by the transcription factor FleQ	70
Figure 1.18. The model of the <i>E. coli</i> degradosome containing the c-di-GMP effector polynucleotide phosphorylase (PNPase) enzyme	72
Figure 1.19. The two domain architecture of a riboswitch	74
Figure 1.20. C-di-GMP turnover, its basic signalling module, and its functions within the bacterial cell	76
Figure 1.21. A Diagram showing the role played by c-di-GMP in controlling sessility and motility in <i>Aeromonas</i> spp	77

Chapter 3: Role played by *A. caviae* GGDEF-EAL domains in motility, biofilm formation, and lateral flagellar genes expression:

Figure 3.1. Detection of conserved domains in <i>A. caviae</i> Sch3N AHA1208 protein	119
Figure 3.2. GGDEF and RxxD motifs in <i>A. caviae</i> protein AHA1208	120

Figure 3.3 Detection of conserved domains in <i>A. caviae</i> Sch3N AHA0382 protein	122
Figure 3.4. EAL residues in of <i>A. caviae</i> protein AHA0382	123
Figure 3.5. Detection of conserved domains in <i>A. veronii</i> bv. Sobria BC88 MshH protein	124
Figure 3.6. Detection of conserved residues in the sequence of <i>A. veronii</i> MshH protein	125
Figure 3.7. Agarose gel showing PCR amplification of <i>A. caviae</i> AHA0382 and AHA1208	126
Figure 3.8. Map of pBBR1MCS5 broad host range plasmid	127
Figure 3.9. Map of pBBR1MCS broad host range plasmid	128
Figure 3.10. A 1% agarose gel showing an <i>E. coli</i> DH5 α colony PCR screen following transformation with pBBR1MCS5-AHA1208	129
Figure 3.11. A 1% agarose gel showing an <i>E. coli</i> DH5 α colony PCR screening following transformation with pBBR1MCS5-AHA0382	129
Figure 3.12. Biofilm assay to test the ability of <i>A. caviae</i> Sch3N pBBR1MCS5-AHA1208 to form a biofilm	131
Figure 3.13. A graph showing biofilm production on borosilicate glass tubes by the strain <i>A. caviae</i> Sch3N pBBR1MCS5-AHA1208	132
Figure 3.14. Colony morphology of <i>A. caviae</i> pBBR1MCS-5-AHA1208 grown on 0.025% Congo Red agar	132
Figure 3.15. Motility test on swim agar plate to test the effect of AHA1208 overexpression in <i>A. caviae</i> Sch3N	133
Figure 3.16. Motility test on swarm plate to test the effect of AHA1208 overexpression in <i>A. caviae</i> Sch3N	133
Figure 3.17. Biofilm assay using borosilicate glass tubes testing the strain <i>A. caviae</i> Sch3N pBBR1MCS- <i>mshH</i>	135
Figure 3.18. Quantitative determination of the biofilm formed by <i>A. caviae</i> Sch3N pBBR1MCS- <i>mshH</i> on borosilicate glass tubes	135
Figure 3.19. Colony morphology of <i>A. caviae</i> Sch3N overexpressing <i>mshH</i> growing on Congo Red (0.025%) agar	136
Figure 3.20. Motility test on swim agar plate to test the effect of <i>A. veronii mshH</i> overexpression in <i>A. caviae</i> Sch3N	137
Figure 3.21. Motility test on swarm plate to test the effect of <i>A. veronii mshH</i> overexpression in <i>A. caviae</i> Sch3N	137
Figure 3.22. Predicted domain architecture of the thirteen GGDEF-EAL containing proteins in <i>A. caviae</i> Sch3N	139
Figure 3.23. Multiple sequence alignment of the amino acid sequences of the thirteen GGDEF-EAL-containing proteins in <i>A. caviae</i> Sch3N	140
Figure 3.24. A 1% agarose gel showing PCR amplification of internal fragments of each of the thirteen GGDEF-EAL encoding genes in <i>A. caviae</i> Sch3N	141
Figure 3.25. Map of the suicide plasmid vector pKNG101	142

Figure 3.26. Schematic presentation of the plasmid insertion mutagenesis technique	143
Figure 3.27. Schematic presentation of the procedure used to knockout the GGDEF-EAL encoding genes in <i>A. caviae</i> Sch3N	144
Figure 3.28. Effects of mutations in the thirteen GGDEF-EAL encoding genes of <i>A. caviae</i> Sch3N on its ability to swim	146
Figure 3.29. Swarm agar plate showing the morphology of a single <i>A. caviae</i> Sch3N colony during swarming motility	146
Figure 3.30. Quantification of the biofilm formed by the GGDEF-EAL <i>A. caviae</i> mutant strains on borosilicate glass tubes	148
Figure 3.31. Qualitative pictures showing the decreased ability of the mutant strain MA12 to form a biofilm on borosilicate glass tubes	149
Figure 3.32. Colony morphology of the <i>A. caviae</i> mutant strains MA2 and MA12 grown on (0.025%) Congo Red (CR) agar	150
Figure 3.33. A Map showing the main features of the plasmid vector pKAGb-2(-)	152
Figure 3.34. A 1% agarose gel of colony PCR screening of <i>E. coli</i> S17-1 cells transformed with pKAGb2(-) <i>lafA1p</i>	152
Figure 3.35. A 1% agarose gel of colony PCR screening of <i>E. coli</i> S17-1 cells transformed with the pKAGb2(-) <i>lafA2p</i>	153
Figure 3.36. A 1% agarose gel of colony PCR screening of <i>E. coli</i> S17-1 cells transformed with the pKAGb2(-) <i>lafKp</i>	153
Figure 3.37. A schematic presentation showing the detailed steps used to fuse the promoters of the three genes <i>lafK</i> , <i>lafA1</i> , and <i>lafA2</i> to pKAGb2(-)	154
Figure 3.38. Analysis of <i>lafA1</i> promoter activity in <i>A. caviae</i> GGDEF-EAL mutants using β -galactosidase assay	157
Figure 3.39. Analysis of <i>lafA2</i> promoter activity in <i>A. caviae</i> GGDEF-EAL mutants using β -galactosidase assay	158
Figure 3.40. Analysis of <i>lafK</i> promoter activity in <i>A. caviae</i> GGDEF-EAL mutants using β -galactosidase assay	159
Figure 3.41. The predicted domain architecture of the three <i>A. caviae</i> Sch3N GGDEF-EAL containing proteins AHA2484, AHA3342, and AHA2698	160
Figure 3.42. A 1% agarose gel showing restriction digestion of the PCR amplicons of the genes <i>AHA2484</i> , <i>AHA3342</i> , and <i>AHA2698</i>	162
Figure 3.43. A 1% agarose gel showing colony PCR screening of <i>E. coli</i> DH5 α transformed with pBBR1MCS5- <i>AHA2484</i>	163
Figure 3.44. A 1% agarose gel showing colony PCR screening of <i>E. coli</i> DH5 α transformed with pBBR1MCS5- <i>AHA3342</i>	163
Figure 3.45. A 1% agarose gel showing colony PCR screening of <i>E. coli</i> DH5 α transformed with pBBR1MCS5- <i>AHA2698</i>	164
Figure 3.46. Swim agar plate showing the effect of complementation and overexpression of the <i>A. caviae</i> genes <i>AHA2484</i> , <i>AHA3342</i> , <i>AHA2698</i>	165
Figure 3.47. Swarm agar plates showing the effect of complementation and overexpression of the <i>A. caviae</i> gene <i>AHA2484</i>	166

Figure 3.48. Colonies of <i>A. caviae</i> strains on Congo Red agar (0.025%) showing the results of complementation and overexpression of the <i>A. caviae</i> gene <i>AHA2484</i>	167
Figure 3.49. Quantitative biofilm assay results following complementing the gene <i>AHA2484</i> and its overexpression in <i>A. caviae</i> Sch3N	168
Figure 3.50. Swarm agar plates showing the effect of complementation and overexpression of the <i>A. caviae</i> gene <i>AHA3342</i>	170
Figure 3.51. Congo red agar plate showing the effect of complementation and overexpression of the <i>A. caviae</i> gene <i>AHA3342</i>	171
Figure 3.52. Quantitative biofilm assay results following complementing the gene <i>AHA3342</i> and its overexpression in <i>A. caviae</i> Sch3N	172
Figure 3.53. Swarm agar plates showing the effect of complementation and overexpression of the <i>A. caviae</i> gene <i>AHA2698</i>	174
Figure 3.54. Congo Red agar plate showing the result of complementation and overexpression of the <i>A. caviae</i> gene <i>AHA2698</i>	175
Figure 3.55. Quantitative biofilm assay results following complementing the gene <i>AHA2698</i> and its overexpression in <i>A. caviae</i> Sch3N	176
<u>Chapter 4: The effect of <i>pilZ</i> gene knockout on <i>A. caviae</i> Sch3N lifestyle</u>	
Figure 4.1. Sites of the custom designed oligonucleotide primers used to check for the expression of <i>pilZ</i> and <i>lafU</i> genes during swarming motility of <i>A. caviae</i> by RT-PCR	190
Figure 4.2. A 1% agarose gel showing the expression of the genes <i>pilZ</i> and <i>lafU</i> during the swarming of <i>A. caviae</i> using RT-PCR	191
Figure 4.3. Schematic presentation of the procedure used in this study to confirm the expression of <i>pilZ</i> and <i>lafU</i> during swarming of <i>A. caviae</i> Sch3N	192
Figure 4.4. Region of <i>A. caviae</i> genomic DNA containing the <i>pilZ</i> gene to be cloned and knocked out	194
Figure 4.5. 0.8% agarose gel showing PCR amplification of <i>pilZ</i> gene using the custom designed primers PilZ-F and PilZ-R and genomic DNA of <i>A. caviae</i> Sch3N	195
Figure 4.6. A map showing the main features of the plasmid pGEM-T-Easy	195
Figure 4.7. A 1% agarose gel showing the ligation mixture containing pGEM-T plasmid and PCR amplified <i>pilZ</i> gene	196
Figure 4.8. A 1% agarose gel showing colony PCR screening of <i>E. coli</i> DH5 α transformed with pGEM- <i>pilZ</i>	198
Figure 4.9. A 1% agarose gel showing the successful construction of pGEM- <i>pilZ</i> ::Km	198
Figure 4.10. A 1% agarose gel showing pKNG101- <i>pilZ</i> ::km extracted from streptomycin- and kanamycin-resistant <i>E. coli</i> CC118 λ pir colony	201
Figure 4.11. A schematic representation of the double cross over event which was used to permanently mutate the <i>pilZ</i> gene in <i>A. caviae</i> Sch3N	201
Figure 4.12. A 1% agarose gel showing the PCR amplification of the mutated <i>A. caviae pilZ</i> gene and the wild type <i>pilZ</i> gene	202
Figure 4.13. Schematic presentation of the complete procedure used to knock out <i>pilZ</i> gene in <i>A. caviae</i> Sch3N	203

Figure 4.14. A swim agar plate showing the effect of <i>pilZ</i> gene mutation on the swimming ability of <i>A. caviae</i>	205
Figure 4.15. Two swarm agar plates showing the effect of <i>pilZ</i> gene mutation on the swarming ability of <i>A. caviae</i>	205
Figure 4.16. Biofilm assay using borosilicate glass tube to test the effect of introducing a mutation in <i>pilZ</i> gene on the ability of <i>A. caviae</i> to form a biofilm	206
Figure 4.17. Graphs showing the effect of <i>pilZ</i> gene knockout on the ability of <i>A. caviae</i> to form a biofilm on borosilicate glass tubes	207
Figure 4.18. Congo red agar plate showing the effect of <i>pilZ</i> gene knockout on the ability of <i>A. caviae</i> to bind the Congo red dye	207
Figure 4.19. Analysis of <i>lafA1</i> promoter activity in <i>A. caviae pilZ</i> mutant grown on swarm agar using β -galactosidase assay	209
Figure 4.20. Analysis of <i>lafA2</i> promoter activity in <i>A. caviae pilZ</i> mutant grown on swarm agar using β -galactosidase assay	209
Figure 4.21. Analysis of <i>lafK</i> promoter activity in <i>A. caviae pilZ</i> mutant grown on swarm agar using β -galactosidase assay	210
Figure 4.22. The putative conserved domains detected in <i>A. caviae</i> protein LafU using the NCBI blastp tool	211
<u>Chapter 5: The role of <i>lafK</i> riboswitch as a cyclic-di-GMP receptor</u>	
Figure 5.1. <i>A. caviae lafK</i> gene promoter prediction	219
Figure 5.2. Prediction of riboswitch within the <i>lafK</i> promoter region	219
Figure 5.3. ClustalW alignment showing the similarity between the <i>V. cholerae</i> Vc2 GEMM RNA type I and the <i>A. caviae lafK</i> GEMM riboswitch type I	219
Figure 5.4. RNA sequence and suggested architecture of the <i>A. caviae lafK</i> GEMM c-di-GMP type I riboswitch	221
Figure 5.5. The secondary structure of the <i>A. caviae lafK</i> GEMM c-di-GMP type I riboswitch in dot-bracket notation	221
Figure 5.6. Putative conserved domains detected within <i>A. caviae</i> LafK protein using the NCBI blastp tool	222
Figure 5.7. The predicted genetic structure of the region upstream of <i>A. caviae lafK</i> gene	223
Figure 5.8. A schematic presentation of the Spliced Overlap Extension (SOE) PCR technique used in this study to delete the <i>lafK</i> riboswitch in <i>A. caviae</i> Sch3N	224
Figure 5.9. A 1% agarose gel showing the products of the first and the second PCR steps of the SOE PCR technique used to delete the <i>lafK</i> riboswitch of <i>A. caviae</i> Sch3N	225
Figure 5.10. A 1% agarose gel showing the single PCR product of the third step of the SOE PCR technique used to delete the <i>A. caviae</i> Sch3N <i>lafK</i> riboswitch	225
Figure 5.11. A 1% agarose gel showing PCR amplification of a 577bp DNA region upstream of <i>lafK</i> which contains a riboswitch	227
Figure 5.12. Agarose gels showing successful cloning of <i>lafK</i> promoter in <i>E. coli</i> DH5 α	227
Figure 5.13. Agarose gels showing successful cloning of <i>lafKp</i> Δ riboswitch in <i>E. coli</i> DH5 α	229

Figure 5.14. A schematic presentation of the procedure used to fuse <i>lafK</i> promoter and the <i>lafKp</i> Δriboswitch to pKAGb2(-)	230
Figure 5.15. Analysis of <i>lafK</i> promoter activity in the presence and absence of the <i>lafK</i> riboswitch in <i>A. caviae</i> and <i>E. coli</i> DH5α using β-galactosidase assay	231
Figure 5.16. A schematic presentation showing the position of each of the four primers used in SOE-PCR to delete the P1 region of the <i>lafK</i> riboswitch	235
Figure 5.17. A 1% agarose gel showing amplicons of the first and second PCR steps of the SOE-PCR technique used to delete the P1 and P2 loops of <i>lafK</i> riboswitch	236
Figure 5.18. A 1% agarose showing amplicons of the third PCR step of the SOE-PCR technique used to delete P1 or P2 loops of the <i>A. caviae</i> <i>lafK</i> riboswitch	236
Figure 5.19. A schematic presentation showing the position of each of the four primers used in SOE-PCR to delete the P2 region of the <i>lafK</i> riboswitch	237
Figure 5.20. A 1% agarose gel showing colony PCR screening of <i>E. coli</i> DH5α cells transformed with pKAG- <i>lafKp</i> ΔP1	237
Figure 5.21. A 1% agarose gel showing colony PCR screening of <i>E. coli</i> DH5α cells transformed with pKAG- <i>lafKp</i> ΔP2	238
Figure 5.22. An overview of the procedure used to separately delete P1 and P2 loops of <i>lafK</i> riboswitch followed by cloning the mutated promoter in pKAGb2(-)	239
Figure 5.23. Analysis of <i>lafK</i> promoter activity in the presence and absence of the <i>lafK</i> riboswitch and following the deletion of P1 and P2 loops of the riboswitch in <i>A. caviae</i> and in <i>E. coli</i> DH5α using β-galactosidase assay	240
Figure 5.24. A schematic presentation showing the positions of the primers Ribodel-P1AG-F and Ribodel-P1AG-R used to change two nucleotides in the stem of P1 loop of <i>lafK</i> riboswitch by SOE-PCR technique	244
Figure 5.25. A schematic presentation showing the positions of the primers Ribodel-P2A-F and Ribodel-P2A-R used to change one nucleotides in the stem of P2 loop of <i>lafK</i> riboswitch by SOE-PCR technique	244
Figure 5.26. A 1% agarose gel showing the first and the second PCR steps of the SOE-PCR technique used to create mutations within the stem of P1 loop of <i>lafK</i> riboswitch	245
Figure 5.27. A 1% agarose showing amplicons of the third PCR step of the SOE-PCR technique used to create mutations within the stems of P1 and P2 loops of <i>lafK</i> riboswitch	245
Figure 5.28. A 1% agarose gel showing the first and the second PCR steps of the SOE-PCR technique used to create a mutation within the stem of the P2 loop of <i>lafK</i> riboswitch	246
Figure 5.29. A 1% agarose gel showing colony PCR screening of <i>E. coli</i> DH5α cells transformed with pKAG- <i>lafKp</i> P1AG	246
Figure 5.30. Analysis of <i>lafK</i> promoter activity using β-galactosidase assay following the change of two nucleotides in the stem of the P1 loop of the <i>lafK</i> riboswitch	247
Figure 5.31. Position of the four custom designed oligonucleotide primers used to amplify <i>lafK</i> gene and delete the riboswitch by SOE-PCR technique	250
Figure 5.32. A 1% agarose gel showing the first and the second PCR steps of the SOE-PCR technique used to both amplify the <i>lafK</i> gene and to delete the <i>lafK</i> riboswitch	250
Figure 5.33. A 1% agarose showing amplicons of the third PCR step of the SOE-PCR technique used to amplify <i>lafK</i> gene and delete the riboswitch	251

Figure 5.34. A 1% agarose gel showing colony PCR screening of <i>E. coli</i> DH5 α cells transformed with pBBR1MCS5- <i>lafK</i> Δ riboswitch	251
Figure 5.35. Testing the ability of CM100 pBBR1MCS5- <i>lafK</i> Δ Ribo to swarm	253
Figure 5.36. Testing the ability of CM100 pBBR1MCS5- <i>lafK</i> Δ Ribo to swim	253
Figure 5.37. Western blot showing specific detection of polar and lateral flagellin proteins expressed following complementing <i>lafK</i> gene in CM100 with pBBR1MCS5- <i>lafK</i> Δ ribo during both swarming and swimming	256
Figure 5.38. Suggested architecture of <i>A. caviae</i> <i>lafK</i> GEMM riboswitch type I after binding to c-di-GMP	261
Figure 5.39. The proposed results for a recommended promoter fusion experiment which can further confirm the role played by the <i>lafK</i> riboswitch as a c-di-GMP receptor	262

List of Tables

Chapter 1:

Table 1.1. The classification of <i>Aeromonas</i> species based on DNA-DNA homology	3
Table 1.2. Bacterial species known to possess two distinct flagellar systems	25
Table 1.3. <i>A. caviae</i> Sch3N polar flagellar genes with their predicted function	29
Table 1.4. Genes composing the <i>A. caviae</i> Sch3N lateral flagellar operon along with their predicted function	33
Table 1.5. Sensory domains commonly linked to GGDEF and EAL domains	57
Table 1.6. Examples of studied enzyme proteins containing GGDEF, EAL, and HD-GYP domains	60
Table 1.7. Examples of c-di-GMP effectors	62

Chapter 2:

Table 2.1. Bacterial strains used in this study	86
Table 2.2. Plasmids used in this study	90

Chapter 3:

Table 3.1. Summary of the results obtained following mutation, complementation, and overexpression of the <i>A. caviae</i> genes <i>AHA2484</i> , <i>AHA3342</i> , and <i>AHA2698</i>	177
--	-----

Abbreviations

Am	Ampicillin
BHIB	Brain Heart Infusion Broth
c-di-GMP	Bis-(3'-5')-cyclic dimeric guanosine monophosphate
CPS	Capsular polysaccharide
CR Agar	Congo Red Agar
Cm	Chloramphenicol
cm	centimetre
DMSO	Dimethyl sulfoxide
DNA	Deoxyribonucleic Acid
dNTPs	Deoxynucleotide triphosphates
Fla	Polar flagellar system
Gm	Gentamycin
Hr	Hour
IPTG	Isopropyl β -D-1-thiogalactopyranoside
Km	Kanamycin
Laf	Lateral flagellar system
LB	Luria Bertani
M	Molar
ml	Millilitre
mM	Millimolar
MOPS	3-(N-morpholino)propanesulfonic acid
μ g	Microgram
μ l	Microlitre
M unit	Miller unit
NA	Nalidixic acid
nm	Nano metre
OD	Optical density
ONPG	Ortho-nitrophenyl- β -galactoside

ORF	Open reading frame
PCR	Polymerase Chain Reaction
PFGE	Pulsed Field Gel Electrophoresis
RNA	Ribonucleic acid
RT-PCR	Reverse Transcriptase Polymerase Chain Reaction
SD	Standard deviation
Sm	Streptomycin
SMART	Simple Modular Architecture Research Tool
TEM	Transmission electron microscope
UTR	Untranslated region
X-gal	5-bromo-4-chloro-3-indolyl- β -D-galactopyranoside

Acknowledgment

Firstly, I would like to thank The University of Sheffield for giving me the opportunity to enjoy a great academic experience and to use the excellent campus facilities. I also would like to thank the Department of Infection and Immunity for giving me a desk to read and for allowing me to use their most recent research facilities to perform my experiments.

Special thanks to both my supervisor Dr. Jon Shaw and my co-supervisor Dr. Mark Thomas for giving me the opportunity to work with one of the most promising fields in molecular microbiology, c-di-GMP signalling, and for the guidance they provided me with throughout this project. I am also thankful for my personal tutor Dr. Bernard Corfe who was very friendly in our regular meetings and who through his guidance and support that I was able to gain a high confidence and to carry on with my study. My thanks are also extended to the post-doctoral fellows in the Department of Infection and Immunity, namely, Dr. Jennifer Parker, Dr. Ed Guccione, Dr. Sarb Pradhananga, Dr. Guta Vitovski, and Dr. Sabela Balboa Mendez for the technical help and for the experimental protocols and the very useful scientific advices they provided me with.

Many thanks to my colleagues, the previous and current students in the Department of Infection and Immunity, namely, Mr. Zeren Liu, Dr. Asma Ahmad, Dr. Richard Jones, Mrs. Magdalena Wierzbicka, Dr. Jing Zhang, Mr. Yu Hang Zhao, Mr. Ramhari Kumbhar, Mr. Md Risat Ul Haque, Miss Ruyue Sun, Mr. Chris Mason, Mr. Christopher Jenkins, Miss Helena Spiewak, and Mr. Jamie Hall for providing me with the help and advice during performing my experiments and when using certain computer softwares, and also for the very useful and enjoyable scientific discussions we carried out together. My thanks also go to the technicians in the Department of Infection and Immunity, namely, Mrs. Yvonne Stephenson (lead technician), Mr. Ian Geary, Mrs. Vanessa Singleton, Mr. John Finner, and Mr. Ben Harvey for the help and support they provided me with in relation to general microbiology, safety, and ordering items for my project being so kind and friendly.

I finally, would like to deeply thank my dear family for the love and support they gave me during my stay in Sheffield, and also to thank the Government of The State of Kuwait for funding this project.

Chapter 1

Introduction

Chapter 1: Introduction

1.1. The genus *Aeromonas*

1.1.1. Taxonomy

Historically the genus *Aeromonas* was considered to be a member of the family *Vibrionaceae* (Janda *et al.*, 1988) and its taxonomy was unclear and confusing (Popoff *et al.*, 1981). The species of the genus *Aeromonas* were basically divided into two groups based on their phenotypic and biochemical characteristics as well as on the temperature required for their optimum growth (Janda *et al.*, 2010). The first group, named the mesophilic aeromonads, included species which are motile, capable of causing human diseases and were optimally growing in a temperature range of 35°C to 37°C (Janda *et al.*, 1988). The second group, referred to as psychrophilic aeromonads, were mainly linked to causing infections in fish with its members being non motile and were best growing in a temperature range of 22°C to 25°C (Janda *et al.*, 1988). The mesophiles were a heterogenous group of species collectively referred to as *A. hydrophila* complex while the psychrophiles were represented by the species *A. salmonicida* (Janda *et al.*, 1988). This broad classification was impractical and inaccurate, for example, it is currently known that *A. hydrophila* is actually capable of causing both human and fish infections (Seshadri *et al.*, 2006). In addition, the recently described *A. salmonicida* subsp. *pectinolytica* was found to be capable of growing at 35°C (Pavan *et al.*, 2000). Thus, the need for a more accurate classification scheme which allows the separation of the heterogenous members of each of these two groups was necessary.

Studies providing extensive revision of the classification of the genus *Aeromonas* have begun after the mid-1970 (Janda *et al.*, 2010). The start was the study of Popoff and colleagues who used the DNA-DNA hybridization technique to determine the relatedness among 55 strains belonging to the mesophilic aeromonads (Popoff *et al.*, 1981). They have described the mesophilic group as consisting of three species, namely, *A. hydrophila*, *A. caviae*, and *A. sobria* with each species containing at least two of what was referred to as DNA-DNA homology groups (HGs). The study described the HGs as biochemically similar and recommended their future taxonomic designation with the accumulation of biochemical and molecular data. In their review, however, Janda and Abbott (Janda *et al.*, 2010) described the term HG as an outdated term used to describe *Aeromonas* strains which are similar at the DNA level but are difficult to be

distinguished based on phenotypic tests. They disagreed on the use of the term HG in *Aeromonas* taxonomy. Table 1.1 lists the classification of *Aeromonas* species based on DNA homology groups. Colwell and co-workers (Colwell *et al.*, 1986) performed a revolutionary phylogenetic study to revise the taxonomy of the genus *Aeromonas* by using the sequences of the rRNA-encoding genes to compare between *Aeromonas* species and some members of the *Vibrionaceae* and *Enterobacteriaceae*, as well as to use the sequence for inter-species relationships among members of the genus *Aeromonas*. Both the nucleotide sequences of the 5S (included in the ribosome's large subunit) and those of the 16S (included in the ribosome's small subunit) were included in the analysis. The study recommended the assignment of the genus *Aeromonas* to a separate family, the *Aeromonadaceae*. This family falls within the *Gammaproteobacteria* and the family includes two more genera, namely, *Oceanimonas*, and *Tolumonas* (Janda *et al.*, 2010) and currently there is a consensus on this classification.

Table 1.1. The classification of *Aeromonas* species based on DNA-DNA homology

Species name	DNA homology group (HG)
<i>A. hydrophila</i>	HG1
<i>A. bestiarum</i>	HG2
<i>A. salmonicida</i>	HG3
<i>A. caviae</i>	HG4
<i>A. media</i>	HG5
<i>A. eucrenophila</i>	HG6
<i>A. sobria</i>	HG7
<i>A. veronii</i> biogroup <i>sobria</i>	HG8
<i>A. jandaei</i>	HG9
<i>A. veronii</i> biogroup <i>veronii</i>	HG10
<i>Aeromonas</i> sp. (unnamed)	HG11
<i>A. schubertii</i>	HG12
<i>Aeromonas</i> sp. (unnamed)	HG13
<i>A. trota</i>	HG14
<i>A. allosaccharophila</i>	HG15
<i>A. encheleia</i>	HG16
<i>A. popoffii</i>	HG17

The classification provided in this table is based on the study of Yanez and colleagues (Yáñez *et al.*, 2003).

The use of the conserved 16S rRNA gene sequence for genetic relatedness analysis was, however, associated with few problems. First, the analysis indicated that the *Aeromonas* is a tight group. For example, *A. caviae* and *A. trota* have been found to be different by only one nucleotide while *A. hydrophila* and *A. media* had only three nucleotides difference (Yáñez *et al.*, 2003). The second problem associated with the use of the 16S rRNA gene sequence in the setting of *Aeromonas* taxonomy was the polymorphisms reported within this region among some species (Kupfer *et al.*, 2006). As a result, many investigations were carried out in the last 20 years exploring the nucleotide sequence of many housekeeping genes in an attempt to find DNA regions with more sequence diversity which can be used as phylogenetic markers to clearly distinguish between *Aeromonas* species.

Many genes were used as alternatives to the 16S rRNA gene and all of them were suggested to be powerful phylogenetic markers for the classification of *Aeromonas* species. Analysis of the nucleotide sequence of the *gyrB* gene clearly indicated that the genus *Aeromonas* forms a distinct line when compared to *Vibrio* spp., *E. coli* and to other members of the *Proteobacteria* (Yáñez *et al.*, 2003). The *gyrB* gene sequence analysis allowed for the splitting *A. veronii/A. culiciola/A. allosaccharophila* (Soler *et al.*, 2004). The mean sequence divergence of the *gyrB* gene was determined to be 7.76% (Kupfer *et al.*, 2006). The sequence divergence value of *rpoB* (which encodes the β subunit of the enzyme RNA polymerase) was determined to be 6.07% a finding which indicates that the *rpoB* is more conserved than the *gyrB* and that the later is a better tool to provide differentiation among *Aeromonas* species and sub-species. (Kupfer *et al.*, 2006). In addition, the mean sequence divergence value of the *recA* gene (which is important for both the repair of damaged DNA and for homologous recombination) was determined to be 7.8% (Sepe *et al.*, 2008). The DNA sequences of the *rpoD* gene was a powerful tool for inter-species differentiation as it helped to differentiate between *A. salmonicida* from *A. bestiarum* (Soler *et al.*, 2004). Sequence analysis of the gene for the heat-shock protein 40 *dnaJ* was found to have a discriminatory power which is highly similar to the power of the *gyrB* and *rpoD* genes (Nhung *et al.*, 2007).

The sequence analysis of all above mentioned housekeeping genes was found to be more powerful than the analysis of the 16S rRNA gene sequence for classification of *Aeromonas* species and for intra-species differentiation. As the sequences of these genes were analysed separately, the accuracy and reliability of the phylogenetic

structure would, however, increase further when more than one of these housekeeping genes was included in the same analysis, as each gene would help in differentiating between certain closely related species thus making the phylogenetic analysis more reliable (Soler *et al.*, 2004). Based on this principle, several recently published studies have used the multi locus sequence typing (MLST) technique for *Aeromonas* species delineation. An example of such studies is the one performed by Martino and colleagues (Martino *et al.*, 2011). The study used the DNA sequence of the six housekeeping genes *gyrB*, *groL*, *gltA*, *metG*, *ppsA*, and *recA* to analyze the relatedness among 100 *Aeromonas* strains isolated from clinical and environmental sources as well as type strains. The group found *Aeromonas* species to be clearly separated. In addition, the four species *A. caviae*, *A. media*, *A. encheleia*, and *A. eucrenophila* which were considered highly related and were described as a controversial group, formed different phylogenetic lines using the MLST approach.

MLST seems to have provided a precise method for differentiating between members of the genus *Aeromonas*, and it has been highly recommended as the reference method to provide the best description of any new species within the genus (Roger *et al.*, 2012). However, a new study has recently re-emphasized on the usefulness of the 16S rRNA gene as a phylogenetic marker for determining the taxonomic structure of the genus *Aeromonas* if this region was properly explored (Roger *et al.*, 2012). The components of the bacterial ribosomal subunits (5S, 23S and 16S) are usually arranged as an operon and co-transcribed together. In some bacterial genera, more than one copy of that operon can be found in the genome. Roger and colleagues used this principle to investigate the diversity in ribosomal operons copy number and copy heterogeneity. *A. hydrophila* subsp. *hydrophila* strain ATCC 7966^T was found to contain 10 operons while the notorious pathogen *Pseudomonas aeruginosa* possessed only 4 operons, a fact which indicated that the operon copy number in *Aeromonas* spp. is higher than other bacteria. Furthermore, *A. caviae* strains showed a noticeable heterogeneity using this phylogenetic approach.

The number of taxonomically valid bacterial species is constantly changing, the latest list of the valid *Aeromonas* species can be found in the List of Prokaryotic names with Standing in Nomenclature (LPSN) website (www.bacterio.net). According to LPSN, there are 31 valid *Aeromonas* species, of these, pathogenic *Aeromonas* species are discussed in section 2 of this chapter.

1.1.2. Morphology, physiology, and biochemistry

All members of the genus *Aeromonas* are non-endospore forming Gram-negative rods (Colwell *et al.*, 1986). The length of *Aeromonas* cells is around 1-3 μm (Janda *et al.*, 1988). The aeromonads are chemoorganotrophs and are able to grow in the presence or absence of Oxygen, i.e., facultative anaerobes (Janda *et al.*, 2010). A study published in 2003 in which the biochemical properties of 193 strains of the genus *Aeromonas* were investigated, all strains were able to ferment D-glucose and trehalose (Abbott *et al.*, 2003). The commonly used laboratory media do support the growth of *Aeromonas* species, examples include sheep blood agar and heart infusion agar (Janda *et al.*, 2010). All species of the genus *Aeromonas* are oxidase-positive and have the ability to reduce nitrate (Abbott *et al.*, 2003). Both mesophilic and psychrophilic aeromonads do exist (Colwell *et al.*, 1986). The mesophilic aeromonads are able to swim using a single polar flagellum, while the psychrophilic aeromonads are non motile (Janda *et al.*, 2010). In addition, an earlier study by Shimada and colleagues (Shimada *et al.*, 1985) have revealed the ability of the mesophilic aeromonads to produce many peritrichous lateral flagella under specific conditions. Both the polar and the lateral types of flagella produced by the mesophilic species *A. caviae* are discussed in detail later in this chapter.

1.1.3. Ecology

Although *Aeromonas* species are ubiquitous in nature, they are often linked with aquatic environments (Janda *et al.*, 2010). In a recently published study from Malaysia the researchers investigated the water quality of the coastal area of Langkawi (Andaman Sea) by collecting samples from four different stations and analysing them microbiologically (Jalal *et al.*, 2012). The study found a high microbial load in samples collected from the station number 4 with the bacterial species identified to be *A. hydrophila*, *Klebsiella oxytoca*, and *Serratia odorifera*. The number of colony forming units (CFU/ml) was around 3400 CFU/ml when samples were collected from the water surface. A high level of nitrates (14.61 $\mu\text{g/L}$) was also detected in the same station. The high concentration of organic matter (containing nitrogen) in this area was due to the different types of wastes and municipal sewage that was being discharged in the studied coast. The temperature of the water surface was 29.45°C and the pH was measured to be 8.16 when samples were collected for microbial analysis. In addition to the sea water and wastewater, *Aeromonas* species were also isolated from drinking water samples

according to a study performed in Southern Brazil (Scoaris *et al.*, 2008). The researchers collected 238 water samples from three different sources, followed by performance of membrane-filtration of each water sample. Each membrane was then cultured on the proper bacteriological culture media and the plates were incubated for 24 hours at 37°C. The presence of *Aeromonas* species in culture plates was then confirmed by both conventional and molecular tests. The group isolated *Aeromonas* species from 12.7%, 8.3%, and 6.5% of the bottled mineral water, artesian well water, and tap water, respectively. *Aeromonas* species have been isolated from ponds and shrimp culture hatcheries (Vaseeharan *et al.*, 2005) as well as rivers (Goñi-Urriza *et al.*, 2000). *A. hydrophila* and *A. sobria* were the only two species belonging to the genus *Aeromonas* isolated from two alkaline lakes in Hungary (Lango *et al.*, 2002).

Aeromonas species have been isolated from fish (Janda *et al.*, 2010), as well as from chicken. In a study performed in Ankara, Turkey, *Aeromonas* species were isolated from more than 80% of chicken carcasses purchased from local supermarkets, with *A. hydrophila* being the most dominant species (56%) and *A. caviae* being the less frequently isolated (14.7%) from chicken samples in this study (Sarimehmetoglu *et al.*, 2001). *Aeromonas* species have been isolated from meat of sheep, pigs, and cattle (Ceylan *et al.*, 2009). In addition, the raw milk and faeces of sheep, cattle, and horses also contained *Aeromonas* species (Ceylan *et al.*, 2009). Isolation of *Aeromonas* species from healthy domestic dogs and cats have been reported (Ghenghesh *et al.*, 1999). Nayduch and colleagues isolated *A. caviae* from houseflies (Nayduch *et al.*, 2002).

It is well known that the mesophilic *Aeromonas* species are soil inhabitants (Goñi-Urriza *et al.*, 2000). Furthermore, in a study performed in Northern Ireland to investigate the occurrence of pathogenic bacteria in organic vegetable samples, *Aeromonas* species were found in 34% of the vegetables tested, with *A. schubertii* being the most commonly isolated species (McMahon *et al.*, 2001).

1.2. *Aeromonas* pathogenesis

1.2.1. *Aeromonas* infections in fish

Fish infections caused by *Aeromonas* species are very well established. Each year, these infections cause huge economical losses in fish farming industry (Janda *et al.*, 2010). The species responsible for fish infections may belong to the psychrophilic or mesophilic aeromonads.

1.2.1.1. Fish infections caused by the psychrophilic aeromonads

The main species responsible for fish infections in this category is *A. salmonicida*. This species is commonly associated with the disease furunculosis which was originally thought to be limited to the salmonids, however, it is also now known to affect other fish species including, for instance, the Atlantic cod, carp, and goldfish (Beaz-Hidalgo *et al.*, 2013). The name of the disease came from the ‘furuncles’ which are skin ulcers (Beaz-Hidalgo *et al.*, 2013). There are different manifestations of the disease which include skin hyperpigmentation, loss of appetite leading to anaemia, lethargy and exophthalmia (Janda *et al.*, 2010, Beaz-Hidalgo *et al.*, 2013). The disease can as well cause septicaemia accompanied by the formation of haemorrhagic lesions both internally (in muscles and organs) and externally (in gills, fins and nares) (Beaz-Hidalgo *et al.*, 2013).

1.2.1.2. Fish infections caused by the mesophilic aeromonads

Both *A. hydrophila* and *A. veronii* are able to cause hemorrhagic septicaemia, which is commonly referred to as ‘motile *Aeromonas* septicaemia’ (Beaz-Hidalgo *et al.*, 2013). The disease can occur in salmon, carp, catfish and other fish (Janda *et al.*, 2010). In addition, *A. hydrophila* is known to be directly involved in the ‘red sore disease’ in bass which is characterized by the formations of red ulcers and sores (Huizinga *et al.*, 1979). Both *A. hydrophila* and *A. veronii* were implicated in ulcerative infections in cod, carp, and catfish (Janda *et al.*, 2010).

1.2.2. *Aeromonas* infections in animals

Both warm-blooded and cold-blooded animals can be infected by *Aeromonas* species (Janda *et al.*, 2010). *Aeromonas* species can cause diseases in amphibians, including turtles and frogs. The most common disease in this setting is the ‘red leg disease’ affecting frogs in which the bacterium causes haemorrhages in the leg muscles, hence the name red leg (Huys *et al.*, 2003). *Aeromonas hydrophila* has been isolated from cases of bovine seminal vesiculitis in bulls (Moro *et al.*, 1999) and from a case of septicaemia in a dog (Pierce *et al.*, 1973). Infections in calves, seals, snakes and lizards caused by *Aeromonas* species have as well been reported (Janda *et al.*, 2010).

1.2.3. *Aeromonas* infections in humans

Human diseases caused by the mesophilic *Aeromonas* species can be divided into three main categories which include: (1) wound and soft tissue infections (2)

gastroenteritis, and (3) extraintestinal infections (von Graevenitz, 2007, Janda *et al.*, 2010). The three most commonly isolated species from the above infections are *A. hydrophila*, *A. caviae*, and *A. veronii* biovar *sobria* (Tomas, 2012).

1.2.3.1. Epidemiology of human infections caused by *Aeromonas* species.

One of the important epidemiological studies investigating the types of infection caused by *Aeromonas* species was a study performed in France screening all types of infection occurring in 70 hospitals from May to October 2006 (Lamy *et al.*, 2009). The researchers found out the most common infections from which *Aeromonas* species were isolated to be wound and soft tissue infections. The study agrees with the published literature in the association of *Aeromonas* wound infections with trauma in contaminated water as >90% of the reported wound and soft tissue infections in otherwise healthy individuals occurred following trauma concomitant with environmental exposure to fresh water and soil in this study. Bacteraemia was determined to be the second most common infection in this study with a fatality rate of 35% and irrelevance to wound infections. Although gastroenteritis is considered to be the most common human infection associated with *Aeromonas* species, Lamy's group considered the *Aeromonas* gastroenteritis as a less common disease in France giving a possible reason that the disease is under reported due to it being self-limiting and that does not require any medical attention. In the same study, *A. hydrophila* was found to be mostly associated with wound infections while *A. caviae* was commonly isolated from cases of bacteraemia. This last finding is supported by another recent study performed in Japan which considered *A. caviae* as the most common species isolated from cases of *Aeromonas* bacteraemia with a mortality rate of 19% (Kimura *et al.*, 2013). However, the number of patients included in the latter study was low (n=36 in a 15 year period). Another study performed in Taiwan has investigated the clinical characteristics of monomicrobial *Aeromonas* bacteraemia in 154 patients during a study period of 8-years. Here the workers found out that *A. hydrophila* was the most frequently isolated species from cases of *Aeromonas* bacteremia followed by *A. veronii* biovar *sobria* (Chuang *et al.*, 2011). In addition, bacteraemia caused by *A. caviae* was less severe than that caused by the other two *Aeromonas* species, with the lowest mortality rate reported according to the clinical records revised in this particular study.

1.2.3.2. Role of *Aeromonas* in gastroenteritis

With regard to gastroenteritis, although *Aeromonas* species are closely linked to causing gastrointestinal infections, their role in this clinical condition has been considered as controversial. The main reasons for this consideration include the lack of reported outbreak of *Aeromonas* gastroenteritis caused by a single clone, as well as a failure to fulfil Koch's postulates (in both its conventional or molecular formats) to prove that *Aeromonas* is a true gastrointestinal pathogen (Janda *et al.*, 2010). In a study published in 1995, Hanninen and colleagues cultivated watery or slimy stool samples from 254 Finnish tourists who had diarrhoea following travel to Morocco (Hänninen *et al.*, 1995). *Aeromonas* species were isolated from 22 faecal samples (8.7%), however, it was only from 14 patients (5.5%) that *Aeromonas* was isolated as the sole pathogen. The diarrhoea in the 14 patients lasted from 2 to 20 days. Some, but not all, of the patients presented with symptoms like fever, nausea, or abdominal pain. The species involved in these cases were identified to be *A. caviae* and *A. veronii* biovar *sobria*, however, ribotyping studies revealed that the strains within each of the identified species had a unique ribotype, thus, an epidemiological link between the *Aeromonas* strains causing diarrhoea in this study was not determined.

Aeromonas species were isolated from four cases of acute diarrhoea in children at a hospital in Czech Republic (Krejci *et al.*, 2006). The main responsible agent was *A. caviae* and only one case was caused by *A. veronii* biovar *sobria*. The researchers found out that each of the isolated strains had a different ribotype and thus they could not determine an epidemiological link, however, they concluded that *Aeromonas* species should be considered as a true pathogen and that *A. caviae* is significantly associated with acute gastroenteritis in children under 1 year of age. Many other studies have as well considered *A. caviae* and *A. veronii* biotype *sobria* as the most frequently isolated *Aeromonas* species from screened cases of gastroenteritis in both adults and children in different geographical regions, estimating the prevalence of *Aeromonas* spp. in this clinical setting to be 1.6% to 2% (Vila *et al.*, 2003, Senderovich *et al.*, 2012).

Recently, a global enteric multicentre study which took place during a three year period has been published in the Lancet (Kotloff *et al.*, 2013). The study investigated the causative agents of diarrhoea in children aged 0-59 months in sub Saharan Africa and South East Asia. Loose stool samples were screened for enteric pathogens at the health centres participating in the study which were located in seven

countries. The number of patients enrolled in the study was 8549 children who had moderate to severe diarrhoea. *Aeromonas* species were considered as one of the significant enteric pathogens involved in children's diarrhoea, although the pathogen was confined to Asia and was not isolated from cases screened in sub Saharan Africa. *Aeromonas* species were considered, in this study, as important causative agents of gastroenteritis in children living in Mirzapur (Bangladesh) and Karachi (Pakistan). This study was just a screening study which did not provide any scientific evidence to consider *Aeromonas* as a true enteric pathogen. The study of Namdari and colleagues strongly supported the role played by *A. caviae* as a causative agent of diarrhoea in children aged from 1 week to 10 years (Namdari *et al.*, 1990). After screening more than a thousand watery stool samples for enteric pathogens, *A. caviae* was isolated from 14 specimens, *A. veronii* biotype *sobria* and *A. hydrophila* each was isolated from one faecal specimen. No other enteric pathogen was isolated with any *Aeromonas* strain. In addition to *A. caviae* being the most frequently isolated species in this study, all strains belonging to this genus were found capable of adhering to HEp-2 cells.

The studies reviewed above found no epidemiologic link between *Aeromonas* strains isolated from human diseases. In spite of this, and although *Aeromonas* species were sometimes isolated along with other pathogens, all published studies emphasized on the importance of the isolated *Aeromonas* species as the causative agents of diarrhoea given the clinical symptoms of the examined patients and the possible synergistic effect created in the presence of *Aeromonas* with other enteric pathogens in mixed infections rather than considering the isolated *Aeromonas* species as a transient colonizer due to its frequent isolation from water and food.

An important study which has been published recently presented evidence for *Aeromonas* spp. water to human transmission (Khajanchi *et al.*, 2010). The study provided a base for clonal relatedness studies which, when followed, will help in accurate determination of the epidemiologic relatedness among clinical and environmental isolates of *Aeromonas* species and thus will help in spotting the source of infection in cases of diarrhoeal outbreaks. The researchers believed that only a specific subset within each of the pathogenic *Aeromonas* species is actually capable of causing diseases to humans. As a result, a specific *Aeromonas* clone might predominate in an environment leading to repeated human infections. The study suggested the ability of *Aeromonas* to differentially express certain virulence genes only following their

transmission from the environment to the human host. Furthermore, the presence of a gene which encodes a specific virulence factor in an environmental strain should not be directly linked to this environment as the same detected gene might be better expressed by the same *Aeromonas* strain while being within the human host.

To prove their hypothesis, the group compared a number of *Aeromonas* stool and water isolates collected from different locations in the United States by performing three tests: (1) measurements of certain biochemical activities (haemolysis, cytotoxicity, proteolysis and *N*-Acyl homoserine lactone [AHL] production), (2) fingerprinting by pulsed-field gel electrophoresis (PFGE), and (3) detection of 11 virulence genes using specific probes.

The *A. hydrophila* group was identified as being the most prevalent group in water samples (59.5%) while *A. caviae*-*A. media* group was isolated from only 14.3% of the examined water samples. *A. veronii*-*A. sobria* group prevalence was determined to be 15.7% in the studied water samples. The prevalence of tested pathogenic *Aeromonas* species among the clinical samples, however, was different with *A. caviae*-*A. media* group being the most prevalent (71.6%), followed by *A. hydrophila* group which was isolated from 13.2% of the total clinical samples, and finally *A. veronii*-*A. sobria* group 5.6%.

Differences in biochemical activities were found among the studied *Aeromonas* isolates. The mean haemolytic activity of the *A. hydrophila* group isolated from clinical samples was 525.5 U, while that of *A. veronii*-*A. sobria* group clinical isolates was 854.5 U. A less haemolytic activity was detected in water isolates belonging to the same two groups. On the other hand, a very low haemolytic activity was detected in both the clinical and the water isolates of *A. caviae*-*A. media* group (less than 3 U). The authors considered *A. caviae* isolates as having no haemolytic activity. As in the case with haemolytic activity, the mean cytotoxic activity was higher in the clinical isolates than the water isolates of the *A. hydrophila* and *A. veronii*-*A. sobria* groups. The cytotoxic activity was measured to be 29,820 U and 19,516 U for *A. hydrophila* group and *A. veronii*-*A. sobria* group, respectively. Unlike the haemolytic activity, however, the cytotoxic activity among the *A. caviae*-*A. media* group was found to exist and was found to equal to 640.1 U in stool isolates compared to 254.8 U in water isolates.

A higher protease activity was noticed among the *A. caviae*-*A. media* stool isolates than the water isolates. The mean protease activity in *A. hydrophila* and *A. veronii-sobria* groups, however, was either higher in water isolates or equal in both water and stool isolates. However, the differences in protease activity between the clinical and environmental isolates for all studied *Aeromonas* groups were considered as statistically insignificant. Furthermore, a high level of AHL was produced by stool isolates belonging to the *A. hydrophila* and the *A. caviae*-*A. media* groups, whereas in *A. veronii*-*A. sobria* group AHL production was higher in water isolates.

Aeromonas strains were screened for the presence of virulence genes which can be used as identification markers for diarrhoea-associated pathogenic strains. The screening results revealed that more than 70% of water isolates and more than 90% of stool isolates in all studied groups possessed the virulence genes *dam* (DNA adenine methyltransferase), *gidA* (glucose-inhibited division A), and enolase. The group suggested that these three genes are important for *Aeromonas* species to survive in the environment and to cause human infection. In addition, the genes *alt* (encoding a heat-labile cytotoxic enterotoxin) and *dam* were more common in stool isolates belonging to the three studied groups than in water isolates. Furthermore, the gene *alt* was detected in more than 90% of the strains belonging to the two groups *A. caviae*-*A. media* and *A. hydrophila*, and in more than 60% of the *A. veronii*-*A. sobria* group. The group described the *alt* encoded enterotoxin as being a major virulence factor for gastroenteritis associated *Aeromonas* strains. Finally, the study found a high prevalence in T3SS genes (*aexU* and *ascV*) in both water and stool isolates belonging to *A. hydrophila* group as well as in water isolates of *A. veronii*-*A. sobria* group. No T3SS genes were detected in *A. caviae*-*A. media* isolates. As a result, the group suggested the involvement of the T3SS in the ability of *A. hydrophila* to cause human diarrhoea.

Khajanchi and colleagues performed PFGE and compared the generated profiles with the virulence signatures of the studied *Aeromonas* strains in order to determine the clonal relationships between these strains. They have found three sets of isolates, each set had a similar PFGE profile and possessed similar virulence genes. The strains within each set originated from both water and stool isolates. In total, the three sets contained seven strains: three strains in set 1, 2 strains in each of set 2 and set 3. All seven strains however were found to belong to *A. caviae*-*A. media* group, and they all harboured the virulence genes *alt*, *dam*, *gidA*, and enolase. The seven strains were found

to have no haemolytic or cytotoxic activities, however, five of them possessed a functional T6SS. This finding was considered by the authors as an evidence of *Aeromonas* water-to-human transmission.

The group emphasized on the necessity to be cautious when performing statistical analyses to detect the prevalence of certain traits. When the analysis was carried out in their study based on the source of samples, i.e., stool and water, the results showed a different trend than when performing the statistical analysis based on comparing the species followed by further dividing them to their sources. They explained that this is due to the Simpson's paradox (or the reversal of inequalities) which is causing a specific pattern to appear when separately analysing each of the *Aeromonas* species but giving a reversed pattern when the *Aeromonas* species under study are combined in one group. Thus, it is highly recommended to first correctly identify the isolates to the species level followed by studying their genotypic and phenotypic traits and finally discriminating between them taking their source in consideration.

They have considered the *Aeromonas* strains causing gastroenteritis to be able to spread from children with diarrhoea to the water through the sewage treatment system. After which the *Aeromonas* strains re-infect humans again by consumption of infected fish or by exposure to contaminated water. These diarrhoea causing strains are stable clonal lineages of the genus *Aeromonas* which have certain genotypic and phenotypic characteristics. This study attempted to determine some of the genotypic and phenotypic characteristics of seven *Aeromonas* isolates which were shown to have transmitted from water to humans in the US. Consequently, other studies which follow the same strategy used here and which use strains from different geographic locations are warranted to further understand *Aeromonas* pathogenesis.

1.2.4. Virulence factors of *Aeromonas* spp.

Within the *Aeromonas* genus a number of potential virulence factors have been proposed, the main ones of these are outlined below.

1.2.4.1. Resistance to antibiotics

The best study which has provided extensive antimicrobial susceptibility data for all known *Aeromonas* taxa (at the time of its publication) was performed by Kampfer and colleagues (Kampfer *et al.*, 1999). The study tested 217 *Aeromonas* strains

against all major antibiotics groups and found out that the majority of the tested strains showed different degrees of resistance to clindamycin (a lincosamide), clarithromycin (a macrolide), as well as to the penicillins: penicillin G, oxacillin, and amoxicillin. Furthermore, the aeromonads are now known to produce different classes of β -lactamases (Janda *et al.*, 2010). A recent study investigated the antibiotic resistance patterns among *Aeromonas* species isolated from drinking and waste water samples reported 88.9 % of nalidixic acid (a quinolone) resistance among *A. punctata* isolates (Figueira *et al.*, 2011). In the same study, *A. veronii* isolates showed more than 75% of resistance to the aminoglycoside streptomycin while also being significantly resistant to ticarcillin, a carboxypenicillin. In addition, *A. hydrophila* subsp. *hydrophila* and *A. punctata* isolates showed a resistance prevalence to the first generation cephalosporin cephalothin of 52% and 72.2%, respectively.

1.2.4.2. Capsule

The capsule is composed of polysaccharides and is located at the outermost layer of the bacterial cell which (Tomas, 2012). The location of the capsule makes it an important virulence factor being involved in resistance to both phagocytosis and complement-mediated serum killing, allowing the bacteria to survive in phagocytes, protecting the bacterial cell from desiccation, and facilitate adhesion of bacteria to host cells (Zhang *et al.*, 2003). The capsule assembly system in *E. coli* is well studied and it is considered a good representative for all other capsular assembly systems in Gram-negative bacteria (Zhang *et al.*, 2003). Capsules in *E. coli* have been divided to four groups and several studies have been published comparing the capsules in *Aeromonas* species to the capsules in *E. coli*. The capsule gene cluster in *A. hydrophila* strain PPD134/91 was studied and was found to be similar to the capsular group II type gene cluster of *E. coli*. The strain was described to belong to the serogroup O:18 (Zhang *et al.*, 2002). In *E. coli*, the genes for group II capsule type are divided to three regions. The genes in regions I and III are conserved (among the bacterial species with group II capsule type) and their products involved in capsule transport. Genes in region II, which function in capsule biosynthesis are, however, serotype specific (Zhang *et al.*, 2003). Genetic analysis of region II in 33 *A. hydrophila* strains revealed the existence of two types of group II capsules, IIA and IIB. The group IIA type of capsule was found in *A. hydrophila* serogroups O:18 and O:34, while *A. hydrophila* serogroups O:21 and O:27 were found to contain the group IIB type of capsule (Zhang *et al.*, 2003). Furthermore,

A. hydrophila serogroups O:11 and O:34 were found to produce a capsule when grown in glucose-rich medium (Martinez *et al.*, 1995). Other *Aeromonas* species which have been reported to produce a polysaccharide capsule include *A. veronii* biovar *sobria* serogroup O:11 (Tomas, 2012), and the fish pathogen *A. salmonicida* strain 80204-1 (Wang *et al.*, 2004), with the latter being grown on tryptic soy agar.

1.2.4.3. Lipopolysaccharide (LPS)

The lipopolysaccharides are embedded in the outer membrane of the Gram-negative bacteria, and are composed of lipid A, core oligosaccharide and O antigen. The surface-exposed LPS prevent not only phagocytosis but also killing of the bacteria by the complement system (Tomas, 2012).

1.2.4.4. Alpha-glucan

A surface α -glucan polysaccharide produced by the mesophilic *Aeromonas* strains has been suggested to play a significant role in biofilm formation by acting as a cement that helps in holding bacteria together within biofilms (Tomas, 2012).

1.2.4.5. The S-layer

The S-layer is the outermost layer of the cell envelope in many bacteria. The layer is composed of either a single protein or glycoprotein and has a significant role in bacterial pathogenicity being important for adhesion to host cells as well as for evasion of the host's immune system. *A. salmonicida* and some mesophilic *Aeromonas* strains have been shown to contain an S-layer (Tomas, 2012).

1.2.4.6. Iron-binding mechanisms

Iron availability is important for bacterial growth and for its pathogenesis, thus bacteria possess efficient mechanisms for iron uptake from both the environment as well as within the host (Tomas, 2012). These mechanisms are necessary due to the limited bioavailability of iron ion (Fe^{3+}) as it is being mostly bound to other compounds both in the environmental setting as well as within the human host (Kraemer, 2004). In addition, the limited bioavailability of iron is directly caused by the low solubility of the iron-bearing minerals as a result of their low rate of dissolution (Kraemer, 2004). *In vivo*, the iron is normally bound to a number of proteins, namely, haemoglobin, ferritin, lactoferrin, and transferrin which makes it little accessible for bacteria (Tomas, 2012). Thus, possession of iron acquisition mechanisms is considered one of the major virulence factors as the bacteria can't survive within their host without iron (Beaz-

Hidalgo *et al.*, 2013). *Aeromonas* species possess two complex mechanisms for iron uptake, namely, siderophore-dependent and siderophore-independent mechanisms (Tomas, 2012).

Siderophores are peptides of a low-molecular weight which bind to the iron ions with a high affinity (iron chelators) (Tomas, 2012). In his review, Kraemer summarized the process of iron uptake by siderophores in four steps: (i) siderophores synthesized by the cells under iron limiting conditions, (ii) the synthesized siderophores are secreted to the surrounding environment, (iii) binding of iron following complex processes to free the iron from the compounds/minerals to which it is bound, and (iv) uptake of ferric siderophores by the cells via a special transport system or dissociation of iron from the siderophore followed by its uptake (Kraemer, 2004). *Aeromonas* species are able to synthesize two types of siderophores which are encoded by two different gene sets, namely, the enterobactin siderophore (encoded by *aeb* genes) and amonabactin siderophore (encoded by *amo* genes) (Tomas, 2012). The enterobactin siderophore has been detected in other Gram-negative bacteria, however, the amonabactin siderophore is unique to *Aeromonas* species (Tomas, 2012, Beaz-Hidalgo *et al.*, 2013).

Within the human host, iron bound to haemoglobin is difficult to obtain by *Aeromonas* cells using their siderophore-dependent mechanisms. The *Aeromonas* cells do, however, synthesize haem-binding proteins which help the bacterial cells, through a complex mechanism, to acquire iron following its removal from haemoglobin. This mechanism of iron acquisition is referred to as the siderophore-independent mechanism (Beaz-Hidalgo *et al.*, 2013).

1.2.4.7. Exotoxins

When bacterial cells produce exotoxins which specifically affect intestinal epithelial cells, these exotoxins are generally referred to as enterotoxins. *Aeromonas* species (many of which are involved in diarrhoea) are able to produce and release several potent enterotoxins. The enterotoxins produced by the aeromonads have been divided to two categories, namely, the cytotoxic (cytolytic) and the cytotoxic enterotoxins. Each of these categories has a different mechanism of action within the human host (Tomas, 2012).

The cytotoxic enterotoxins were found to be involved in enterotoxicity, cytotoxicity, as well as haemolysis (Tomas, 2012). A well-studied example of the cytotoxic enterotoxins is the toxin protein (Act) produced by *A. hydrophila* SSU (Ferguson *et al.*, 1997). The mechanism of action of the toxin protein Act has been described as a pore-forming mechanism which basically means that the toxin oligomerizes to form pores in the membranes of the human host cells leading to cell lysis as a result of swelling of cells following water entry (Ferguson *et al.*, 1997). Act has as well been found to have immune-modulatory effects while attacking the host's epithelial cells leading to high fluid secretion and host-induced tissue damage (Tomas, 2012).

Another important toxin produced by *A. hydrophila* is the pore forming Aerolysin (Bernheimer *et al.*, 1974) which has been described in some papers as a haemolysin while described in others as a synonym of the cytotoxic enterotoxin Act, thus creating a confusing status of the Aerolysin toxin. Chopra and Houston, however, emphasized that Act is better described as an Aerolysin-like molecule and that Act and Aerolysin are different in the following aspects: (i) the amino acid sequence of Act was found to be different from that of Aerolysin (ii) cholesterol was determined as a receptor for the Act toxin but not for the Aerolysin toxin (iii) unlike Aerolysin, Act toxin was unable to bind to glycophorin, the membrane spanning protein present in the red blood cells (Buckley *et al.*, 1999). The detailed mechanism of pore formation by Aerolysin has recently been described by Bucker and colleagues who presented a model which describes the binding of the proaerolysin to the cells, its oligomerization to form a heptameric β -barrel pore, and the detailed cellular response to such binding and pore formation leading eventually to a leak flux (Bucker *et al.*, 2011). Through their model the group were able to explain the mechanism of action of the produced Aerolysin in the infected host cells which eventually can lead to either diarrhoea or defective wound closure.

Two cytotoxic enterotoxins have been identified in *Aeromonas* species, the first one is a heat-labile toxin referred to as Alt (Chopra *et al.*, 1996) and the second one is the heat-stable Ast toxin (Chopra *et al.*, 1994). Both toxins were tested at 56°C for 20 minutes and both were identified in the diarrhoeal isolate SSU of *A. hydrophila*. When *A. hydrophila* gets into the host intestinal tract, it produces the Alt and Ast enterotoxins both of which cause the intestinal epithelial cells to produce high levels of 3'-5'-cyclic

adenosine monophosphate (cAMP) resulting in fluid accumulation, i.e., diarrhoea (Chopra *et al.*, 1996). In addition, the Alt toxin was as well able to induce elevated levels of the prostaglandin E₂ (PGE₂), which consequently induces diarrhoea (Chopra *et al.*, 1996). Furthermore, the Ast toxin was found to cause elongation in the Chinese hamster ovary (CHO) cells (Chopra *et al.*, 1994). Finally, *Aeromonas* species were also found to be able to produce various haemolysins, namely, HlyA, Ahh1, and Asa1 (Bucker *et al.*, 2011).

1.2.4.8. Extracellular enzymes

Proteolysis of proteins and hydrolysis of gelatin in host tissues can be done, respectively, by proteases and gelatinases produced by *Aeromonas* species. During the pathogenic process of *Aeromonas*, cleavage of the phosphodiester bonds within nucleic acids can be accomplished by the production of nucleases, and the breakdown of cellular lipids is achieved by the production of lipases. Other extracellular enzymes produced by *Aeromonas* species include amylases and chitinases (Tomas, 2012).

1.2.4.9. Type II, III and VI protein secretion systems

It is well known that there are six different types of secretion systems produced by the Gram negative bacteria which have a direct role in bacterial virulence. Although these secretion systems are highly conserved among Gram-negative bacteria, they, however, do possess certain characteristics (see below) which help in differentiating them from one another (Suarez *et al.*, 2008). The main function of these diverse secretion systems is to deliver specific effector proteins produced by the bacterial cells directly to the cytoplasm of the host cells after which the effector proteins will exert their powerful pathogenic actions within host cells which can include activation of signalling cascades, causing cytoskeletal changes, and immunomodulation (Fadl *et al.*, 2006, Tseng *et al.*, 2009). Principally, the effectors are translocated across the inner and outer membrane of the Gram-negative bacteria in either a single step (via the T1SS, T3SS, T4SS, and T6SS) or in two steps (T2SS, T5SS, and less commonly, T1SS, T4SS). The two steps involves first the use of either the general secretion Sec-pathway or the two-arginine (Tat) pathway to export the effector proteins to the periplasmic space followed by their translocation across the outer membrane via one of the secretion systems described above (Tseng *et al.*, 2009).

Generally, the T2SS is composed of an outer membrane translocation pore, pseudopilin subunits located in the periplasm, inner membrane subunits, and finally an intracellular ATPase which provides the necessary energy for the proper functioning of the apparatus (Tseng *et al.*, 2009). The T2SS has been well characterized in *Aeromonas* species (Schoenhofen *et al.*, 2005, Li *et al.*, 2011a, Strozen *et al.*, 2011). The effector proteins which have been found to be secreted via the T2SS in *Aeromonas* include the cytotoxic enterotoxin Act (described above) (Fadl *et al.*, 2006) and the Aerolysin (Strozen *et al.*, 2011).

The T3SS in *Aeromonas* has been well-studied, particularly in strains belonging to *A. hydrophila* and *A. salmonicida* (see below). The T3SS in *Aeromonas* was found to be composed of a needle-like structure referred to as an injectisome which allows the bacterial cells to inject their effector proteins into host cells via the translocation pore located at the tip of the needle (Fadl *et al.*, 2006, Tseng *et al.*, 2009). The injectisome, which is the hallmark of this secretion system, is connected to several basal rings located in both the inner and the outer membranes of the bacterial cell, and an ATPase is located at the base of the apparatus to provide energy for the secretion process (Tseng *et al.*, 2009). Furthermore, the T3SS shares structural and sequence similarities with bacterial flagella, thus, suggesting an evolutionary relationship (Blocker *et al.*, 2003). Genes of the T3SS were detected in clinical isolates of *A. hydrophila*, *A. veronii*, and *A. caviae*, with their incidence in *A. caviae* being much lower than in the other two *Aeromonas* species (Chacon *et al.*, 2004). More importantly, the complete DNA sequence of the T3SS gene cluster in *A. hydrophila* AH-3 has been published (Vilches *et al.*, 2004). The cluster was found to comprise 35 genes. Furthermore, a functional T3SS has been described for the psychrophilic species *A. salmonicida* (Burr *et al.*, 2002). Four T3SS effector proteins have been identified so far in the fish pathogen *A. salmonicida*, these include AexT, AopP, AopH, AopO (Vilches *et al.*, 2009). In *A. hydrophila*, on the other hand, two T3SS effector proteins have been identified, namely, AexT and AexU (Vilches *et al.*, 2009). Both AexT and AexU have been described as ADP-ribosylating toxins (Suarez *et al.*, 2008, Vilches *et al.*, 2008). The detailed mechanism of action of AexU toxin has recently been published (Sierra *et al.*, 2010). In Sierra and colleagues study, the AexU effector protein was found to inhibit bacterial phagocytosis, induce host cell apoptosis, and stimulate overproduction of cytokines and chemokines. In the same study, a high death rate was observed among

infected mice when they were challenged with AexU. Vilches and colleagues have investigated the relationship between the T3SS and the flagella in *A. hydrophila* AH-3 (Vilches *et al.*, 2009). Since *A. hydrophila* AH-3 is one of the mesophilic aeromonads which possess two types of flagellar systems, namely the polar (for swimming) and lateral (for swarming) flagellar systems (see below), the researchers investigated the crosstalk between the T3SS and both types of flagella in *A. hydrophila* AH-3. The crosstalk investigation was performed by checking the promoter activity of the two genes *aopN* (translocation regulator) and *aopB* (translocation apparatus) encoded in the T3SS operon as well as the promoter activity of the T3SS effector *AexT* in strains with different background mutations in which the biosynthesis and assembly of both the polar and the lateral flagella were affected. The group found out that the activity of the two tested promoter regions have decreased in *A. hydrophila* AH-3 mutant with defects in the polar flagellar system, but the activity of the tested promoters was not affected when the master regulator of the lateral flagellar operon was knocked out. Their findings indicate a positive cross talk between the T3SS and the polar flagellar system (but not the lateral flagellar system) in *A. hydrophila* AH-3. In the same study, however, neither the overexpression of the T3SS transcriptional activator AxsA nor the deletion of its gene *axsA* in *A. hydrophila* AH-3 showed any effect in the ability of the tested strain to swim or swarm. In another study, however, a relationship between the lateral flagellar system of *A. hydrophila* and its T3SS was clearly demonstrated using both a different strain, *A. hydrophila* AH-1, and different laboratory growth condition (Yu *et al.*, 2007). Thus, it seems clear that crosstalk does exist between the T3SS of *Aeromonas* species and both of their polar and lateral flagellar systems. The crosstalk between the two systems, however, shows intra-species differences and might be affected by the surrounding environmental factors (Vilches *et al.*, 2009).

The T6SS is a recently discovered secretion system which its machinery seems to resemble that of the T3SS except for a T4 phage tail spike-like injectisome (Tseng *et al.*, 2009). Bioinformatic analysis indicated the existence of the T6SS gene cluster in many Gram-negative bacteria, however, the role of T6SS in virulence and the detailed mechanism of protein secretion by this system are still largely unknown (Suarez *et al.*, 2008). Based on the limited available studies concerned with the T6SS in different bacteria, a model was recently proposed for the T6SS which includes a channel extending from the inner to the outer membrane of the bacterial cell, a needle which has

a pore forming protein at its tip, and a chaperone with an ATPase activity located in the cytoplasm of the bacterial cell (Tseng *et al.*, 2009). The clinical strain *Aeromonas hydrophila* SSU has been reported recently to possess a functional T6SS (Suarez *et al.*, 2008). In addition, the environmental isolate *A. hydrophila* ATCC 7966 has also been reported to carry the T6SS gene cluster. The T6SS effectors which have recently been identified in bacteria include the haemolysin coregulated protein (Hcp) and the valine glycine repeat G (VgrG) family of proteins (Sha *et al.*, 2013). In fact, Hcp and VgrG, seem not only to act as effectors, but are themselves considered to be structural components of the T6SS (Sha *et al.*, 2013). They seem to protrude from the bacterial surface forming a pilus-like structure in which the Hcp forms the tube while the VgrG both punctures the host cell and also act as an effector through its C-terminal domain (Pukatzki *et al.*, 2009). These effectors have been previously identified and studied in *P. aeruginosa* and *V. cholerae* (Suarez *et al.*, 2008), however, a recent study have investigated the roles played by Hcp and VgrG paralogues in the SSU clinical strain of *A. hydrophila* (Sha *et al.*, 2013). Although the exact mechanism by which these two paralogues function in *A. hydrophila* is not yet clear, Sha and colleagues demonstrated an effect on the ability of *A. hydrophila* to swim and form a biofilm following deletion of the genes encoding the Hcp and VgrG and even suggested the two effectors to play a regulatory role in the expression of genes involved in both motility and biofilm formation in *A. hydrophila* SSU. Furthermore, a proteomic analysis of the VgrG effector protein present in both *A. hydrophila* SSU and *A. hydrophila* ATCC 7966 was previously performed (Suarez *et al.*, 2010a). Out of the known members of the VgrG family, Suarez and colleagues specifically determined the toxin to be a VgrG1 with an actin ADP-ribosylating activity which have caused apoptosis in the used HeLa Tet-Off cell lines. The authors indicated that the VgrG1 in both *A. hydrophila* ATCC 7966 and *V. cholerae* showed a 55% sequence homology in their NH₂-terminal domains and that both were able to induce a rounded-cell phenotype, each with a different mechanism. The researchers suggested the *A. hydrophila* T6SS-effector VgrG1 to play a significant role in *A. hydrophila*-caused gastroenteritis as it could induce actin depolymerisation within infected intestinal epithelial cells. Finally, the role of the secreted form of Hcp, the T6SS effector in *A. hydrophila* has recently been investigated (Suarez *et al.*, 2010b). Suarez and colleagues, demonstrated that Hcp has immunomodulatory effects within the host which include its binding to macrophages, resulting in the prevention of phagocytosis, and its trigger of the production of the cytokines IL-10 and TGF- β , which

results in inefficiency of host immune cells recruitment due to these cytokines being immunosuppressive.

1.2.4.10. Pili

Pili (short appendages made up of the protein pilin) do exist in large numbers on the surface of many Gram-negative bacteria. Some *Aeromonas* species have been reported to possess type IV pili which is the type of pili involved in three main processes in Gram negative bacteria, namely, adhesion to host epithelial cells, twitching motility, and biofilm formation (Tomas, 2012). Type IV pili are mainly described in gastroenteritis-causing strains of *Aeromonas* species (Hadi *et al.*, 2012). Based on their N-terminal amino acid sequences and their molecular weights, the type IV pili in *Aeromonas* species can be divided to two distinct families, namely, the bundle-forming pili (Bfp) and the Type IV *Aeromonas* Pili (Tap) (Hadi *et al.*, 2012). Studying the *Aeromonas* clinical strains isolated from cases of human diarrhoea revealed that the Tap pili don't seem to have a significant role in the initial stage of colonization (the first and most important step for causing gastroenteritis) while the Bfp seem to have a crucial role in human gastroenteritis, being purified from all studied *Aeromonas* strains isolated from these cases (Kirov *et al.*, 2000). Recently, the genetic characterization of the Bfp of the mesophilic *Aeromonas veronii* bv. Sobria has been published (Hadi *et al.*, 2012). In the study of Hadi and colleagues, the Bfp locus was found to contain 17 pilus-related genes. Mutations in each of the encoded genes of this locus resulted in a great reduction in the ability of the studied strain to adhere to HEp-2 cells and to form biofilms in borosilicate glass tubes. Searching for homology to the studied gene cluster revealed a similarity to the surface pilus produced by *Vibrio cholerae* El Tor and which is referred to as mannose-sensitive hemagglutinin (MSHA).

1.2.4.11. Flagella

1.2.4.11.1. Types of flagella possessed by *Aeromonas* species

Mesophilic *Aeromonas* species are well known to constitutively express a single polar unsheathed flagellum when grown in any culture condition (Canals *et al.*, 2006a). Furthermore, around 50 to 60% of the mesophilic aeromonads are able to express many peritrichous lateral flagella (in addition to their ability to express the single polar flagellum) when grown on surfaces or in viscous environments (Canals *et al.*, 2006a), i.e., an inducible lateral flagellar system (Merino *et al.*, 2006).

These two distinct flagellar systems in *Aeromonas* species are encoded by two different gene sets designated (*fla*) for the polar system and (*laf*) for the lateral system (Rabaan *et al.*, 2001, Gavín *et al.*, 2002). The main function of the single polar flagellum is to allow the aeromonads to swim in liquid environments while the peritrichous lateral flagella help them to swarm as a group over surfaces (Kirov *et al.*, 2002). The flagellated bacteria, in general, are known to express only one type of the several well-known flagellar systems. They can express a single polar flagellum and be described as monotrichous bacteria, or can express many flagella with different arrangements over their surfaces, i.e., amphitrichous, lophotrichous, and peritrichous lateral flagella, with the later type being an uninduced system as seen for example in *Proteus mirabilis*, *E. coli*, and *Salmonella enterica* (Merino *et al.*, 2006). However, the unique property possessed by some of the mesophilic *Aeromonas* species is that they are able to express two distinct flagellar systems, as discussed below.

1.2.4.11.2. Evidence for the possession of two distinct flagellar systems by mesophilic *Aeromonas* species.

Gavín and colleagues performed a study in which they have clearly demonstrated the ability of both *A. caviae* Sch3N and *A. hydrophila* AH-3 to produce two different types of flagella (Gavín *et al.*, 2002). Following growing the two species in broth and on agar, the group visualized the flagella expressed in each of the two growth conditions using electron microscopy and found both species being able to express a single polar flagellum when grown in brain heart infusion broth (BHIB) and able to express multiple lateral flagella when grown on tryptic soy agar (TSA). The workers have then applied mechanical shearing to dissociate the two types of flagella followed by purification of the flagellin proteins formed during growth of the bacteria in broth and on agar. When the purified flagellin proteins were run on SDS-PAGE two flagellin protein bands were visualized: a large band (35.5 kDa) and a small band (31.5 kDa). The large band was obtained when both *Aeromonas* species were grown in broth and solid media (constitutive expression) while the small band was only obtained following growing them on solid media (induced expression). Comparing the N-terminal amino acid sequence of the larger protein to the database indicated a similarity to the *A. caviae* polar flagellin previously studied by the same group while comparing the N-terminal amino acid sequence of the small protein to other bacteria showed a high

homology to the lateral flagellin of *Vibrio parahaemolyticus*. These findings crucially indicate the existence of a dual flagella system in *Aeromonas* species.

1.2.4.11.3. Other bacteria which possess two flagellar systems

The number of bacterial species which possess a dual flagellar system is limited and include, in addition to *Aeromonas* (Shimada *et al.*, 1985), *V. parahaemolyticus* (Shinoda *et al.*, 1977) which causes human gastroenteritis and which its dual flagellar system has been extensively studied, the wound infections-causing *V. alginolyticus* (Kawagishi *et al.*, 1995), the enteric pathogen *Plesiomonas shigelloides* (Inoue *et al.*, 1991) and the three clinically non-significant species *Helicobacter mustelae* (O'Rourke *et al.*, 1992), *Azospirillum brasilense* (Hall *et al.*, 1983), and *Rhodospirillum centenum* (McClain *et al.*, 2002) (table 1.2). In addition, Ren and colleagues have described a new locus (gene cluster) in *E. coli* 042 which they have called Flag-2 and which they have suggested to encode a novel flagellar system in *E. coli* 042 that is highly similar to the lateral flagellar system in *Aeromonas* and *Vibrio* (Ren *et al.*, 2005). The process of synthesizing flagella by any bacterial cell requires a large number of cellular resources and a high amount of energy (i.e., metabolically costly). Consequently, flagella synthesis is a highly regulated process in bacteria (Gavín *et al.*, 2002, Merino *et al.*, 2006).

Table 1.2. Bacterial species known to possess two distinct flagellar systems

Species	Reference
<i>Aeromonas</i> spp.	Shimada <i>et al.</i> , 1985
<i>Azospirillum brasilense</i>	Hall <i>et al.</i> , 1983
<i>Helicobacter mustelae</i>	O'Rourke <i>et al.</i> , 1992
<i>Plesiomonas shigelloides</i>	Inoue <i>et al.</i> , 1991
<i>Rhodospirillum centenum</i>	McClain <i>et al.</i> , 2002
<i>Vibrio alginolyticus</i>	Kawagishi <i>et al.</i> , 1995
<i>Vibrio parahaemolyticus</i>	Shinoda <i>et al.</i> , 1977

1.2.4.11.4. *Aeromonas* polar flagellar system

Genes involved in the synthesis and regulation of the single polar flagellum of both *A. caviae* Sch3N (Rabaan *et al.*, 2001, Kirov *et al.*, 2004) and *A. hydrophila* AH-3 (Rabaan *et al.*, 2001, Altarriba *et al.*, 2003, Canals *et al.*, 2006b) have been identified.

According to the above three studies, the polar flagellar genes in *A. caviae* Sch3N and *A. hydrophila* AH-3 are located in five non-contiguous chromosomal regions, as shown in figure 1.1. The three studies isolated different genetic regions in the two indicated *Aeromonas* species and then performed extensive sequence analysis detecting regulatory regions, e.g., promoter sequences and transcription terminators. The three studies also compared the nucleotide and amino acid sequences to the database to predict the functions of the isolated genes in the five regions. Such comparison showed similarities to gene sequences in other bacteria and allowed the authors to predict genes functions (table 1.3).

Genes functions were also predicted based on extensive studies performed by the same research groups which included the generation of mutants followed by studying the mutant strains by some or all of the following assays/techniques: motility assays, biofilm assay, adherence to HEp-2 cells, detection of flagella production by transmission electron microscope (TEM), assessment of flagellin protein expression, and complementation studies.

The first identified region was region 2 by Rabaan and colleagues who have isolated and described in detail five contiguous polar flagellum genes in *A. caviae* Sch3N, namely, *flaA*, *flaB*, *flaG*, *flaH*, *flaJ* (Rabaan *et al.*, 2001). These genes were named by the author as their homologs in *V. parahaemolyticus* and *A. salmonicida*. Of notable importance in the study of Rabaan and co-workers is the finding that the polar flagellum filament is made up of two flagellin proteins, FlaA and FlaB (Rabaan *et al.*, 2001). The same polar flagellar region 2, however, in *A. hydrophila* AH-3 was identified and studied by Canals and colleagues who, in addition to the above five ORFs, identified a sixth ORF which they have referred to as *maf-1* (for modification accessory factor or motility accessory factor) (Canals *et al.*, 2006b). Parker and colleagues have recently suggested the Maf-1 protein in *A. caviae* to help in assembly of the polar flagellum by acting as a glycosyltransferase enzyme which catalyzes the addition of the sugar pseudaminic acid to the polar flagellin proteins (Parker *et al.*, 2012).

Chromosomal polar flagellar region 1 was studied in *A. hydrophila* AH-3 by Altarriba and colleagues (Altarriba *et al.*, 2003). The identified locus was referred to as the *flg* region and was found to contain a total of 16 ORFs named as their homologs in

V. parahaemolyticus. The identified genes were predicted to have structural, chemotactic, and regulatory functions. Altarriba and colleagues have determined the distribution of the *flg* genes in mesophilic *Aeromonas* species (other than *A. hydrophila* AH-3) using the dot blot hybridization technique. Their results indicated the presence of the *flg* genes in *A. caviae* Sch3N and *A. veronii* bv. *sobria* AH-1.

The other three chromosomal polar flagellar regions (3, 4, and 5) in *A. hydrophila* AH-3 were described in detail by Canals and colleagues (Canals *et al.*, 2006b). The authors found region 3 in *A. hydrophila* AH-3 to contain 29 ORFs. Sequence analysis of the detected ORFs revealed their similarity to proteins in other bacteria, namely, *Vibrio parahaemolyticus*, *V. vulnificus*, *Shewanella oneidensis*, *Photobacterium profundum*, *Pseudomonas aeruginosa*, *Pseudomonas putida*, and *Pseudomonas syringae*. The homologous proteins in other bacteria were found to be involved in polar flagellum biogenesis and assembly as well as in chemotaxis. Consequently, Canals and colleagues have nominated the detected ORFs in *A. hydrophila* AH-3 with similar names as in the other above mentioned bacteria and predicted them to have the same functions.

Only one ORF was detected in polar flagellum chromosomal region 4 in *A. hydrophila* AH-3 (Canals *et al.*, 2006b). The sequence of the detected ORF was found to be similar to the sequence of a sodium derived flagellar motor protein, referred to as MotX, in *Vibrio* species. Canals and colleagues have determined the sequence similarity between MotX in *A. hydrophila* and that in *V. alginolyticus* to be equal to 54%.

Lastly, Canals and co-workers have identified three ORFs composing the polar flagellar region number 5 in the chromosome of *A. hydrophila* AH-3 which they have named *flrA*, *flrB*, and *flrC* (Canals *et al.*, 2006b). Canals and colleagues have predicted the functions of the three ORFs to be regulatory proteins based on finding their sequence homologs in the database. FlrA and FlrB were showing 53% and 40% identity, respectively, to their homologs in *V. cholerae*, while FlrC was showing 58% sequence identity to its homolog in *V. fischeri*.

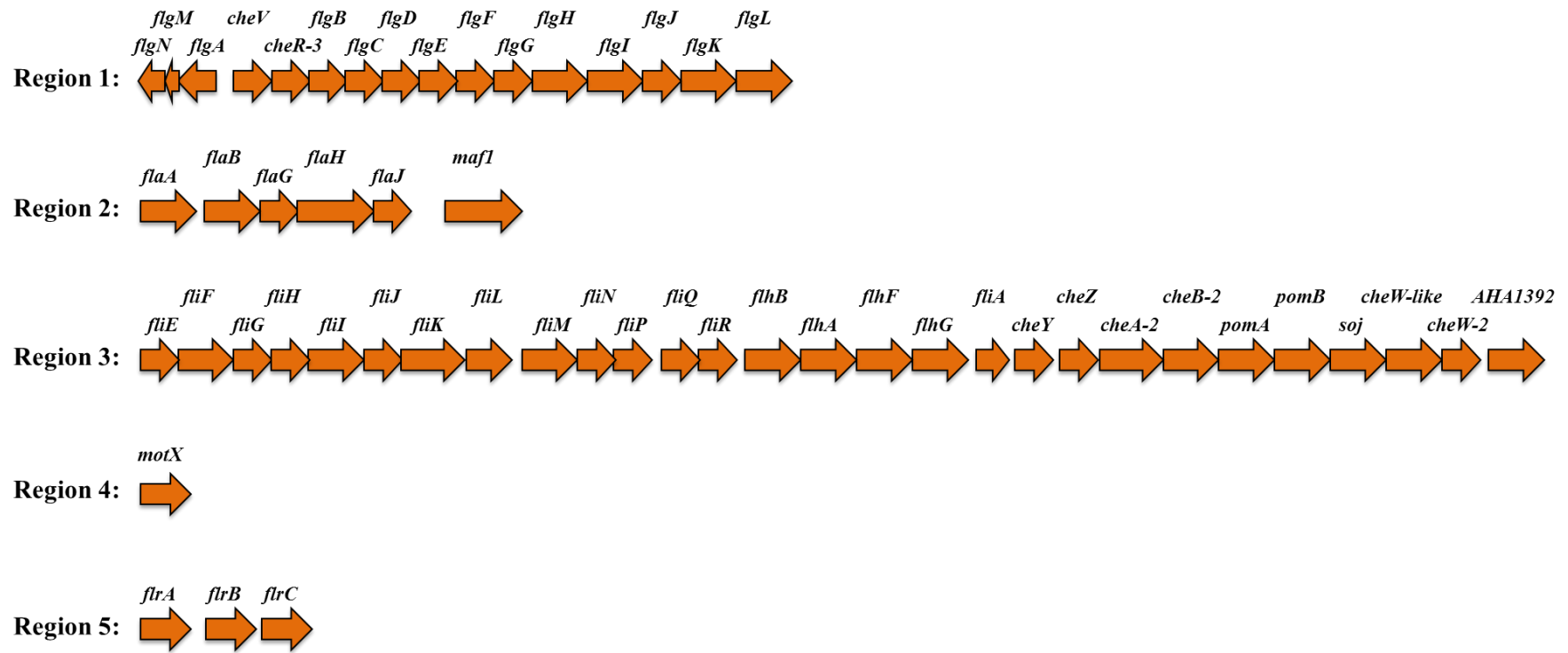


Figure 1.1. The five chromosomal regions containing the polar flagellar genes of *A. caviae* Sch3N, based on information provided by Dr. Jon Shaw. The figure shows the identified ORFs in each of the chromosomal regions with their transcriptional direction.

Table 1.3. *A. caviae* Sch3N polar flagellar genes with their predicted function

Gene name	Predicted function	Speceis containing homologous genes
<u>Region 1:</u>		
<i>flgN</i>	Potential chaperone	<i>Vibrio parahaemolyticus</i>
<i>flgM</i>	Negative regulation of flagellar synthesis	<i>V. parahaemolyticus</i> / <i>V. cholerae</i>
<i>flgA</i>	Necessary for P-ring addition	<i>V. parahaemolyticus</i>
<i>cheV</i>	Chemotaxis CheY/CheW hybrid	<i>V. parahaemolyticus</i> / <i>V. cholerae</i>
<i>cheR</i>	Chemotaxis protein methyltransferase	<i>V. parahaemolyticus</i> / <i>V. cholerae</i> / <i>V. anguillarum</i>
<i>flgB</i>	Flagellar basal-body rod protein	<i>V. parahaemolyticus</i> / <i>V. cholerae</i> / <i>Pseudomonas aeruginosa</i>
<i>flgC</i>	Flagellar basal-body rod protein	<i>V. parahaemolyticus</i> / <i>V. cholerae</i> / <i>Pseudomonas aeruginosa</i>
<i>flgD</i>	Basal-body rod modification protein	<i>V. parahaemolyticus</i> / <i>V. cholerae</i> / <i>Pseudomonas aeruginosa</i>
<i>flgE</i>	Flagellar hook protein	<i>V. parahaemolyticus</i> / <i>V. cholerae</i> / <i>Pseudomonas aeruginosa</i>
<i>flgF</i>	Flagellar basal-body rod protein	<i>V. parahaemolyticus</i> / <i>V. cholerae</i> / <i>Pseudomonas aeruginosa</i>
<i>flgG</i>	Flagellar basal-body rod protein	<i>V. parahaemolyticus</i> / <i>V. cholerae</i> / <i>Pseudomonas aeruginosa</i>
<i>flgH</i>	Flagellar L-ring protein	<i>V. cholerae</i> / <i>Pseudomonas aeruginosa</i> / <i>Yersinia pestis</i>
<i>flgI</i>	Flagellar P-ring protein precursor	<i>V. parahaemolyticus</i> / <i>V. cholerae</i> / <i>Pseudomonas aeruginosa</i>
<i>flgJ</i>	Peptidoglycan hydrolase	<i>V. parahaemolyticus</i> / <i>V. cholerae</i>
<i>flgK</i>	Flagellar hook-associated protein type 1	<i>Pseudomonas aeruginosa</i>
<i>flgL</i>	Flagellar hook-associated protein type 3	<i>V. parahaemolyticus</i> / <i>V. cholerae</i> / <i>Pseudomonas aeruginosa</i>

Table 1.3. to be continued on the next page

Table 1.3 (continued). *A. caviae* Sch3N polar flagellar genes with their predicted function

Gene name	Predicted function	Speceis containing homologous genes
<u>Region 2:</u>		
<i>flaA</i>	Polar flagellin	<i>Aeromonas salmonicida</i>
<i>flaB</i>	Polar flagellin	<i>A. salmonicida</i>
<i>flaG</i>	Filament length control	<i>A. salmonicida</i>
<i>flaH</i>	HAP-2	<i>A. hydrophila AH-3</i>
<i>flaJ</i>	Chaperone protein that facilitates flagellin export	<i>A. hydrophila AH-3</i>
<i>maf1</i>	Modification (or motility) accessory (or associated) factor 1 for post-translational glycosylation of flagellin proteins	<i>Campylobacter jejuni</i>
<u>Region 3:</u>		
<i>fliE</i>	MS-ring/ rod adaptor	<i>Vibrio vulnificus</i>
<i>fliF</i>	M-ring	<i>Shewanella oneidensis</i>
<i>fliG</i>	Switch	<i>S. oneidensis</i>
<i>fliH</i>	Export / assembly	<i>Photobacterium profundum</i>
<i>fliI</i>	Export ATP synthase	<i>V. parahaemolyticus</i>
<i>fliJ</i>	Export / assembly	<i>Pseudomonas syringae</i>
<i>fliK</i>	Hook length	<i>V. parahaemolyticus</i>
<i>fliL</i>	Flagellar protein	<i>Photobacterium profundum</i>
<i>fliM</i>	Switch	<i>Photobacterium profundum</i>
<i>fliN</i>	Switch	<i>Photobacterium profundum</i>
<i>fliP</i>	Export/ assembly	<i>V. parahaemolyticus</i>
<i>fliQ</i>	Export/ assembly	<i>V. vulnificus</i>
<i>fliR</i>	Export/ assembly	<i>S. oneidensis</i>

Table 1.3. to be continued on the next page

Table 1.3 (continued). *A. caviae* Sch3N polar flagellar genes with their predicted function

Gene name	Predicted function	Speceis containing homologous genes
<u>Region 3 (continued):</u>		
<i>flhB</i>	Export/ assembly	<i>S. oneidensis</i>
<i>flhA</i>	Export/ assembly	<i>S. oneidensis</i>
<i>flhF</i>	Polar flagellar site determinant	<i>V. vulnificus</i>
<i>flhG</i>	Flagellar number regulator	<i>S. oneidensis</i>
<i>fliA</i>	σ^{28}	<i>S. oneidensis</i>
<i>cheY</i>	Chemotaxis	<i>S. oneidensis</i>
<i>cheZ</i>	Chemotaxis	<i>S. oneidensis</i>
<i>cheA-2</i>	Chemotaxis	<i>Photobacterium profundum</i>
<i>cheB-2</i>	Chemotaxis	<i>V. vulnificus</i>
<i>pomA</i>	Redundant stator protein involved for polar flagellum rotation	<i>Pseudomonas aeruginosa (motA)</i>
<i>pomB</i>	Redundant stator protein involved for polar flagellum rotation	<i>Pseudomonas putida (motB)</i>
<i>soj</i>	Unknown	<i>Photobacterium profundum</i>
<i>cheW-like</i>	Chemotaxis	<i>V. parahaemolyticus</i>
<i>cheW-2</i>	Chemotaxis	<i>V. parahaemolyticus</i>
<i>AHA1392</i>	Unknown	<i>Photobacterium profundum</i>
<u>Region 4:</u>		
<i>motX</i>	Stator	<i>V. alginolyticus</i>
<u>Region 5:</u>		
<i>flrA</i>	Flagellum regulator	<i>V. cholerae</i>
<i>flrB</i>	Two-component sensor kinase	<i>V. cholerae</i>
<i>flrC</i>	Two-component response regulator	<i>V. parahaemolyticus (flaM)</i>

Information provided in this table is based on the studies of Rabaan and colleagues (Rabaan *et al.*, 2001), Altarriba and colleagues (Altarriba *et al.*, 2003), and Canals and colleagues (Canals *et al.*, 2006b).

1.2.4.11.5. *Aeromonas* lateral flagellar system

Unlike the polar flagellar genes which are located in different regions within the chromosome of *Aeromonas* species, the lateral flagellar genes of *A. caviae* and *A. hydrophila* are located in a single chromosomal region (personal communication with Dr. Jon Shaw). Different lateral flagellar genes within this single chromosomal region have been studied in *A. caviae* Sch3N (Gavín *et al.*, 2002) and in *A. hydrophila* AH-3 (Gavín *et al.*, 2002, Canals *et al.*, 2006a). The DNA and amino acid sequence analyses performed in these studies indicated that most, but not all, of the detected ORFs are similar to the lateral flagellar genes in *V. parahaemolyticus*, and as a result, the detected ORFs in *Aeromonas* species were given the same names of their homologs in *V. parahaemolyticus* and the few other bacteria.

Gavin and colleagues have studied the lateral flagellin loci (in which the lateral flagellin protein is encoded) in both *A. caviae* Sch3N and *A. hydrophila* AH-3 (Gavín *et al.*, 2002). They have identified four open reading frames and nine ORFs in the locus of *A. caviae* Sch3N and the locus of *A. hydrophila* AH-3, respectively. The four genes identified in the lateral flagellin locus of *A. caviae* Sch3N were designated *lafA1*, *lafA2*, *lafB*, and *fliU* and the nine ORFs included in the lateral flagellin locus of *A. hydrophila* AH-3 were designated as *lafA*, *lafB*, *lafC*, *lafX*, *lafE*, *lafF*, *lafS*, *lafT*, and *lafU* (Gavín *et al.*, 2002).

Following the study of Gavin and colleagues, Canals and co-workers have published an extensive study on the lateral flagellar system in *A. hydrophila* AH-3 which provided a complete description of the lateral flagellar operon in *A. hydrophila* AH-3 (Canals *et al.*, 2006a). The study described five additional lateral flagellar gene clusters (29 ORFs) within the single *laf* operon other than the lateral flagellin locus described earlier by Gavin and colleagues, which makes the total number of gene clusters constituting the lateral flagellar region in *A. hydrophila* AH-3 equal to six (38 ORFs). As with the above described nine ORFs, most of the 29 ORFs showed high homology to genes within the lateral flagellar system of *V. parahaemolyticus* (with few exceptions) and thus were designated by the authors with the same gene names and were predicted to have the same functions described for those in *V. parahaemolyticus* or the other few bacteria.

Based on these studies and based on a personal communication with Dr. Jon Shaw the lateral flagellar genes of *A. caviae* Sch3N, the focus of our study, with their predicted functions are listed in table 1.4. In addition, the genetic organization of the lateral flagellar operon in *A. caviae* is shown in figure 1.2 and a schematic presentation showing the basic structure of one of the many *A. caviae* lateral flagella is provided in figure 1.3.

Table 1.4. Genes composing the *A. caviae* Sch3N lateral flagellar operon along with their predicted function

Gene name	Predicted function	Speceis containing homologous genes
<i>fliM_L</i>	Switch (C-ring)	<i>V. parahaemolyticus</i>
<i>fliN_L</i>	Switch (C-ring)	<i>V. parahaemolyticus</i>
<i>fliP_L</i>	Export/assembly	<i>V. parahaemolyticus</i>
<i>fliQ_L</i>	Export/assembly	<i>V. parahaemolyticus</i>
<i>fliR_L</i>	Export/assembly	<i>V. parahaemolyticus</i>
<i>flhB_L</i>	Export/assembly	<i>V. parahaemolyticus</i>
<i>flhA_L</i>	Export/assembly	<i>V. parahaemolyticus</i>
<i>LafK</i>	Regulation	<i>V. parahaemolyticus</i>
<i>fliE_L</i>	Basal body	<i>V. parahaemolyticus</i>
<i>fliF_L</i>	M-ring	<i>V. parahaemolyticus</i>
<i>fliG_L</i>	Switch (C-ring)	<i>V. parahaemolyticus</i>
<i>fliH_L</i>	Export/assembly	<i>V. parahaemolyticus</i>
<i>fliI_L</i>	Export ATP synthase	<i>V. parahaemolyticus</i>
<i>fliJ_L</i>	Export/assembly	<i>P. putida</i>
<i>flgN_L</i>	Chaprone	<i>Photobacterium profundum</i>
<i>flgM_L</i>	Anti-sigma factor	<i>V. parahaemolyticus</i>
<i>flgA_L</i>	P-ring assembly	<i>V. parahaemolyticus</i>
<i>flgB_L</i>	Rod	<i>V. parahaemolyticus</i>
<i>flgC_L</i>	Rod	<i>V. parahaemolyticus</i>
<i>flgD_L</i>	Rod	<i>V. parahaemolyticus</i>
<i>flgE_L</i>	Hook	<i>V. parahaemolyticus</i>

Table 1.4. is to be continued on the next page

Table 1.4 (continued). Genes composing the *A. caviae* Sch3N lateral flagellar operon along with their predicted function

Gene name	Predicted function	Speceis containing homologous genes
<i>flgF_L</i>	Rod	<i>V. parahaemolyticus</i>
<i>flgG_L</i>	Rod	<i>V. parahaemolyticus</i>
<i>flgH_L</i>	L-ring	<i>V. parahaemolyticus</i>
<i>flgI_L</i>	P-ring	<i>V. parahaemolyticus</i>
<i>flgJ_L</i>	Peptidoglycan hydrolase	<i>V. parahaemolyticus</i>
<i>flgK_L</i>	Hook associated protein 1 (HAP1)	<i>V. parahaemolyticus</i>
<i>flgL_L</i>	Hook associated protein 3 (HAP3)	<i>V. parahaemolyticus</i>
<i>ASA0374/lafW</i>	Unknown function	<i>V. parahaemolyticus</i>
<i>fliU</i>	Flagellar protein	<i>Salmonella choleraesuis</i>
<i>lafA1</i>	Lateral flagellin	<i>V. parahaemolyticus</i>
<i>lafA2</i>	Lateral flagellin	<i>V. parahaemolyticus</i>
<i>lafB</i>	Flagella capping protein (HAP2)	<i>V. parahaemolyticus</i>
<i>lafC</i>	Flagellar protein	<i>V. parahaemolyticus</i>
<i>lafX</i>	Unknown function	<i>V. parahaemolyticus</i>
<i>lafE</i>	Hook length control protein	<i>V. parahaemolyticus</i>
<i>lafF</i>	Flagellar protein	<i>V. parahaemolyticus</i>
<i>lafS</i>	Lateral flagellar sigma factor	<i>V. parahaemolyticus</i>
<i>lafT</i>	Chemotaxis motor protein	<i>V. parahaemolyticus</i> (and <i>motA</i> in <i>P. aeruginosa</i>)
<i>lafU</i>	Chemotaxis motor protein	<i>V. parahaemolyticus</i> (and <i>motB</i> in <i>P. aeruginosa</i>)
<i>pilZ</i>	c-di-GMP receptor protein	<i>Moritella</i> sp. / <i>Shewanella</i> sp.

Information provided in this table is based on the studies of Gavin and colleagues (Gavín *et al.*, 2002), Canals and colleagues (Canals *et al.*, 2006a), and the review of Merino and colleagues (Merino *et al.*, 2006).

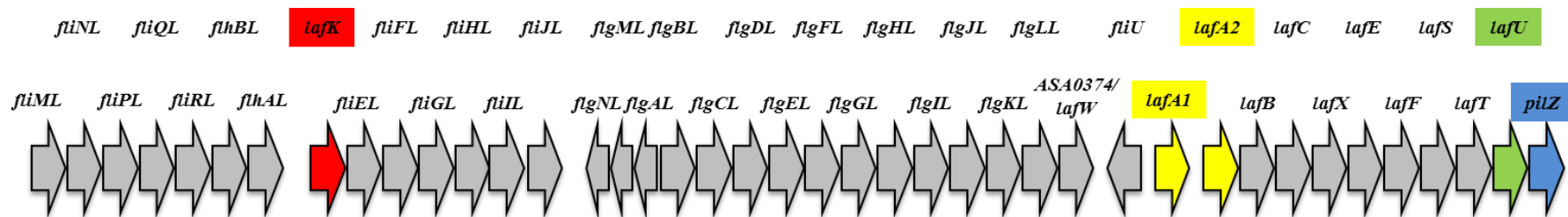


Figure 1.2. The lateral flagellar operon of *Aeromonas caviae* Sch3N. The operon is composed of 41 genes. The arrows depict open reading frames (ORFs) and show their direction of transcription. The gene for the major regulator LafK is coloured red, the genes for the two flagellins LafA1 and LafA2 are coloured yellow, the genes for LafU is coloured green, and the gene for the PilZ domain is coloured blue. The lateral flagellar gene cluster is found as one large locus on the *A. caviae* chromosome, this information was gained from the unpublished genome sequence of *A. caviae* Sch3N.

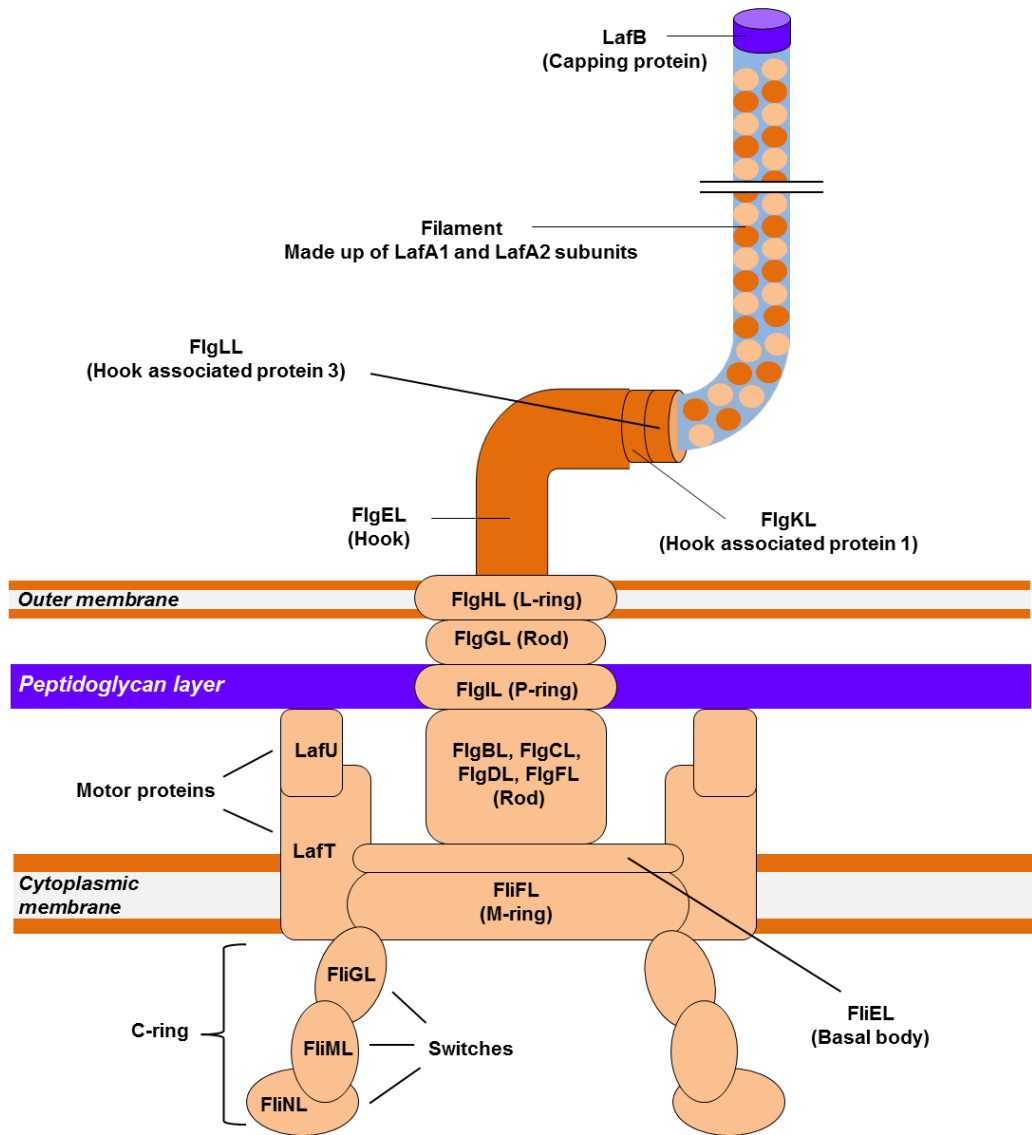


Figure 1.3. A diagram showing the structure of a lateral flagellum in *A. caviae* Sch3N. The diagram depicts the important structural proteins forming this apparatus.

Gavin and colleagues have reported the existence of two genes encoding the lateral flagellin proteins LafA1 and LafA2 (Gavín *et al.*, 2002). Both LafA1 and LafA2 proteins do compose the filaments of *A. caviae* lateral flagella. The reserachers have performed DNA sequence analysis and predicted putative promoter sequences upstream of the two genes *lafA1* and *lafA2* and also predicted terminator sequences downstream of the same two genes. Gavin and co-workers have, thus, suggested the two genes to be transcribed independently and, because of their sequences being highly similar to each other, the genes *lafA1* and *lafA2* were suggested to result from a gene duplication event. Gavin and co-workers have also proved that the purified lateral flagellin proteins from both *A. caviae* Sch3N and *A. hydrophila* AH-3 were modified by glycosylation (Gavín *et al.*, 2002).

Of notable importance in the lateral flagellar operon of *A. caviae* Sch3N is the existence of the *lafK* gene. The LafK protein has been identified by Stewart and colleagues as the master regulator of the lateral flagellar operon (Laf) expression in *V. parahaemolyticus* (Stewart *et al.*, 2003). The researchers in the indicated study have found the architecture of the LafK protein to be similar to four proteins in *Vibrio* spp that function as transcriptional regulators for the polar flagellar genes expression, namely, FlaK and FlaM in *V. parahaemolyticus*, as well as FlrA and FlrC in *V. cholerae*. Furthermore, LafK architecture shared similarities to FleQ and FleR, the transcriptional regulators of flagella gene expression in *P. aeruginosa* (Ritchings *et al.*, 1995, Stewart *et al.*, 2003, Baraquet *et al.*, 2012). The Laf operon expression in *V. parahaemolyticus* was found to be LafK-dependant and the expression of LafK itself (which is the transcriptional activator of the Laf system) was determined to be RopN (σ^{54})-dependant (Stewart *et al.*, 2003).

Kim and McCarter performed different experiments and concluded that when *flaK* gene (encoding the master regulator of the polar flagellum) function was lost then *lafK* can substitute for it but the opposite was not true in *V. parahaemolyticus* (Kim *et al.*, 2004). Since LafK plays an important role in the overlapping regulation between Laf and Fla systems in *V. parahaemolyticus*, and since mesophilic *Aeromonas* share the characteristic of possessing a dual flagellar system as in *V. parahaemolyticus*, with many of the flagellar proteins in the two species being homologous to each other, the possibility of *Aeromonas* LafK to play a similar overlapping regulatory role is worth studying.

Wilhelms and colleagues have recently described the lateral flagellar gene transcription hierarchy in *A. hydrophila* AH-3 (Wilhelms *et al.*, 2013). The study concluded that the transcription cascade of the lateral flagellar genes in *A. hydrophila* AH-3 occurs in three levels involving genes which are divided into three classes, Class I, II, and III. The transcription of *LafK* in *A. hydrophila* AH-3 was found to be σ^{70} -dependant and the *lafK* gene was considered one of the class I genes. The group suggested that although *LafK* is essential for the formation of the lateral flagella in *A. hydrophila* AH-3 it can't, however, be considered as a strict master regulator of the *A. hydrophila* Laf genes (as in *V. parahaemolyticus*) because many *A. hydrophila* Laf gene clusters were found to be *LafK*-independently-transcribed.

Wilhelms and colleagues have previously proposed a transcriptional hierarchy for the *A. hydrophila* AH-3 polar flagellum genes (Wilhelms *et al.*, 2011). They have proposed the transcriptional cascade to be divided to four classes (Class I-IV) and suggested *FlrA* to be the master regulator of the polar flagellar genes transcription. The transcription of *flrA* was also found to be σ^{70} -dependant. Being different from the *LafK* of *V. parahaemolyticus*, the *A. hydrophila* *LafK* protein does not compensate for the loss of *FlrA* and the latter is required for both polar flagellar genes expression and swimming motility exactly as the *LafK* being required for the lateral flagellar genes expression and the swarming motility.

The *LafK* encoded in the *A. caviae* Laf operon has not been previously studied. Wilhelms and co-workers, however, detected a σ^{70} promoter sequence upstream of *lafK* gene following an *in silico* analysis of the lateral flagellar region of *A. caviae* Sch3N (Wilhelms *et al.*, 2013). Furthermore, and based on information provided by Dr. Jon Shaw, the promoter sequence upstream of the *lafK* gene in *A. caviae* Sch3N contains a riboswitch. Riboswitches are regulatory segments found in the 5'untranslated regions (5'-UTRs) of some mRNA molecules in many bacteria (Batey, 2006). Their main function is to control gene expression following a direct binding to a specific metabolite, for example c-di-GMP, without the involvement of any intermediate protein in this process (Batey, 2006). The Bis-(3'-5')-cyclic dimeric guanosine monophosphate (c-di-GMP) has been suggested to control the switch of bacterial cells from a motile to sessile lifestyle, and vice versa (Hengge, 2009). More information about c-di-GMP is provided below. Whether the riboswitch identified upstream of *lafK* gene in *A. caviae* Sch3N is a c-di-GMP receptor which controls the expression of lateral flagellar genes in

this bacterium (and consequently has a role in determining the lifestyle of *A. caviae*) is worth studying.

Another important gene found in the *laf* operon of *A. caviae* Sch3N is the *pilZ* gene which encodes a PilZ domain-containing protein. PilZ domain-containing proteins have been extensively studied in recent years and have been described as c-di-GMP effector proteins used by the second messenger to exert its functions in many bacterial cells (Hengge, 2009). The PilZ domain was first identified in *P. aeruginosa* as being involved in type 4 fimbrial biogenesis (Alm *et al.*, 1996). The domain was then identified in other bacterial species as a c-di-GMP binding domain being part of the post-translational level of signalling by this second messenger (Sondermann *et al.*, 2012). The PilZ domain was described as a phylogenetically widely distributed domain which can either occur as a single domain or be linked to other domains that have different cellular functions (Sondermann *et al.*, 2012). Not all PilZ domains, however, do directly bind c-di-GMP but they still become involved, indirectly, in the c-di-GMP signalling pathway (Ryan *et al.*, 2012). Most bacterial genomes do encode more than one of the PilZ domain-containing proteins (Sondermann *et al.*, 2012). Those multiple PilZ domains within a single species which are unlinked to other domains have shown a considerable sequence variation (Ryan *et al.*, 2012).

Although structural differences have been reported among the PilZ-domain-containing proteins, however, their fold was found to be highly similar and a loop referred to as a “c-di-GMP switch” was determined in the majority of these domains (Sondermann *et al.*, 2012). Furthermore, comparing the amino acid sequences of different PilZ domains shows the existence of certain conserved motifs which were suggested to be required for c-di-GMP binding (Sondermann *et al.*, 2012). The PilZ domain-containing proteins have been reported to play roles in processes which include: twitching motility, alginate production, biofilm formation, intestinal colonization, cellulose synthesis, flagella rotation, and virulence gene expression (Hengge, 2009, Sondermann *et al.*, 2012). The PilZ domain encoded in the *A. caviae* Sch3N has not been studied previously. This domain is worth studying as a potential effector for the c-di-GMP being involved in bacterial lifestyle determination. More information about PilZ domains as effectors for c-di-GMP is provided below.

1.2.4.11.6. Pathogenicity of *Aeromonas* during motility and sessility and the roles played by flagella in each setting

In mesophilic *Aeromonas* species the main function of the single polar flagellum is to allow the cells to swim in liquid environments, while the function of the lateral flagella is basically to allow the bacteria to swarm as a group over surfaces or in viscous environments. However, reviewing the medical literature indicates the involvement of *Aeromonas* polar and lateral flagella in other functions related to *Aeromonas* pathogenicity.

Swarming is a type of motility, powered by flagella, which allows bacterial cells to move rapidly as a group over a moist surface or in a viscous environment (Verstraeten *et al.*, 2008, Kearns, 2010). There is almost a consensus that swarmer cells become elongated during swarming due to suppression of cell division (Kearns, 2010). It is not known, however, whether cell elongation is actually required by the cells to be able to swarm or it is just an indication of the process (Kearns, 2010). Both *Aeromonas* and *V. parahaemolyticus* swarmer cells have been reported to become elongated and hyper-flagellated (figure 1.4) (Gavín *et al.*, 2002), however, in *V. parahaemolyticus* the swarmer cells become as well multi-nucleated (Stewart *et al.*, 1997), a morphology which does not seem to occur in *Aeromonas* swarmer cells (Gavín *et al.*, 2002).

The role played by the lateral flagella in swarming motility in both *A. caviae* Sch3N and *A. hydrophila* AH-3 has been clearly demonstrated by Gavin and colleagues (Gavín *et al.*, 2002). In the indicated study, the researchers have generated two *A. caviae* Sch3N mutant strains, the first strain was a tandem mutant in which both lateral flagellin genes *lafA1* and *lafA2* were inactivated and the second strain contained a mutation in its *lafB* gene (encoding the flagellar capping protein HAP2). The two *A. caviae* Sch3N mutant strains showed 50% less ability to swarm on motility agar plates in comparison to the wild type when the swarm zone size was measured. Their findings clearly indicate the direct role of lateral flagella in swarming motility. *Aeromonas* lateral flagella were also found to be directly involved in biofilm formation (Kirov *et al.*, 2004). Biofilms are formed when a group of bacterial cells produce an extracellular matrix and become embedded as a sessile community within this matrix (Verstraeten *et al.*, 2008, Kearns, 2010). Bacterial biofilms in general are directly associated with the establishment of most human infections (Kirov *et al.*, 2002). Examples of human diseases in which bacterial biofilms were found to be directly involved in disease

establishment and progression include cystic fibrosis, native valve endocarditis, otitis media and chronic bacterial prostatitis (Kokare *et al.*, 2009). Following biofilm formation the bacteria do not only establish the infection and start to release its toxins and invade host cells, however, it also becomes more resistant to both antibiotics and host immune cells by being embedded in such a biofilm (Lindsay *et al.*, 2006). In addition, bacteria in a mature biofilm reaches a certain density which allows the quorum sensing system to be used by bacteria to exchange stimuli which leads to the activation of gene expression of more virulence factors than when the bacteria are in their planktonic state (Merino *et al.*, 2006). Bacterial biofilms constitute a major healthcare problem (Kokare *et al.*, 2009). This is basically due to formation of bacterial (and non-bacterial) biofilms on or in the indwelling medical devices such as central venous catheters, prosthetic heart valves, urinary catheters, and intrauterine devices (Kokare *et al.*, 2009). The microorganisms which form such medical device-associated biofilms may originate from the patient's own flora, the flora of healthcare workers, or from the hospital environment (Kokare *et al.*, 2009). It should be noted, however, that motility and sessility are very much interrelated processes (Verstraeten *et al.*, 2008). Motility is required by bacteria to reach a certain niche and form a biofilm with a defined architecture (Verstraeten *et al.*, 2008). In addition, flagella do help the bacterial cells to attach to a surface in order for them to form a biofilm and establish infection (Verstraeten *et al.*, 2008). Furthermore, the bacterial cells need to convert from sessility to motility in order for them to detach from the formed biofilm whenever needed (Verstraeten *et al.*, 2008).

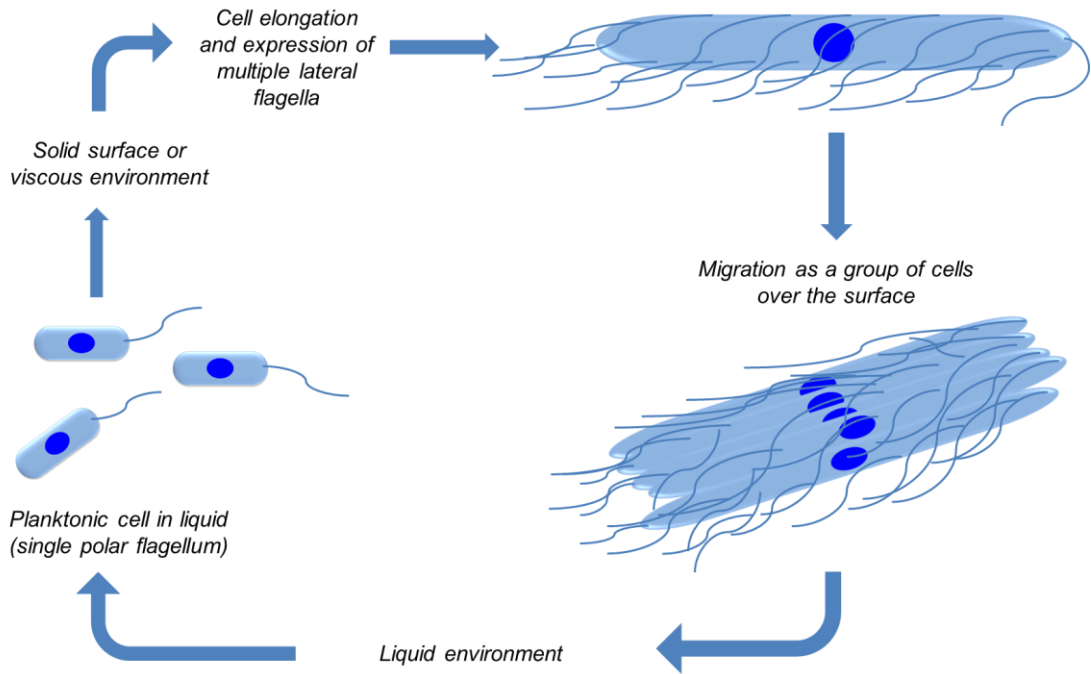


Figure 1.4. A diagram showing the ability of a mesophilic *Aeromonas* cell to switch between its polar and lateral flagellar systems to differentiate from a unicellular planktonic cell to an elongated cell which will then swarm over surfaces as a group along with other elongated cells using their induced multiple lateral flagella. When the inducer of the lateral flagellar system becomes absent, i.e., cells move from a solid/viscous surface to a liquid environment, all giant cells dedifferentiate to planktonic cells.

Both *A. caviae* polar and lateral flagella were suggested to act as adhesins required for attachment to human cell lines and that both are necessary for biofilm formation by *A. caviae* during gastrointestinal infections (Kirov *et al.*, 2004). Generally, there is a consensus that efficient bacterial pathogenesis occurs firstly by initial attachment (mediated by pili and flagella) and colonization of the host mucosal surfaces (Kirov *et al.*, 2002, Merino *et al.*, 2006). In addition, it has been strongly suggested that bacterial colonization directly involves biofilm formation, which itself formed following the movement of bacterial cells over mucosal surfaces by swarming (Merino *et al.*, 2006). It is thought that swarming motility expands the colonization area (Merino *et al.*, 2006). Kirov and colleagues investigated the role played by both polar and lateral flagella of *A. caviae* Sch3, a diarrhoeal isolate, in adhesion of bacterial cells to two types of intestinal cell lines, namely, Henle 407 and Caco-2 (Kirov *et al.*, 2004). The study has showed that both polar and lateral flagella were directly involved in *A. caviae* Sch3 adhesion to intestinal cell lines. A mutated strain in which both the polar flagellin genes *flaA* and *flaB* genes were knocked out resulting in a loss of the polar flagellum was not able to adhere to the tested cell lines. The same strain, however, restored 80% of its adhesion ability following complementation of the mutated genes. In the same study, inducing mutations in the lateral flagellin genes *lafA1* and *lafA2* caused *A. caviae* Sch3 to lose its ability to form the peritrichous lateral type of flagella. Loss of lateral flagella in *A. caviae* Sch3 resulted in more than 50% reduction in its ability to attach to the tested cell lines. More importantly, the study found that mutant strains with defects in either swimming or swarming motility were less able to adhere to human cells even if they were able to express polar and lateral flagella, a fact which crucially indicates the importance of motility itself in establishment of infection in human.

Gavin and co-workers emphasized the fact that hyper flagellation occurring following the expression of lateral flagella is associated with a higher degree of adherence to human host cells even though both polar and lateral flagella are important for such adherence (Gavín *et al.*, 2002). Specifically, production of peritrichous lateral flagella forms bacterial-bacterial linkages which allows the bacterial cells to form microcolonies on the mucosal surfaces of the infected host (Kirov *et al.*, 2002). In addition, the lateral flagella forms bacterial-surface linkages allowing for a firm attachment to the agar (or host cells) surface (Kirov *et al.*, 2002).

Kirov and colleagues used borosilicate glass tubes as an *in vitro* model to test the ability of both polar flagellar and lateral flagellar mutant strains of *A. caviae* Sch3 to form a biofilm (Kirov *et al.*, 2004). They found a reduction in the ability of both polar and lateral mutants to form a biofilm of 60% and 50%, respectively. Furthermore, the study confirmed that the chemotaxis sensory system is equally important for motility and biofilm formation as the *A. caviae* chemotactic mutant strain (in which the *cheA* chemotaxis protein was mutated) failed to swim and swarm and its ability to form a biofilm on borosilicate glass tubes was reduced by 83% in comparison to the wild type strain. The chemotaxis sensory system was found to be important for swarming in several bacterial species, namely, *V. parahaemolyticus*, *Proteus mirabilis*, *E. coli*, and *Salmonella typhimurium*, and *Serratia marcescens* (Verstraeten *et al.*, 2008). The main function of the chemotaxis system is to switch between the two types of flagellar rotation which include the counter-clockwise (required for swimming) and the clockwise (leads to tumbling), with the chemotaxis protein CheY being essential for switching to the latter type of rotation (and thus supports swarming) following its interaction with the switch proteins of the flagellar complex (Verstraeten *et al.*, 2008).

A co-ordination in the expression of both the polar and the lateral systems in *Aeromonas* species seem to exist. When the lateral flagella genes *lafB*, *lafS*, and *lafT* were knocked out in *A. hydrophila* AH-3, the formed mutant strains not only lost their ability to swarm on motility agar, but also were unable to swim using the single polar flagellum (Gavín *et al.*, 2002). Although western blot analysis detected the polar flagellin protein in all mutant strains and detected the lateral flagellin protein in the *lafT* mutant strain, these formed flagella were inactive (i.e., paralysed). This indicates that defects in lateral flagella expression or assembly might affect the functionality of the polar flagellum. In addition, the same study mentioned that mutations in *A. caviae* causing defects in the polar flagellum production have also lead to the elimination of lateral flagella in the same mutant strains. These findings indicate the existence of a co-ordination with in the dual flagellar system of *A. hydrophila* and *A. caviae*.

Defects in the polar flagellum in *V. parahaemolyticus* has been reported to cause constitutive expression of the lateral flagellar system in the indicated species (McCarter *et al.*, 1988). Thus, the polar flagellum in *V. parahaemolyticus* seems to act as a mechano-sensor which immediately induces lateral flagellar formation following its movement being slowed down due to the cell being in a viscous environment or due to

its attachment to a surface (McCarter *et al.*, 1988). The polar flagellum of mesophilic *Aeromonas* species has not been reported to act as a mechano-sensor that causes a constitutive expression of the lateral flagellar genes in *Aeromonas* (Merino *et al.*, 2006). Figure 1.5 illustrates the role played by both polar and lateral types of flagella in establishment of infection in human.

Finally, it should as well be mentioned here that the bacterial flagellin protein (specifically the conserved flagellin domain) is known to trigger inflammatory or adaptive host immune responses (Ramos *et al.*, 2004, Zgair, 2012).

Studying the mechanisms by which the bacterial cells decide to switch from motility to sessility (and vice versa) is important to further understand bacterial pathogenesis as well as to develop powerful strategies to prevent and eliminate bacterial infections in humans. The bacterial second messenger c-di-GMP, has been suggested recently to play a direct role in controlling the switch between motility and sessility in bacterial cells (Hengge, 2009). The c-di-GMP molecule, its effector and targets and its specific role in motility/ sessility determination are discussed in the following section.

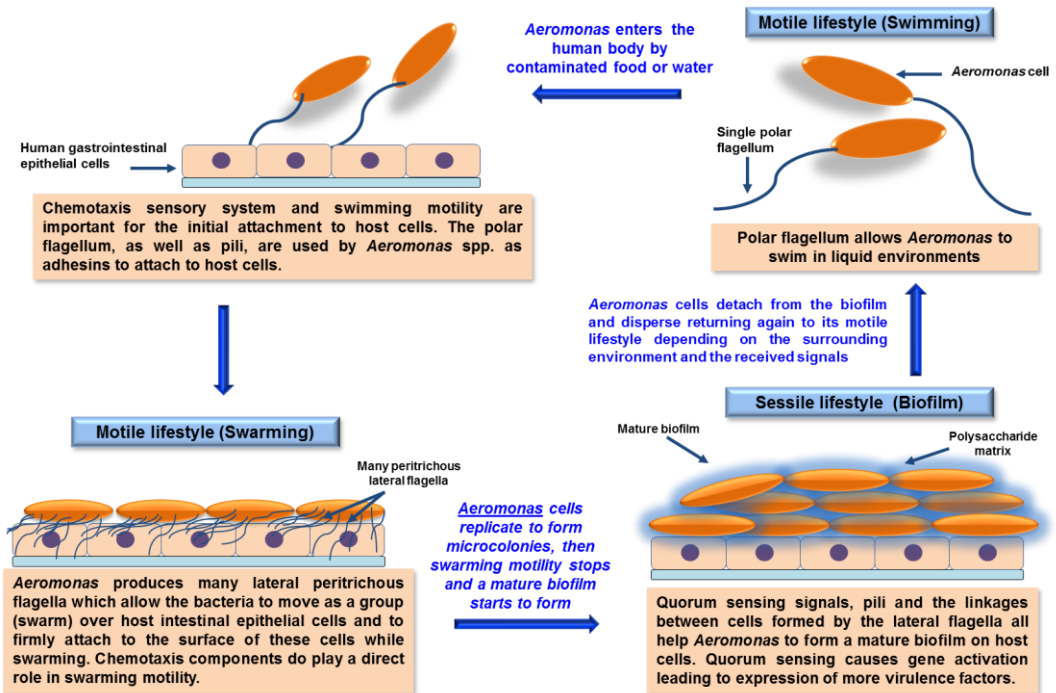


Figure 1.5. A diagram summarizes the cycle of swimming motility, swarming motility, and biofilm formation in human gastroenteritis caused by *A. caviae*. The figure illustrates the roles played by both polar and lateral types of flagella possessed by *A. caviae* in establishing human gastrointestinal infection and the important role of biofilms in this clinical setting. The same cycle can be applied on the other types of human infections caused by *Aeromonas* spp. as well as in the environmental setting.

1.3. Cyclic dimeric guanosine monophosphate (c-di-GMP)

1.3.1. Discovery of and roles played by c-di-GMP

C-di-GMP (figure 1.6) is a recently discovered second messenger in bacteria (Hengge, 2009). The first report describing its importance was published in 1987 by Ross and colleagues who were studying the regulation of cellulose biosynthesis in *Acetobacter xylinum* and suggested the existence of a complex signalling network in which c-di-GMP was directly affecting the activity of the enzyme cellulose synthase in the studied bacterium (Ross *et al.*, 1987). Since then, many studies have been published concerned with the role played by c-di-GMP in the bacterial cells. Such studies emphasized the direct involvement of c-di-GMP in cellular processes which include motility, biofilm formation, virulence genes expression, as well as bacterial cell division (Hengge, 2009), figure 1.7.

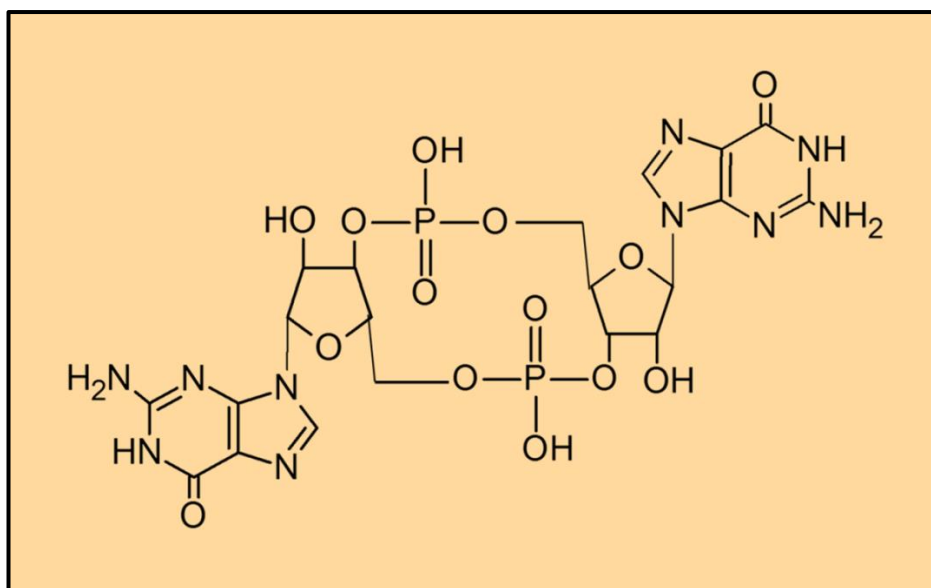


Figure 1.6. The chemical structure of c-di-GMP drawn using the ChemSketch software.

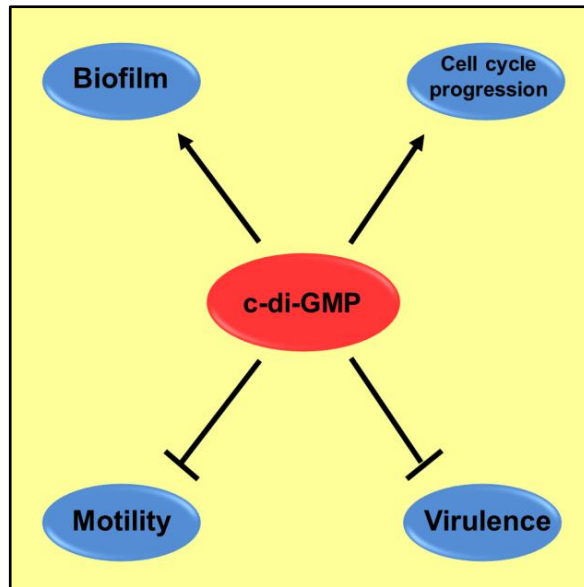


Figure 1.7. Effects of c-di-GMP on certain cellular processes as revealed by different studies in the medical literature.

1.3.2. c-di-GMP turnover

1.3.2.1. Synthesis of c-di-GMP

The c-di-GMP molecule is known to be produced by diguanylate cyclases (DGC) (Ryjenkov *et al.*, 2005) (figure 1.8). The DGC produce c-di-GMP from two molecules of guanosine triphosphate (GTP) which is the substrate specific to this enzyme (Hengge, 2009, Romling *et al.*, 2013). The GTP substrate binds to the active site (A site) of the DGC enzyme which contains the GGDEF motif (Hengge, 2009). The GGDEF motif name is based on its conserved amino acid sequence (Gly-Gly-Asp-Glu-Phe) (Romling *et al.*, 2013). The DGC enzyme is active only when the signature sequence (GG[DE]EF) is present in its A-site (Hengge, 2009, Romling *et al.*, 2013). Once the two GTP substrate molecules bind to the A site, the DGC enzyme catalyzes the formation of a phosphoester bond between them with the aid of either two Mg^{2+} or two Mn^{2+} and eventually the formation of c-di-GMP (Romling *et al.*, 2013).

Several researchers have attempted to study the DGC enzyme regulation (i.e., what makes this enzyme active and what cause it to be inhibited) and some research groups have provided structural details about DGC transformation from an inactive to an active states (and vice versa) and have also suggested models to illustrate their findings (see below). Structurally, the DGC enzyme is composed of two similar

monomers (a homodimer) which must physically come very close to each other in order to form the “complete” A-site at the interface between the two monomers and thus causing the DGC enzyme to be catalytically-competent (Hengge, 2009, Romling *et al.*, 2013). While that’s the general principle of DGC activation, it seems from reviewing the few published studies that there are different mechanisms which are suggested to allow this catalytically competent homodimer to form (Romling *et al.*, 2013).

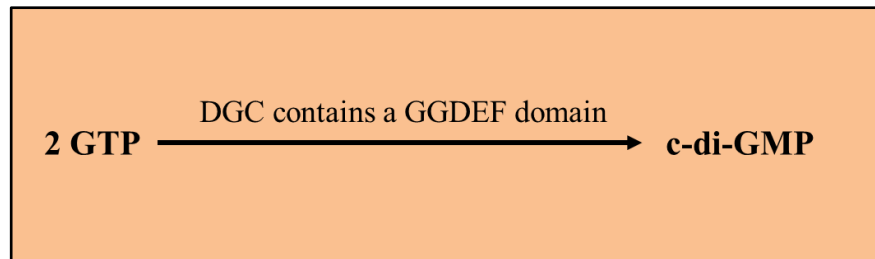


Figure 1.8. Chemical formula for the formation of bis-(3’-5’)-cyclic dimeric guanosine monophosphate (c-di-GMP). **GTP:** guanosine triphosphate. **DGC:** Diguanylate cyclase enzyme.

1.3.2.1.1. Mechanisms of DGC activation/ inactivation

1.3.2.1.1.1. Phosphorylation-dependent regulation

Few published studies have suggested different mechanisms for DGC regulation. Malone and colleagues have suggested a mechanism which involves the constitutive inhibition of the C-terminal GGDEF domain of the DGC protein by the N-terminal (receiver) domain of the same protein until the latter becomes phosphorylated after which the inhibition is relieved (Malone *et al.*, 2007, Giardina *et al.*, 2013). They have proposed a model of phosphorylation-dependent activation for the DGC protein WspR in *Pseudomonas fluorescens*. The WspR is known as a response regulator which controls the ability of *Pseudomonas* species to form a biofilm (De *et al.*, 2008). Although Malone and colleague have well proved their hypothesis, they, however, did not consider their model to be the final one and they have warranted more research to be done to investigate other possible mechanisms of regulation for WspR. Figure 1.9 shows Malone and colleagues mechanism of WspR activation in *P. fluorescens*.

1.3.2.1.1.2. Product feed back inhibition

The second mechanism of DGC regulation was also proposed by studying the WspR by De and co-workers but this time in *P. aeruginosa* (De *et al.*, 2008, De *et al.*,

2009). The mechanism was described as a non-competitive product feedback inhibition resulting from binding of two intercalating c-di-GMP molecules to an inhibitory site (I-site) located upstream of the A-site of the DGC enzyme (Romling *et al.*, 2013). This binding results in complete prevention of the movement of the GGDEF domains toward each other (dimerization) and consequently stops c-di-GMP synthesis (Romling *et al.*, 2013). When the level of c-di-GMP becomes low, the two bound c-di-GMP molecules become detached from the I-site allowing a catalytically competent dimer to form followed by c-di-GMP synthesis (Romling *et al.*, 2013). The I-site is known to contain the RxxD motif, with the “x” indicating any amino acid (Romling *et al.*, 2013). The same mechanism of feedback inhibition was also proposed for PleD in *Caulobacter crescentus* (Chan *et al.*, 2004, Wassmann *et al.*, 2007). Figure 1.10 shows the basic steps of the second mechanism.

1.3.2.1.1.3. Environmental signals-based regulation

The third model of GGDEF domain activation was suggested by Giardina and colleagues who studied the DGC protein YfiN in *Pseudomonas aeruginosa* (Giardina *et al.*, 2013). The DGC enzyme YfiN is part of a signalling module referred to as YfiBNR present in the genome of *P. aeruginosa* (Giardina *et al.*, 2013). This signalling module is involved in the formation of the so called small-colony variants of *P. aeruginosa* isolated from cystic fibrosis patients and which are (the colonies) characterized by high level of c-di-GMP production and are known to have a high ability to form a biofilm within the human host and are noticeably resistant to both immune cells and antibiotics (Giardina *et al.*, 2013). The YfiN is composed of a GGDEF domain, a HAMP domain, two transmembrane helices and a PAS domain. The YfiR is the negative regulator of the signalling module and the YfiB is an outer-membrane protein. The YfiR seems to be able to sense the redox stress occurring in the periplasm while the YfiB seems to sense the cell wall stress. According to Giardina and coworkers, the YfiN DGC enzyme is constitutively inhibited by YfiR binding to the PAS domain of the YfiN protein. Once there is a redox stress or a cell wall stress, YfiR becomes detached from the PAS domain of the YfiN and becomes instead bound to the YfiB protein. Once the PAS domain becomes free from the YfiR, conformation changes occur in the YfiN resulting in the dimerized GGDEF domains to move toward each other and the catalytically competent homodimer becomes ready for binding 2GTPs and eventually synthesis of c-di-GMP. Figure 1.11 describes in detail the proposed model of *P. aeruginosa* YfiN

activation. This model is similar to the above discussed phosphorylation-dependent model suggested by Malone and colleagues, however, no phosphorylation reaction has been detected in this model and only environmental signals were involved in the DGC enzyme regulation. In addition, the YfiN contained a degenerate I-site and there was no evidence of a feedback inhibition mechanism being involved in YfiN regulation.

1.3.2.1.1.4. Competitive inhibition of DGCs

Half of the GGDEF domain DGCs can not be controlled by the non-competitive feed back inhibition mechanism described above due to the lack of an I-site (Romling *et al.*, 2013). However, a recent study has shown that two molecules of c-di-GMP can actually bind to the active site (A-site) of the DGC enzyme XCC4471 in *Xanthomonas campestris* implying that regulation of DGCs by competitive inhibition can occur (Yang *et al.*, 2011). The reserachers have described the studied A-site to contain a highly conserved sequence and have provided important structural details. They, however, they have not provided a model for their proposed novel mechanism.

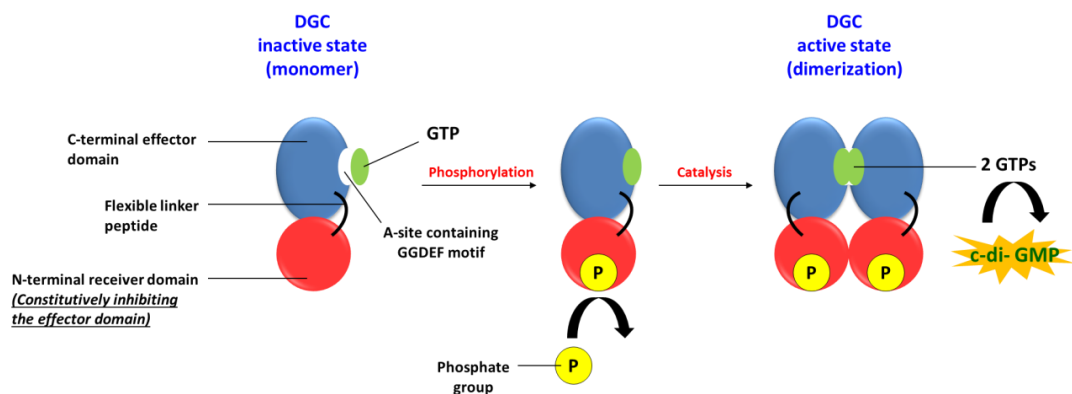


Figure 1.9. Phosphorylation-dependent mechanism of DGC activation proposed for the WspR in *Pseudomonas fluorescens* (Malone *et al.*, 2007). The N-terminal receiver domain constitutively inhibits the C-terminal GGDEF-containing domain from dimerization and production of c-di-GMP. When c-di-GMP is needed by the cell, addition of a phosphate group to the N-terminal domain relieves the inhibition and allows for dimerization (in which the two active sites come together) and consequently c-di-GMP synthesis. Modifications of or mutations in the N-terminal domain might also result in constitutive c-di-GMP synthesis.

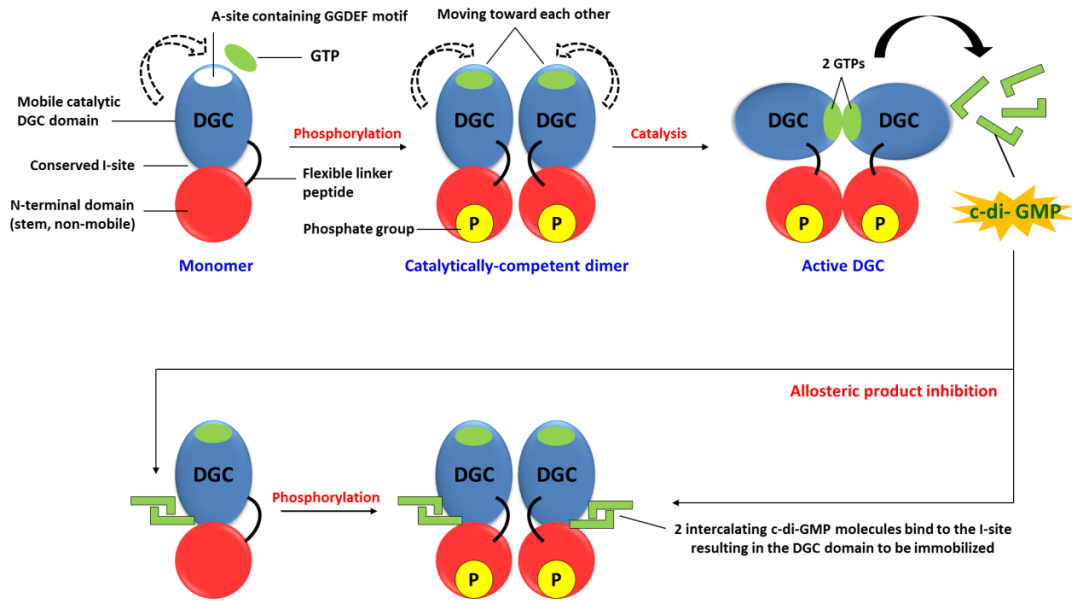


Figure 1.10. Regulation of DGC activity by non-competitive feedback inhibition. The model proposed for *Caulobacter crescentus* PleD enzyme regulation (Chan *et al.*, 2004, Wassmann *et al.*, 2007) is illustrated. A single GTP molecule binds to the A-site of the previously non-active DGC monomer after which a phosphorylation reaction results in the formation of a catalytically-competent homodimer. The mobile DGC domains of the PleD enzyme move toward each other while being still attached to the N-terminal (stem) domain causing the two A-sites to face each other and the formation of the fully active DGC. A condensation reaction results in the formation of c-di-GMP from the two GTP molecules after which the c-di-GMP will reach its desired cellular targets and exert its functions, and once in excess, c-di-GMP will bind to the inhibitory site (I-site) of the DGC enzyme resulting in immobilization of the GGDEF-containing domains which blocks the formation of the active state of DGC enzyme (and eventually blocking the production of more c-di-GMP) by product feedback inhibition mechanism. The same mechanism has been also proposed to control the DGC enzyme WspR in *P. aeruginosa* (De *et al.*, 2008, De *et al.*, 2009).

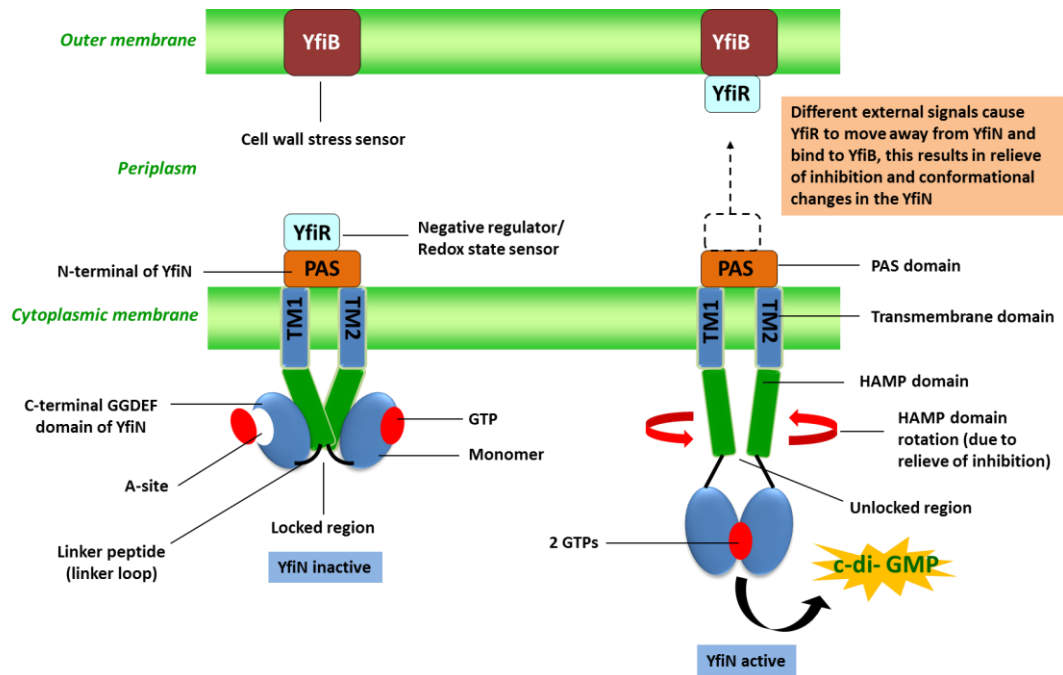


Figure 1.11. Mechanism of regulation of the DGC protein YfiN (part of YfiBNR signalling system) in *P. aeruginosa* as proposed by Giardina and colleagues (Giardina *et al.*, 2013). The YfiN is inhibited by the binding of YfiR to the PAS domain of the YfiN. The YfiN is activated only as a result of the YfiR and/or YfiB receiving certain environmental signals after which the negative regulator YfiR moves away from the PAS domain and binds to the YfiB. The detachment of the suppressor YfiR causes rearrangement of domains composing the YfiN resulting in rotating the HAMP domains and loosening of the linker peptide and movement of the GGDEF domains toward each other (catalytically competent GGDEF dimer). The formed dimer is then ready to bind to two molecules of GTP and eventually c-di-GMP synthesis.

1.3.2.2. Hydrolysis of c-di-GMP

The molecule c-di-GMP can be hydrolysed by phosphodiesterases (PDEs) which are proteins containing either EAL domain or HD-GYP domain, with the former domain being more common in these enzymes (Hengge, 2009). Chemically, the complete hydrolysis of c-di-GMP means its breakdown to the linear form di-GMP (5'-pGpG) and then this will further be broken down to two molecules of guanosine monophosphate (2 GMP) (Hengge, 2009).

It seems from the few studies concerned with EAL domain phosphodiesterases that the first step of hydrolysis (formation of pGpG) is done by c-di-GMP-specific EAL PDEs while the second step is performed by different (non-c-di-GMP-specific) enzymes

which have an affinity for pGpG (Romling *et al.*, 2013). The HD-GYP domain PDEs, however, seem to carry out the complete hydrolysis of c-di-GMP to 2 GMP and thus they can't be described as c-di-GMP-specific PDEs because they have an equal affinity to pGpG (Stelitano *et al.*, 2013). The chemical formula of c-di-GMP hydrolysis is shown in figure 1.12.

Hydrolysis of c-di-GMP to its linear form pGpG by EAL domain PDEs strictly requires either Mg^{2+} or Mn^{2+} and this step is strongly inhibited by Ca^{2+} (Tchigvintsev *et al.*, 2010). The EAL domain PDEs can occur as monomers, dimers, or even oligomers with the dimer form being the most common and the one important for the domain activation by different stimuli (Romling *et al.*, 2013). One of the best published structural studies concerned with EAL domains activation is the study of Barends and colleagues who have proposed the mechanism of c-di-GMP hydrolysis by the EAL PDE enzyme BlrP1 in *K. pneumoniae* to occur by light activation (Barends *et al.*, 2009). First the BLUF sensor domain attached to the EAL domain becomes activated by blue light (photon absorption) resulting in conformational changes in the BLUF domain and the transfer of a signal to the EAL domain which contains c-di-GMP in its active site and following rearrangements of the now activated BlrP1 protein strands the hydrolysis of the c-di-GMP takes place (Barends *et al.*, 2009). It seems that the E residue (glutamic acid) plays a direct role in interaction with the catalytic metal ions during c-di-GMP hydrolysis (Romling *et al.*, 2013). The E residue was found to be conserved in all of the studied “enzymatically active” EAL PDEs (Romling *et al.*, 2013).

The c-di-GMP hydrolysis reaction carried out by the HD-GYP domain PDE (Bd1817) in *Bdellovibrio bacteriovorus* seems to depend on Fe^{2+} or Mn^{2+} (Lovering *et al.*, 2011). Also, only one very recent study has shown the actual crystal structure of the HD-GYP domain PDE (*pmGH*) of the bacterium *Persephonella marina* while being complexed with c-di-GMP (Wigren *et al.*, 2014).

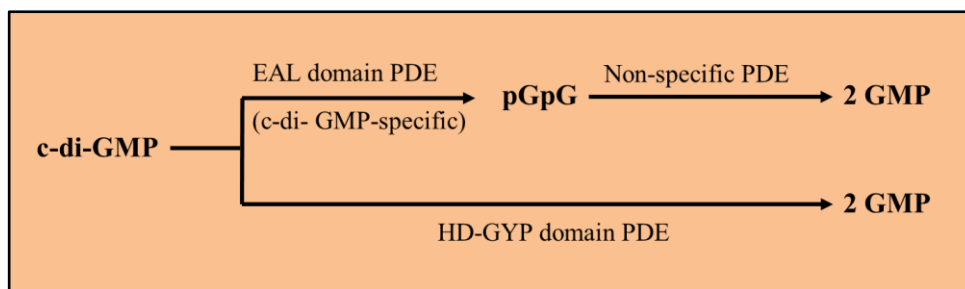


Figure 1.12. Chemical formula for the hydrolysis of bis-(3'-5')-cyclic dimeric guanosine monophosphate (c-di-GMP). **pGpG**: 5'-phosphoguanylyl-(3'-5')-guanosine. **GMP**: guanosine monophosphate. **PDE**: Phosphodiesterase enzyme.

1.3.3. Presence of GGDEF and EAL domains in bacterial genomes

Examining the DNA sequence data accumulating from bacterial whole genome sequencing reveals a large number of genes encoding GGDEF and EAL domains (Hengge, 2009). Basically, some bacterial proteins contain one of these domains or have both of them in tandem, i.e., GGDEF-EAL or GGDEF-HD-GYP (Romling *et al.*, 2013). Among the phylum *Proteobacteria*, the whole genomes of 794 members of the phylum were sequenced from the period of January 2012 till March 2013, of these, 2,461 EAL-containing proteins, 1,453 HD-GYP-containing proteins, 7,029 GGDEF-containing proteins, and 4,867 proteins containing both GGDEF and EAL domains were detected (Romling *et al.*, 2013).

More related to our study, the genome of *Vibrio parahaemolyticus* encodes 12 EAL-containing proteins, 28 GGDEF-containing proteins, two HD-GYP-containing proteins, and 15 proteins containing both GGDEF and EAL domains (Kim *et al.*, 2007). Also, the genome of *V. cholerae* encodes 12 EAL-containing proteins, 31 GGDEF-containing proteins, and 10 proteins containing both GGDEF and EAL domains (Lim *et al.*, 2007).

The sequenced genome of *A. hydrophila* ATCC7966^T contains 7 EAL-containing proteins, 23 GGDEF-containing proteins, and 15 proteins containing both GGDEF and EAL domains (Seshadri *et al.*, 2006, Kozlova *et al.*, 2011). In addition, and based on our unpublished data provided by Dr. Jon Shaw, the genome sequence of *A. caviae* Sch3 contains 8 EAL-containing proteins, 4 HD-GYP-containing proteins, 31 GGDEF-containing proteins, and 13 proteins containing both GGDEF and EAL domains.

1.3.4. Sensory domains linked to GGDEF and EAL domains

The GGDEF and EAL domains are often found linked to other intracellular sensory domains, domains that are trans-membrane-located or extracellular domains. (Hengge, 2009, Sondermann *et al.*, 2012). Examples of these sensory domains and their functions are listed in table 1.5. Altogether, these sensory domains allow for the environmental and cellular signals to be sensed and responded to by the bacterial cell using a network in which c-di-GMP takes control of a large number of cellular activities (Hengge, 2009, Sondermann *et al.*, 2012).

Table 1.5. Sensory domains commonly linked to GGDEF and EAL domains

Domain name	Function	Reference
Blue Light Using FAD (BLUF) domain	Blue light sensing	(Hasegawa <i>et al.</i> , 2006)
Cyclases/Histidine kinases Associated Sensing Extracellular (CHASE) domain	Binding to low molecular weight ligands	(Mougel <i>et al.</i> , 2001)
cyclic GMP Adenylyl cyclase FhlA (GAF) domain	Binding of cyclic GMP and cyclic AMP	(Hurley, 2003)
Light-Oxygen-Voltage (LOV) sensing domain	Blue light and Oxygen sensor	(Cao <i>et al.</i> , 2010)
Membrane-Associated Sensor 1 (MASE1) domain	A redox-responsive regulator of aspartate taxis Iron and Oxygen sensing	(Lacey <i>et al.</i> , 2013) (Nikolskaya <i>et al.</i> , 2003)
Membrane-Associated Sensor 2 (MASE2) domain	Membrane sensory domain (nature of sensed signals still unknown)	(Nikolskaya <i>et al.</i> , 2003)
Oxygen-binding haemerythrin domain	Oxygen binding	(French <i>et al.</i> , 2008)
Per-Arnt-Sim (PAS) domain	Oxygen sensing	(Sasakura <i>et al.</i> , 2002)
Receiver (REC) domain	Phosphoryl acceptor	(Kazmierczak <i>et al.</i> , 2006)
Red light bacteriophytochromes	Red and far red light sensing	(Tarutina <i>et al.</i> , 2006)

1.3.5. Tandemly arranged domains (composite proteins) and their functions

The arrangement of the GGDEF and EAL domains in tandem is more common than their presence as single domains in bacterial proteins and there are three possibilities for the exact function of a composite protein (Romling *et al.*, 2013).

Firstly, the composite proteins can have both of their domains to be catalytically active (bifunctional enzymes) but the domains are differentially regulated by the cell making the enzyme show only one of its two activities in response to certain external stimuli (Romling *et al.*, 2013). One example is the ScrC in *V. parahaemolyticus* (Ferreira *et al.*, 2008). The ScrC is part of a novel operon referred to as *scrABC* which regulates both swarming motility and capsular polysaccharide (CPS) production in *V. parahaemolyticus* (Boles *et al.*, 2002, Ferreira *et al.*, 2008). Researchers have found the ScrC protein to work only in the context of the other two proteins encoded within the same operon, ScrA and ScrB, which modulate its activity (Ferreira *et al.*, 2008). *In vivo*, i.e., in the presence of the ScrAB, the ScrC protein functions as a phosphodiesterase which degrades c-di-GMP and thus swarming motility becomes enhanced (Ferreira *et al.*, 2008). When the activity of ScrC was experimentally tested in the absence of the ScrAB, it acted as a diguanylate cyclase, with the enhancement of the *cps* transcription being noticed (Ferreira *et al.*, 2008).

Secondly, one of the two domains of a composite protein may act as a DGC or PDE but the other domain is catalytically inactive, however, the latter is still involved in other important functions including for example its interaction with other proteins or RNA molecules (Romling *et al.*, 2013). In addition, some inactive GGDEF domains can still bind GTP molecules with no further proceeding to c-di-GMP synthesis, but with this binding seemingly activating the PDE activity of the EAL domain (Romling *et al.*, 2013). The same is true for inactive EAL domains suggested to bind c-di-GMP and allow the enzymatically active GGDEF domain to function (Christen *et al.*, 2005, Schmidt *et al.*, 2005). Examples include the dual domain containing proteins CC3396 in *Caulobacter crescentus* (Christen *et al.*, 2005) and FimX in *P. aeruginosa* (Kazmierczak *et al.*, 2006) both of which were found to act as phosphodiesterase enzymes with their GGDEF domain lacking any DGC activity yet able to bind GTP, a step which was found to be important for EAL domain activation and hydrolysis of c-di-GMP by these two proteins. Another example is the ScrG protein in *V. parahaemolyticus* (Ferreira *et al.*, 2008) which was found to play a role in regulating

swarming motility and CPS production in this bacterial species (Kim *et al.*, 2007). The main function of the ScrG protein *in vivo* was to act as a phosphodiesterase which causes enhancement of motility and suppression of capsular polysaccharides production (Kim *et al.*, 2007). However, deletion of the EAL domain caused exactly opposite effects on motility and CPS production in the tested bacterium. The GGDEF domain sequence was poorly conserved and after doing mutational analysis to test the activity of this potential DGC domain the authors did not directly assign a DGC activity to the degenerate GGDEF domain of the ScrG (although they did not rule it out), they, instead, suggested its interaction with other proteins involved in c-di-GMP signalling which may result in indirect but important effects on the lifestyle of *V. parahaemolyticus* and they have suggested more investigations of the ScrG protein (Kim *et al.*, 2007).

Thirdly, both domains of a composite protein can be enzymatically inactive and have no roles to play in the c-di-GMP signalling network (Romling *et al.*, 2013). A good example is the CsrD protein in *E. coli* which was shown to contain enzymatically inactive GGDEF and EAL domains both of which had no roles to play in the c-di-GMP signalling system of *E. coli*, however, they both were found to be actively involved in RNA degradation (Suzuki *et al.*, 2006). Table 1.6 lists some of the studied enzyme proteins containing GGDEF and/or EAL/HD-GYP domains along with their enzymatic functions.

Table 1.6. Examples of studied enzyme proteins containing GGDEF, EAL, and HD-GYP domains

Name of protein	Detected domains	Host bacteria	Enzymatic activity	Reference
<u>GGDEF-containing proteins:</u>				
PleD	REC-REC-GGEEF	<i>Caulobacter crescentus</i>	DGC	(Chan <i>et al.</i> , 2004, Paul <i>et al.</i> , 2004)
DgcA	Coiled coil-GGDEF	<i>Caulobacter crescentus</i>	DGC	(Schirmer <i>et al.</i> , 2009)
WspR	REC-GGEEF	<i>Pseudomonas aeruginosa</i>	DGC	(Hickman <i>et al.</i> , 2005)
YfiN	PAS-TM-TM-HAMP-GGDEF	<i>Pseudomonas aeruginosa</i>	DGC	(Giardina <i>et al.</i> , 2013)
<u>EAL-containing proteins:</u>				
RocR	REC-EVL	<i>Pseudomonas aeruginosa</i>	PDE	(Rao <i>et al.</i> , 2008)
YahA	HTH-EVL	<i>Escherichia coli</i>	PDE	(Schmidt <i>et al.</i> , 2005)
BlrP1	BLUF-EAL	<i>Klebsiella pneumoniae</i>	PDE	(Barends <i>et al.</i> , 2009)
<u>HD-GYP-containing proteins:</u>				
RpfG	REC-HD-GYP	<i>Xanthomonas campestris</i>	PDE	(Ryan <i>et al.</i> , 2006, Ryan <i>et al.</i> , 2010)
<i>pmGH</i>	GAF-HD-GYP	<i>Persephonella marina</i>	PDE	(Wigren <i>et al.</i> , 2014)
<u>GGDEF-EAL-containing proteins:</u>				
BphG1	PAS-GAF-PHY-GGDEF-EAL	<i>Rhodobacter sphaeroides</i>	Bifunctional	(Tarutina <i>et al.</i> , 2006)
PdeA	PAS-GEDEF-EAL	<i>Caulobacter crescentus</i>	PDE	(Christen <i>et al.</i> , 2005)
Dgc1	PAS-GGDEF-EAL	<i>Acetobacter xylinus</i>	DGC	(Tal <i>et al.</i> , 1998, Bae <i>et al.</i> , 2004)
MSDGC1	GAF-GGDEF-EAL	<i>Mycobacterium smegmatis</i>	Bifunctional	(Bharati <i>et al.</i> , 2012)
ScrC	TM-TM-GGDEF-EAL	<i>Vibrio parahaemolyticus</i>	Bifunctional	(Ferreira <i>et al.</i> , 2008)
ScrG	PAS-HDDDF-ESL	<i>Vibrio parahaemolyticus</i>	PDE	(Kim <i>et al.</i> , 2007)
Lpl0329	REC-GGDEF-EAL	<i>Legionella pneumophila</i>	Bifunctional	(Levet-Paulo <i>et al.</i> , 2011)

1.3.6. Receptors (effectors) for c-di-GMP

In order for c-di-GMP to exert its function, it needs to bind to an effector molecule which will then transfer the signal to a target component allowing a specific output to appear (Hengge, 2009). Specifically, binding of c-di-GMP will cause allosteric changes to the receptor molecule thus allowing the signal to be transferred (Furukawa *et al.*, 2012). Many c-di-GMP effector molecules have been identified and they have been found to be either protein domains or RNA domains (riboswitches) (Sondermann *et al.*, 2012). The c-di-GMP binding proteins can themselves be divided to four categories which include (i) the PilZ domain-containing proteins, (ii) enzymatically-inactive GGDEF and EAL domain-containing proteins, (iii) proteins functioning as transcription factors, and (iv) the enzyme polynucleotide phosphorylase (PNPase) (Ryan *et al.*, 2012, Sondermann *et al.*, 2012). A list of c-di-GMP effectors is provided in table 1.7.

1.3.6.1. PilZ domain

The PilZ domain containing proteins have been described as effector molecules which bind to c-di-GMP with a high affinity (Romling *et al.*, 2013). The dissociation constant (K_d) for the c-di-GMP-PilZ complex was estimated to be from <50 nM to 1 μ M (Hengge, 2009).

The name “PilZ” was originally given to the PilZ protein of the Gram negative bacterium *P. aeruginosa* during a novel study which have identified its coding gene (*pilZ*) and assigned a role for the PilZ protein as being involved in type 4 pili biogenesis in *P. aeruginosa* (Alm *et al.*, 1996). The PilZ domain was first suggested to function as a c-di-GMP receptor in a study published in 2006 by Amikam and colleagues who did sequence analyses for different proteins in different bacterial species from which they noticed the existence of the amino acid sequence of the previously identified PilZ domain in all of them (Amikam *et al.*, 2006). From 2006 onward many studies have been published which have experimentally supported the fact that the PilZ domain is a c-di-GMP receptor (effector), examples of the studied proteins containing the PilZ domain are listed in table 1.7. The indicated examples of the PilZ domain have been suggested to control cellular functions which include, for instance, twitching motility, alginate production, polysaccharide synthesis, biofilm formation, flagella rotation, virulence genes expression, and DNA binding (Hengge, 2009, Ryan *et al.*, 2012, Sondermann *et al.*, 2012, Romling *et al.*, 2013).

Table 1.7. Examples of c-di-GMP effectors

Effector name	Organism	Role played	Reference
<u>Proteins containing PilZ domain:</u>			
Alg44 (PA4608)	<i>Pseudomonas aeruginosa</i>	Alginate biosynthesis	(Merighi <i>et al.</i> , 2007)
BcsA	<i>Gluconacetobacter xylinus</i>	Cellulose synthesis	(Weinhouse <i>et al.</i> , 1997)
DgrA	<i>Caulobacter crescentus</i>	Control of flagellar motor function	(Christen <i>et al.</i> , 2007)
MrkH	<i>Klebsiella pneumoniae</i>	Control of biofilm formation by regulation of type 3 fimbriae expression	(Wilksch <i>et al.</i> , 2011)
PilZ (PA2960)	<i>P. aeruginosa</i>	Type 4 fimbrial biogenesis	(Alm <i>et al.</i> , 1996)
PlzA,B,C,D, E	<i>Vibrio cholerae</i>	Regulation of biofilm formation, motility, and virulence	(Pratt <i>et al.</i> , 2007)
PP4397	<i>P. putida</i>	Unknown	(Ko <i>et al.</i> , 2010)
XAC1133 (PilZ)	<i>Xanthomonas axonopodis</i>	Control of type IV pilus biogenesis	(Guzzo <i>et al.</i> , 2009)
XC1028	<i>X. campestris</i>	Type IV fimbriae assembly	(Li <i>et al.</i> , 2009)
XCC6012 (PilZ)	<i>X. campestris</i>	Virulence	(Li <i>et al.</i> , 2011b)
YcgR	<i>Escherichia coli</i> , <i>Salmonella</i> spp.	Regulation of flagellum-based motility	(Ryjenkov <i>et al.</i> , 2006)
<u>Enzymatically inactive GGDEF domains (I-site effectors):</u>			
PopA (CC_1842)	<i>C. crescentus</i>	Cell cycle progression	(Duerig <i>et al.</i> , 2009)
SgmT (MXAN_4640)	<i>Myxococcus xanthus</i>	Regulation of extracellular matrix production	(Petters <i>et al.</i> , 2012)
CdgA (Bd3125)	<i>Bdellovibrio bacteriovorus</i>	Switch between free living growth and predation	(Hobley <i>et al.</i> , 2012)
PelD (PA3061)	<i>P. aeruginosa</i>	PEL polysaccharide production	(Lee <i>et al.</i> , 2007, Whitney <i>et al.</i> , 2012)
<u>Enzymatically inactive EAL domains:</u>			
FimX	<i>P. aeruginosa</i>	Type IV pilus biogenesis and twitching motility	Qi <i>et al.</i> , 2011
LapD	<i>P. fluorescens</i>	Biofilm formation	Newell, 2009
<u>Transcription factors (main function is the regulation of genes expression):</u>			
FleQ	<i>P. aeruginosa</i>	Flagella biosynthesis and exopolysaccharide (EPS) biosynthesis	(Hickman <i>et al.</i> , 2008)
VpsT	<i>V. cholerae</i>	Motility and extracellular matrix production	(Krasteva <i>et al.</i> , 2010)
Clp	<i>X. campestris</i> , <i>X. axonopodis</i>	Virulence	(Leduc <i>et al.</i> , 2009, Tao <i>et al.</i> , 2010)
Bcam1349	<i>Burkholderia cenocepacia</i>	Virulence and biofilm formation	(Fazli <i>et al.</i> , 2011)
<u>Riboswitches:</u>			
Cd1 (c-di-GMP-type-I)	<i>Clostridium difficile</i>	Flagella biosynthesis	(Sudarsan <i>et al.</i> , 2008)
Vc1 (c-di-GMP-type-I)	<i>V. cholerae</i>	Chitin binding protein production and colonization	(Sudarsan <i>et al.</i> , 2008)
Vc2 (c-di-GMP-type-I)	<i>V. cholerae</i>	Competence (DNA uptake)	(Sudarsan <i>et al.</i> , 2008)
Cd84 (c-di-GMP-type-II)	<i>C. difficile</i>	Self-splicing ribozyme	(Lee <i>et al.</i> , 2010)
<u>Other effectors:</u>			
PNPase	<i>E. coli</i>	3'-5' exoribonuclease	(Tuckerman <i>et al.</i> , 2011)

*This table was created based on the information provided in the reviews written by Sondermann *et al.*, 2012; Ryan *et al.*, 2012; and Hengge, 2009.

Basically, the PilZ domain appears to be widespread among bacterial species (Romling *et al.*, 2013), however, the number of PilZ-encoding genes vary from one species to another. The unpublished genome sequence of *A. caviae* Sch3N contains five scattered PilZ-encoding genes, while the genome of *Bdellovibrio bacteriovorus* contains 15 PilZ-encoding genes (Hobley *et al.*, 2012). In addition, the studied PilZ domains were reported to be either single domains or linked to other regulatory or sensing domains (Romling *et al.*, 2013). For example, PilZ domains can be found linked to GGDEF, EAL or HD-GYP domains (Amikam *et al.*, 2006). Moreover, not all PilZ domains are able to bind to c-di-GMP (i.e., non-active domains) (Romling *et al.*, 2013). Once the c-di-GMP molecule binds to an active PilZ domain, it causes conformational changes which eventually leads to the transfer of the signal to the cellular target (Shin *et al.*, 2011).

Once the protein containing the PilZ domain gets activated by binding to c-di-GMP (which has been produced by the cell as a result of receiving a specific signal) it then (the PilZ protein) can regulate certain cellular processes. The two known mechanisms of regulation by PilZ domain include its direct interaction with other proteins and its binding to DNA (Ryan *et al.*, 2012).

The protein-protein interaction mechanism was suggested as to be the mechanism of slowing down the speed of *E. coli* flagella by direct interaction of the PilZ protein (YcgR) with either the MotA stator protein (Boehm *et al.*, 2010) or the interface between the rotor proteins FliG and FliM (Paul *et al.*, 2010) resulting in interrupting the coordinated movement of the flagellar stator and rotor and eventually slowing down the flagella speed by the so called “brake action”. Figure 1.13 illustrates the protein-protein interaction mechanism proposed for the *E. coli* PilZ protein YcgR.

The best example for the second mechanism of regulation by PilZ domain proteins, which is through DNA binding, is the PilZ protein MrkH in *K. pneumoniae* which was found to directly bind to the promoter region upstream of a type 3 fimbriae genes operon and activate its transcription after which the bacterium is able to express fimbriae and form a biofilm (Wilksch *et al.*, 2011) (figure 1.14).

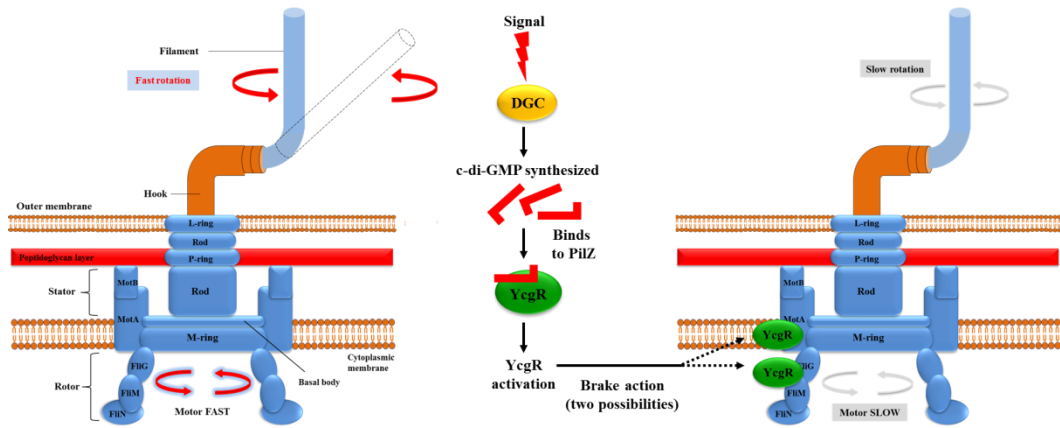


Figure 1.13. The protein-protein interaction mechanism of regulation proposed for the *E. coli* PilZ domain containing protein YcgR. Following synthesis of c-di-GMP by a diguanylate cyclase (DGC) enzyme as a result of receiving a specific signal, c-di-GMP molecule will bind to the PilZ domain contained in the YcgR protein which then becomes activated and proceeds toward slowing down the flagellar motor speed by directly interacting with either the stator protein MotA (Boehm *et al.*, 2010) or the interface between the rotor proteins FliG and FliM (Paul *et al.*, 2010). The model in this figure is based on the model presented in the review written by Armitage and colleagues (Armitage *et al.*, 2010).

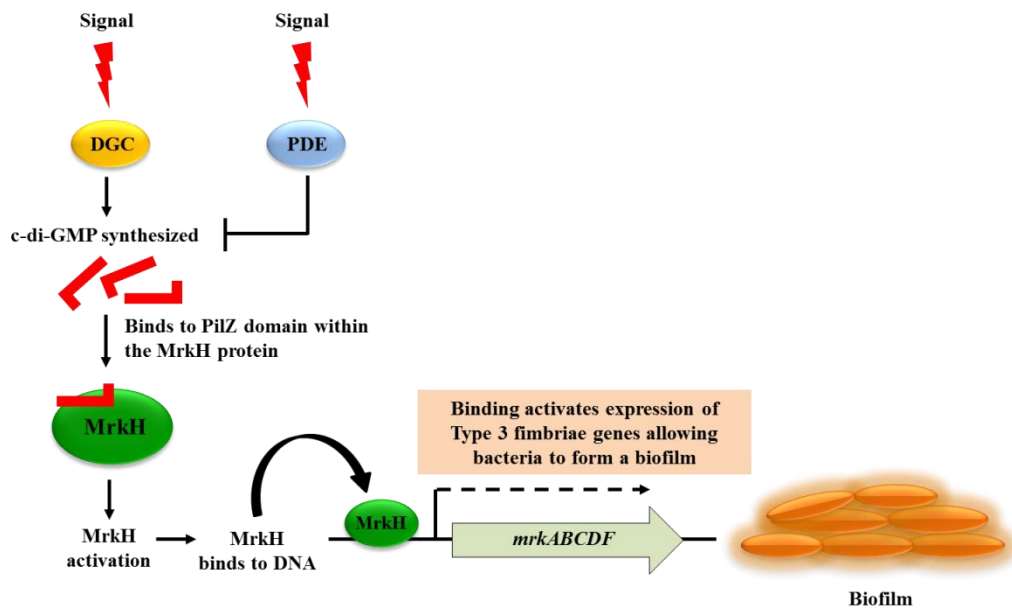


Figure 1.14. Activation of Type 3 fimbriae genes expression by PilZ protein MrkH in *K. pneumoniae* by binding to the promoter region upstream of the operon. This figure is based on the model presented in the study of Wilksch and colleagues (Wilksch *et al.*, 2011).

1.3.6.2. Enzymatically inactive GGDEF and EAL domains

Enzymatically inactive GGDEF domains have been suggested to function as receptors for c-di-GMP through their I-site (Ryan *et al.*, 2012). They are no longer able to synthesize c-di-GMP, however they can function as effectors being part of the c-di-GMP signalling network (Romling *et al.*, 2013). The same principle applies to some enzymatically inactive EAL domains that are unable to breakdown the c-di-GMP any more but still can act as effector molecules which bind to c-di-GMP and help in regulating certain cellular processes (Ryan *et al.*, 2012). Examples of enzymatically inactive GGDEF and EAL domains known to act as c-di-GMP effectors are listed in table 1.7.

According to the review of Romling and colleagues, no enzymatically inactive HD-GYP domains have yet been reported to act as c-di-GMP effector molecules although they, logically, are expected to exist (Romling *et al.*, 2013). Ryan and colleagues have studied the protein PA2572 in *P. aeruginosa* which contains a degenerate HD-GYP domain (YN-GYP) and which they have reported to possess no phosphodiesterase activity (Ryan *et al.*, 2009). Ryan and coworkers have suggested some regulatory roles played by the enzymatically inactive YN-GYP domain in *P. aeruginosa*, as mutations within the protein PA2572 have affected biofilm architecture and the ability of the bacterium to swarm, in addition to causing an overproduction of rhamnolipids (Ryan *et al.*, 2009). The latter study, however, did not confirm the actual binding of c-di-GMP to the YN-GYP domain neither did it explain the exact mechanism of regulation of the above processes by this domain although they have suggested the degenerate domain to function by protein-protein interaction (Ryan *et al.*, 2009). Consequently, we can not consider PA2572 as a c-di-GMP effector until further investigations confirm this role (Ryan *et al.*, 2012).

1.3.6.3. Transcription factors

Transcription factors are proteins which bind to DNA regions and regulate the transcription of certain genes by either facilitating the binding of RNA polymerase to perform transcription (i.e., activators) or they can prevent the process of transcription from occurring (i.e., repressors) (Latchman, 1997). Recently, it has been found out that the activity of some of these transcriptional factors (regulators) can be c-di-GMP responsive, in other words, some of the transcriptional factors can be considered as c-di-

GMP receptors (Romling *et al.*, 2013). Examples of the transcription factors which have been described as c-di-GMP responsive are listed in table 1.7.

Of notable importance is the FleQ protein in *P. aeruginosa* which has been described to act as both an activator and a repressor (Baraquet *et al.*, 2012). Basically, FleQ protein has two important regulatory roles to play in *P. aeruginosa*, first, it functions as the major (positive) regulator for genes responsible for polar flagellum biosynthesis, second, it regulates the expression of genes responsible for exopolysaccharides production (and thus biofilm formation) (Baraquet *et al.*, 2013). FleQ is an enhancer binding protein (EBP) (Dasgupta *et al.*, 2001) which is composed of three domains namely, a FleQ domain (N-terminus), an AAA [ATPase] domain (centre), and a helix-turn-helix (HTH) DNA-binding domain (C-terminus) (Hickman *et al.*, 2008). FleQ binds to promoters of the genes and operons under its control through its HTH domain and activates or represses their transcription.

Dasgupta and colleagues have identified FleN protein in *P. aeruginosa* which its activity is directly related to that of FleQ (Dasgupta *et al.*, 2000), as will be discussed below. The identified FleN does not possess a DNA binding domain (Dasgupta *et al.*, 2001), however, it does contain an ATP-binding motif in its N-terminus (Dasgupta *et al.*, 2000). Originally, FleN was suggested to play a role in controlling the flagellar number and chemotaxis in *P. aeruginosa* (Dasgupta *et al.*, 2000). Mutating *fleN* gene resulted in *P. aeruginosa* cells to produce multiple flagella (a tuft) at one pole instead of producing the characteristic single polar flagellum (Dasgupta *et al.*, 2000). In addition, *fleN* deletion causes *P. aeruginosa* cells to lose their chemotactic ability as they were randomly moving (tumbling) when examined under the microscope (Dasgupta *et al.*, 2000). The relationship between FleN and FleQ has been noticed when this deletion of *fleN* was found to result in further upregulation of the expression of *P. aeruginosa* flagellar genes and operons originally upregulated by FleQ (Dasgupta *et al.*, 2000). Thus, FleN seem to have an inhibitory effect against FleQ during the synthesis of *P. aeruginosa* polar flagellum (Dasgupta *et al.*, 2000).

Few studies have been published which provide useful information about the probable mechanism of flagellar genes regulation by FleQ (Dasgupta *et al.*, 2000, Dasgupta *et al.*, 2001, Dasgupta *et al.*, 2002) and the role of c-di-GMP in this regulation (Baraquet *et al.*, 2013). Based on the four sources, we provide a model for FleQ

flagellar regulation in Figure 1.15. FleN was found to specifically interact with FleQ using a yeast two hybrid system (Dasgupta *et al.*, 2001). ATP binding to FleN seems to cause changes in its folding and results in a specific conformation which might be important for its binding to FleQ (Dasgupta *et al.*, 2001). A direct binding of FleN to FleQ results in the formation of a FleN-FleQ complex after which the whole complex binds to any of the flagellar genes promoters under the control of FleQ, in other words, FleN does not seem to prevent FleQ from binding to DNA (Dasgupta *et al.*, 2001). FleQ activity requires the binding of ATP to its Walker A site after which ATP is hydrolysed and FleQ proceeds with its positive regulatory action (Baraquet *et al.*, 2013). According to a recent study, FleN might inhibit the ATPase activity of FleQ (Baraquet *et al.*, 2013). More importantly, further inhibition of FleQ ATPase activity (and consequently flagellar biosynthesis) seems to come from c-di-GMP which competitively inhibits ATP binding to FleQ by itself being able to bind to the Walker A (ATP binding) motif of FleQ and thus rendering FleQ inactive and consequently unable to activate flagellar genes expression in *P. aeruginosa* (Baraquet *et al.*, 2013).

Opposite to its activity in the setting of flagellar genes expression, FleQ acts as a repressor for the exopolysaccharide genes in *P. aeruginosa*, until the level of c-di-GMP become high enough to bind to FleQ and activates polysaccharide biosynthesis gene expression. Two published studies have investigated the mechanism of regulation of the *pel* operon by the c-di-GMP-responsive FleQ protein in *P. aeruginosa* and suggested a model for such regulation.

The first model was proposed by Hickman and colleagues (Hickman *et al.*, 2008). As shown in figure 1.16, when c-di-GMP level is low, FleQ is suggested to bind to the *pel* promoter in a location which prevents the RNA polymerase from binding to DNA to initiate transcription of exopolysaccharides genes. Binding of FleN to FleQ weakens the ATPase activity of FleQ as well as the strength of its binding to the *pel* promoter. Elevation of c-di-GMP level and binding of the second messenger to the central AAA domain of FleQ is suggested by the authors to lead to a complete dissociation of the FleQ/FleN complex from the *pel* promoter and thus allowing for binding of RNA polymerase to DNA to perform transcription of the exopolysaccharide biosynthesis genes in *P. aeruginosa*.

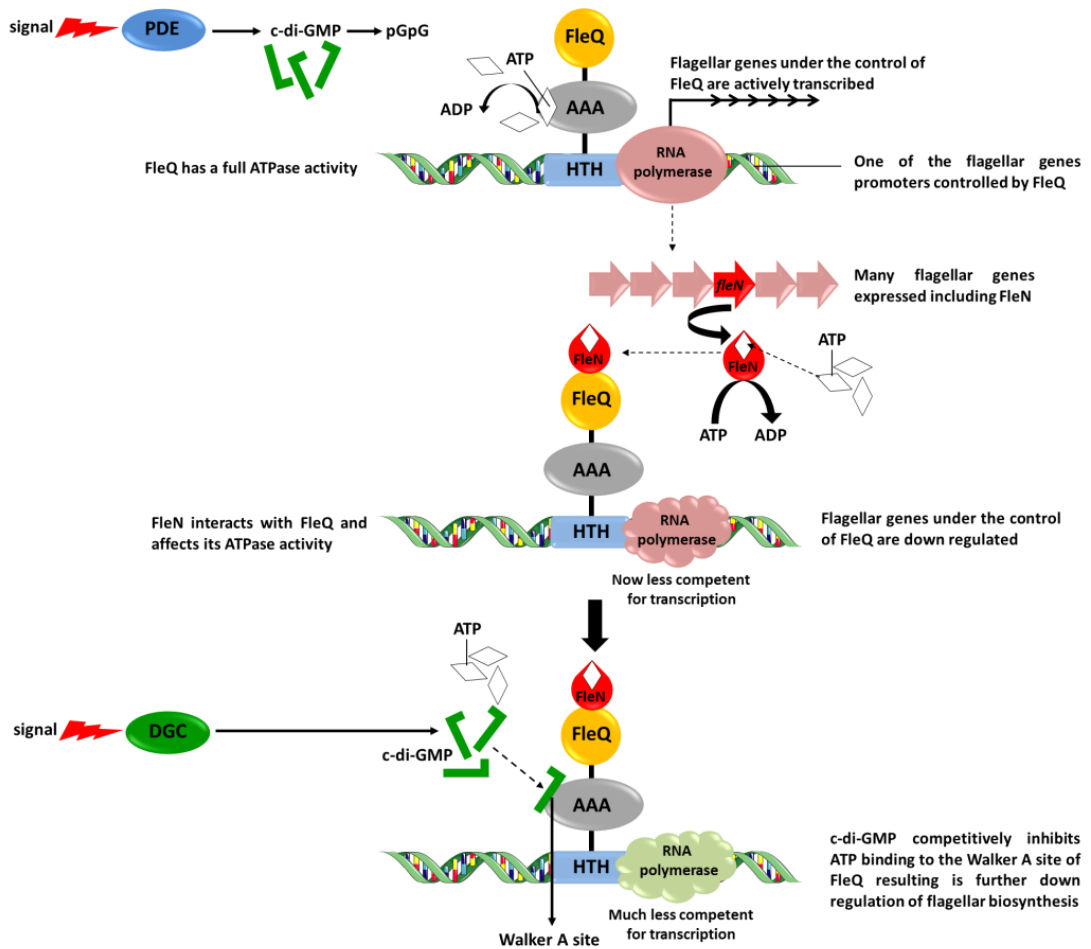


Figure 1.15. The proposed model for the regulation of *P. aeruginosa* polar flagellar genes expression mediated by the transcription factor FleQ. FleQ protein is composed of the FleQ domain, AAA (ATP binding) domain, and HTH (DNA binding) domain. FleQ binds to the promoters of the genes and operons under its control in order to activate their expression and consequently flagellar biosynthesis in the absence of c-di-GMP. ATP hydrolysis by FleQ is required activate flagellar genes expression. Along with the expressed flagellar genes is the FleN protein which then binds to FleQ and allows for some degree of down regulation of its ATPase activity. Elevated levels of c-di-GMP results in further down regulation of flagellar genes expression following c-di-GMP binding to the Walker A (ATP binding) motif of FleQ and thus competitively inhibiting ATP binding which is required for FleQ activity. Thus, c-di-GMP strongly inhibits FleQ ATPase activity and flagellar biosynthesis in *P. aeruginosa*. More studies are required to confirm this regulatory model. This figure is based on all references indicated in the text.

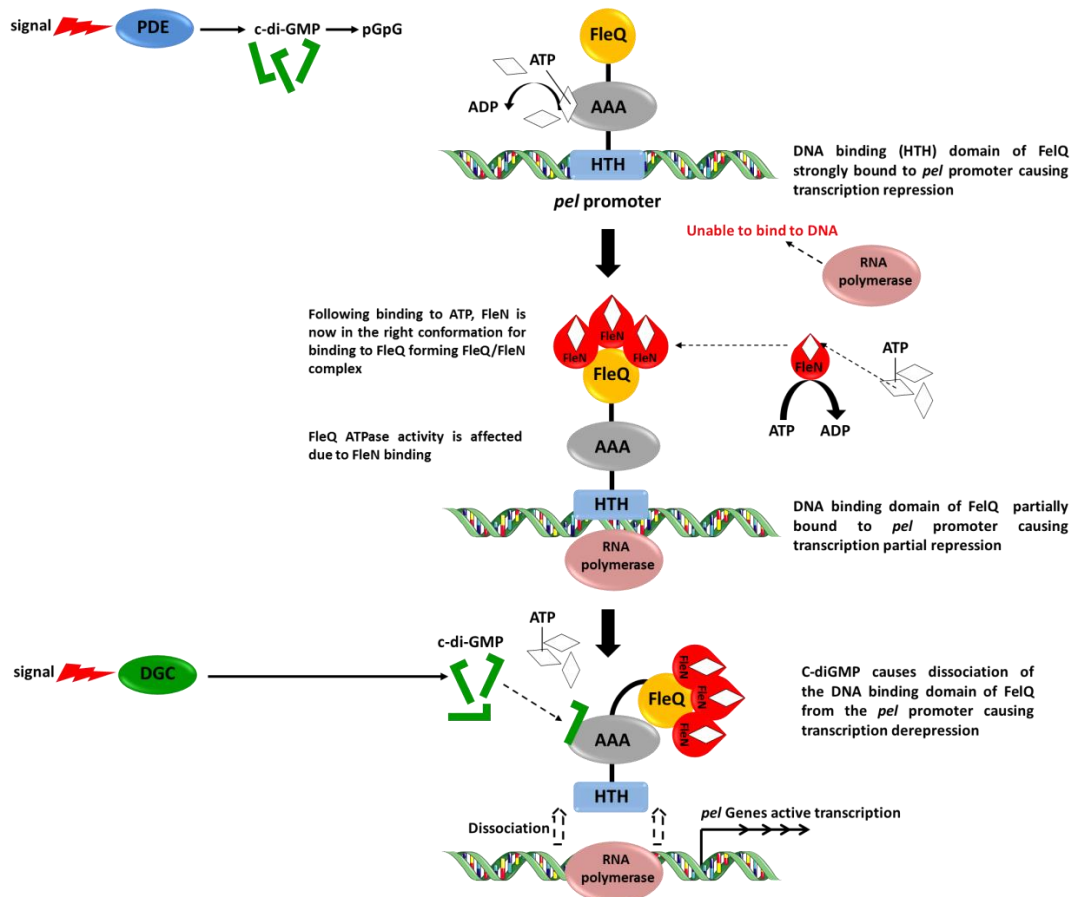


Figure 1.16. First model of *pel* promoter regulation by FleQ transcription factor as suggested by Hickman and colleagues (Hickman *et al.*, 2008). Pel polysaccharides are expressed during the high level of c-di-GMP which binds to the AAA central domain of the FleQ transcription factor and causes detachment of the HTH domain of FleQ from the *pel* promoter and consequently derepressing (activating) the transcription of *pel* genes in *P. aeruginosa*.

The second model was proposed by Baraquet and colleagues who suggested FleQ to bind to two positions on the *pel* promoter after which FleN interacts with FleQ and leads to distortion of *pel* promoter and as a result repression of exopolysaccharide gene transcription (figure 1.17) (Baraquet *et al.*, 2012). Once the c-di-GMP level is high enough, the second messenger is suggested to bind to FleQ (at the AAA site) and causes conformational changes to the FleQ resulting in the relief of DNA distortion and activation of exopolysaccharide gene transcription leading to the formation of a biofilm.

FleQ is the best studied c-di-GMP-dependent transcriptional factor, however, more studies are required to confirm the proposed models for its mechanism of action. FleQ homologous proteins in other bacteria include FlrA in both *Aeromonas* species and *V. cholerae* as well as FlaK in *V. parahaemolyticus* (Dasgupta *et al.*, 2002), the three FleQ homologues are considered the major regulators for polar flagellum biosynthesis in their corresponding species. Possibly these indicated homologous flagellar regulators follow a similar mechanism of regulation as the FleQ.

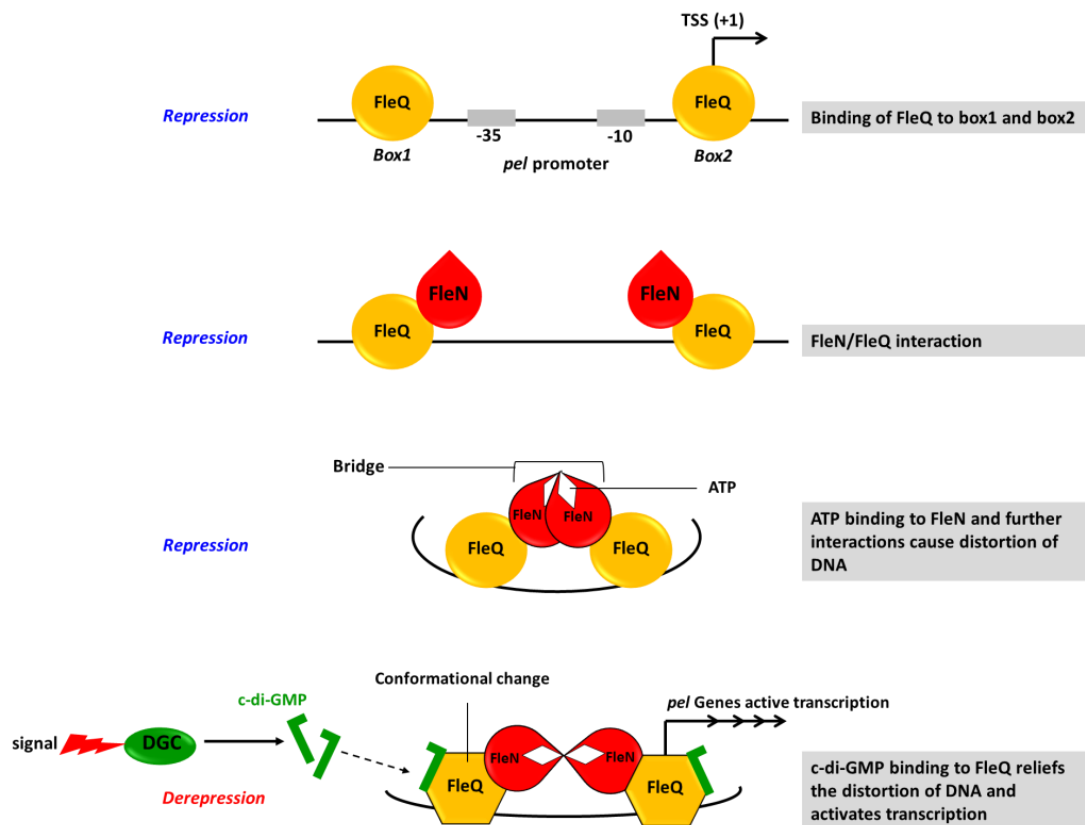


Figure 1.17. The second suggested model of repression and derepression of *pel* genes transcription in *P. aeruginosa* by the transcription factor FleQ in the presence of ATP and c-di-GMP. The mechanism is based on binding of FleQ to two positions within the *pel* promoter followed by its interaction with FleN. The presence of ATP will take the FleQ/FleN interaction a further step by allowing bridge formation between the two bound FleQ proteins and distortion of DNA. The presence of c-di-GMP induces conformational changes in FleQ a step that is required for *pel* genes expression. The steps presented in this figure are based on the suggested model presented in the study of Baraquet and colleagues (Baraquet *et al.*, 2012). This is a proposed model and not considered a final and complete one.

1.3.6.4. Polynucleotide phosphorylase (PNPase)

Tuckerman and colleagues have described a ribonucleoprotein complex (RNA degradosome) in *E. coli* which mainly functions in mRNA degradation in a c-di-GMP dependent manner (Tuckerman *et al.*, 2011). The proteins composing the degradosome include the enzyme PNPase (which directly degrades mRNA molecules), DosC protein (which acts as a diguanylate cyclase), DosP protein (which function as a phosphodiesterase), in addition to other enzymes including RNase E, enolase, and RNA helicase. The degradation of mRNA by PNPase depends on its activation by c-di-GMP which depends on the presence and absence of O₂ (figure 1.18).

The O₂ sensors DosC and DosP regulate mRNA degradation in a c-di-GMP-dependent manner. In the absence of O₂, the GGDEF domain-containing protein DosC will synthesize c-di-GMP which then binds to the PNPase enzyme after which the enzyme becomes active and degrades the selected mRNA molecule. In the presence of O₂, the EAL domain-containing protein DosP will hydrolyze c-di-GMP resulting in the PNPase enzyme to be inactive and lose its ability to degrade mRNA molecules.

Tuckerman and co-workers have experimentally confirmed the direct binding of c-di-GMP to PNPase and have measured their dissociation constant K_d to equal to 2.9 μ M. PNPase has been categorized as one of the c-di-GMP effectors (Ryan *et al.*, 2012, Sondermann *et al.*, 2012) and its role (described above) clearly demonstrates the direct involvement of c-di-GMP in regulating the stability of mRNA molecules within bacterial cells (Tuckerman *et al.*, 2011). Tuckerman and colleagues have linked their findings with the well known role of c-di-GMP in controlling the switch of bacteria from a motile lifestyle to a biofilm state indicating that controlling the stability of certain subsets of mRNA during the presence and absence of O₂ seems to be a mechanism by which c-di-GMP controls the formation of a biofilm. They also suggested the existence of other degradosomes in which c-di-GMP activation of PNPase is mediated by signals other than O₂, and thus, the role of c-di-GMP in controlling the stability of mRNA can be taken to a broader range reflecting the large number of processes controlled by the second messenger.

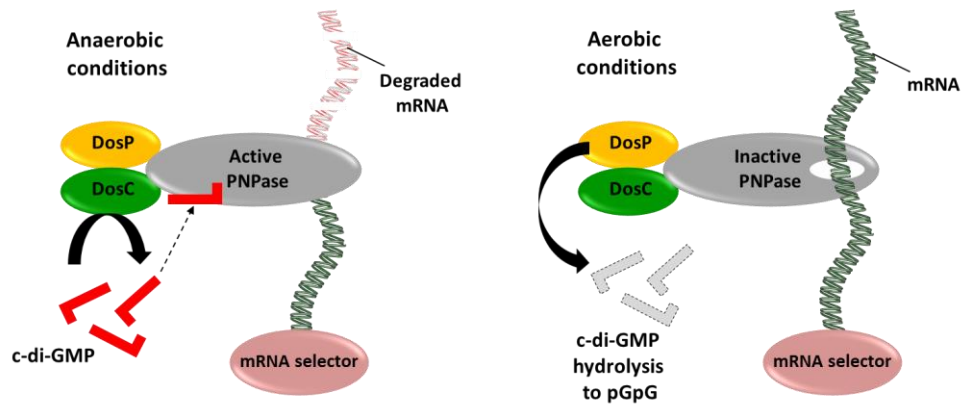


Figure 1.18. The model of the *E. coli* degradosome containing the c-di-GMP effector polynucleotide phosphorylase (PNPase) enzyme, a direct O₂-sensing cyclase (DosC) which contains a GGDEF domain and which synthesizes c-di-GMP, a direct O₂-sensing phosphodiesterase (DosP) which contains an EAL domain and which hydrolyzes c-di-GMP to pGpG, and an mRNA selector which can be either a small RNA molecule or an RNA binding domain. This figure is based on the model presented in the study of Tuckerman and colleagues (Tuckerman *et al.*, 2011).

1.3.6.5. Riboswitches

Riboswitches are RNA domains which are present in the 5'-UTR region of many genes and which basically perform regulatory functions within the cell being directly involved in controlling gene expression (Hengge, 2009). Riboswitches are formed when a non-coding mRNA molecule folds and forms a complex structure (Romling *et al.*, 2013) which is composed of an aptamer and an expression platform (Breaker, 2008) (Figure 1.19). The regulatory function of the riboswitch depends on its binding (through its aptamer) to a ligand (an ion or a small molecule) which causes changes in the riboswitch structure and consequently affects the expression of genes under the control of the riboswitch (Romling *et al.*, 2013). Binding of a ligand to the riboswitch aptamer stabilizes its structure (Furukawa *et al.*, 2012) after which the aptamer can either induce or repress genes expression (Ryan *et al.*, 2012) by modulating the folding of the expression platform (Furukawa *et al.*, 2012). The riboswitches can thus be divided to either an "OFF" or an "ON" riboswitch and can control genes at either transcriptional or translational levels (Smith *et al.*, 2011a).

Termination of transcription by an "OFF riboswitch" can be achieved by one of two mechanisms (Breaker, 2008). The first one is a Rho-independent transcription termination mechanism (Weinberg *et al.*, 2007) which depends on the formation of a

hairpin (stem-loop) structure which acts as a transcription terminator (hence the term “OFF riboswitch”) and then the formation of another hairpin which acts as an anti-terminator which allows gene expression to proceed depending on the concentration of the ligand molecule (Breaker, 2008). The second mechanism by which an “OFF riboswitch” terminates transcription occurs simply when the ribosomal binding site becomes hidden due to its sequence being overlapped with the riboswitch (Weinberg *et al.*, 2007), more specifically, when the ribosomal binding site becomes located within the ligand-bound aptamer and will not be exposed for ribosomal binding until the transcription of genes becomes necessary (Breaker, 2008). On the other hand, the “ON riboswitches” do activate the transcription of genes under their control by simply reversing the principle of the above mentioned mechanisms of inhibition used by the “OFF riboswitch” (Breaker, 2008).

Riboswitches can bind to their metabolites with a very high affinity ($K_d =$ picomolar to nanomolar range) and they are able to differentiate between highly similar ligands based on the differences in their affinities (Breaker, 2008). The time factor is very important for the control of genes expression by a riboswitch, and thus, riboswitches are suggested to use different strategies to respond to a wide range of their ligand concentration (Breaker, 2008). For example, riboswitches may exist in tandem or may possess multiple aptamers (but a single expression platform) to catch their ligand very quickly and decide whether to terminate or allow the expression of genes under their control (Breaker, 2008). Moreover, the latter arrangement of riboswitches in tandem or their possession of multiple aptamers may allow interaction with different metabolites during different conditions to control the expression of a single gene (or a single operon). Perhaps a single riboswitch can have the ability to differentiate between and bind to different metabolites without having to exist in tandem or to possess multiple aptamers (Breaker, 2008). Riboswitches, thus, seem to be a powerful tool to control genes expression and are worth more future studies. Until today, thousands of riboswitches have been identified and they been grouped to different classes based on the metabolite they sense (Sudarsan *et al.*, 2008).

C-di-GMP is one of the many small molecules sensed by riboswitches, with its binding to riboswitches been described as highly specific and with high affinity (Romling *et al.*, 2013). Two types (or classes) of c-di-GMP-specific riboswitches exist with their division to two types being based on the different sequences of their aptamers

(Sondermann *et al.*, 2012) as well as on the presence of some structural differences (Lee *et al.*, 2010). Examples of the studied c-di-GMP-types I and II are listed in table 1.7.

The c-di-GMP type-I riboswitch is mainly found in the mRNA (i.e., in the 5'-UTR) of a group of genes commonly referred to as GEMM (for genes of environment, membrane, and motility) (Hengge, 2009). As a result, in the medical literature, c-di-GMP type-I riboswitch is also referred to as the GEMM conserved motif. As c-di-GMP is directly involved in motility, biofilm formation, and the expression of virulence factors, then its relationship to the GEMM motif (by being its ligand) seems to be direct and strong. Chapter 5 of this study provides extensive details about the *lafK* riboswitch present upstream of the gene encoding the lateral flagellar major regulatory protein LafK in *A. caviae*. The *lafK* riboswitch belongs to the c-di-GMP type-I riboswitches (GEMM motif) and which we believe is involved in c-di-GMP-mediated lateral flagellar genes expression. The c-di-GMP-type-II riboswitch Cd84 has been detected in a self-splicing ribozyme in *C. difficile* (Lee *et al.*, 2010). The activity of the studied ribozyme has been experimentally proven to be c-di-GMP-controlled and the structure of the detected riboswitch was found to be different from that of c-di-GMP-type-I.

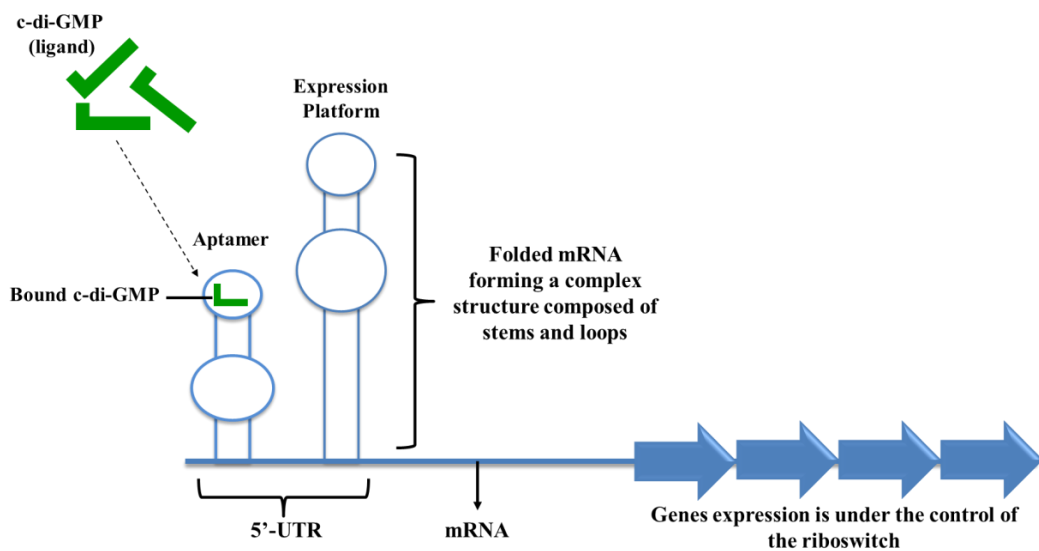


Figure 1.19. The two domain architecture of a riboswitch upstream of genes under its control. The riboswitch is composed of an aptamer, to which ions and metabolites bind, and an expression platform which undergoes structural rearrangements following binding of the ligand to the aptamer resulting in activation or repression of gene expression.

1.3.7. Targets of c-di-GMP

Although the targets of c-di-GMP have been directly or indirectly mentioned during the above discussion of the c-di-GMP effectors, we shall briefly mention them here. Firstly, c-di-GMP can target genes transcription (Hengge, 2009). An example is the control of the *pel* operon transcription and the flagellar genes transcription by c-di-GMP in *P. aeruginosa* through the effector protein FleQ (Hickman *et al.*, 2008). Secondly, translation initiation can as well be a target for c-di-GMP, for example riboswitches can control translation of genes following modulation of their structure as a result of c-di-GMP binding (Hengge, 2009). Thirdly, c-di-GMP can directly control the activity of certain enzymes which were found to contain a PilZ domain as part of their structure (Hengge, 2009). For example, c-di-GMP (after binding to the PilZ domain) can control the activity of the enzyme cellulose synthase (responsible for cellulose synthesis) in *Acetobacter xylinum* (Amikam *et al.*, 2006) and the activity of the enzyme Alg44 (responsible for synthesis and transportation of alginate) in *P. aeruginosa* (Merighi *et al.*, 2007). Finally, complex structures within the bacterial cell can as well be targets for the action of c-di-GMP (Hengge, 2009). The best example is the PilZ domain-containing protein YcgR in *E. coli* which (following binding to c-di-GMP) was found to directly bind to the flagellar motor proteins (a complex cellular structure) and causing the flagellar movement to slow down after direct protein-protein interaction (Armitage *et al.*, 2010). Figure 1.20 illustrates c-di-GMP turnover, its receptors and targets, and finally its outputs.

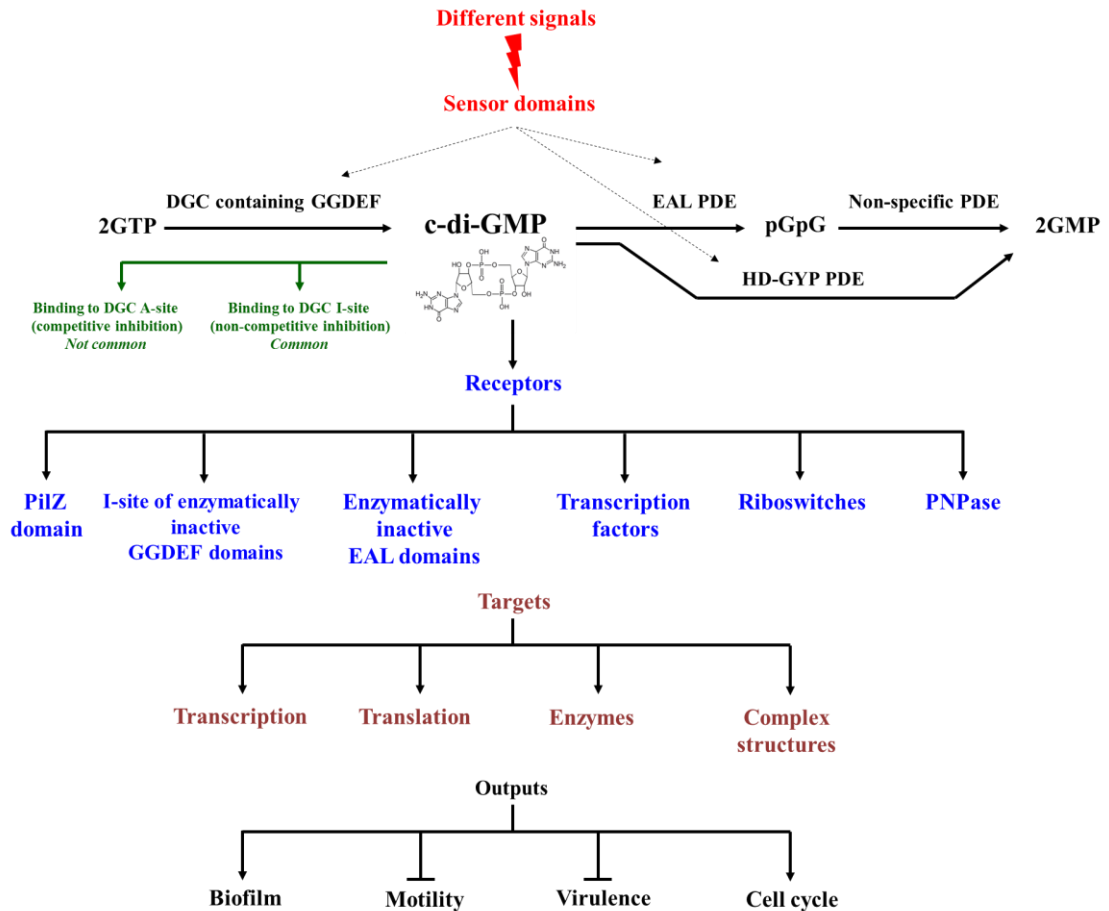


Figure 1.20. C-di-GMP turnover, its basic signalling module, and its functions within the bacterial cell. The diguanylate cyclases are responsible for c-di-GMP synthesis while the phosphodiesterases are the enzymes responsible for the breakdown of the second messenger. Upon its formation, c-di-GMP binds to a variety of effector domains and causes them to undergo conformational changes which leads to the transfer of the signal to many target processes or structures leading to outputs mainly related to motility, sessility, virulence and cell cycle progression.

1.3.8. The c-di-GMP signalling network in *Aeromonas* species

Searching the medical literature revealed the existence of only three studies which has investigated the role of c-di-GMP signalling in *Aeromonas* spp. (Rahman *et al.*, 2007, Kozlova *et al.*, 2011, Kozlova *et al.*, 2012) Below is a review of the major findings of the three studies.

1.3.8.1. Role of c-di-GMP in controlling the switch between motility and sessility in *Aeromonas* species.

It is generally accepted that the production of c-di-GMP is coupled with the ability of bacterial cells to form a biofilm while a low concentration of the second messenger in the cell enhances a motile lifestyle, as illustrated in figure 1.21 (Tamayo *et al.*, 2007). All types of bacterial motility including swimming, swarming, and twitching are inhibited when c-di-GMP levels in the cell are elevated (Tamayo *et al.*, 2007). These findings came from studies which investigated several domains with DGC and PDE activities in different Gram-negative bacteria, including, *P. aeruginosa*, *Salmonella* Typhimurium, *Y. pestis*, *Vibrio cholerae*, and *V. parahaemolyticus*. In a study by Rahman and colleagues, the researchers introduced a GGDEF domain-containing protein AdrA and the EAL domain-containing protein YhjH separately into *A. veronii* biovar *sobria* and found that the c-di-GMP level has significantly increased in the strain containing the protein AdrA (Rahman *et al.*, 2007). In addition, the strain containing the GGDEF domain showed a reddish colony morphotype on Congo Red agar and its ability to form a biofilm on the wall of glass tubes was noticeably enhanced. The opposite phenotype was obtained for the strain containing the YhjH protein which was described as less able to produce extracellular polysaccharides and thus its sessile lifestyle could not be manifested. The strain overexpressing the EAL domain-containing protein was shown to be actively motile by testing its ability to swim using 0.3% agar plates.

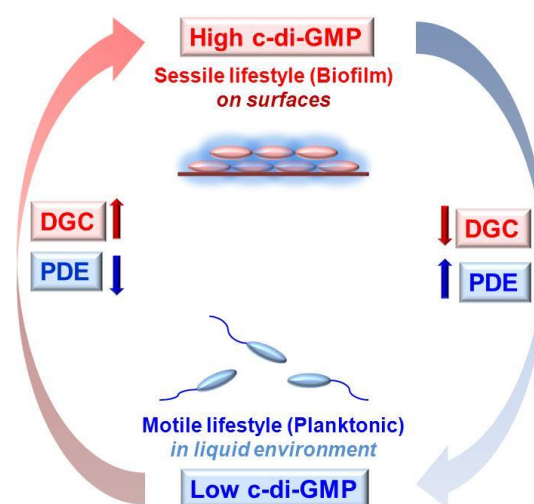


Figure 1.21. A Diagram showing the role played by c-di-GMP in controlling sessility and motility in *Aeromonas* spp. Based on information provided by Tamayo and colleagues (Tamayo *et al.*, 2007).

1.3.8.2. Interrelation between c-di-GMP signalling system and quorum sensing (QS) system in *Aeromonas* species.

Kozlova and colleagues have recently published two important studies in which they examined the relationship between the quorum sensing system and c-di-GMP signalling system in *A. hydrophila* SSU (Kozlova *et al.*, 2011, Kozlova *et al.*, 2012). Quorum sensing (cell-cell signalling) is the ability of bacteria to communicate by producing certain chemicals called autoinducers (AI) (Miller *et al.*, 2001, Safari *et al.*, 2014). Quorum sensing allows bacteria to control gene expression upon reaching a certain cellular density which is sensed by the group of cells as a result of the accumulation of the AIs (Miller *et al.*, 2001). Bacterial cell-cell signalling is very well known to regulate a large number of cellular processes examples of which include motility, biofilm formation, virulence, and antibiotic production (Miller *et al.*, 2001). As mentioned elsewhere in this study, c-di-GMP signalling system is also involved in controlling motility, biofilm formation, and virulence, and so attempts to study the interrelation between the quorum sensing system and the c-di-GMP signalling system seems to be a wise step.

The strain *A. hydrophila* SSU is known to possess three QS systems (Kozlova *et al.*, 2012). The first one is the *N*-acylhomoserine lactone (AHL)-based system (also referred to as AI-1 or *ahyRI* system) (Khajanchi *et al.*, 2009), the second one is the *S*-ribosylhomocysteinase (LuxS)-based system (also referred to as AI-2 system) (Kozlova *et al.*, 2008), and the third one is the QseBC system (Kozlova *et al.*, 2012). Kozlova and co-workers have carried extensive experiments to investigate a possible interrelation between the three QS systems and also between the QS systems and the c-di-GMP signalling system in *A. hydrophila* SSU.

In their first study, Kozlova and colleagues focused on the AI-1 and AI-2 systems in *A. hydrophila* SSU (Kozlova *et al.*, 2011). They have attempted to determine the existence of any interplay between the two QS systems by generating two mutant strains *A. hydrophila* Δ *ahyRI* (in which the AI-1 system was deleted) and *A. hydrophila* Δ *luxS* (in which the AI-2 system was deleted). This was followed by testing the transcriptional level for *ahyR* and *ahyI* genes using the *A. hydrophila* Δ *luxS* mutant as a background, and testing the transcriptional level of *luxS* in *A. hydrophila* Δ *ahyRI*. The transcription level was determined by first performing an RT-PCR followed by performance of densitometric analysis to quantify the level of cDNA.

The authors found the transcription of the *luxS* gene to be upregulated when checked in the Δ *ahyRI* background in comparison to its transcriptional level in the wild type strain *A. hydrophila* SSU (Kozlova *et al.*, 2011). They also found the transcriptional level of both genes *ahyR* and *ahyI* to be down regulated in the *A. hydrophila* Δ *luxS* background in comparison to their transcriptional level in the wild type strain (Kozlova *et al.*, 2011). Furthermore, the transcription of each of the two genes *ahyR2* and *ahyR3* in the background *A. hydrophila* Δ *luxS* was higher in level than its level in the wild type strain *A. hydrophila* SSU (Kozlova *et al.*, 2011). It should be mentioned here that the *ahyR2* and *ahyR3* genes were previously identified by the same group as homologs to the *ahyR* gene during their sequence analysis of the *A. hydrophila* SSU genome (Kozlova *et al.*, 2011). The above results allowed Kozlova and co-workers to conclude that the two QS systems AI-1 and AI-2 in *A. hydrophila* SSU are connected at the transcriptional level.

Kozlova and colleagues have also tested the transcription of genes other than the *ahyRI* and *luxS* which were encoded in the genome of *A. hydrophila* SSU and are known to be involved in biofilm formation and motility using the backgrounds *A. hydrophila* Δ *ahyRI* and *A. hydrophila* Δ *luxS* (Kozlova *et al.*, 2011). These investigated genes included *litR* (similar to *hapR* in *V. cholerae* which encodes the transcription factor HapR implicated in controlling the expression of genes involved in biofilm formation), *csgAB* (similar to *vpsT* in *V. cholerae* which is a transcriptional activator involved in polysaccharide gene expression), *fleQ* (homologous to the *fleQ* gene encoding FleQ protein, the flagellar genes expression master regulator in *P. aeruginosa*), and *fleN* (homologous to the FleQ anti-activator encoding gene, *fleN*, in *P. aeruginosa*).

In comparison to the wild type strain *A. hydrophila* SSU there was an upregulation of the genes *litR* and *fleQ* genes transcription and a lower transcription level for the genes *csgAB* and *fleN* in *A. hydrophila* Δ *luxS* (Kozlova *et al.*, 2011). There were, however, different effects on the deletion of *ahyRI* on the transcription of the latter genes in *A. hydrophila* SSU. A down regulation for *litR* transcription and an upregulation of the *fleN* gene were reported in the background *A. hydrophila* Δ *ahyRI* (opposite to their transcription level when *luxS* was deleted) (Kozlova *et al.*, 2011). In addition, the transcriptional level of the two genes *fleQ* and *csgAB* in both *A. hydrophila* Δ *ahyRI* and the wild type strain has not changed (Kozlova *et al.*, 2011). The

transcriptional level analysis of these genes supports the above mentioned conclusion of Kozlova and co-workers that the AI-1 and AI-2 QS systems in *A. hydrophila* SSU are interrelated at the transcriptional level.

Kozlova and colleagues have then overexpressed the GGDEF domain AHA0701h (a diguanylate cyclase enzyme encoded in the genome of *A. hydrophila*) in the wild type strain *A. hydrophila* SSU and the mutant strain *A. hydrophila* Δ *ahyRI* (Kozlova *et al.*, 2011). The over expression was based on cloning *AHA0701h* into pBAD/Myc-HisB. As expected, the elevated level of c-di-GMP caused an increase in biofilm density by the wild type strain which was detected after 24 hrs. There was, however, a very little increase in the biofilm formed by the mutant strain *A. hydrophila* Δ *ahyRI* overexpressing the GGDEF domain and which was detected after 48 hrs of incubation (Kozlova *et al.*, 2011). This indicated that the AI-1 QS system and the c-di-GMP signalling system might be interconnected to allow the *A. hydrophila* SSU to form a biofilm.

Furthermore, the upregulation of the *luxS* gene transcription previously noticed in the mutant *A. hydrophila* Δ *ahyRI* was reduced again and normalized to the transcriptional level observed in the wild type strain following overexpressing the GGDEF domain in the *A. hydrophila* Δ *ahyRI* mutant (Kozlova *et al.*, 2011). The last fact allowed Kozlova and co-workers to suggest a modulation of the transcription of certain QS genes by the second messenger c-di-GMP.

To further confirm the possible modulation of the transcription of QS-associated genes by c-di-GMP, the same group of researchers have overexpressed the GGDEF domain AHA0701h in *A. hydrophila* Δ *ahyRI* followed by determining the transcriptional level of the same above tested genes which are involved in biofilm and motility (Kozlova *et al.*, 2011). The transcription level of both *litR* and *fleQ* was higher than the wild type strain while that of the *csgAB* was lower than the wild type strain (Kozlova *et al.*, 2011). Also there was a down regulation for the transcription of the genes *luxS*, *ahyR2*, and *ahyR3* due to the overexpression of the GGDEF domain in *A. hydrophila* Δ *ahyRI* compared to *A. hydrophila* SSU (Kozlova *et al.*, 2011). The transcriptional profile for these genes was different from when measured in the mutant strain *A. hydrophila* Δ *ahyRI* before the overexpression of the GGDEF domain. The authors found these results to support their previous suggestion that the c-di-GMP does

modulate the functions of QS systems AI-1 and AI-2 in *A. hydrophila* SSU by modulating the transcription of genes under their control.

In their second study, Kozlova and co-workers focused on the third QS (QseBC) system in *A. hydrophila* SSU and its connection with the other QS systems and with the c-di-GMP signalling system in the same bacterium (Kozlova *et al.*, 2012). The genes *ahyRI*, *luxS*, and *qseB* were separately deleted from the genome of *A. hydrophila* SSU followed by testing the transcription of each of these genes in the other two backgrounds.

An increase in the transcription level of *qseB* and *qseC* was detected in *A. hydrophila* Δ *ahyRI*, however, there was a down regulation of the *ahyR* and *ahyI* transcription following the separate deletion of *qseB* and *luxS* (Kozlova *et al.*, 2012). This seems to indicate that the three QS systems in *A. hydrophila* SSU are interconnected at the transcriptional level.

Kozlova and colleagues have then overexpressed the above mentioned GGDEF domain AHA0701h in different backgrounds to observe any interrelation between the three QS systems and the c-di-GMP system in *A. hydrophila* SSU (Kozlova *et al.*, 2012). Over production of c-di-GMP in Δ *ahyRI* background has caused the previously high *qseB* and *qseC* transcription to be normalized to their level of transcription in the wild type strain which seems to indicate that QS in *A. hydrophila* SSU is c-di-GMP dependent (Kozlova *et al.*, 2012).

Overproduction of AHA0701h in the wildtype strain resulted in a noticeable reduction in swarming but no effect on swimming and the strain was able to form a thick biofilm on the surface of polystyrene tubes (Kozlova *et al.*, 2012). Overproduction of AHA0701h in the *A. hydrophila* Δ *qseB* resulted in a swarming migration zone similar to the one formed by *A. hydrophila* pBAD::*AHA0701h* (Kozlova *et al.*, 2012). The mutant strain *A. hydrophila* Δ *qseB* was, however, completely unable to swim and formed less biofilm on the surface of polystyrene tubes when c-di-GMP level was artificially elevated (Kozlova *et al.*, 2012). This result also supports the authors previous conclusion that the QseBC system and the c-di-GMP signalling system are interrelated.

1.4. Hypothesis of this study

As several GGDEF-EAL containing proteins were determined to possess diguanylate cyclase and/or phosphodiesterase activities in Gram negative bacteria, and as c-di-GMP was reported to be used by some bacterial cells to control motility and biofilm formation, we think that mutations in the GGDEF-EAL encoding genes in *A. caviae* will affect the turnover of the second messenger and consequently will give phenotypic manifestations and molecular indications on the general role played by c-di-GMP in determining the lifestyle of *A. caviae*.

The lateral flagella system of *Aeromonas* plays a direct role in both swarming motility and biofilm formation. As the lateral flagellar operon (*laf*) includes two important genetic regions, the first one is an ORF which is similar in sequence to the PilZ domain (a c-di-GMP effector previously studied in several bacteria) and the second one is a GEMM motif which is similar in sequence to the well studied Vc2 c-di-GMP type I riboswitch in *V. cholerae* (and which is located upstream of the gene encoding LafK, the potential major regulatory protein for *laf* operon expression) we think that c-di-GMP in *A. caviae* directly controls the expression of lateral flagella using PilZ and/or *lafK* riboswitch as effectors. We believe that genetic manipulations affecting PilZ domain and *lafK* riboswitch in *A. caviae* will have phenotypic and molecular manifestations which will provide a direct evidence of the specific role of c-di-GMP in controlling lateral flagella expression in *A. caviae*.

1.5. Objectives of this study

1. To mutate thirteen GGDEF-EAL encoding genes in *A. caviae* genome followed by determining the effects of such mutations phenotypically and on the activities of the three lateral flagellar promoters *lafA1p*, *lafA2p*, and *lafKp*.
2. To mutate *pilZ* gene and observe the phenotypic effects of this mutation as well as its effect on the activity of the three lateral flagellar promoters *lafA1p*, *lafA2p*, and *lafKp*.
3. To delete and dissect the *lafK* riboswitch followed by performing transcriptional fusions to detect the effect of its complete deletion or some of its parts on the activity of the *lafK* promoter.

Chapter 2

Materials and Methods

Chapter 2: Materials and methods

2.1. Bacterial strains and plasmids

The names and characteristics of the bacterial strains and plasmids used in this study are provided in tables 2.1 and 2.2, respectively.

2.2. Bacterial growth and maintenance conditions

2.2.1. Liquid media

Brain Heart Infusion Broth (BHIB), Luria-Bertani (LB) broth, and Super Optimal Broth (SOB) were used to grow bacterial strains with the addition of appropriate antibiotics or other supplements. LB broth was prepared by mixing the following components: 1% (w/v) tryptone (Oxoid, UK), 0.5% (w/v) yeast extract (Oxoid, UK), 1% (w/v) NaCl, and H₂O was added to the desired volume. SOB components included 2% (w/v) tryptone (Oxoid, UK), 0.5% (w/v) yeast extract (Oxoid, UK), 10 mM NaCl, 2.5 mM KCl, and finally H₂O was added to the desired volume.

2.2.2. Incubation of broth cultures

The broth cultures were incubated overnight at 37°C at 155 rpm in a C25KC incubator shaker (New Brunswick Scientific, Edison, NJ, USA).

2.2.3. Solid media

Columbia agar with horse blood (CBA) was used to grow the wild type strain *A. caviae* Sch3N. CBA was prepared in the department of Infection and Immunity, Medical School, University of Sheffield and was composed of 4.2 % (w/v) Columbia agar base, plus 5% of defibrinated horse blood. LB agar supplemented with appropriate antibiotics or other supplements was used to grow mutant strains or plasmid-containing strains of *A. caviae* Sch3N, *E. coli*, and *Salmonella*. LB agar was prepared by mixing the components indicated above in the liquid media section with 1.5% w/v bacteriological agar (Oxoid, UK) as a solidifying agent. Motility agar was prepared in this study to test the ability of *Aeromonas* to swim or swarm. The components of the motility agar medium were as follows:

Swarm agar

- Difco Nutrient broth powder (BD, UK) 0.8% (w/v)
- NaCl 0.5% (w/v)
- Eiken agar (Eiken Chemical Co., Ltd. Japan) 0.6% (w/v)
- Tap water to 100 ml

Swim agar

- Tryptone powder (Oxoid, UK) 1% (w/v)
- NaCl 0.5% (w/v)
- Bacteriological agar (Oxoid, UK) 0.25% (w/v)
- Distilled H₂O to 100 ml

The sodium salt 3,3'-([1,1'-biphenyl]-4,4'-diyl)bis(4-aminonaphthalene-1-sulfonic acid) also known as Congo Red (CR) dye was used to prepare CR agar. The dye is known to bind the extracellular polymers produced by bacterial cells while forming a biofilm, and thus was added to bacteriological media as an indicator for extracellular polysaccharide production. The components of Congo Red agar were:

- Brain Heart Infusion Broth (Oxoid, UK) 3.7% (w/v)
- Bacteriological agar (Oxoid, UK) 1.5% (w/v)
- Congo Red (Fisher Scientific, UK) dissolved in absolute ethanol 0.025% (v/v)
- CaCl₂ 5 mM
- Distilled H₂O to 100 ml

Both the CR colloidal solution and the CaCl₂ were added after the medium was autoclaved. The CaCl₂ stock solution was filter sterilized prior to its addition to the medium.

2.2.4. Incubation and storage of agar-based cultures

Bacterial cultures grown on CBA and LB plates were incubated overnight in an ambient air incubator at 37°C. Inoculated swarm and swim agar plates were kept on the bench for 24 hours to allow the bacteria to swim or swarm at room temperature. Inoculated CR agar plates were incubated in an ambient air incubator at 37°C for 24 hours followed by keeping them on the bench for 2-4 days to allow for colour development at room temperature. The bacterial culture plates were stored in 4°C for a maximum of one week. For long term storage of bacteria, strains were collected in glass beads vials and stored at -80°C.

Table 2.1. Bacterial strains used in this study

Strain name	Characteristics	Reference
<u>Aeromonas caviae strains:</u>		
Sch3N (wildtype)	Spontaneous Nal ^R	(Rabaan <i>et al.</i> , 2001)
Sch3N pBBR1MCS- <i>mshH</i>	Sch3N overexpressing MshH protein of <i>A. veronii</i> bv. <i>sobria</i> , Nal ^R , Cm ^R	This study
Sch3N pBBR1MCS5- <i>AHA1208</i>	Sch3N overexpressing <i>A. caviae</i> GGDEF domain <i>AHA1208</i> , Nal ^R , GM ^R	This study
Sch3N pBBR1MCS5- <i>AHA2484</i>	Sch3N overexpressing <i>A. caviae</i> protein <i>AHA2484</i> , Nal ^R , GM ^R	This study
Sch3N pBBR1MCS5- <i>AHA3342</i>	Sch3N overexpressing <i>A. caviae</i> protein <i>AHA3342</i> , Nal ^R , GM ^R	This study
Sch3N pBBR1MCS5- <i>AHA2698</i>	Sch3N overexpressing <i>A. caviae</i> protein <i>AHA2698</i> , Nal ^R , GM ^R	This study
Sch3N pKAGb2(-)	Nal ^R , Cm ^R	This study
Sch3N pKAGb2- <i>lafA1p</i>	Nal ^R , Cm ^R	This study
Sch3N pKAGb2- <i>lafA2p</i>	Nal ^R , Cm ^R	This study
Sch3N pKAGb2- <i>lafKp</i>	Nal ^R , Cm ^R	This study
Sch3N pKAGb2- <i>lafKp</i> Δriboswitch	Nal ^R , Cm ^R	This study
Sch3N pKAGb2- <i>lafKp</i> ΔP1	Nal ^R , Cm ^R	This study
Sch3N pKAGb2- <i>lafKp</i> ΔP2	Nal ^R , Cm ^R	This study
Sch3N pKAGb2- <i>lafKp</i> P1AG	Nal ^R , Cm ^R	This study
MA1	<i>Azoto</i> ::pKNG101 Sm ^R Nal ^R	This study
MA1 pKAGb2- <i>lafA1p</i>	Nal ^R , Sm ^R , Cm ^R	This study
MA1 pKAGb2- <i>lafA2p</i>	Nal ^R , Sm ^R , Cm ^R	This study
MA1 pKAGb2- <i>lafKp</i>	Nal ^R , Sm ^R , Cm ^R	This study
MA2	<i>AHA2484</i> ::pKNG101 Sm ^R Nal ^R	This study
MA2 pKAGb2- <i>lafA1p</i>	Nal ^R , Sm ^R , Cm ^R	This study
MA2 pKAGb2- <i>lafA2p</i>	Nal ^R , Sm ^R , Cm ^R	This study
MA2 pKAGb2- <i>lafKp</i>	Nal ^R , Sm ^R , Cm ^R	This study
MA2 pBBR1MCS5- <i>AHA2484</i>	Nal ^R , Sm ^R , Gm ^R	This study

Table 2.1. is continued on the next page

Table 2.1. Bacterial strains used in this study (continued)

Strain name	Characteristics	Reference
MA3	<i>AHA0383mshH::pKNG101 Sm^R Nal^R</i>	This study
MA3 pKAGb2- <i>lafA1p</i>	Nal ^R , Sm ^R , Cm ^R	This study
MA3 pKAGb2- <i>lafA2p</i>	Nal ^R , Sm ^R , Cm ^R	This study
MA3 pKAGb2- <i>lafKp</i>	Nal ^R , Sm ^R , Cm ^R	This study
MA4	<i>Coma::pKNG101 Sm^R Nal^R</i>	This study
MA4 pKAGb2- <i>lafA1p</i>	Nal ^R , Sm ^R , Cm ^R	This study
MA4 pKAGb2- <i>lafA2p</i>	Nal ^R , Sm ^R , Cm ^R	This study
MA4 pKAGb2- <i>lafKp</i>	Nal ^R , Sm ^R , Cm ^R	This study
MA5	<i>AHA1800::pKNG101 Sm^R Nal^R</i>	This study
MA 5 pKAGb2- <i>lafA1p</i>	Nal ^R , Sm ^R , Cm ^R	This study
MA5 pKAGb2- <i>lafA2p</i>	Nal ^R , Sm ^R , Cm ^R	This study
MA5 pKAGb2- <i>lafKp</i>	Nal ^R , Sm ^R , Cm ^R	This study
MA6	<i>AHA4237::pKNG101 Sm^R Nal^R</i>	This study
MA6 pKAGb2- <i>lafA1p</i>	Nal ^R , Sm ^R , Cm ^R	This study
MA6 pKAGb2- <i>lafA2p</i>	Nal ^R , Sm ^R , Cm ^R	This study
MA6 pKAGb2- <i>lafKp</i>	Nal ^R , Sm ^R , Cm ^R	This study
MA7	<i>AHA0093::pKNG101 Sm^R Nal^R</i>	This study
MA7 pKAGb2- <i>lafA1p</i>	Nal ^R , Sm ^R , Cm ^R	This study
MA7 pKAGb2- <i>lafA2p</i>	Nal ^R , Sm ^R , Cm ^R	This study
MA7 pKAGb2- <i>lafKp</i>	Nal ^R , Sm ^R , Cm ^R	This study
MA8	<i>AHA0862::pKNG101 Sm^R Nal^R</i>	This study
MA8 pKAGb2- <i>lafA1p</i>	Nal ^R , Sm ^R , Cm ^R	This study
MA8 pKAGb2- <i>lafA2p</i>	Nal ^R , Sm ^R , Cm ^R	This study
MA8 pKAGb2- <i>lafKp</i>	Nal ^R , Sm ^R , Cm ^R	This study
MA9	<i>MorA::pKNG101 Sm^R Nal^R</i>	This study
MA9 pKAGb2- <i>lafA1p</i>	Nal ^R , Sm ^R , Cm ^R	This study
MA9 pKAGb2- <i>lafA2p</i>	Nal ^R , Sm ^R , Cm ^R	This study
MA9 pKAGb2- <i>lafKp</i>	Nal ^R , Sm ^R , Cm ^R	This study

Table 2.1. is continued on the next page

Table 2.1. Bacterial strains used in this study (continued)

Strain name	Characteristics	Reference
MA10	<i>AHA3342</i> ::pKNG101 Sm ^R Nal ^R	This study
MA10 pKAGb2- <i>lafA1</i> p	Nal ^R , Sm ^R , Cm ^R	This study
MA10 pKAGb2- <i>lafA2</i> p	Nal ^R , Sm ^R , Cm ^R	This study
MA10 pKAGb2- <i>lafK</i> p	Nal ^R , Sm ^R , Cm ^R	This study
MA10 pBBR1MCS5- <i>AHA3342</i>	Nal ^R , Sm ^R , Gm ^R	This study
MA11	<i>AHA3469</i> ::pKNG101 Sm ^R Nal ^R	This study
MA11 pKAGb2- <i>lafA1</i> p	Nal ^R , Sm ^R , Cm ^R	This study
MA11 pKAGb2- <i>lafA2</i> p	Nal ^R , Sm ^R , Cm ^R	This study
MA11 pKAGb2- <i>lafK</i> p	Nal ^R , Sm ^R , Cm ^R	This study
MA12	<i>AHA2698</i> ::pKNG101 Sm ^R Nal ^R	This study
MA12 pKAGb2- <i>lafA1</i> p	Nal ^R , Sm ^R , Cm ^R	This study
MA12 pKAGb2- <i>lafA2</i> p	Nal ^R , Sm ^R , Cm ^R	This study
MA12 pKAGb2- <i>lafK</i> p	Nal ^R , Sm ^R , Cm ^R	This study
MA12 pBBR1MCS5- <i>AHA2698</i>	Nal ^R , Sm ^R , Gm ^R	This study
MA13	<i>AHA2092</i> ::pKNG101 Sm ^R Nal ^R	This study
MA13 pKAGb2- <i>lafA1</i> p	Nal ^R , Sm ^R , Cm ^R	This study
MA13 pKAGb2- <i>lafA2</i> p	Nal ^R , Sm ^R , Cm ^R	This study
MA13 pKAGb2- <i>lafK</i> p	Nal ^R , Sm ^R , Cm ^R	This study
MA124	<i>pilZ</i> ::Km ^R Nal ^R	This study
MA124 pKAGb2- <i>lafA1</i> p	Nal ^R , Km ^R , Cm ^R	This study
MA124 pKAGb2- <i>lafA2</i> p	Nal ^R , Km ^R , Cm ^R	This study
MA124 pKAGb2- <i>lafK</i> p	Nal ^R , Km ^R , Cm ^R	This study
CM100	<i>lafK</i> ::Km ^R Nal ^R	(Mason, 2013)
CM100 pBBR1MCS5- <i>lafK</i> Δribo	Nal ^R , Km ^R , Gm ^R	This study
AAR6	<i>lafA1</i> ::Cm ^r <i>lafA2</i> ::Km ^R Nal ^R	(Gavín <i>et al.</i> , 2002)
AAR9	<i>lafB</i> ::Km ^R Nal ^R	(Gavín <i>et al.</i> , 2002)

Table 2.1. is continued on the next page

Table 2.1. Bacterial strains used in this study (continued)

Strain name	Characteristics	Reference
<i>Escherichia coli:</i>		
DH5 α	F ⁻ <i>endA hdsR17</i> (r _K ⁻ ,m _K ⁺) <i>supE44 thi-1 recA1 gyrA96 Φ80 lacZ</i>	(Hanahan, 1983)
CC118 λ <i>pir</i>	Δ (<i>ara leu</i>)7697 <i>araD139 ΔlacZX74 glaE glaK phoA20 thi-1 rspE rpoB</i> (Rf ^R) <i>argE</i> (Am) <i>recA1</i> <i>pir</i> ⁺	(Herrero <i>et al.</i> , 1990)
S17-1	<i>thi pro hsdR hsdM</i> ⁺ <i>recA</i> [RP4 2-Tc::Mu-Km::Tn7 (Tp ^R Sm ^R) Tra ⁺] Mobilizing donor for conjugation	(Simon <i>et al.</i> , 1983)

Table 2.2. Plasmids used in this study

Name	Characteristics	Reference
pGEM [®] -T-Easy	Cloning vector, linearized with thymidine overhangs, contains <i>lacZ</i> , Amp ^R	Promega, USA
pBBR1MCS	Broad host range cloning vector, medium copy number, IncP, -W, -Q, ColE1 and p15A compatible, contains pBluescript IIS-lacZ α -polylinker, Cm ^R	(Kovach <i>et al.</i> , 1994)
pBBR1MCS5	Broad host range cloning vector, medium copy number, IncP, -W, -Q, ColE1 and p15A compatible, contains pBluescript IIS-lacZ α -polylinker, Gm ^R	(Kovach <i>et al.</i> , 1995)
pKNG101	Suicide plasmid vector, <i>oriR6K mobRK2 strAB sacBR</i> , Sm ^R	(Kaniga <i>et al.</i> , 1991)
pKAGb-2(-)	Broad host range vector, <i>ori</i> ₁₆₀₀ , contains promoterless <i>lacZ</i> gene, Cm ^R	(Thomas)
pUC4KIXX	Source of Tn5-derived <i>nptII</i> gene, Km ^R	Pharmacia, GE Healthcare Life Sciences, USA
pRK2013	Helper plasmid Col E1::RK2 <i>tra</i> ⁺ <i>ori</i> ⁻ Km ^R	(Figurski <i>et al.</i> , 1979)
pBBR1MCS <i>mshH</i>	<i>A. veronii</i> bv. <i>sobria mshH</i> gene ligated to pBBR1MCS, Cm ^R	This study
pGEM- <i>pilZ</i>	<i>A. caviae pilZ</i> gene ligated to pGEM-T-Easy cloning vector, Amp ^R	This study
pGEM- <i>pilZ</i> ::km	Kanamycin cassette inserted into <i>pilZ</i> gene of <i>A. caviae</i> , <i>pilZ</i> ::Km ligated to pGEM-T-Easy vector, Amp ^R	This study
pKNG- <i>Azoto</i>	<i>Azoto</i> gene of <i>A. caviae</i> ligated to pKNG101, Sm ^R	This study

Table 2.2. to be continued on the next page

Table 2.2. Plasmids used in this study, continued

Name	Characteristics	Reference
pKNG-AHA2484	<i>AHA2484</i> gene of <i>A. caviae</i> ligated to pKNG101, Sm ^R	This study
pKNG-AHA0383 <i>mshH</i>	<i>mshH</i> gene of <i>A. caviae</i> ligated to pKNG101, Sm ^R	This study
pKNG- <i>Coma</i>	<i>Coma</i> gene of <i>A. caviae</i> ligated to pKNG101, Sm ^R	This study
pKNG-AHA1800	<i>AHA1800</i> gene of <i>A. caviae</i> ligated to pKNG101, Sm ^R	This study
pKNG-AHA4237	<i>AHA4237</i> gene of <i>A. caviae</i> ligated to pKNG101, Sm ^R	This study
pKNG-AHA0093	<i>AHA0093</i> gene of <i>A. caviae</i> ligated to pKNG101, Sm ^R	This study
pKNG-AHA0862	<i>AHA0862</i> gene of <i>A. caviae</i> ligated to pKNG101, Sm ^R	This study
pKNG- <i>MorA</i>	<i>MorA</i> gene of <i>A. caviae</i> ligated to pKNG101, Sm ^R	This study
pKNG-AHA3342	<i>AHA3342</i> gene of <i>A. caviae</i> ligated to pKNG101, Sm ^R	This study
pKNG-AHA3469	<i>AHA3469</i> gene of <i>A. caviae</i> ligated to pKNG101, Sm ^R	This study

Table 2.2. is to be continued on the next page

Table 2.2. Plasmids used in this study, continued

Name	Characteristics	Reference
pKNG-AHA2698	AHA2698 gene of <i>A. caviae</i> ligated to pKNG101, Sm ^R	This study
pKNG-AHA2092	AHA2092 gene of <i>A. caviae</i> ligated to pKNG101, Sm ^R	This study
pKNG-pilZ::km	Kanamycin cassette inserted into <i>A. caviae</i> pilZ gene, pilZ::Km ligated to pKNG101, Sm ^R	This study
pKAG-lafA1p	<i>A. caviae</i> lafA1 promoter ligated to promoterless vector pKAGb2(-), Cm ^R	This study
pKAG-laA2p	<i>A. caviae</i> lafA2 promoter ligated to promoterless vector pKAGb2(-), Cm ^R	This study
pKAG-lafKp	<i>A. caviae</i> lafK promoter ligated to promoterless vector pKAGb2(-), Cm ^R	This study
pKAG-lafKpΔribo	GEMM riboswitch deleted from lafK promoter, lafKpΔribo riboswitch ligated to promoterless vector pKAGb2(-), Cm ^R	This study
pKAG-lafKpΔP1	P1 hairpin of lafK GEMM riboswitch deleted, lafKpΔP1 ligated to promoterless vector pKAGb2(-), Cm ^R	This study
pKAG-lafKpΔP2	P2 hairpin of lafK GEMM riboswitch deleted, lafKpΔP2 ligated to promoterless vector pKAGb2(-), Cm ^R	This study
pKAG-lafKpΔP1AG	Nucleotides number 8 and 9 P2 hairpin of lafK GEMM riboswitch deleted, lafKpΔP2 ligated to promoterless vector pKAGb2(-), Cm ^R	This study

Table 2.2. is to be continued on the next page

Table 2.2. Plasmids used in this study, continued

Name	Characteristics	Reference
pBBR1MCS5- <i>AHA0382</i>	<i>A. caviae</i> EAL domain encoding gene <i>AHA0382</i> ligated to pBBR1MCS5, Gm ^R	This study
pBBR1MCS5- <i>AHA1208</i>	<i>A. caviae</i> GGDEF domain encoding gene <i>AHA1208</i> ligated to pBBR1MCS5, Gm ^R	This study
pBBR1MCS5- <i>AHA2484</i>	<i>A. caviae</i> <i>AHA2484</i> gene ligated to pBBR1MCS5, Gm ^R	This study
pBBR1MCS5- <i>AHA3342</i>	<i>A. caviae</i> <i>AHA3342</i> gene ligated to pBBR1MCS5, Gm ^R	This study
pBBR1MCS5- <i>AHA2698</i>	<i>A. caviae</i> <i>AHA2698</i> gene pBBR1MCS5, Gm ^R	This study
pBBR1MCS5- <i>lafKΔribo</i>	<i>A. caviae</i> <i>lafK</i> GEMM riboswitch deleted, <i>lafKΔribo</i> ligated to pBBR1MCS5, Gm ^R	This study

2.2.5. Sterilization of bacteriological media

The prepared bacteriological media were sterilized by autoclaving at 121°C, 15 psi for 15 minutes. Heat-sensitive components were added after autoclaving of media at a temperature of 55°C. All heat sensitive solutions were sterilized by filtration using a 0.22 µm syringe driven 33 mm membrane filter unit (Millipore).

2.2.6. Antibiotics

Nalidixic acid, ampicillin, kanamycin, and streptomycin were used at final concentrations of 50 µg/ml while chloramphenicol and gentamicin were used at a final concentration of 25 µg/ml and 10 µg/ml, respectively. Stock solutions of ampicillin, kanamycin, streptomycin and gentamicin were prepared in distilled water. The stock solutions of nalidixic acid and chloramphenicol were prepared in 1M NaOH and absolute ethanol, respectively. All stock solutions were filter sterilized. The stock solutions of the prepared antibiotics were stored at -20°C, with the exception of the stock solution of nalidixic acid which was stored at 4°C.

2.2.7. Other media supplements

5-bromo-4-chloro-3-indolyl- β -D-galactopyranoside (X-gal) and isopropyl β -D-thiogalactoside (IPTG) were added to media whenever required. The stock solution of X-gal was prepared as 20 mg/ml in DMSO and stored at -20°C . The stock solution of IPTG was prepared as 100 mM in distilled water followed by its filter sterilization and storage at -20°C until required. The final concentration of X-gal and IPTG used in media was 40 $\mu\text{g}/\text{ml}$ and 0.1 mM, respectively.

2.3. Conventional tests

2.3.1. Oxidase test

In this study, *A. caviae* Sch3N was differentiated from *E. coli* and other bacteria based on the production of the enzyme cytochrome *c* oxidase by *A. caviae* Sch3N (oxidase positive) while the other bacteria are unable to produce this enzyme (oxidase negative). A few crystals of N,N,N',N'-tetramethyl-*p*-phenylenediamine (TMPD) powder (Sigma, UK) was dissolved in 0.5 ml of distilled water. A few drops of the formed solution were applied to a filter paper. A single colony from the strain to be tested was picked up by a toothpick and placed on the wet filter paper. An immediate purple colour formation indicates an oxidase positive reaction while an oxidase negative reaction was indicated when no colour change was detected.

2.4. DNA and RNA techniques

2.4.1. Extraction of bacterial chromosomal DNA

The extraction of bacterial chromosomal DNA was performed using the E.Z.N.A. Bacterial DNA Kit (OMEGA bio-tek) according to the supplier's instructions. Briefly, a single bacterial colony was inoculated to 5 ml of a bacteriological broth medium and incubated overnight at 37°C with shaking. The overnight culture was harvested by centrifugation at 2782 *g* for 10 minutes at 15°C using AllegraTM X-22R Centrifuge (Beckman Coulter). The broth medium was discarded and the bacterial pellet was resuspended in 100 μl of TE buffer followed by the addition of 10 μl of a 50 mg/ml Lysozyme Solution. The cells were incubated in a 37°C water bath for 10 minutes. A 100 μl volume of BTL buffer was then added followed by addition of 20 μl of Proteinase K. The components were mixed by vortexing for 10 seconds. The mixture was incubated for one hour in a 55°C water bath and the sample was briefly vortexed every 20 minutes to complete cell lysis. Next, 5 μl of RNase A was added to the sample

and the components were mixed by inverting the tube several times. This was followed by an incubation step at room temperature for 5 minutes. The sample was then centrifuged at 16,100 *g* for 2 minutes at room temperature using an Eppendorf Centrifuge 5415D. The supernatant was carefully aspirated and transferred to a clean microcentrifuge tube. To the clear supernatant a 220 μ l of BDL buffer was added and was mixed with the sample by brief shaking. This was followed by an incubation step at 65°C for 10 minutes. Ethanol precipitation of DNA was done by addition of 220 μ l of absolute ethanol to the sample followed by thorough mixing by vortexing for 20 seconds. The sample was then transferred into the supplied HiBind DNA Column assembled into a 2 ml Collection tube. The column was centrifuged at 16,100 *g* for 1 minute to allow the binding of DNA. The flow-through was discarded and 500 μ l of Buffer HB was added to the column. This was followed by another centrifugation step at 16,100 *g* for 1 minute. The flow-through was discarded and 700 μ l of DNA Wash Buffer (diluted with absolute ethanol) was added to the column. The column was centrifuged at 16,100 *g* for 1 minute and the flow-through was discarded. The step of washing the column with the DNA Wash Buffer was done twice. The empty column was centrifuged for 2 minutes to ensure a complete removal of ethanol. The HiBind DNA Column was then placed into a clean 1.5 ml microfuge tube and 100 μ l of Elution Buffer was added to the column. The column was incubated for 5 minutes at room temperature and then was centrifuged for 1 minute at 16,100 *g* to elute the DNA. The DNA sample was stored at -20°C until needed.

2.4.2. Plasmid extraction (miniprep)

Plasmids were extracted using e.Z.N.A Plasmid Mini Kit II (OMEGA bio-tek) according to the manufacturer instructions. Briefly, a single bacterial colony containing the plasmid was inoculated into 5 – 10 ml of the desired broth medium containing the appropriate antibiotic to maintain the plasmid. The broth culture was incubated overnight with shaking at 37°C. Next day, the bacterial cells were harvested by centrifugation at 2782 *g* for 10 minutes at 15°C using Allegra™ X-22R Centrifuge (Beckman Coulter). The bacterial pellet was resuspended using 250 μ l of Solution I (containing RNase A). The resuspended pellet was then transferred to a 1.5ml microfuge tube followed by addition of 250 μ l of Solution II with proper mixing by inverting and rotating several times. Once a clear lysate was obtained, 350 μ l of Solution III was added followed by immediate mixing by inverting several times. The

obtained lysate was then centrifuged at 16,100 *g* for 10 minutes at room temperature using an Eppendorf centrifuge 5415D. The cleared supernatant was then carefully aspirated and added to the provided HiBind DNA Miniprep Column assembled in the 2 ml collection tube. The column was then centrifuged at 16,100 *g* for 1 minute at room temperature to bind the DNA and pass the lysate through the column. The flow-through was then discarded and 500 μ l of the provided HB Buffer was added to the column. A further step of centrifugation for 1 minute was needed to pass the liquid through the column to ensure the removal of the residual proteins. The flow through was then discarded and 700 μ l of the provided Wash Buffer (diluted with absolute ethanol) was added to wash the column. Another step of centrifugation was carried out to pass the liquid through the column. The flow through was discarded and the empty column was centrifuged again for 2 minutes at 16,100 *g* to completely dry the column matrix ensuring a good plasmid yield. The column was removed from the 2 ml collection tube and was placed into a clean 1.5 ml previously labelled microcentrifuge tube. Finally, 50 μ l of the provided Elution Buffer was added to the column followed by centrifugation of the column at 16,100 *g* for 1 minute at room temperature to elute the plasmid DNA into the clean microcentrifuge tube. The extracted plasmid was then stored at -20°C until needed.

2.4.3. DNA purification

PCR amplicons and plasmid DNA were cleaned up in this study before and after restriction digestion using the PCR purification kit (QIAGEN) according to the manufacturer instructions. Briefly, the Binding Buffer (Buffer PB) was added as a five times volume of the DNA sample to be cleaned up. The PB Buffer containing the DNA was placed in the centre of a universal spin filter column assembled in a 2 ml collection tube (UPrep Spin Columns, Dutscher Scientific). The column was then centrifuged at room temperature for 1 minute at 16,100 *g* using an Eppendorf Centrifuge 5415D. The flow through was then discarded and 650 μ l of the Wash Buffer (Buffer PE) containing ethanol was added to the column and another centrifugation step was carried out as described above. The flow-through was discarded followed by addition of 50 μ l of the Elution Buffer (Buffer EB) to the column. For a more concentrated DNA sample, 30 μ l of Buffer EB was added. The column was allowed then to stand for 1 minute followed by its placement in a clean microfuge tube. A final centrifugation step was carried out as described above and the eluted DNA sample was stored at -20°C until needed.

2.4.4. DNA Restriction digestion

PCR amplicons and plasmid DNA were digested in this study using restriction enzymes supplied from Promega. The enzymes were stored at -20°C until needed and were placed on ice during the preparation of the restriction digestion reaction mixture. The concentration of each restriction enzyme used was 10 units per reaction. The DNA to be cut was first purified from endonucleases using the PCR Purification kit (QIAGEN) as described elsewhere in this chapter. Restriction digestion reaction mixture and incubation conditions were performed according to the instructions of the manufacturer. The cut DNA was then cleaned from both the restriction enzymes and the buffers using the PCR purification kit (QIAGEN). The sample was eluted using 30 µl of Elution Buffer provided in the PCR purification kit. The cleaned cut DNA sample was stored at -20°C until needed.

2.4.5. DNA ligation

The PCR amplicons were ligated to the previously cut DNA plasmids using the T4 DNA Ligase kit (Promega). The concentration of T4 DNA ligase used in this study to carry out a ligation reaction was 3 units per reaction. The ligation reaction was carried out in a PCR Genius machine (Techne) at 15°C. The ligation mixture was prepared according to the instructions provided by the manufacturer.

2.4.6. Polymerase chain reaction (PCR)

PCR was used in this study to amplify certain DNA regions using different polymerase enzymes including GoTaq® DNA polymerase (Promega, UK), KOD Hot Start DNA Polymerase (Novagen®, Japan), and Platinum *Pfx* DNA Polymerase (Invitrogen, Life technologies Ltd., UK) and to generate cDNA from RNA using the GoScript™ Reverse Transcription System (Promega, UK). All reactions were done using a G-Storm Thermal Cycler (Gene technologies Ltd, UK) using nuclease-free 0.2 ml PCR Tubes with Attached Cap (Fisher Scientific, UK).

2.4.6.1. Primer design

The primers used in this study were synthetic primers obtained from Eurogentec Ltd., UK. The primers were designed based on the *A. caviae* whole genome DNA sequence (provided by Dr. Jonathan Shaw). The primers were generally designed to have from 18 to 22 bp length and to have a GC content ranging from 40% to 60%. If the PCR products were to be cloned, suitable restriction digestion linkers plus GC

clamps were added to the primers at their 5' end. The runs and repeats of bases were avoided as much as possible while designing the primers and the self-complementarity of the primers was checked using the Oligo Calc online software (<http://www.basic.northwestern.edu/biotools/oligocalc.html>). In some experiments, the SnapGene software (GSL Biotech LLC, Chicago, IL) was as well used to design DNA primers. The ordered primers were provided by the company at a concentration of 100 μM in MilliQ water. The DNA primers were designed during this study for different purposes including amplification of a whole gene or part of it as well as for amplification of a DNA region that contains a promoter or a riboswitch. Primers used in this study are listed in tables included in the appendix section.

2.4.6.2. PCR amplification using GoTaq® DNA polymerase

In this study, the GoTaq DNA polymerase was found to give robust PCR amplification when compared to the standard *Taq* DNA polymerase which showed inferior PCR performance. The GoTaq DNA polymerase enzyme is supplied in different formulations. The GoTaq Flexi DNA polymerase was the kit chosen to be used throughout this study because it gave a flexibility in adjusting the final MgCl_2 concentration. The components needed for a PCR amplification reaction using the GoTaq DNA polymerase were as the following:

<u>Component</u>	<u>Final volume</u>	<u>Final concentration</u>
Colourless GoTaq Flexi Buffer (5X)	10 μl	1X
MgCl_2 solution (25 mM)	2 μl	1.0 mM
Nucleotide mix (10 mM each)	1.5 μl	0.3 mM each
Forward primer (100 μM)	1.5 μl	3 μM
Reverse primer (100 μM)	1.5 μl	3 μM
GoTaq DNA Polymerase (5 Units/ μl)	0.25 μl	1.25 Units
Template DNA (genomic or plasmid DNA)	3 μl	
H_2O (nuclease-free)	Up to 50 μl	

The reaction tubes were then placed in the thermal cycler to amplify the DNA using the following programme:

<u>Temperature</u>	<u>Time</u>	<u>Number of cycles</u>	<u>Outcome</u>
95°C	2 minutes	1	Initial denaturation
95°C	30 seconds	} 30	Denaturation
40°C-60°C*	40 seconds		Annealing
72°C	1 minute/kb		Extension
72°C	5 minutes	1	Final extension
4°C	Indefinite	1	Hold

*The temperature was set at 5°C below the melting temperature (T_m) of the used primers.

2.4.6.3. Colony PCR screening using GoTaq DNA polymerase

A colony PCR screening technique is a method used to screen a large number of colonies for the presence of certain genes or DNA plasmids by directly using the colonies as the template DNA without performing a genomic DNA or plasmid DNA extractions. When performing colony PCR screening, each bacterial colony to be screened was picked up from the plate using a sterile tooth pick, and was then swirled into the bottom of the PCR tube. The above listed components of the PCR Reaction using GoTaq® DNA polymerase were then added to each PCR tube containing the bacterial colony followed by the addition of 2.5 µl of dimethyl sulfoxide (DMSO) into each tube. The DMSO is a solvent which helps in stabilizing the nucleic acid against depurination and allow for fast renaturation of the denatured DNA during the PCR.

2.4.6.4. PCR amplification using KOD Hot Start DNA Polymerase

The KOD Hot Start DNA Polymerase was used in this study to generate blunt-ended PCR amplicons needed for the blunt end ligation reactions. The blunt ends were generated by the enzyme due to its proofreading ability, i.e., its 3'-5' exonuclease activity. In comparison to the Taq DNA polymerase, the KOD Hot Start DNA Polymerase provided both a high fidelity and a fast extension. The components of the PCR reaction using the KOD Hot Start DNA Polymerase were as the following:

<u>Component</u>	<u>Final volume</u>	<u>Final concentration</u>
KOD Hot Start DNA Polymerase buffer (10X)	5 µl	1X
MgSO ₄ solution (25 mM)	3 µl	1.5 mM
Nucleotide mix (2 mM each)	5 µl	0.2 mM each
Forward primer (100 µM)	1.5 µl	3 µM
Reverse primer (100 µM)	1.5 µl	3 µM
KOD Hot Start DNA Polymerase (1 Unit/µl)	1 µl	0.02 Units
Template DNA (genomic DNA)	3 µl	
H ₂ O (nuclease-free)	Up to 50 µl	

The reaction tubes were placed in the thermal cycler which was set to the following programme:

<u>Temperature</u>	<u>Time</u>	<u>Number of cycles</u>	<u>Outcome</u>
95°C	2 minutes	1	Initial denaturation
95°C	30 seconds	} 30	Denaturation
40°C-60°C*	40 seconds		Annealing
72°C	1 minute/kb		Extension
72°C	5 minutes	1	Final extension
4°C	Indefinite	1	Hold

*The temperature was set at 5°C below the melting temperature (T_m) of the used primers.

2.4.6.5. PCR amplification using Platinum *Pfx* DNA Polymerase

Platinum *Pfx* DNA Polymerase was used in this study due to its advanced properties that include fast extension and 3'-5' exonuclease (proofreading) activity. The kit also included an enhancer solution which can be used to further improve the PCR performance in certain settings. The enzyme was chosen in this study specifically for creating deletions by the Spliced Overlap Extension (SOE) PCR technique. The PCR reaction components when using the Platinum *Pfx* DNA Polymerase were as the following:

<u>Component</u>	<u>Final volume</u>	<u>Final concentration</u>
<i>Pfx</i> Amplification Buffer (10X)	5 µl	1X
MgSO ₄ solution (50 mM)	1 µl	1 mM
Nucleotide mix (10 mM each)	1.5 µl	0.3 mM each
Forward primer (100 µM)	1.5 µl	3 µM
Reverse primer (100 µM)	1.5 µl	3 µM
Platinum® <i>Pfx</i> DNA Polymerase (2.5 Units/µl)	0.4 µl	1 Unit
Template DNA (genomic DNA)	3 µl	
Enhancer solution* (10X)	2.5 µl	0.5X
H ₂ O (nuclease-free)	Up to 50 µl	

*This is an optional component used only for problematic and/ or GC-rich templates

The reaction tubes were then placed in the thermal cycler and the following programme was run:

<u>Temperature</u>	<u>Time</u>	<u>Number of cycles</u>	<u>Outcome</u>
94°C	2 minutes	1	Initial denaturation
94°C	20 seconds	} 30	Denaturation
40°C-60°C*	30 seconds		Annealing
68°C	1 minute/kb		Extension
68°C	2 minutes	1	Final extension
4°C	Indefinite	1	Hold

*The temperature was set at 5°C below the melting temperature (T_m) of the used primers.

2.4.7. RNA extraction

RNA extraction from swarming cells was performed in this study using two kits, the RNeasy Protect Bacteria Mini Kit (QIAGEN) and the RNase-Free DNase Set (QIAGEN) according to the supplier's instructions with few modifications. *A. caviae* cells were made to swarm by growing them on swarming agar plates as described above. To the plate containing the swarming bacteria 1 ml of RNAProtect® Bacteria Reagent was added. Using a sterile inoculation loop the swarming *A. caviae* cells were

detached from the agar and the whole RNeasy Protect[®] Bacteria Reagent containing the swarming bacterial cells was collected using a sterile filter tip and added to an RNase-free 1.5 ml microfuge tube. The bacterial suspension was homogenized within the tube by up and down pipetting. The sample was vortexed for 5 seconds and then centrifuged at 8000 g for 10 minutes at room temperature using Eppendorf Centrifuge 5415D. The pellet was resuspended in 100 µl of RNase-free water containing 15mg/ml lysozyme. Next, 10 µl of Proteinase K (QIAGEN >600 mAU/ml, solution) was added to the sample. The tube was then incubated for 10 minutes at room temperature, with a brief vortex every 2 minutes. A volume of 350 µl of Buffer RLT was added to the sample followed by a vigorous vortexing for 10 to 15 seconds. Absolute ethanol was added to the sample in a volume of 250 µl followed by a brief vortexing. The lysate was transferred to the RNeasy Mini Spin Column assembled in the 2 ml collection tube, both provided by the kit supplier. The column was then centrifuged for 1 minute at 8000 g and the flow-through was discarded. On-column DNase digestion was then performed using several steps. First, 350 µl of Buffer RW1 was added to the RNeasy Spin Column. The column was centrifuged at 8000 g for 1 minute and the flow-through was discarded. A mixture of 70 µl of Buffer RDD and 10 µl of DNase I RNase-free solution was prepared in a separate tube, mixed well and then applied to the column containing the RNA. The column was incubated on the bench for 15 minutes. Next, a 350 µl of Buffer RW1 was added to the column which was then centrifuged for 1 minutes at 8000 g. The flow-through was discarded and 500 µl of Buffer RPE was added to the column followed by centrifugation at 8000 g for 1 minute and the flow-through was discarded. The Buffer RPE washing step was repeated twice. The column was then placed in a clean RNase-free microfuge tube to elute the RNA. By adding 50 µl of RNase-free water to the centre of the column followed by centrifugation at 8000 g for 1 minute. The eluted RNA was then analysed by gel electrophoresis to check for its presence. The RNA sample was stored at -20°C for until needed.

2.4.8. Reverse Transcriptase Polymerase Chain Reaction (RT-PCR)

The reverse transcription reaction was done using GoScript[™] Reverse Transcription System (Promega, UK). Briefly, 2 µl of the extracted RNA was placed in a 0.5 ml micro tube followed by addition of 2 µl of the random primers provided in the kit (to reach a final concentration of 1 µg per reaction) and 1 µl of nuclease free water. A second tube containing exactly the same components was labelled as a positive

control, and a third tube in which the RNA was replaced by nuclease free water was labelled as a no-RNA negative control. The components in each tube were mixed together by gentle pipetting. The samples were then incubated at 70°C for 5 minutes followed by chilling on ice while preparing the reverse transcription reaction components. The reverse transcription mixture included the following:

<u>Component</u>	<u>Final volume</u>	<u>Final concentration</u>
GoScript 5X Reaction Buffer	4 µl	1X
MgCl ₂ (25 mM)	1.2 µl	1.5 mM
PCR nucleotide mix (10 mM)	1 µl	0.5 mM each
Recombinant RNasin Ribonuclease Inhibitor	0.5 µl	20 Units
GoScript reverse transcriptase	1 µl	Not indicated*
Nuclease-free water	up to 15 µl	

* The concentration of the GoScript reverse transcriptase was not specified by the supplier. The supplier instructions indicated an efficient performance when 1 µl of the enzyme is added to 20 µl of the reverse transcription reaction mixture.

Reverse transcription reaction mixtures were prepared in separate tubes for each sample as well as for the positive and negative control samples. The sample as well as the positive and negative controls were each added to the corresponding reverse transcriptase reaction mixture tubes to make a final volume of 20 µl in each tube. The samples were then placed in the thermal cycler to generate the first strand of cDNA using the following programme:

<u>Temperature</u>	<u>Duration</u>	<u>Outcome</u>
25°C	5 minutes	Annealing
Next, one cycle of:		
42°C	1 hour	Extension
70°C	15 minutes	Inactivation of reverse transcriptase

The generated first strand of cDNA was then used as a template in a normal PCR reaction to generate the complementary DNA strand using the GoTaq Flexi DNA polymerase (Promega, UK) kit as described previously. The second strand synthesis was carried out using primers specifically designed to amplify certain regions of cDNA. The final PCR reaction volume for the second strand synthesis was 25 μ l using 5 μ l of the cDNA first strand as a template. The carry over of both the $MgCl_2$ and dNTPs was carefully considered when determining the final volume of $MgCl_2$ and dNTPs to be added in the second PCR in order to optimize the final concentration of both components in the second reaction mixture. The products of the second PCR reaction were then analysed by agarose gel electrophoresis.

2.4.9. Agarose gel electrophoresis

The agarose gel electrophoresis technique was used to analyse DNA and RNA samples whenever required throughout this study. The agarose gel was prepared by dissolving the agarose powder (1% w/v) in 1X TAE buffer (containing 40 mM Tris, 20 mM acetic acid, and 1 mM EDTA). For samples to be gel extracted, the agarose concentration was reduced to 0.8% (w/v) to facilitate the gel extraction of DNA. Once dissolved, the agarose was poured into a UV-gel tray containing a comb, and was allowed to solidify at room temperature. Depending on the number of samples to be loaded, a small (10 x 7 cm) or a large (15 x 10 cm) UV-gel tray can be used. The gel was then placed in a horizontal gel tank (GeneFlow Ltd., UK) containing 1X TAE buffer. Each sample to be analysed was mixed with a 5X DNA loading buffer (Yorkshire Bioscience Ltd, UK) in a ratio of 5 μ l of sample to 2 μ l of the loading buffer. The components of the 5X DNA loading buffer include 50 mM Tris-HCl, 50 mM EDTA, 0.025% Bromophenol Blue, and 60% glycerol, with a pH of 7.6 (Yorkshire Bioscience Ltd, UK). The samples were then loaded into the gel wells. An appropriate DNA ladder was as well loaded in a separate well. A supercoiled DNA ladder (Promega, UK, or New England Biolabs, UK) was loaded to check the size of the extracted DNA plasmids. Either the HighRanger 1 kb DNA ladder (Norgen Biotek Corp., Ontario, Canada) or the Q-Step 4 DNA ladder (Yorkshire Bioscience Ltd., UK) were used to check the size of the linear DNA samples. The gel tank was then connected to the power supply (PowerPac 300, Bio-Rad). A voltage of 90 was applied to the small gel tank while a voltage of 110 was applied to the large gel tank. The gels were left to run for 70 minutes. The gel was then stained by immersion in a 5 μ g/ml

solution of ethidium bromide for 30 minutes with gentle shaking. The stained gel was then rinsed with water to remove the traces of ethidium bromide and the DNA or RNA samples were visualized under UV using the Dual-Intensity Chromato-Vue Transilluminator TM-20 (UVP, San Gabriel, USA). A picture of the gel containing the samples was then taken using the Kodak EDAS 290 Electrophoresis Documentation and Analysis System.

2.4.9.1. Extraction of DNA fragment from agarose gel

Gel extraction was performed using QIAquick Gel Extraction Kit (QIAGEN) according to the manufacturer's instructions. Briefly, the DNA sample to be extracted was run on a 0.8% agarose gel at 90 volts for 70 minutes. The DNA fragment was then visualized under UV light and quickly cut using a clean sharp blade. The gel slice was then placed in a clean 1.5 µl microfuge tube and its exact weight was determined in milligrams. Three volumes of Buffer QG was added to the gel slice and the sample was incubated at 50°C for 10 minutes with quick vortexing every 3 minutes during the period of incubation to help dissolving the agarose gel. A QIAquick Spin Column was placed in a 2 ml collection tube (both provided in the kit). The sample was added to the column followed by a centrifugation step at 16,100 g for 1 minute at room temperature using an Eppendorf Centrifuge 5415D. The flow-through was discarded and 750 µl of Buffer PE was added to the column followed by another centrifugation step for 1 minute. The flow-through was discarded and the empty column was further centrifuged for 2 minutes for a complete removal of residual ethanol. The column was then placed into a clean 1.5 ml microfuge tube and 50 µl of the elution buffer (Buffer EB) was added to the column. For an increased DNA concentration the elution buffer was added in a 30 µl volume. The column was allowed to stand for 1 minute at room temperature before a final centrifugation step of 1 minute at 16,100 g was done to elute the DNA. Finally, the purified extracted DNA was analysed on a 1% agarose gel to check for a successful gel extraction. The DNA sample was stored at -20°C until needed.

2.5. Introduction of genetic material into bacterial cells

The term transformation is used to describe the genetic alteration of the bacterial cell due to the introduction of a foreign DNA. The foreign DNA can be introduced into the cell by either the uptake of the DNA through the bacterial cell membrane or by bacterial conjugation. The transfer of the DNA material through the bacterial cell membrane can be induced in the laboratory by either heat shock or by

electrical shock (electroporation). In addition, the bacterial cells must be in a state of competence in order for them to be able to up take a plasmid DNA through the membrane. In this study the bacterial cells were made artificially competent in the laboratory using certain procedures which are described in the following paragraphs. Bacterial conjugation is the transfer of DNA from a donor cell to a recipient cell by cell to cell contact mediated by pili. Detailed procedures describing heat shock transformation, electroporation, bacterial conjugation and triparental conjugation are provided below described below.

2.5.1. Transformation by heat shock

The foreign DNA can be introduced through the bacterial cell membrane by first making the bacterial cells competent followed by the application of a heat pulse. The sudden application of heat will increase the permeability of the cell membrane allowing the plasmid DNA to enter the cell through the cell membrane. A detailed protocol on how to make the bacterial cells competent is provided below. The heat shock transformation was performed as the following: the competent cells were obtained from the -80°C freezer and were thawed on ice. Once thawed, a 100 μl of the competent cells was mixed with 5 μl of the plasmid DNA to be introduced into the cells. The mixture was incubated on ice for one hour. The 1.5 ml microfuge tube containing the mixture was then placed in a 42°C water bath for 60 seconds followed by immediate placement of the tube on ice again for one minute. The mixture was then removed from ice and 900 μl of BHI broth was added gently to the transformed cell suspension. The cell suspension was mixed by pipetting up and down and was then incubated in a water bath previously set to 37°C . Next, a serial dilution of the transformed bacterial suspension was performed in a BHI broth for up to 10^{-3} . The dilutions were then plated on previously prepared LB agar plates containing the appropriate antibiotic, i.e., as the antibiotic encoded by the introduced plasmid. From each dilution, a 100 μl was placed on the LB agar and was then spread using a sterile glass spreader. The plates were then incubated over night at 37°C . Next day, the plates were examined for the presence of colonies, the colonies were then screened by either plasmid miniprep extraction, or colony PCR, both of which are described elsewhere in this chapter.

2.5.1.1. Preparation of competent cells for heat shock transformation

Competent cells were prepared for this study using the method of Hanahan (Hanahan, 1983) with a few modifications. Briefly, 99 ml of BHI broth was inoculated with 1 ml of an overnight broth culture of the *E. coli* bacterial strain which its cells need to be made competent. The 100 ml bacterial culture was then incubated at 37°C for 2 hours with shaking. After completion of the two hours of incubation the OD₆₀₀ was checked every 20 minutes until OD₆₀₀ of 0.3 was reached. Once the desired absorbance of cellular density was reached, the cells were placed on ice immediately followed by centrifugation of the bacterial broth culture at 3900 g for 20 minutes at 4°C. The broth was then discarded and the pellet was then resuspended in 33 ml of ice cold RF1 solution, the components of which are indicated below. Next, the bacterial suspension was incubated on ice for 15 minutes. Another step of centrifugation was carried out at 3900 g for 20 minutes at 4°C. The supernatant was discarded and the pellet was resuspended in 8 ml of ice cold RF2 solution. The components of RF2 solution are listed below. The bacterial suspension was incubated on ice for 15 minutes followed by its aliquot into chilled microfuge tubes. The competent cells were stored at – 80°C until required.

RF1 solution

- KCl 100 mM
- MnCl₂ 50 mM
- CaCl₂ 10 mM
- Potassium acetate 30 mM
- Glycerol 15% (v/v)

The pH of the RF1 solution was adjusted to 5.8 with glacial acetic acid followed by its filter sterilization and storage at 4°C.

RF2 solution

- KCl 10mM
- CaCl₂ 75mM
- MOPS (pH 6.8) 10mM
- Glycerol 15% (v/v)

The RF2 solution was then filter sterilized and stored at 4°C.

2.5.2. Bacterial conjugation

In some experiments during this study, the bacterial plasmids were transferred from cell to cell using the bacterial conjugation technique. Mobilizing strains of *E. coli* containing the mobilisable plasmid and the *A. caviae* Sch3N strain to which the plasmid was to be transferred are grown separately overnight at 37°C in 10 ml of BHI broth with shaking. The appropriate antibiotics were added to the BHI broth whenever necessary. The cells were then pelleted by centrifugation and the formed pellets were then washed twice with 20 ml of phosphate buffered saline (PBS). The cells were pelleted again by centrifugation and the formed pellets were then resuspended in 100 µl of PBS. The 100 µl suspension of *E. coli* was added to the 100 µl suspension of *A. caviae* Sch3N. After thorough mixing by pipetting, the mixture was transferred to a CBA plate. The CBA plate was then incubated overnight in a face-up position at 37°C. Next day, the growth on the plate was collected by a sterile loop and was added to a 1.5 ml microfuge tube containing 1 ml of sterile PBS. The suspension was thoroughly mixed by pipetteing and a serial dilution in PBS was made down to 10⁻³. From each diluted suspension, a 100 µl was plated on LB plates containing the antibiotic nalidixic acid plus the antibiotic encoded by the plasmid. The included antibiotics allowed for the selection of the *A. caviae* Sch3N strain to which the plasmid was successfully transferred. The colonies were then screened by plasmid miniprep extraction or by PCR.

2.5.3. Bacterial triparental conjugation

The procedure for the triparental mating was the same as the one for the bacterial conjugation mentioned above, except that, a helper plasmid was used to allow for the mobilization of the desired plasmid. The helper plasmid used in this study was pRK2013 (hosted in *E. coli* HB101). A third bacterial broth culture containing the helper plasmid was washed twice with PBS and the resultant pellet was resuspended and added to the pellet of the other two bacteria, namely the *E. coli* containing the mobilisable plasmid and the *A. caviae* Sch3N which will receive the plasmid.

2.6. The β-galactosidase assay

This assay was performed to check the activity of certain promoters from the *A. caviae* Sch3N genome. The promoter to be studied was first fused to a promoter-less plasmid vector which contains the reporter gene *lacZ* which encodes the β-galactosidase enzyme. The promoter-less plasmid used in this study was pKAGb-2(-). The promoter fusion technique was done by PCR amplification of the DNA region encoding the

promoter using primers with the proper restriction digestion sites. A restriction digestion reaction was then carried out for the PCR amplicons as well as the promoter-less vector and a directional insertion of the promoter region was achieved by a ligation reaction. The plasmid construct was then introduced into *E. coli* DH5 α following a heat-shock transformation reaction. The construct was then transferred to the strain in which the promoter activity needed to be studied either by bacterial conjugation or electroporation techniques. The last two techniques as well as the PCR and cloning techniques are all described elsewhere in this chapter. A strain containing pKAGb-2(-) with no insert (empty vector) was used as a negative control whenever needed. The promoter activity was studied during either swarming or swimming of the bacterial cells. For studying the promoter activity within swarming bacteria, the bacterial cells were first allowed to swarm by growing them on swarming agar plates, as described above. Following overnight incubation, a 1 ml of Z-buffer was added to the swarming bacteria in the swarm agar plate.

Z-buffer

- Na₂HPO₄·7H₂O 0.06M
- NaH₂PO₄·2H₂O 0.04M
- KCl 0.01M
- MgSO₄·7H₂O 0.001M
- Distilled H₂O Up to 1 litre

The Z-buffer was then stored at 4°C. The swarming bacteria were then detached from the agar by a sterile loop and the Z-buffer containing the bacteria was then collected using a sterile pipette and placed in a microfuge tube. The bacterial suspension was then adjusted to OD_{600nm} of 0.5 to 0.7 using Z-buffer as a diluent. The bacterial suspension was placed in a disposable cuvette and the optical density was read using a spectrophotometer (Ultrospec III, Pharmacia LKB Biotechnology, England). The exact OD_{600nm} value was recorded for later use. Once the desired optical density was reached, the cuvette containing the bacterial suspension was kept on ice. Testing the activity of a promoter in swimming bacteria requires first growing the bacterial cells overnight with shaking at 37°C in 10 ml of BHI broth. Next day, 5 μ l of the overnight culture was added to 10 ml of BHI broth. Following two hours of incubation, the OD_{600nm} was checked every 20 minutes until OD_{600nm} 0.5-0.7 was reached. The exact value of the optical density was recorded and the broth culture was immediately stored on ice ready to be used for the β -galactosidase assay. Once the proper optical density of

either the swimming or the swarming bacteria was obtained, two solutions were prepared on the same day of the experiment, the working solution and the substrate solution. Both solutions were composed of the Z-buffer and 0.05 M of β -mercaptoethanol plus an additional 4 mg/ml of *o*-nitrophenyl- β -D-galactoside (ONPG) powder which was added to make the substrate solution. The substrate solution was mixed by vortexing to allow for the ONPG powder to dissolve properly. The compound ONPG was the synthetic substrate used for the β -galactosidase enzyme encoded by the *lacZ* gene. Upon its recognition and cleavage by the enzyme β -galactosidase, the ONPG splits into two compounds, the *o*-nitrophenol which gives a yellow colour and galactose. It is the intensity of the formed yellow colour which was measured in this assay. The β -galactosidase assay was performed using borosilicate glass tubes (12 mm with rim, Fisher Scientific, UK) and each strain was tested in triplicate. To study the promoter activity, the bacterial cells need first to be permeabilized. A permeabilization solution was prepared in each glass tube by addition of 840 μ l of the working solution, 100 μ l of the bacterial suspension, 30 μ l of 0.1% SDS, and finally 30 μ l of chloroform. The mixture was vortexed for 15 seconds to allow the proper mixing of components and permeabilization of bacterial cells. The glass tubes containing the permeabilized cells were then placed in a 30°C water bath for 15 minutes. Next, 200 μ l of the substrate solution was added to the glass tube containing the permeabilized cells to start measuring the activity of the promoter under study. The time at which the ONPG substrate was added was recorded as “the start time” and the reaction was done in a 30°C water bath. The tube was vortexed for 15 seconds and returned back into the water bath. As soon as the colour of the incubated suspension changes from transparent to a yellow colour, the reaction was stopped by addition of 500 μ l of 1M Na₂CO₃. The mixture was vortexed for 15 seconds and the exact “stop time” was recorded. The yellow coloured suspension was then placed into a disposable plastic 1 cm cuvette and both the OD₄₂₀ and OD₅₅₀ were recorded. The Miller units were then calculated to assess the activity of the promoter using the following formula:

$$1\text{Miller Unit} = 1000 \times \text{Abs}_{420} - (1.75 \times \text{Abs}_{550}) / \text{Time (min)} \times \text{Volume of cells (ml)} \times \text{Abs}_{600}$$

Finally, a graph was plotted showing the promoter activity in comparison to the negative control strain possessing the pKAGb2(-) with no promoter.

2.7. Biofilm assay

One colony of the bacterial strain to be studied was inoculated to a 10 ml of BHIB containing the appropriate antibiotics. The broth was incubated overnight at 37°C with vigorous shaking. Next day, the optical density (OD_{600nm}) for the overnight culture was then measured and was adjusted to 0.6. From the adjusted broth culture a 10 µl was removed and was added to a sterile borosilicate glass tube containing 990 µl of BHIB. As the test was done in triplicate, and readings were to be taken after 24h and 48h, six glass tubes were inoculated. Each inoculated test tube was immediately covered with a sterile piece of foil. The borosilicate glass tubes containing the bacterial suspensions were incubated at 37°C with shaking for 48 hours with the first reading was taken at 24 h of incubation. To quantitatively determine the amount of the formed biofilm, three of the six tubes were removed from the incubator shaker after 24 hours. The bacterial suspension was discarded and the tubes were washed twice with sterile distilled water. To each of the empty tubes 1300 µl of 0.5% crystal violet (CV) dye was added and the tubes were incubated at room temperature for 15 minutes. The CV was then discarded and the tubes were washed three times with distilled water. Pictures of the stained biofilms (if any) were taken after this washing step. To dissolve the biofilm, 1.5 ml of absolute ethanol was added to each tube followed by 10 minutes of incubation at room temperature. The ethanol (containing the dissolved CV) was then poured into a disposable cuvette and the quantity of the formed biofilm was determined by measuring the OD_{570nm} of the solution. The average of the three readings was taken, and the same steps of biofilm staining and quantification were followed for the bacterial suspensions which were to be incubated for 48 hours. A graph was then plot comparing the readings of each time point. Since many *A. caviae* Sch3N strains were tested in this study, the graph was comparing different strains in addition to comparing the 24h and 48h incubation time points.

2.8. Western blot analysis

The Western blot analysis was performed to detect the expression of the polar flagellin protein and the lateral flagellin protein in *A. caviae* Sch3N during swarming and swimming of the bacterium. The Western blot analysis required samples to be first run on a gel to separate the cellular proteins by the Sodium Dodecyl Sulphate Polyacrylamide Gel Electrophoresis (SDS-PAGE) technique after which the specific polar or lateral flagellin proteins can be detected by Western blotting. To preform an

SDS-PAGE, samples of swimming and swarming bacteria need first to be prepared, as described below.

2.8.1. Preparation of swimming bacteria for SDS-PAGE

One colony of *A. caviae* was inoculated to 10 ml of BHI broth and the inoculated broth was incubated overnight with shaking at 37°C. As the test was done in triplicate, three tubes were needed. Next day, the broth cultures were diluted with PBS to reach a density within a range of 0.3 to 0.5 when read at 570 nm by spectrophotometer. A volume of 1 ml from each culture was centrifuged at room temperature for 10 minutes at 16,100 g using an Eppendorf centrifuge 5415D. Next, the broth was discarded and the pelleted cells were resuspended in 60µl of 1X Laemmli sample buffer, the components of which are listed below. The resuspended cells were then boiled for 15-20 minutes to lyse the cells and denature proteins. After boiling, the suspensions were spun for few seconds and were then ready to be loaded on the gel to perform an SDS-PAGE.

1X Laemmli sample buffer:

- 63 mM Tris-HCl (pH 6.8)
- 2% (w/v) sodium dodecyl sulphate (SDS)
- 10% (v/v) glycerol
- 0.0005% (w/v) bromophenol blue

2.8.2. Preparation of swarming bacteria for SDS-PAGE

One colony of *A. caviae* was inoculated to 10 ml of BHI broth followed by an overnight incubation of the inoculated broth with shaking at 37°C. As the test was done in triplicate, three tubes were needed. Next day, swarm agar plates were freshly prepared, as described elsewhere in this chapter. The overnight liquid cultures were then centrifuged at 10°C for 10 minutes at 2782 g using Allegra™ X-22R Centrifuge (Beckman Coulter). The liquid medium was then discarded and a volume of 1 µl was drawn by pipette from the formed pellet and was used to inoculate the swarm agar plates. The swarm agar plates were then incubated at room temperature for 24hrs. Next day, the swarm for each strain to be tested was collected in a microcentrifuge tube containing PBS. Collection of swarm was done by sterile toothpicks. The density of the formed suspensions was then adjusted with PBS to be within a range of 0.3 to 0.5 when read at 570nm by spectrophotometer. A volume of 1ml from each suspension was then

centrifuged at room temperature for 10 minutes at 16,100 g using an Eppendorf centrifuge 5415D. Next, the broth was discarded and the pelleted cells were resuspended in 60µl of 1X Laemmli sample buffer. The resuspended cells were then boiled for 15-20 minutes to lyse the cells and to denature proteins. After boiling, the suspensions were spun for few seconds and were then ready to be loaded on the gel to perform an SDS-PAGE.

2.8.3. Sodium Dodecyl Sulphate Polyacrylamide Gel Electrophoresis (SDS-PAGE)

To perform an SDS-PAGE we first assembled the vertical gel electrophoresis unit (OmniPAGE Mini, Geneflow Ltd, UK) containing two glass plates with a dimension of 10cm x 10cm and a thickness of 2mm. This was followed by preparation of a 12% running gel to be added in each of the two assembled glass plates.

12% Running gel

- 4 ml 30% Acrylamide
- 3.3 ml dH₂O
- 2.5 ml Tris-HCl, 1.5M (pH 8.8)
- 50 µl 20% SDS
- 200 µl 10% Ammonium persulphate
- 7 µl TEMED

After pouring the gel in each of the two glass plates, isopropanol was added on the top of the running gel to get rid of any formed bubbles. The gels were set at room temperature for 30 minutes. After solidification, the isopropanol was washed off with 1 ml of distilled water. Next, the stacking gel was prepared to be added on the top of the running gel and in which the comb would be inserted.

5% Stacking gel

- 670 µl 30% Acrylamide
- 2.7 ml dH₂O
- 500 µl Tris-HCl, 1M (pH6.8)
- 40 µl 10% SDS
- 40 µl 10% Ammonium persulphate
- 5 µl TEMED

After addition of the stacking gel and fixation of the combs, the device was left for 30 minutes at room temperature for the stacking gel to solidify. After solidification, the glass plates containing the gels were placed into the OmniPAGE Mini tank. This

was followed by addition of a 1X SDS running buffer to the tank and between the glass plates containing the gels:

10X SDS Running buffer

- 30.3 g Tris base
- 144 g Glycine
- 10 g SDS
- Up to 1L dH₂O

Next, the comp was carefully removed and the protein samples were loaded. The OmniPAGE Mini tank was then covered with its lid and its anode and cathode were properly connected to the power supply (PowerPac 300, BioRad, UK). The SDS-PAGE was carried out to separate proteins within samples by adjusting the voltage to 160 and the time to 1 hour (or until the loaded protein samples reach the end of the gel).

2.8.4. Performing Western blotting

Western blotting was performed using Mini Protean 3 Western transblot system (BioRad, UK). To use this system, the SDS-PAGE gel (prepared as described above) was removed from the glass plates and was placed on a 0.45 µm nitrocellulose membrane (Whatman, GE Healthcare Life Sciences, UK). The membrane was then placed on a filter paper and the filter paper was placed on a fiber pad. The gel was also covered with a filter paper which was then covered with a fiber pad. The gel and the membrane (along with the filter papers and fiber pads) were placed in a gel holder cassette which was then closed to press them together. The closed cassette was then placed into the buffer tank.

The tank was filled with 1X transfer buffer and a magnetic stir bar was placed in the bottom of the tank. The tank was then covered properly with its lid and was placed on the top of a magnetic stirrer. The tank was connected to the power supply (PowerPac 300, BioRad, UK) and the voltage was adjusted to 10 volts. The blotting system was left overnight with stirring to transfer the proteins from the gel to the membrane.

10X Transfer buffer

- 30.3 g Tris
- 144 g Glycine

1X Transfer buffer

- 100 ml 10X Transfer buffer
- 100 ml Methanol
- 800 ml dH₂O

Next day, the gel holder cassette was removed from the tank, the gel was discarded, and the membrane was placed in a new container. The membrane was blocked by adding 20 ml of 5% dried skimmed milk (prepared in PBS). To complete blocking, the membrane was allowed to rotate at room temperature for 1 hour. The membrane was then washed with PBS. A volume of 20 ml of 2.5% dried skimmed milk was then added to the membrane with the primary antibody diluted to 1:500. In this study, the primary antibodies used were either the rat anti-polar flagellin antibody or the rabbit anti-lateral flagellin antibodies. The membrane was incubated on a rotor for 1 hour at room temperature to complete interaction. The membrane was then washed three times with PBS. Next, a volume of 20 ml of 2.5% dried skimmed milk prepared in PBS was directly added to the membrane with the secondary antibody diluted 1:5000. The secondary antibodies used in this study include the anti-rat IgG (for the polar flagellin) and the anti-rabbit IgG (for the lateral flagellin), both of which were labelled with horseradish peroxidase (HRP). The membrane was incubated for 1 hour on a rotor at room temperature following the addition of the secondary antibodies. The membrane was then washed three times with PBS. Finally, the membrane was immersed in Pierce Enhanced Chemiluminescent (ECL) Western blotting substrate (Thermo Scientific) to interact with the HRP enzyme and thus the protein under study will be specifically detected. The membrane was promptly visualised and a picture of it was immediately taken using ChemiDocTMXRS+System with Image LabTM Software (BioRad, UK).

2.9. Statistics

Graphs and data analysis were carried out using Microsoft Excel 2010 software.

Chapter 3

**Role played by *A. caviae* GGDEF-EAL domains
in motility, biofilm formation, and lateral
flagellar genes expression**

Chapter 3: Role played by *A. caviae* GGDEF-EAL domains in motility, biofilm formation, and lateral flagellar genes expression

3.1. Introduction

As indicated in chapter 1, when the novel *scrABC* operon was identified in *Vibrio parahaemolyticus* its role in controlling swarming motility and capsular polysaccharide production was clearly demonstrated (Boles *et al.*, 2002). The ScrC protein encoded in this operon contains both GGDEF and EAL domains and it was shown by a later study that ScrC is able to act as both a diguanylate cyclase and a phosphodiesterase depending on the environmental conditions surrounding the bacterium with the other two proteins in the same operon (ScrAB) directly controlling its activities (Ferreira *et al.*, 2008). Furthermore, ScrG which is another GGDEF-EAL containing protein also identified in *V. parahaemolyticus* was found to play a role in the expression of both lateral flagella (Laf) and capsular polysaccharide (CPS) genes, and its main activity was to degrade c-di-GMP (i.e., a phosphodiesterase) (Kim *et al.*, 2007). Although the genome of *A. caviae* Sch3N does not encode any direct orthologues of ScrC or ScrG, it does encode thirteen GGDEF-EAL domain-containing proteins.

As mentioned earlier, the mesophilic aeromonads are similar to *V. parahaemolyticus* in their possession of two distinct flagellar systems and the lateral flagellar genes in *Aeromonas* species show significant homology to those in *V. parahaemolyticus*. Thus, as in the case with the ScrC and ScrG proteins of *V. parahaemolyticus*, we believe that some of the thirteen GGDEF-EAL-containing proteins in *A. caviae* Sch3N will play a role in the expression of the Laf genes and probably the CPS genes leading to different lifestyles in different settings. To test this hypothesis, this chapter illustrates the effects of overexpressing a GGDEF domain encoding gene, an EAL domain encoding gene, and a gene encoding both GGDEF-EAL domains in *A. caviae* Sch3N on its motility, and its ability to form a biofilm and to bind Congo Red dye. The chapter also shows the effects of knocking out the GGDEF-EAL-encoding genes in the genome of *A. caviae* Sch3N on its motility, its ability to form a biofilm and to bind Congo Red dye, as well as the effects on the activity of certain promoters.

3.2. Overexpression of the genes *AHA1208*, *AHA0382*, and *mshH* in *A. caviae* Sch3N

3.2.1. About the genes *AHA1208*, *AHA0382*, and *mshH*

Before knocking out the GGDEF-EAL domain encoding genes, it was decided first to test our hypothesis by introducing three genes in multi-copy into *A. caviae* Sch3N to check their effects on *A. caviae* lifestyle. These genes were: *AHA1208*, which is a GGDEF domain-encoding gene from *A. caviae* Sch3N, *AHA0382*, an EAL domain-encoding gene from *A. caviae* Sch3N, and *mshH* which is a GGDEF-EAL domain encoding gene of *A. veronii* bv. Sobria strain BC88. The first two genes had never been studied before, while the *mshH* gene was previously isolated, cloned, and studied in our laboratory (Hadi *et al.*, 2012). The genes *AHA1208* and *AHA0382* were chosen from the list of the single domain encoding genes in the genome of *A. caviae* Sch3N. As our group possess the complete genome sequence of *A. caviae* Sch3N, the amino acids sequences of the two genes *AHA1208* and *AHA0382* were subjected to bioinformatics analyses before being cloned in order to check whether they possess the conserved amino acids residues which allow them to be enzymatically active. The amino acids sequence of the *A. veronii* bv Sobria strain BC88 MshH protein was retrieved from the NCBI database and was then subjected to bioinformatics analysis before being overexpressed in *A. caviae* Sch3N to check whether it possesses the signature sequences necessary for the diguanylate cyclase or phosphodiesterase enzymatic activities.

The *AHA1208* gene is composed of 927bp and the encoded protein is composed of 308aa. The domain architecture analysis of *AHA1208* by Simple Modular Architecture Research Tool (SMART) revealed the existence of a single GGDEF domain composed of 168aa (starts at position 141 and ends at position 308) (figure 3.1, A). The amino acids sequence of *AHA1208* was used to search the NCBI protein database by the NCBI blastp tool. The *AHA1208* protein was identified by the blastp tool as a diguanylate cyclase enzyme present in several bacterial species (figure 3.1, B). We have then aligned the amino acids sequence of *AHA1208* with nine other *A. caviae* Sch3N GGDEF containing-proteins (figure 3.2, A). The alignment showed that the active site (A-site) of *AHA1208* contains the conserved signature sequence GGDEF necessary for the diguanylate cyclase activity. The alignment also determined the presence of an I-site containing the sequence RGTD upstream of the A-site.

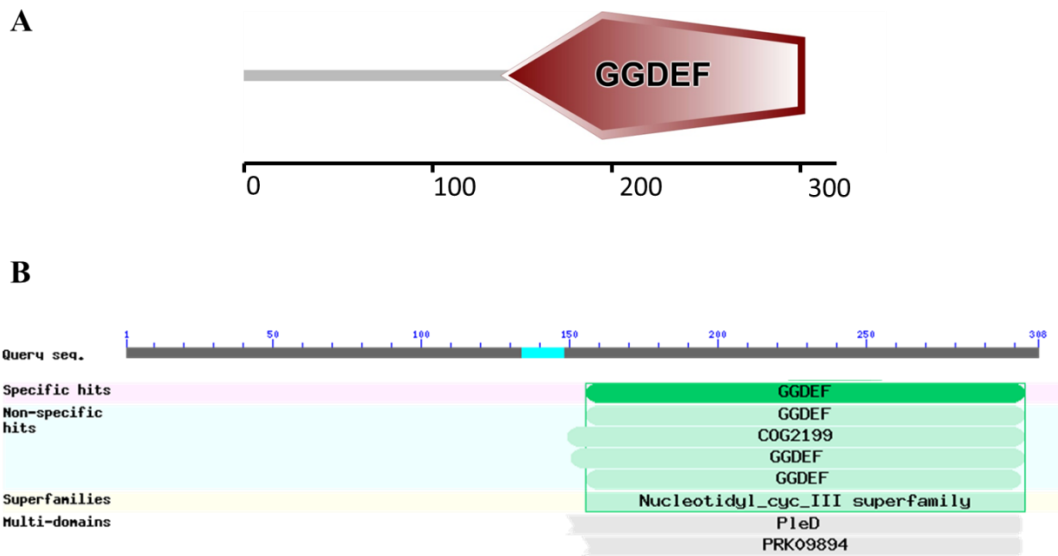
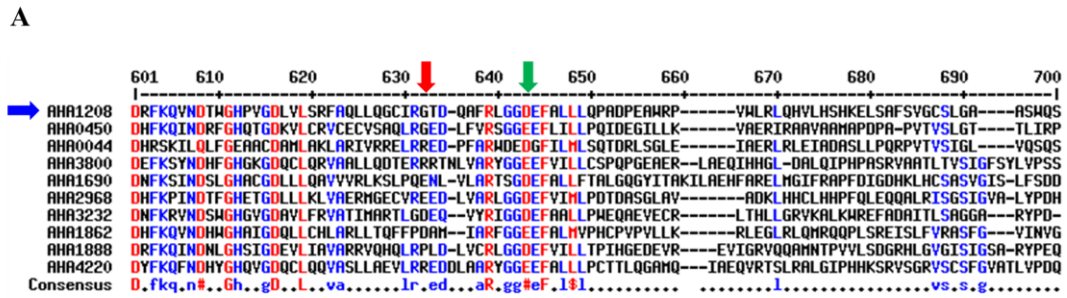


Figure 3.1. Detection of conserved domains of the *A. caviae* Sch3N protein AHA1208 (A) Detection of a GGDEF domain using Simple Modular Architecture Research Tool (SMART). The AHA1208 protein is composed of 308aa. The GGDEF domain was found to be composed of 168aa (starting at position 141 to 308). (B) Detection of a GGDEF domain using the NCBI blastp tool. Specific hits (green-coloured bar) represent the statistically significant sequences that highly matched the sequence of AHA1208 (high confidence). The non-specific hits (light green-coloured bars) represent the statistically less significant matches (less confidence). The AHA1208 protein was placed in the class III nucleotidyl cyclases superfamily. The multi-domains hits (grey-coloured bars) represent a detected similarity to one of several domains contained in multi-domain containing proteins. The scales in A and B represent the number of amino acids.



B

```
MERCKGCNVENTSSLNGFGHGIEQWVQQMERLAPLTGQDRYQQIEQLLQQRDLDA
LLAIFAERVANIVRIHSLQFDCGQPHPLISHPPQARLTLHAYRFEELRGRHEQLLG
QLHYELEHPLSDGQRRLLQYHQFLSLPLP.LYLRLDRLEQQVRLDHLTGLGNRAY
FDEAIGRAVEQHSREPHGLVLVLLDLDLDRFKQVNDTWGHPVGDVLSRFAQLLQGC
IRGTDQAFRLGGDEFALLLQPADPEAWRPVWLRRLQHVLSHSHKELSAFVSGCSLGA
ASWQSGMDVQRLYETADTHLYARKKAGGSGLPE
```

Figure 3.2. Detection of the GGDEF signature sequence and the RxxD motif in the *A. caviae* Sch3N protein AHA1208. **(A)** Multiple sequence alignment comparing the amino acids sequence of AHA1208 (blue arrow) with amino acids sequences of nine other GGDEF domain-containing proteins in *A. caviae* Sch3N using MultAlin online software (<http://multalin.toulouse.inra.fr/multalin/>). The AHA1208 protein contains a conserved GGDEF signature sequence (green arrow) and a conserved RxxD motif (RGTD, red arrow). **(B)** The complete amino acids sequence of *A. caviae* Sch3N protein AHA1208. The sequence contains a GGDEF domain (green colour), a conserved GGDEF signature sequence (yellow colour), a conserved RxxD motif (RGTD, red colour).

The *AHA0382* gene is composed of 1536bp and its encoded protein is composed of 511aa. The domain architecture analysis of *AHA0382* by SMART revealed the existence of a single EAL domain composed of 239aa (starts at position 253 and ends at position 491) (figure 3.3, A). SMART analysis also revealed the existence of two trans-membrane helix regions. The first transmembrane helix region is composed of 23aa (position 6 to 28) while the second region is composed of 20aa (starts at position 231 and ends at position 250). The amino acids sequence of the *A. caviae* protein *AHA0382* was used to search the NCBI protein database by the NCBI blastp tool. The *AHA0382* protein was identified by the blastp tool as a phosphodiesterase enzyme present in several bacterial species (figure 3.3, B). We have then aligned the amino acids sequence of *AHA0382* with five other *A. caviae* Sch3N EAL domain containing-proteins (figure 3.4, A). The alignment showed that *AHA0382* protein contains the conserved EAL motif found in enzymatically active phosphodiesterases.

The *A. veronii* bv. Sobria BC88 *mshH* gene is composed of 1959bp and the encoded protein is composed of 652aa. The domain architecture analysis of MshH by SMART revealed the existence of two transmembrane helix regions, a single GGDEF domain and a single EAL domain (figure 3.5, A). Both transmembrane helix regions are composed of 23aa, the first region starts at position 18 and ends at position 40 while the second transmembrane helix region starts at position 140 and ends at position 162. The GGDEF domain is composed of 171aa (starting at position 221 to 391). The EAL domain is composed of 245aa (starting at position 403 to 647). The amino acids sequence of the *A. veronii* bv Sobria MshH protein was used to search the NCBI protein database by the NCBI blastp tool. The blastp analysis placed the GGDEF domain of the MshH protein in the class III nucleotidyl cyclases superfamily and placed the EAL domain of the same protein in the EAL superfamily (figure 3.5, B). We have then aligned the amino acids sequence of *A. veronii* MshH with the amino acids sequence of thirteen GGDEF-EAL-containing proteins in *A. caviae* Sch3N (figure 3.6, A). The alignment showed that the predicted GGDEF domain in *A. veronii* MshH does not contain the conserved signature sequence and instead the active site contained the sequence AGQVF. The I-site contained the residues RKHN, and the residues ELL were found in the active site of the predicted EAL domain.

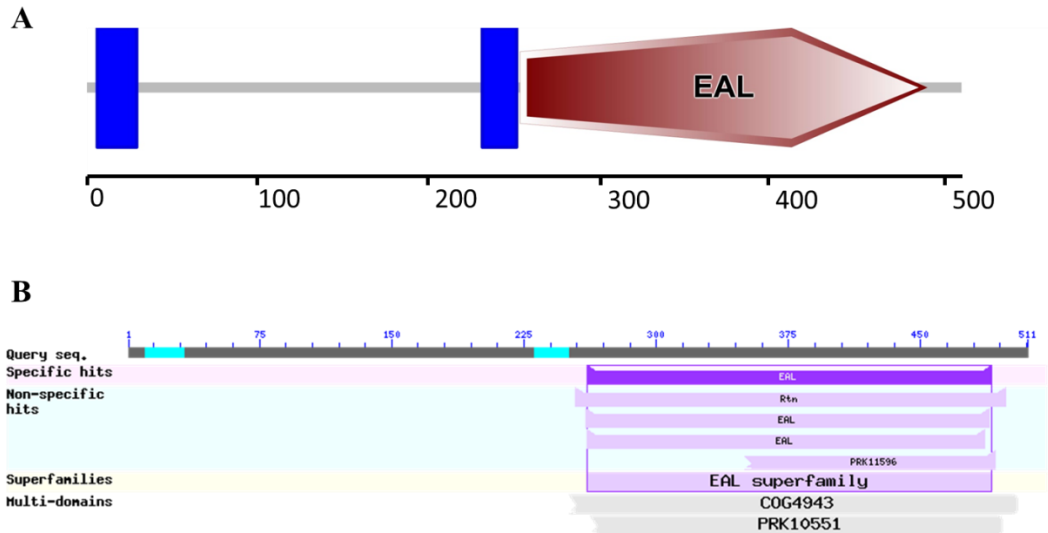


Figure 3.3. Detection of conserved domains of the *A. caviae* Sch3N protein AHA0382 (A) EAL domain and two transmembrane helix regions detected using the Simple Modular Architecture Research Tool (SMART). The AHA0382 protein is composed of 511aa. The first transmembrane helix region is composed of 23aa (starts at position 6 and ends at position 28). The second transmembrane helix region is composed of 20aa (starts at position 231 and ends at position 250). The EAL domain is composed of 239aa (start at position 253 and ends at position 491). (B) EAL domain detected using the NCBI blastp tool. The protein was placed in the EAL superfamily. Specific hits (purple-coloured bar) represent the statistically significant sequences that highly matched the sequence of *AHA0382* (high confidence). The non-specific hits (light purple-coloured bars) represent the statistically less significant matches (less confidence). The multi-domains hits (grey-coloured bars) represent a detected similarity to one of several domains contained in multi-domain containing proteins. The scales in A and B represent the number of amino acids.

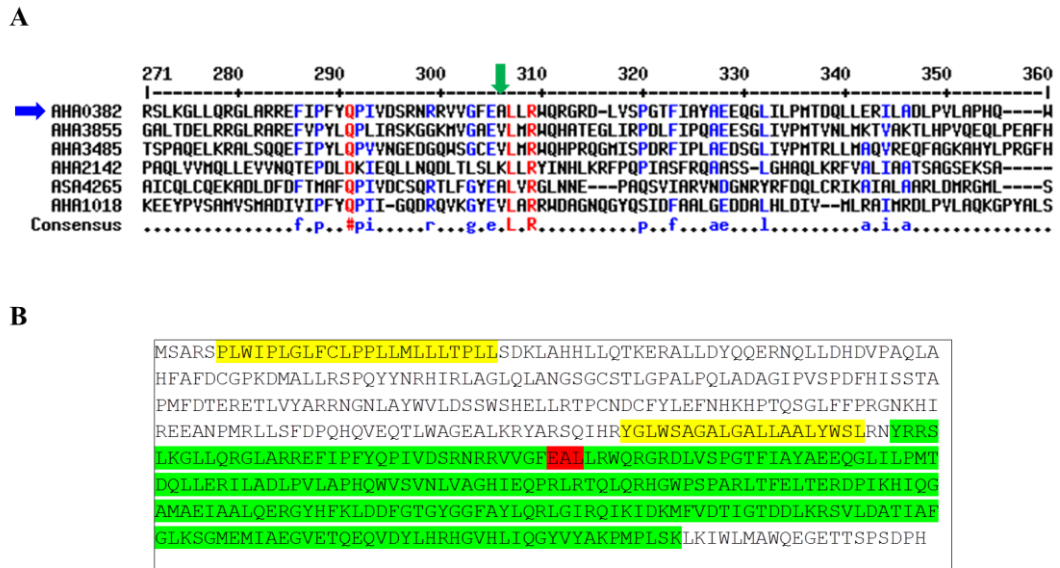


Figure 3.4. Detection of EAL residues in the amino acids sequence of the *A. caviae* protein AHA0382. (A) Multiple sequence alignment comparing the amino acids sequence of AHA0382 (blue arrow) with the amino acids sequences of 5 other EAL domain-containing proteins in *A. caviae* Sch3N using MultAlin online software (<http://multalin.toulouse.inra.fr/multalin/>). A conserved EAL motif was detected in the AHA0382 protein (green arrow) (B) The complete amino acids sequence of AHA0382 protein. The sequence shows the two transmembrane helix regions (yellow), the EAL domain (green) with the exact location of the three EAL residues (red).

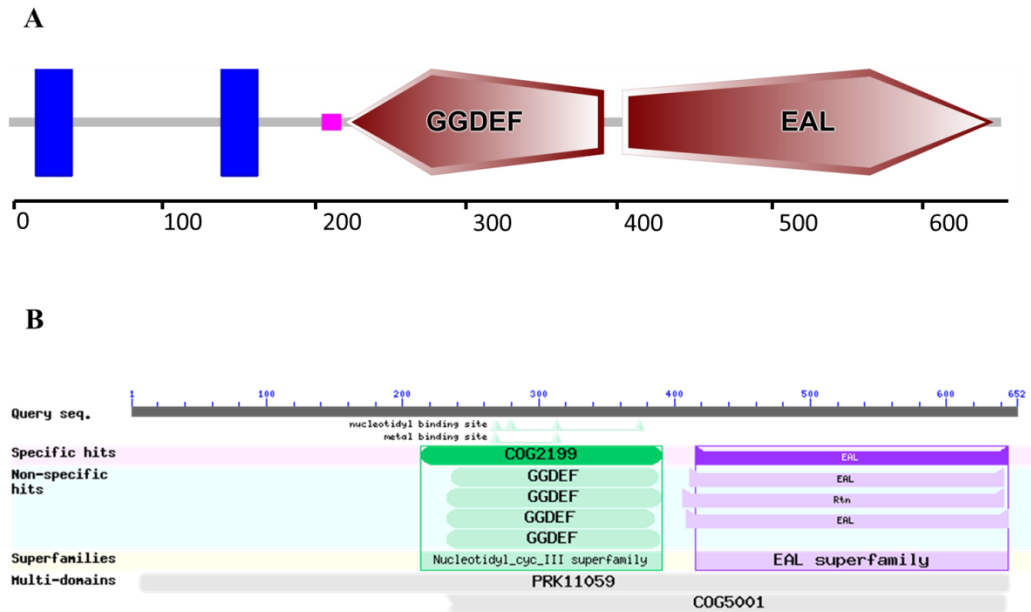


Figure 3.5. Detection of conserved domains of the *A. veronii* bv. Sobria BC88 MshH protein (A) GGDEF domain, EAL domain, and two transmembrane helix regions (blue colour) detected using the Simple Modular Architecture Research Tool (SMART). The MshH protein is composed of 652aa. Both transmembrane helix regions are composed of 23aa, the first region starts at position 18 and ends at position 40 while the second transmembrane helix region starts at position 140 and ends at position 162. The GGDEF domain is composed of 171aa (starting at position 221 to 391). The EAL domain is composed of 245aa (starting at position 403 to 647). (B) Conserved domains detected by the NCBI blastp tool. The specific hits represent the statistically significant sequences that highly matched the sequence of MshH (high confidence). The non-specific hits represent the statistically less significant matches (less confidence). The results placed the GGDEF domain of the MshH protein in the class III nucleotidyl cyclases superfamily and placed the EAL domain of the same protein in the EAL superfamily. The multi-domains hits (grey-coloured bars) represent a detected similarity to one of several domains contained in multi-domain containing proteins. The scales in A and B represent the number of amino acids.

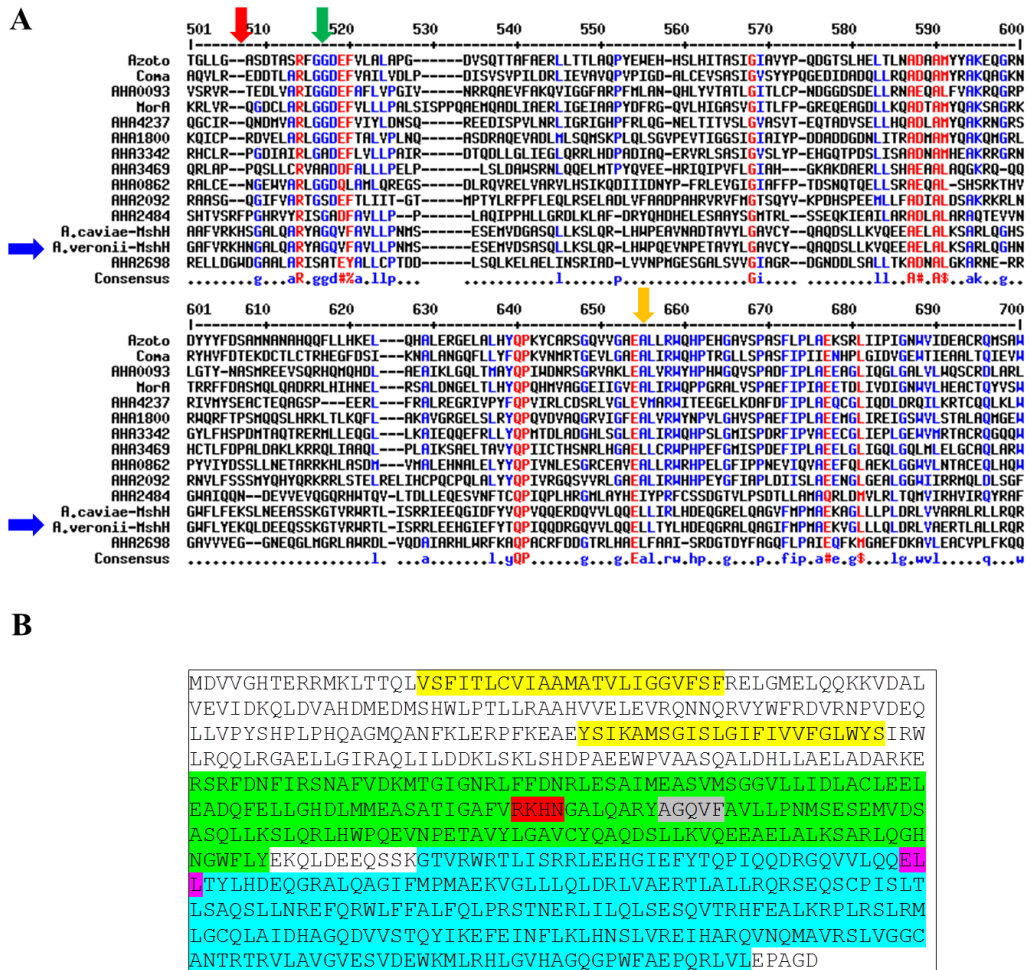


Figure 3.6. Detection of conserved residues in the amino acids sequence of the *A. veronii* bv. Sobria BC88 MshH protein. (A) Multiple sequence alignment comparing the amino acids sequence of *A. veronii* MshH (blue arrows) with the amino acids sequences of thirteen *A. caviae* GGDEF-EAL-containing proteins using MultAlin online software (<http://multalin.toulouse.inra.fr/multalin/>). The I-site contains the sequence RKHN (red arrow), the active site of the predicted GGDEF domain contains the sequence AGQVF (green arrow), and the active site of the predicted EAL domain contains the residues ELL (B) The complete amino acids sequence Of *A. veronii* MshH protein. The sequence shows the two transmembrane helix regions (yellow), the predicted GGDEF domain (green), the predicted I-site (RxxD motif) (red colour), the active site of the predicted GGDEF domain containing the non-conserved sequence AGQVF (gray colour), the predicted EAL domain (light blue), the active site of the predicted EAL domain containing the residues ELL (pink).

3.2.2. Cloning of the genes *AHA1208* and *AHA0382* in *E. coli* DH5 α

The genes *AHA0382* and *AHA1208* were first amplified (figure 3.7) using specifically designed primers which contained restriction digestion linkers for *Xho*I and *Xba*I for later cloning into the plasmid vector pBBR1MCS5 (Gm^R) (figure 3.8). The gene *mshH* was previously ligated in our group to the plasmid pBBR1MCS (Cm^R) (figure 3.9). Both plasmids are of a medium copy number (15-20 copies per cell). The multiple cloning sites of both plasmids are within the *lacZa* gene which is located downstream of a *lac* promoter. The PCR amplicons of the genes *AHA0382* and *AHA1208* and the plasmid pBBR1MCS5 were digested using *Xho*I and *Xba*I followed by performing a ligation reaction. The resulting two constructs pBBR1MCS5-*AHA1208* and pBBR1MCS5-*AHA0382* were then introduced separately by heat-shock into *E. coli* DH5 α . Selection for the correct clones was then carried out by plating the transformed *E. coli* DH5 α cells on LB plates containing the appropriate antibiotics, colony PCR screening as well as DNA sequence analysis. Cloning of *A. caviae* genes *AHA1208* and *AHA0382* in *E. coli* DH5 α was successful (figures 3.10 and 3.11). Cloning of *A. veronii* *mshH* gene in *E. coli* DH5 α was previously done and confirmed by our group.

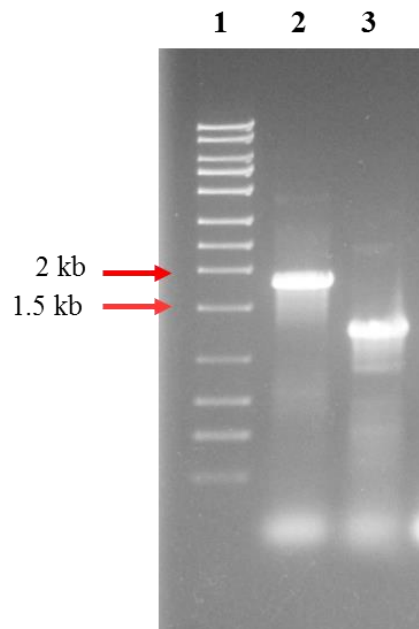


Figure 3.7. A 1% agarose gel showing PCR amplification of *A. caviae* *AHA0382* and *AHA1208*. Lane 1: Norgen biotek DNA ladder, lane 2: EAL domain encoding gene *AHA0382* (1833bp), lane 3: GGDEF domain encoding gene *AHA1208* (1219bp).

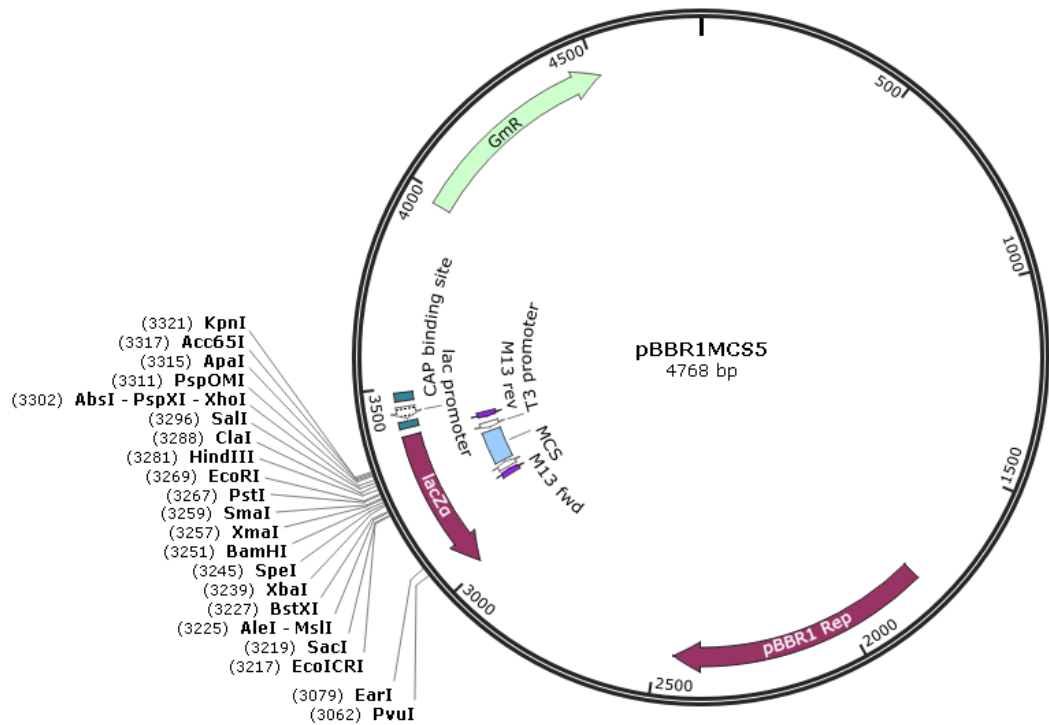


Figure 3.8. A map showing important features of the pBBR1MCS5 broad host range plasmid vector used to clone and overexpress the genes *AHA0382* (encoding EAL domain) and *AHA1208* (encoding GGDEF domain). The plasmid includes a gentamycin resistance marker and a multiple cloning site (MCS) within the *lacZα* gene. The positions of the *lac* and T3 promoters are shown as well as the binding sites for the M13 forward (fwd) and M13 reverse (rev) primers. The map was generated using SnapGene Viewer 2.1.

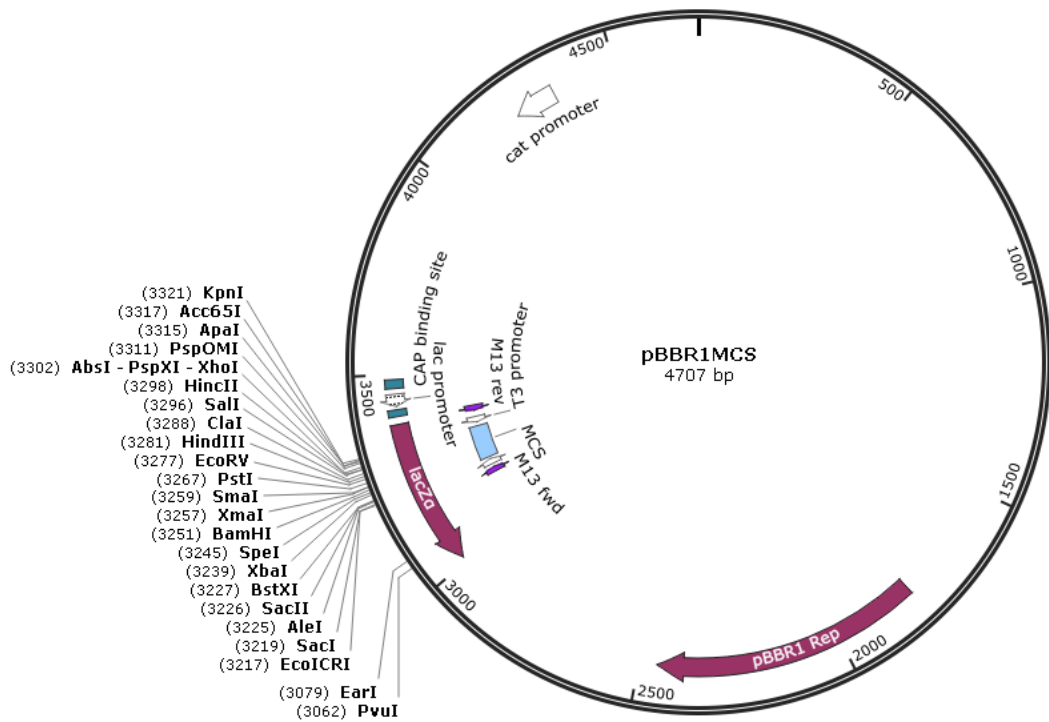


Figure 3.9. A map showing important features of the pBBR1MCS broad host range plasmid vector used to clone and overexpress the *mshH* gene. The plasmid includes a chloramphenicol resistance marker and a multiple cloning site (MCS) within the *lacZα* gene. The map was generated using SnapGene Viewer 2.1.

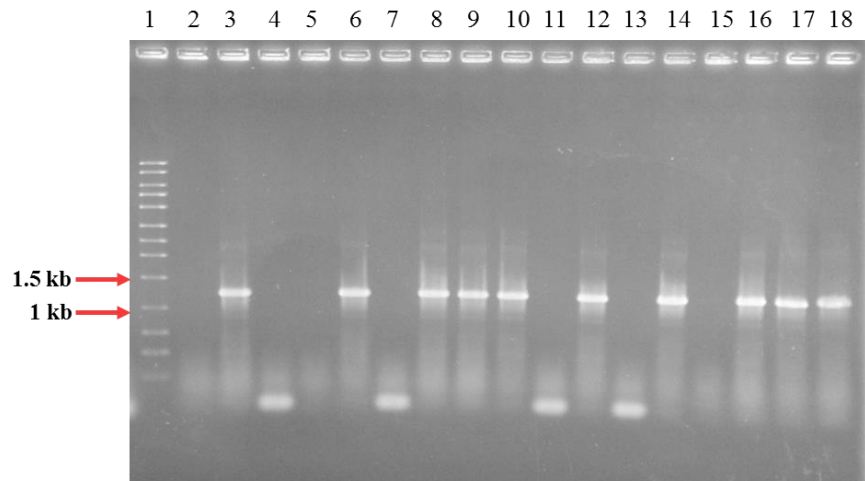


Figure 3.10. A 1% agarose gel showing an *E. coli* DH5 α colony PCR screening following transformation with pBBR1MCS5+*AHA1208*. Gentamicin-resistant *E. coli* colonies were PCR screened using primers *AHA1208*-F and *AHA1208*-R that annealed to the gene *AHA1208*; a positive result would give amplicons size of 1219bp. Lane 1: Norgen biotek DNA ladder, lanes 2-18 transformed *E. coli* DH5 α colonies. Correct size (1219bp) was obtained from colonies number 3, 6, 8, 9, 10, 12, 14, 16, 17, and 18.

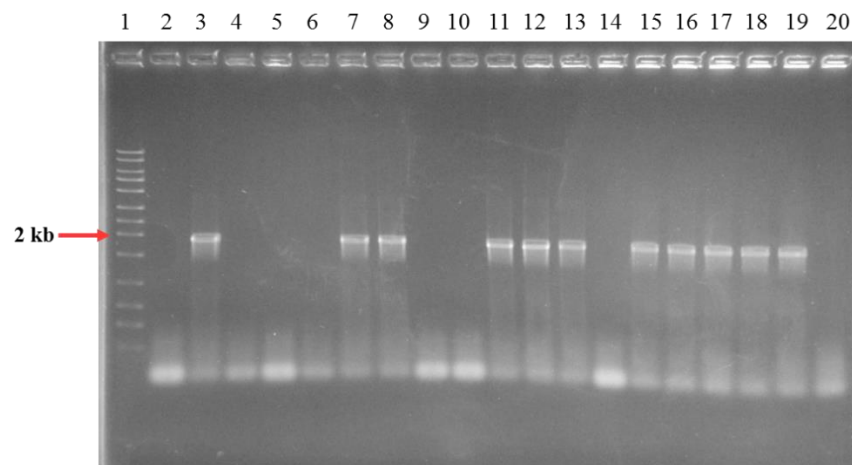


Figure 3.11. A 1% agarose gel showing an *E. coli* DH5 α colony PCR screening following transformation with pBBR1MCS5+ *AHA0382*. Gentamicin-resistant *E. coli* colonies were PCR screened using primers *AHA0382*-F and *AHA0382*-R that annealed to gene *AHA0382*, a positive result would give a fragment of 1833bp. Lane 1: Norgen biotek DNA ladder, lanes 2-20 transformed *E. coli* DH5 α colonies. Correct size (1833bp) was obtained from colonies number 3, 7, 8, 11, 12, 13, 15, 16, 17, 18, and 19.

3.2.3. Introducing multiple copies of *AHA1208* and *mshH* into *A. caviae* Sch3N by bacterial conjugation

The plasmid constructs pBBR1MCS5-*AHA0382*, pBBR1MCS5-*AHA1208*, and pBBR1MCS-*mshH* were then transformed by heat shock to *E. coli* S17-1 in order to transfer them to *A. caviae* Sch3N by conjugation. The transformation to *E. coli* S17-1 was successful for all plasmid constructs. Conjugation was then carried out followed by selection of the *A. caviae* trans-conjugants using LB plates containing the appropriate antibiotics. While the pBBR1MCS5-*AHA1208* and pBBR1MCS-*mshH* were each successfully introduced by conjugation into *A. caviae* Sch3N, the *A. caviae* strain, however, failed to grow on LB plates following the several attempts to introduce the EAL domain encoding gene *AHA0382* into the cell. The effects of overexpressing the *A. caviae* *AHA1208* and the *A. veronii* *MshH* on the ability of *A. caviae* to form a biofilm and on its ability to swarm and swim were then determined using the biofilm assay and the motility assay. No phenotypic studies were carried out for the *A. caviae* EAL encoding gene *AHA0382* due to the failure of its introduction into *A. caviae* by conjugation.

3.2.4. Effects of overexpression of *AHA1208* on *A. caviae* phenotype

Introduction of the GGDEF domain encoding gene *AHA1208* in multi-copy number in *A. caviae* Sch3N resulted in an increase in the ability of *A. caviae* to form a biofilm on a borosilicate glass tube (figure 3.12 and figure 3.13). The relatively thick biofilm was clear by visual inspection and the increase in biofilm density was determined to be statistically significant when compared to the biofilm density formed by the wild type ($p=0.007$). Overexpression of *AHA1208* in *A. caviae* Sch3N has as well resulted in the formation of reddish-coloured rugose type of colonies on Congo Red agar (figure 3.14) in comparison to the translucent colonies with a dark red centre formed by the wild type strain. No noticeable change was observed in the ability of *A. caviae* to swim when *AHA1208* was overexpressed. The migration diameter of *A. caviae* pBBR1MCS5-*AHA1208* during swimming (4cm) was the same as the diameter obtained with the wild type strain after 24hrs of incubation at room temperature (figure 3.15). Also, no effect on swarming motility was detected when *AHA1208* was overexpressed in *A. caviae* (figure 3.16). The diameter of the migration zones formed by the wild type strain measured in each of the three swarm agar plates was 4.7, 4.6, and 3.7cm (average 4.3cm) while that formed by *A. caviae* pBBR1MCS5-*AHA1208* was

2.8, 1.7, and 6.65cm (average 3.7cm) after 24hrs of incubation at room temperature. This reduction in migration zones diameter during swarming of *A. caviae* pBBR1MCS5-*AHA1208* was found to be statistically non-significant ($p=0.70$) when compared to the wild type strain.

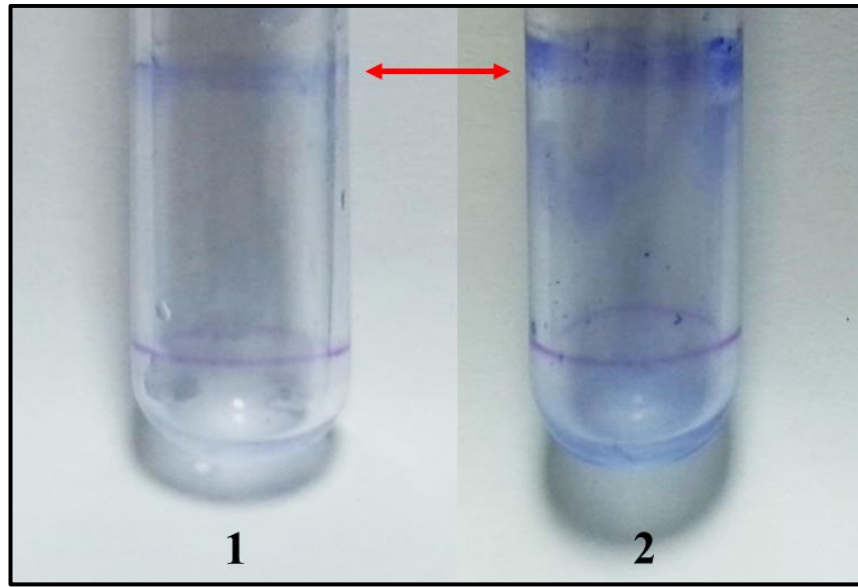


Figure 3.12. Biofilm assay using borosilicate glass tubes and crystal violet stain. Bacteria were grown in BHI broth for 24hrs at 37°C. The test was done in triplicate for each tested strain. (1) *A. caviae* Sch3N (wild type strain). (2) *A. caviae* Sch3N pBBR1MCS5-*AHA1208* (GGDEF domain-encoding gene). The red arrow indicates the formed biofilm by each strain. The picture shows that over expression of *AHA1208* in *A. caviae* results in the formation of a thicker biofilm.

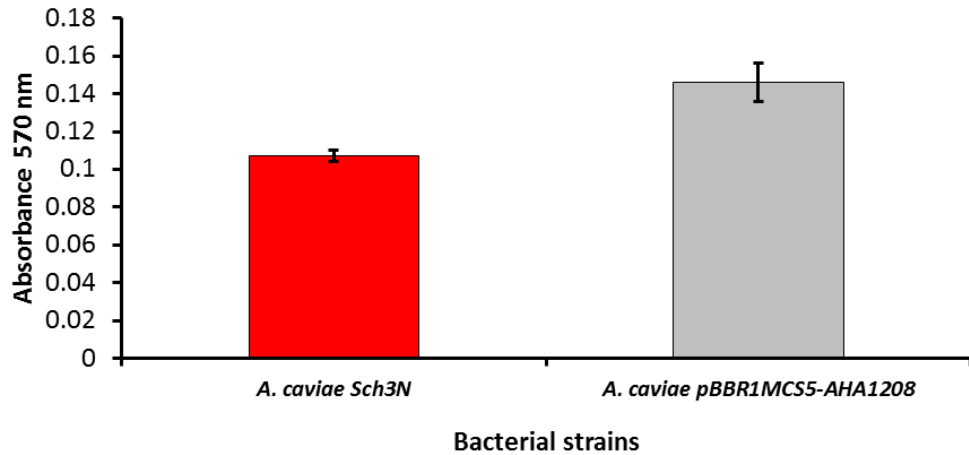


Figure 3.13. Biofilm development on borosilicate glass at 37°C for 24hrs. **Red-coloured bar:** *A. caviae* Sch3N (wild type strain). **Grey-coloured bar:** *A. caviae* Sch3N pBBR1MCS5-AHA1208 (GGDEF domain-encoding gene). The test was done in triplicate. Bars represent the mean value of the three readings. Error bars represent the standard deviation around the mean. Variation was significant (p -value <0.05) using Student's t -Test.



Figure 3.14. A single colony of two strains of *A. caviae* grown on 0.025% Congo Red agar and incubated for 5 days at room temperature to check their ability to form a biofilm (1) *A. caviae* pBBR1MCS-5-AHA1208 (rugose reddish colony) (2) *A. caviae* Sch3N (wild type) showing a translucent colony with a dark red centre. The rugose reddish colony seems to indicate more expression of polysaccharides due to overexpression of the GGDEF domain encoding gene *AHA1208*.



Figure 3.15. Motility test on swim agar plate (0.25% agar) to test the effect of *AHA1208* overexpression in *A. caviae* Sch3N after 24hrs of incubation at room temperature. **(1)** *A. caviae* Sch3N (wild type strain). **(2)** *A. caviae* Sch3N pBBR1MCS5-*AHA1208*. Both tested strains are shown in the pictures to be actively swimming. The test was repeated three times with similar results obtained.

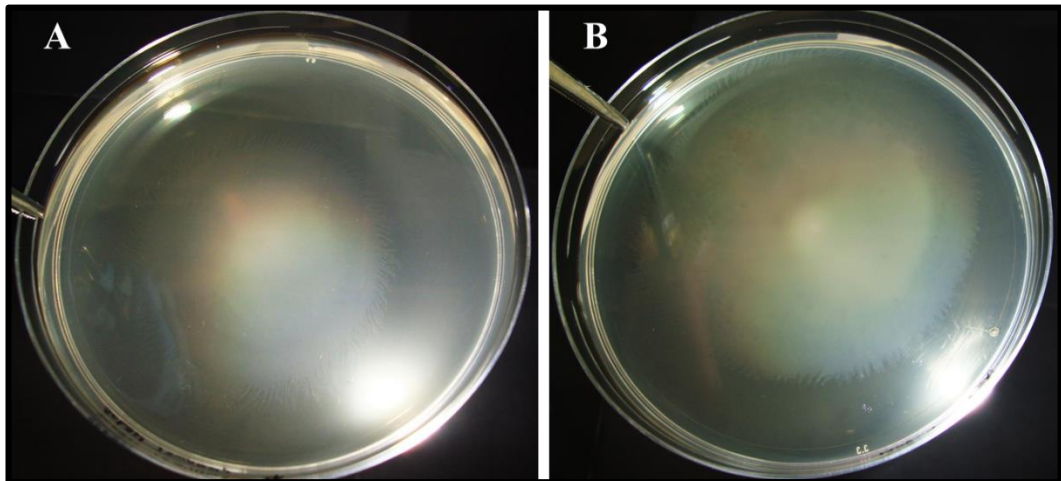


Figure 3.16. Motility test on swarm plate (0.6% Eiken agar) to test the effect of the GGDEF-domain encoding gene *AHA1208* overexpression in *A. caviae* Sch3N after 24hrs of incubation at room temperature. **(A)** *A. caviae* Sch3N (wild type strain). **(B)** *A. caviae* Sch3N pBBR1MCS5-*AHA1208*. Both strains are shown to be actively swarming.

3.2.5. Effects of overexpression of *mshH* on *A. caviae* phenotype

When the GGDEF-EAL encoding gene of *A. veronii* bv. Sobria, *mshH*, was introduced into *A. caviae* Sch3N, the strain's ability to form a biofilm was found to be reduced (figure 3.17). The clear reduction in biofilm formation by the *A. caviae* strain containing the *mshH* gene was not only observed by visual inspection of the glass tubes but was also determined quantitatively as shown in the graph plotted in figure 3.18. The reduction in biofilm production by *A. caviae* pBBR1MCS-*mshH* was found to be statistically significant ($p= 0.01$) when compared to the amount of biofilm produced by the wild type strain.

When the *A. caviae* strain overexpressing the *mshH* gene was grown on Congo Red (CR) agar, no rugose morphology was obtained. The colonies of both the wild type strain and *A. caviae* pBBR1MCS-*mshH* showed a dark red centre and translucent margins (figure 3.19). The colony margins of *A. caviae* pBBR1MCS-*mshH* were more undulated than the margins of the wild type strain. The centre of the colonies of *A. caviae* pBBR1MCS-*mshH* appeared a bit shallower than the margins, i.e., crateriform elevation (having a shape similar to a saucer).

Overexpression of *A. veronii* MshH in *A. caviae* cells did not affect the ability of *A. caviae* to either swim or swarm. The migration diameter of *A. caviae* pBBR1MCS-*mshH* during swimming (4cm) was the same as the diameter obtained with the wild type strain after 24hrs of incubation at room temperature (figure 3.20). Testing the wild type strain and the *A. caviae* strain overexpressing MshH on swarm agar in triplicate gave swarm diameters which ranged from around 3.7cm to filling the entire swarm agar plate (figure 3.21).

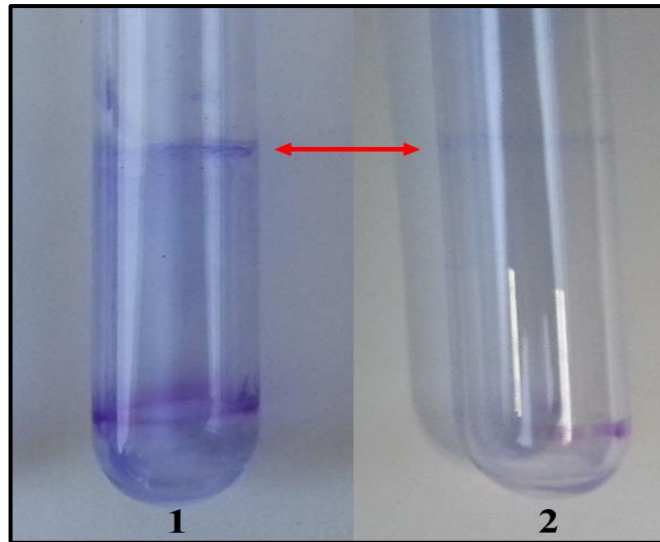


Figure 3.17. Biofilm assay using borosilicate glass tubes and crystal violet stain. Bacteria were grown in BHI broth for 24hrs at 37°C. The test was done in triplicate for each tested strain. (1) *A. caviae* Sch3N (wild type strain). (2) *A. caviae* Sch3N pBBR1MCS-*mshH*. The red arrow indicates the position of the formed biofilm by each strain. The picture shows that overexpression of *A. veronii mshH* gene in *A. caviae* Sch3N caused a reduction in the ability of *A. caviae* Sch3N to produce a biofilm.

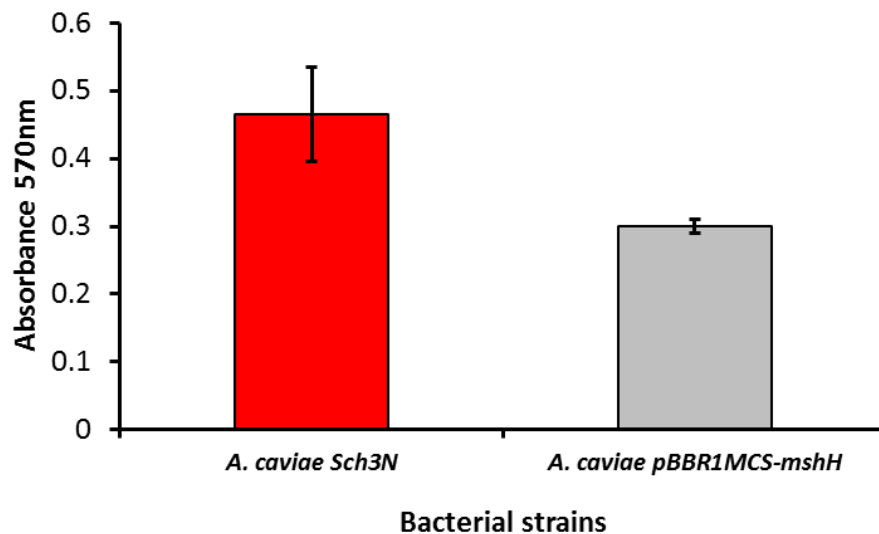


Figure 3.18. Quantitative determination of the formed biofilms on borosilicate glass following 24hrs of incubation at 37°C. **Red-coloured bar:** *A. caviae* Sch3N (wild type strain). **Grey-coloured bar:** *A. caviae* pBBR1MCS-*mshH*. The test was done in triplicate. Bars represent the mean value of the three readings. Error bars represent the standard deviation around the mean. Variation in the formed biofilm was determined to be significant (p -value < 0.05) using Student's t -Test.

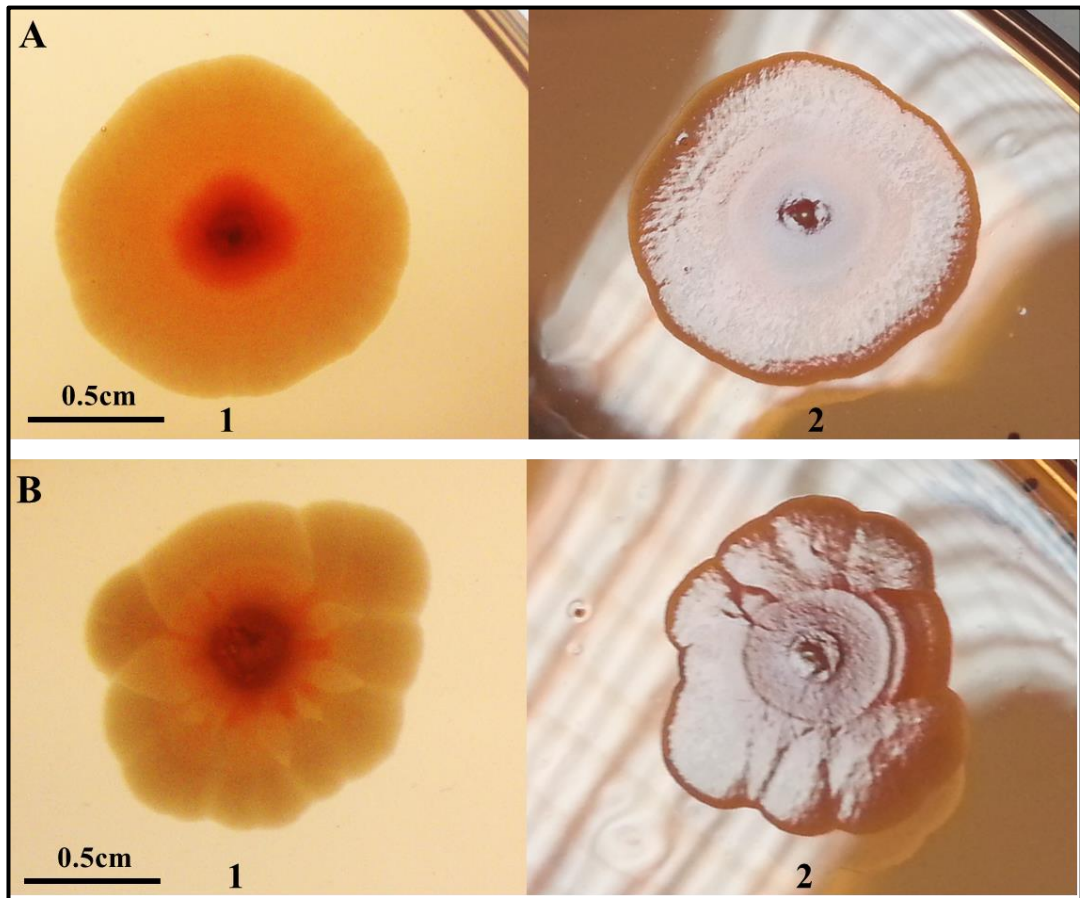


Figure 3.19. Congo Red (0.025%) agar plates showing the effect of MshH overexpression on the colony morphology of *A. caviae* Sch3N following room temperature incubation for 5 days. Pictures were taken at different angles. **A-1:** *A. caviae* Sch3N (wildtype), photo taken directly over the colony. **A-2:** *A. caviae* Sch3N (wildtype), photo taken from an angle. **B-1:** *A. caviae* pBBR1MCS-*mshH*, photo taken directly over the colony. **B-2:** *A. caviae* pBBR1MCS-*mshH*, photo taken from an angle. MshH overexpression in *A. caviae* Sch3N seems to cause the formation of colonies with a crateriform elevation and undulated margins.



Figure 3.20. Motility test on swim agar plate (0.25% agar) to test the effect of *A. veronii* MshH overexpression in *A. caviae* Sch3N after 24hrs of incubation at room temperature. **(1)** *A. caviae* Sch3N (wild type strain). **(2)** *A. caviae* Sch3N pBBR1MCS-*mshH*. Both tested strains are shown in the pictures to be actively swimming. The test was repeated three times with similar results obtained.

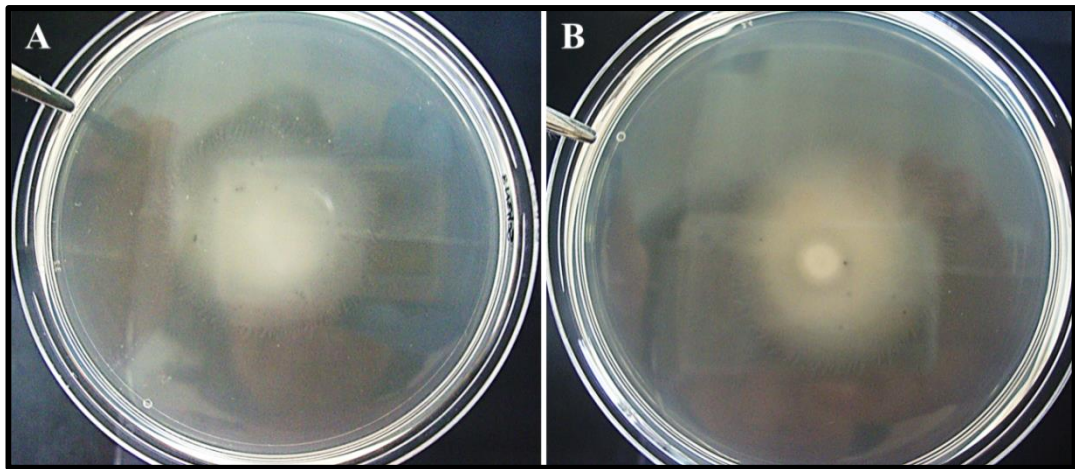


Figure 3.21. Motility test on swarm plate (0.6% Eiken agar) to test the effect of *A. veronii* MshH overexpression in *A. caviae* Sch3N after 24hrs of incubation at room temperature. **(A)** *A. caviae* Sch3N (wild type strain). **(B)** *A. caviae* Sch3N pBBR1MCS-*mshH*. Both tested strains are shown in the pictures to be actively swarming. The test was done in triplicate.

3.3. Phenotypic and molecular effects of mutating each of the thirteen GGDEF-EAL encoding genes in *A. caviae*

3.3.1. Creating mutations in *A. caviae* Sch3N GGDEF-EAL encoding genes

The unpublished *A. caviae* Sch3N genome sequence contained thirteen GGDEF-EAL encoding genes. Figure 3.22 shows the predicted domain architecture for each of the thirteen *A. caviae* Sch3N GGDEF-EAL-containing proteins. Figure 3.23 shows an alignment of the amino acids sequences of the same thirteen proteins with predictions of enzymatically active and inactive domains. The thirteen GGDEF-EAL encoding genes in *A. caviae* Sch3N were mutated. The method chosen to quickly generate the desired mutations was the plasmid insertion mutagenesis technique. The DNA sequence of each of the genes was retrieved from the unpublished *A. caviae* Sch3N genome sequence and oligonucleotide primers were custom designed to amplify internal regions within each of the genes that ranged from 300bp to 800bp. Successful amplification was obtained for the genes except for *AHA2484*, *AHA0383mshH*, *AHA3342*, *AHA3469*, and *AHA2698* for which the PCR reaction gave weak amplification signals or multiple bands (figure 3.24). A gradient annealing temperature PCR reaction was performed to get an optimum amplification for genes *AHA0383mshH*, *AHA3342*, *AHA3469*, and *AHA2698*. New primers were designed for genes *AHA2484* and *Coma*. Successful amplifications of internal fragments for all thirteen genes were eventually obtained.

All primers were designed to contain a 5' linker sequence containing a *Bam*HI restriction site to facilitate cloning. Following PCR amplification, each fragment was digested with *Bam*HI restriction enzyme. The digested fragments were then ligated to the suicide plasmid pKNG101 (figure 3.25) previously cut with *Bam*HI. The ligation mixture was then transferred to *E. coli* CC118 λ *pir* by heat shock as described in materials and methods. Transformed *E. coli* CC118 λ *pir* cells were then plated on LB agar plates containing streptomycin (Sm). *E. coli* CC118 λ *pir* colonies that were streptomycin resistant were successfully obtained for all genes. A colony PCR screening was carried out for the colonies using previously designed primers (primer pKNG101-F and primer pKNG101-R) which flank the polylinker region in pKNG101. Successful cloning of inserts for all genes was obtained as the colony PCR screening gave the correct sizes of inserts. The DNA sequence of PCR amplicons of each insert was determined. All inserts showed the correct DNA sequence.

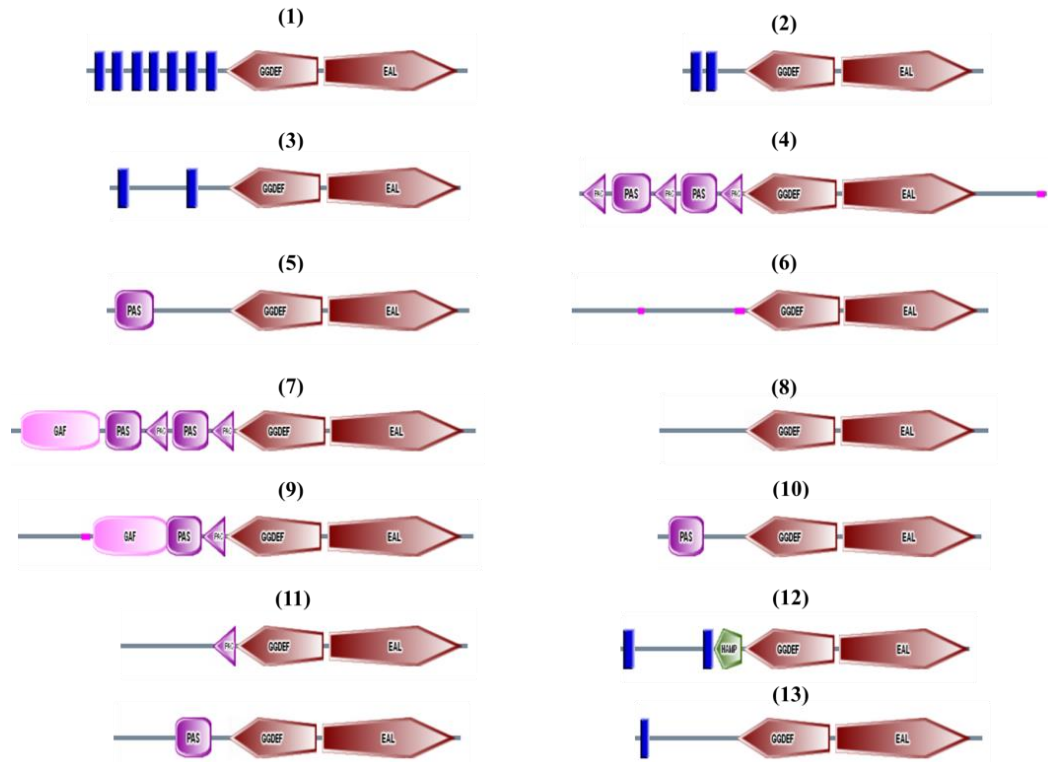


Figure 3.22. Domain architecture of the thirteen GGDEF-EAL containing proteins in *A. caviae* Sch3N performed using the Simple Modular Architecture Research Tool (SMART). (1) *Azoto*, (2) *AHA2484*, (3) *AHA0383mshH*, (4) *Coma*, (5) *AHA1800*, (6) *AHA4237*, (7) *AHA0093*, (8) *AHA0862*, (9) *MorA*, (10) *AHA3342*, (11) *AHA3469*, (12) *AHA2698*, (13) *AHA2092*. In addition to the GGDEF and EAL domains, the picture shows REC, PAS, GAF, and HAMP domains. The blue rectangles indicate transmembrane helix regions.

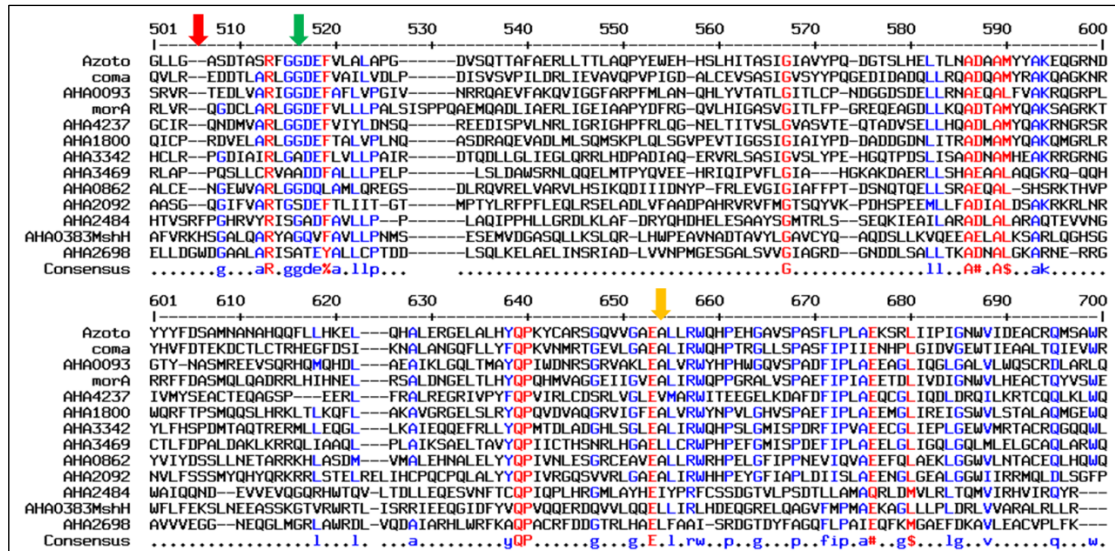


Figure 3.23. Multiple sequence alignment of the amino acids sequences of the thirteen GGDEF-EAL-containing proteins in *A. caviae* Sch3N using MultAlin online software (multalin.toulouse.inra.fr/multalin/). The red arrow indicates the RxxD motif (present in the I-site), the green arrow indicates the GGDEF signature sequence (necessary for diguanylate cyclase activity), and the yellow arrow indicates the EAL residues (necessary for phosphodiesterase activity). Proteins predicted to have two enzymatically active domains include: Azoto, Coma, AHA0039, MorA, and AHA1800. Of these, the proteins Coma, AHA0093, and MorA contain a conserved RxxD motif upstream of the GGDEF domain. The protein AHA4237 is predicted to have an enzymatically active GGDEF domain and a conserved RxxD motif in its I-site. The three proteins AHA3342, AHA0862, and AHA2092 are predicted to have an enzymatically active EAL domain with the protein AHA3342 also possessing a conserved RxxD motif upstream of its non-conserved GADEF sequence.

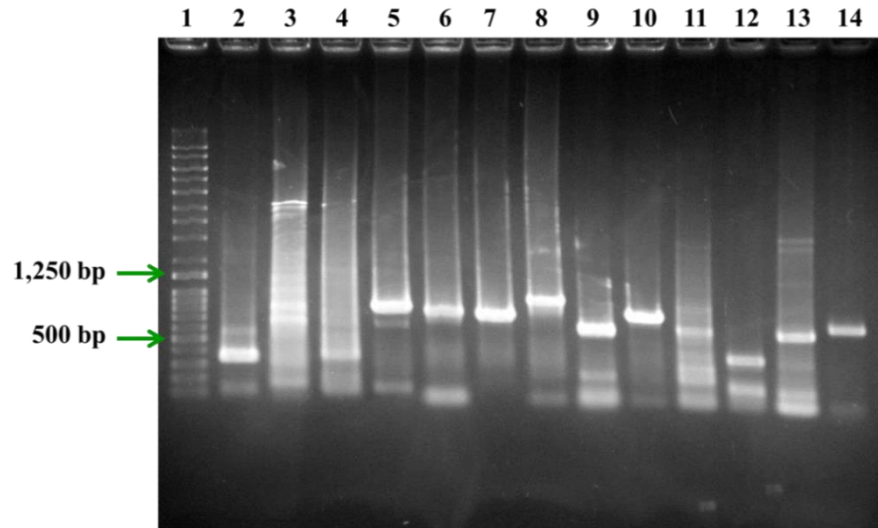


Figure 3.24. A 1% agarose gel showing PCR amplification of internal fragments of each of the thirteen GGDEF-EAL encoding genes using genomic DNA extracted from *A. caviae* Sch3N. The screening was done using custom designed primers to amplify internal gene fragments that ranged in size from 300 to 800bp. Lane (1) Q-step 4 quantitative DNA ladder, lanes (2 to 14) Amplified internal fragments of each gene as the following: (2) *Azoto*, (3) *AHA2484*, (4) *AHA0383mshH*, (5) *Coma*, (6) *AHA1800*, (7) *AHA4237*, (8) *AHA0093*, (9) *AHA0862*, (10) *MorA*, (11) *AHA3342*, (12) *AHA3469*, (13) *AHA2698*, (14) *AHA2092*. PCR reactions were repeated for internal fragments of the genes *AHA2484*, *AHA0383mshH*, *AHA3342*, *AHA3469*, and *AHA2698* using a gradient annealing temperature. Reappearance of multiple bands for some regions was solved by repeating the PCR using newly custom designed primers. All correct sizes were eventually obtained. Amplicons were later cloned into pKNG101.

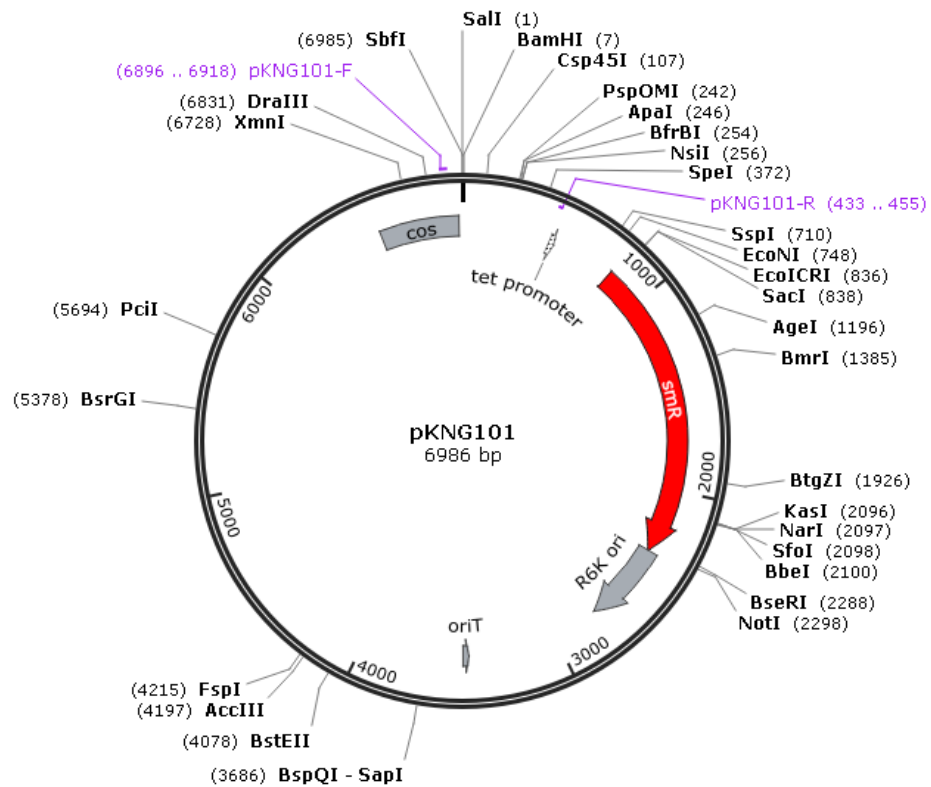


Figure 3.25. A map showing the main features of the suicide plasmid vector pKNG101 used in this study. The custom designed primers pKNG101 forward (pKNG101-F) and reverse (pKNG101-R) flanking the polylinker region are shown in purple colour. Other features shown are the *tet* promoter, Sm^R the streptomycin resistance gene, *oriT* the origin of transfer, and *oriR6K* the origin of replication. This map was generated using SnapGene Software.

The pKNG101 derived plasmids containing each of the thirteen inserts were then transferred separately to *A. caviae* Sch3N by triparental mating technique in which an *E. coli* strain containing the helper plasmid pRK2013 was used to help mobilization of the pKNG101 derivative plasmid from the donor strain (*E. coli* CC118 λ *pir*) to the recipient strain *A. caviae* Sch3N. Once pKNG101 construct plasmid is inside the *A. caviae* cell, homologous recombination occurs between the gene to be knocked out in the *A. caviae* genome and the insert within the plasmid resulting in a single cross over event. This homologous recombination step is followed by insertion of the whole pKNG101 plasmid into the gene resulting in a permanent gene mutation (figure 3.26).

The triparental mating mixture was plated on LB agar containing both nalidixic acid and streptomycin. The nalidixic acid allowed for the selection of *A. caviae* (as it is spontaneously resistant to nalidixic acid) and inhibited the growth of *E. coli*, while streptomycin allowed for the selection of only those *A. caviae* cells containing the plasmid pKNG101. As *Aeromonas* species are known to be oxidase-positive, the isolated colonies were further screened using the oxidase test. The isolated colonies were found to be oxidase-positive and thus the knockout of each gene by a homologous recombination event was confirmed. All thirteen GGDEF-EAL genes in *A. caviae* Sch3N were successfully mutated. Figure 3.27 illustrates the gene knockout procedure explained above. This procedure gave rise to the mutant strains MA1 to MA13 listed in table 2.1.

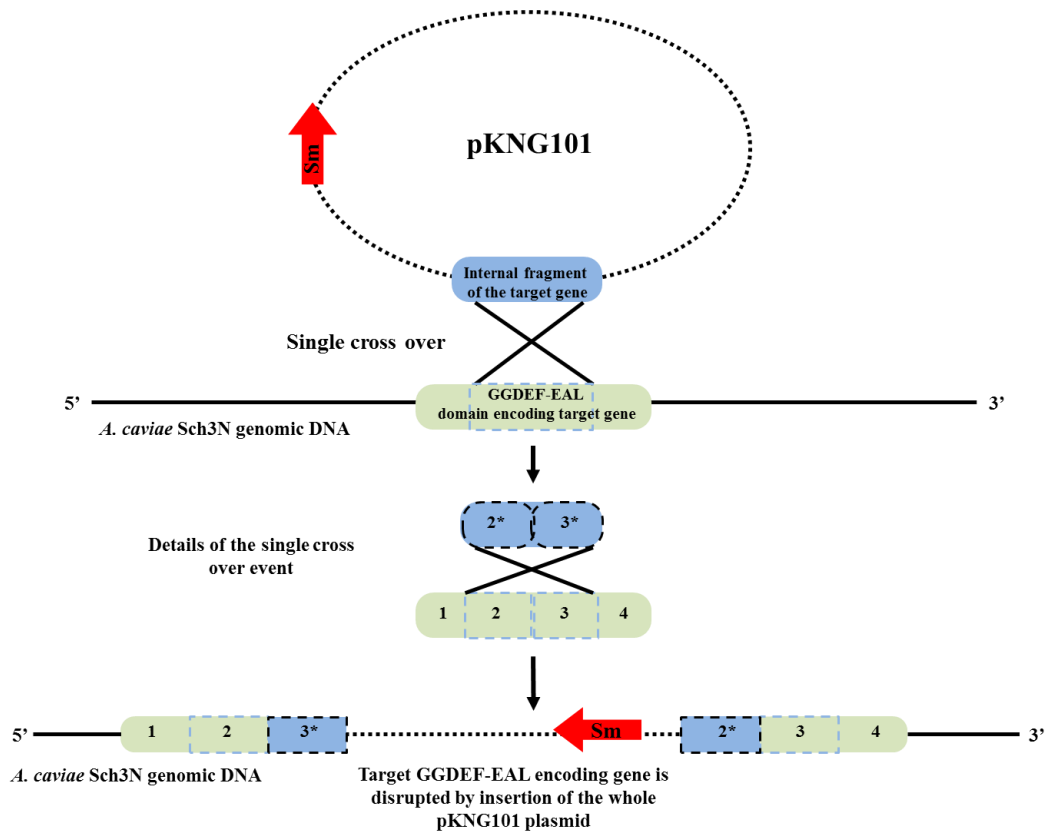


Figure 3.26. Schematic presentation of the plasmid insertion mutagenesis technique used in this study to knockout genes encoding the GGDEF-EAL domains in *A. caviae* Sch3N. Sm: Streptomycin resistance encoding gene.

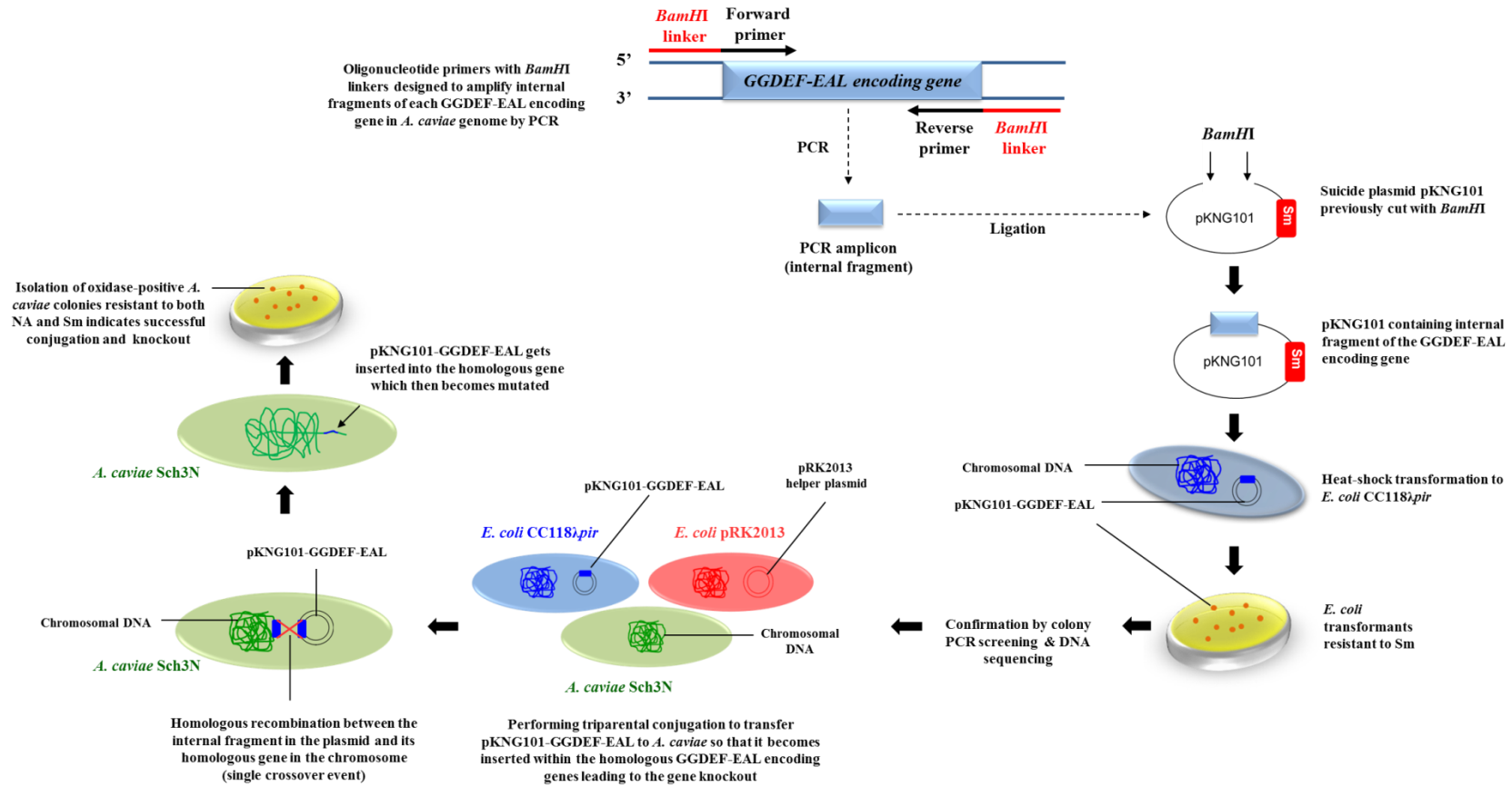


Figure 3.27. Schematic presentation of the procedure used to knockout the GGDEF-EAL encoding genes in *A. caviae* Sch3N.

3.3.2. Effects of mutations on *A. caviae* Sch3N motility and its ability to form a biofilm

To test the effect(s) of the introduced mutations on the ability of *A. caviae* Sch3N to swarm and swim, motility assays were performed. In addition, the effects of the introduced mutations on the ability of *A. caviae* Sch3N to produce a biofilm was tested using borosilicate tubes and by growing the mutant strains on Congo red (CR) agar.

3.3.2.1. Motility assays

Motility assays were performed as described in materials and methods. All mutant strains were inoculated on swim agar and swarm agar plates. All mutant strains were able to actively swim (figure 3.28) with no noticeable inhibitory effects caused by the introduced mutations. Plates were examined by eye and were repeated twice. The mutant strains MA2 (*AHA2484*) and MA7 (*AHA0093*) showed a smaller swimming migration diameter, however, when those two strains were re-inoculated to a separate swim agar plate along with the wild type strain, they had a similar migration diameter and rate of migration as the wild type which indicated that the limited migration in the first plate was only due to the pressure from other colonies but not due to a reduced ability to swim by the mutant strain. All mutant strains were able to swarm giving a uniform migration over the agar surface and ending the growth with a serrated margin. This particular swarming morphology was obtained following the use of bacteriological agar number 1(Oxoid) and incubation of the inoculated plates in a humid box at 30°C. Figure 3.29 shows the typical swarming morphology of *A. caviae* Sch3N on 0.7% Oxoid bacteriological agar. Inoculation of the swim agar and swarm agar plates was carried out from both a 24hr liquid culture as well as from a single freshly grown colony (24hr culture), both inoculation types gave the same motility results.

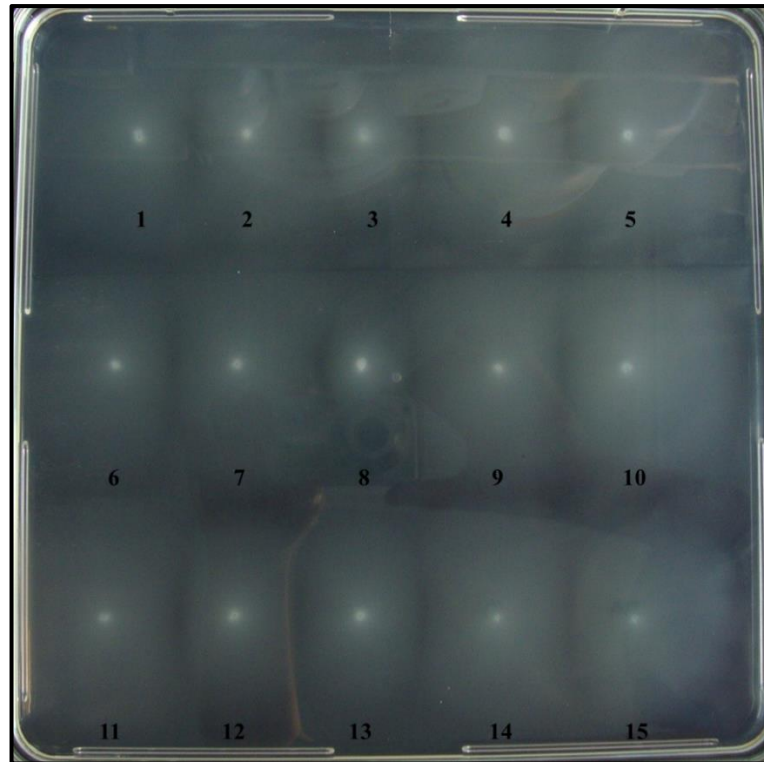


Figure 3.28. Effects of mutations in the thirteen GGDEF-EAL encoding genes of *A. caviae* Sch3N on its ability to swim in 0.25% agar after 24hrs of incubation at room temperature. All mutant strains are shown to be actively swimming. **1:** *A. caviae* Sch3N (wild type). **2:** MA1(*Azoto*), **3:** MA2 (*AHA2484*), **4:** MA3 (*AHA0383mshH*), **5:** MA4 (*Coma*), **6:** MA5 (*AHA1800*), **7:** MA6 (*AHA4237*), **8:** MA7 (*AHA0093*), **9:** MA8 (*AHA0862*), **10:** MA9 (*MorA*), **11:** MA10 (*AHA3342*), **12:** MA11(*AHA3469*), **13:** MA12 (*AHA2698*), and **14:** MA13 (*AHA2092*). **15:** *A. caviae* Sch3N (wild type).

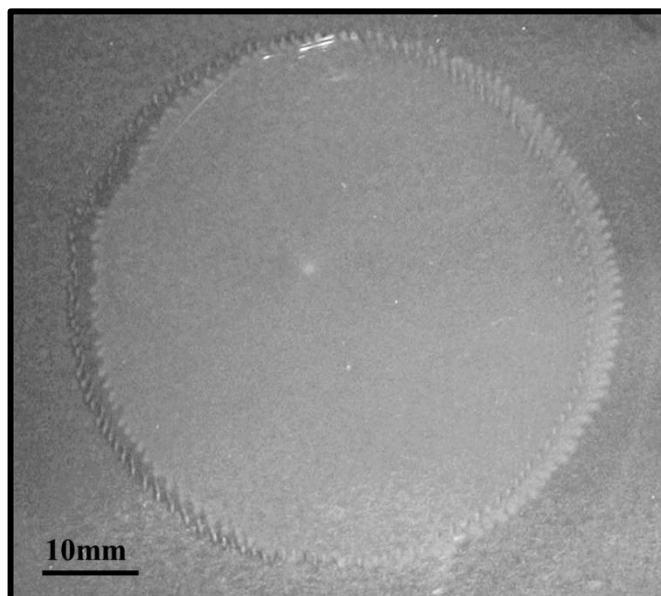


Figure 3.29. Swarm (0.7% Oxoid agar) plate showing the morphology of a single *A. caviae* Sch3N colony during swarming motility. The migration ends with serrated margins.

3.3.2.2. Biofilm formation

The effects of the generated mutations on the ability of the *A. caviae* Sch3N to form a biofilm on borosilicate glass tubes was investigated. The thirteen strains were tested and compared with the wild type following 24 hours and 48 hours of incubation (figure 3.30). Performing statistical analysis on the obtained data indicated a significant variation in the ability of the mutant strains to form a biofilm ($p < 0.05$). Furthermore, examining the graphs in figure 3.30 revealed that biofilm formation was higher after 24hrs of incubation and became weaker after 48hrs of incubation. The variation in biofilm production among mutant strains incubated in glass tubes for 48hrs was also found to be statistically significant ($p = 0.0001$). The mutant strain MA12 (in which the gene *AHA2698* was knocked out) showed noticeable reduction in biofilm formation with approximately a three-fold reduction in biofilm production compared to the wild type strain following 24hrs of incubation ($p = 0.0006$) and with approximately two-fold reduction in biofilm production compared to the wild type strain following 48hrs of incubation ($p = 0.0003$), figure 3.31.

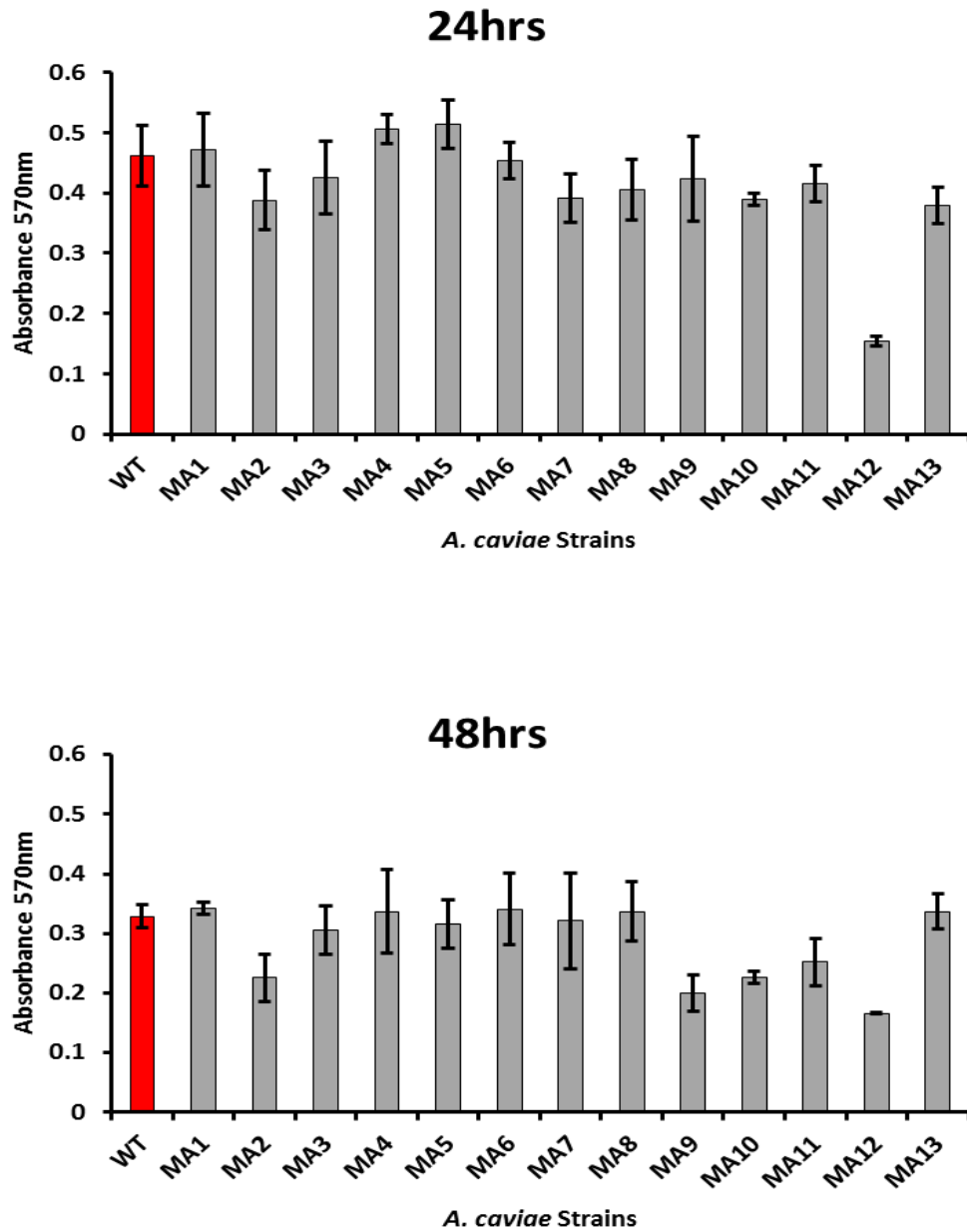


Figure 3.30. Biofilm assay results quantified. GGDEF-EAL *A. caviae* mutant strains were tested for their ability to form a biofilm on borosilicate glass tubes following their incubation in such tubes for 24hr and 48hrs. Tests were done in triplicate. Bars represent the mean of the three readings. Error bars represent the standard deviation around the mean. Red-coloured bars represent the wild type strain Sch3N. Variation was significant (p -value <0.05) using ANOVA-Single Factor test.

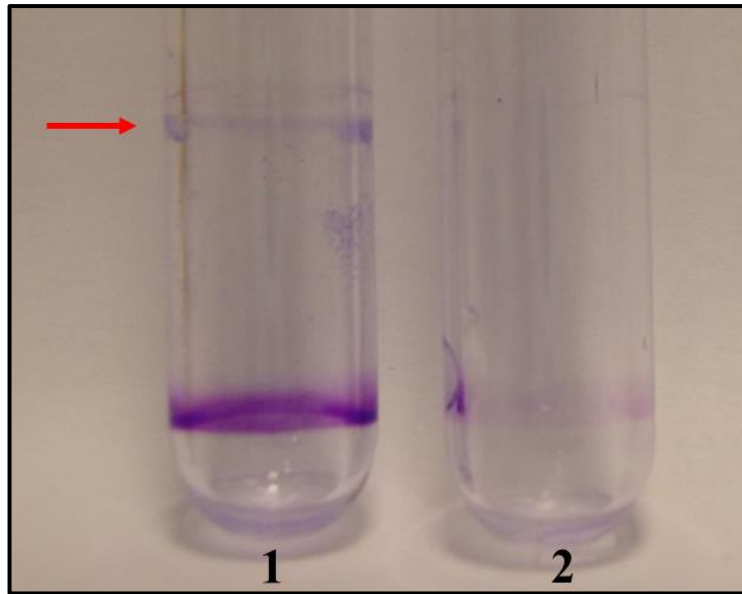


Figure 3.31. Biofilm assay using borosilicate glass tubes. Qualitative pictures showing the decreased ability of the mutant strain MA12 (*AHA2698::pKNG101*) to form a biofilm in comparison to the wild type strain following 24hrs of incubation. **(1)** *A. caviae* Sch3N (WT). **(2)** *A. caviae* mutant strain MA12 (*AHA2698::pKNG101*). Red arrow points to the biofilm formed by the wild type strain which was almost lacking in the mutant strain MA12.

3.3.2.3. Growth of *A. caviae* mutants on Congo Red (CR) agar

Another attempt to test the ability of the mutant strains to form a biofilm was further carried out by growing them on CR agar which contains the dye Congo Red which, once absorbed, indicates an active production of extracellular polysaccharides which are crucially needed to form a matrix in which the sessile cells get embedded and which helps in attachment to surfaces. Each mutant was freshly grown on LB agar plates and following 24hrs of incubation one colony of each mutant was picked up by a sterile tooth pick and inoculated on CR agar. The inoculated CR agar plates were then incubated at 37°C for 24hrs followed by their incubation at room temperature for 5 to 7 days to allow for colour development. With the exception of the colonies of the mutants MA2 and MA12, all other mutants showed slightly raised translucent colonies with a dark red centre and slightly undulate (wavy) margins. The colonies of the mutant strain MA2 (*AHA2484::pKNG101*) and MA12 (*AHA2698::pKNG101*) both showed smooth colonies with a faint red-coloured centre (figure 3.32). The faint coloured centre in the colonies of MA2 and MA12 seem to indicate a less ability to uptake the Congo Red dye, thus, the mutations in genes *AHA2484* and *AHA2698* might have caused a reduction in the ability of *A. caviae* Sch3N to form a biofilm.

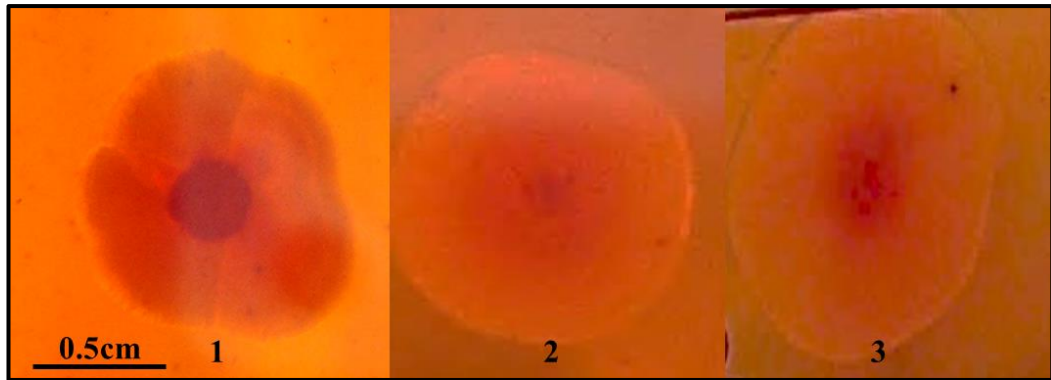


Figure 3.32. Colony morphology of the *A. caviae* mutant strains MA2 (*AHA2484::pKNG101*) and MA12 (*AHA2698::pKNG101*) on (0.025%) Congo Red (CR) agar compared to the colony morphology of the wild type strain *A. caviae* Sch3N after 24hrs of incubation at 37°C followed by 5 days of incubation at room temperature to allow for colour development. (1) *A. caviae* Sch3N (wild type). (2) MA2 (*AHA2484::pKNG101*) (3) MA12 (*AHA2698::pKNG101*). The wild type strain showed slightly raised translucent colonies with a dark red centre and slightly undulate margins. The colonies of MA2 and MA12 showed slightly raised translucent colonies which were smooth and with a faint reddish centre. The faint coloured centre in the colonies of MA2 and MA12 seem to indicate a less ability to uptake the Congo Red dye, thus, the mutations in genes *AHA2484* and *AHA2698* might have caused a reduction in the ability of *A. caviae* Sch3N to form a biofilm.

3.3.3. Transcriptional analysis of *lafA1*, *lafA2*, and *lafK* genes expression in the background of *A. caviae* mutants

To examine the effect of the introduced mutations on the ability of *A. caviae* to express the lateral flagellin genes *lafA1* and *lafA2*, and their effects on the expression of the *lafK* gene that encodes the lateral flagella system master regulator, gene fusion experiment was carried out followed by a β -galactosidase assay to quantitatively determine the effects of the mutations on the expression of the three indicated genes in an attempt to determine a relationship between the GGDEF-EAL dual domain proteins and the expression of the Laf system in *A. caviae* Sch3N.

3.3.3.1. Construction of plasmids containing promoters of the *A. caviae* genes *lafA1*, *lafA2*, and *lafK*.

Analysis of the transcription of *lafA1*, *lafA2*, and *lafK* genes was carried out by first designing specific oligonucleotide primers which flank the promoter region (by approximately 200bp) to PCR amplify each of the three promoters followed by their cloning into pKAGb2(-) (figure 3.33). The primers used to amplify *lafA1p*, *lafA2p*, and

lafKp were designated pARL23-LafA1p-F/R, *lafA2p*-F/R, and *lafKp*-F/R, respectively, and were all contained *Bam*HI and *Hind*III linkers to allow cloning of the promoter regions in the correct orientation.

The custom primers were used to amplify each of the promoter regions by PCR. Amplification was successful as the correct band size was obtained (828bp for *lafA1p*, 550bp for *lafA2p*, and 420bp for *lafKp*) and the DNA sequence of each of the three promoter regions was confirmed. Each of the three promoters was then fused to a promoter-less vector, pKAGb2(-), which encodes the *lacZ* reporter gene downstream of the polylinker region and a chloramphenicol (Cm) resistance cassette. Fusion was done by first digesting both the PCR amplicons containing the promoter regions as well as the pKAGb2(-) with both *Bam*HI and *Hind*III as previously described. Both inserts and plasmid were successfully digested and were then ligated using T4 DNA ligase. Plasmids containing each of the three promoters were transferred by heat shock to *E. coli* S17-1. Transformation was successful as *E. coli* S17-1 cells were selected on LB plates containing Cm. Colony PCR screening using custom designed pKAGb2 primers (pKAG-F and pKAG-R) flanking the polylinker region gave the correct size (figure: 3.34, 3.35, and 3.36) and final confirmation of successful cloning of each of the promoter regions was obtained by DNA sequencing.

Each of the three plasmids (containing each of the three promoters) was then separately transferred to all of the *A. caviae* GGDEF-EAL mutants by bacterial conjugation and also to the wild type strain to be used as a positive control. Conjugation was successful as oxidase-positive colonies were selected on LB plates containing both nalidixic acid and chloramphenicol. Conjugation was further confirmed by colony PCR using pKAGb2 custom designed primers. A pKAGb2(-) empty vector (with no fused promoter) was introduced into *A. caviae* Sch3N using a procedure similar to the one described above in order to use the strain as a negative control in the β -galactosidase assay. Figure 3.37 summarizes the whole procedure of promoter fusion.

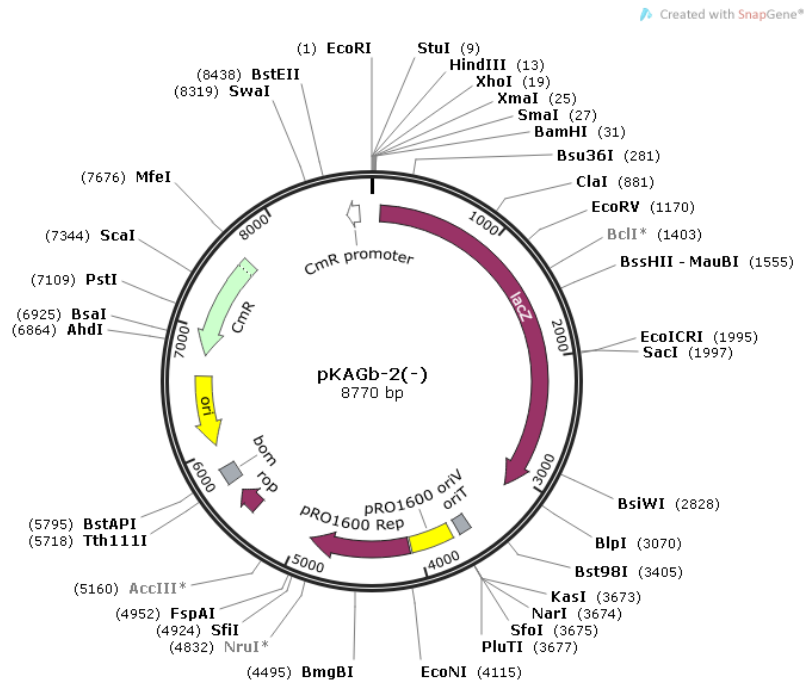


Figure 3.33. A map showing the main features of the plasmid vector pKAGb-2(-) used in this study. Features shown include the reporter gene *lacZ*, the chloramphenicol resistance gene (Cm^R), and the origin of transfer (*oriT*). This map was generated using SnapGene Software.

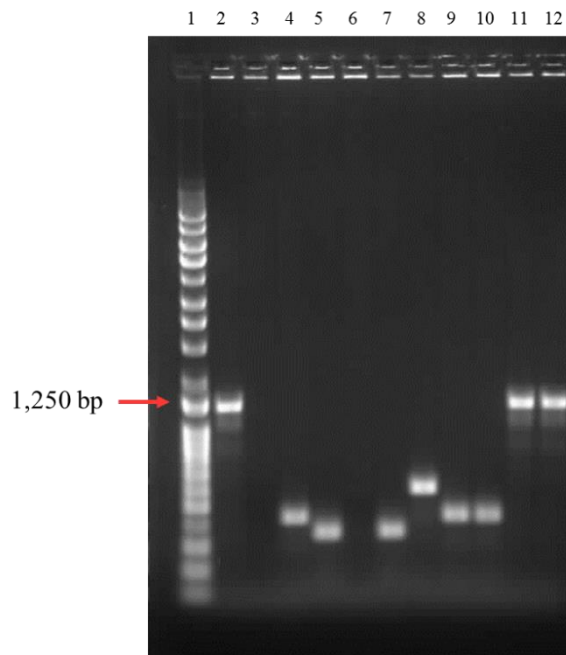


Figure 3.34. A 1% agarose gel of colony PCR screening of *E. coli* S17-1 cells transformed with pKAGb2(-)*lafA1p* using primers pKAG-F and pKAG-R. **Lane 1:** Q-Step 4 DNA ladder. **Lane 2-12:** *E. coli* strains that were chloramphenicol resistant after transformation subjected to colony PCR. Expected band size (1234bp) was obtained from screening colonies in lanes 2, 11, and 12.

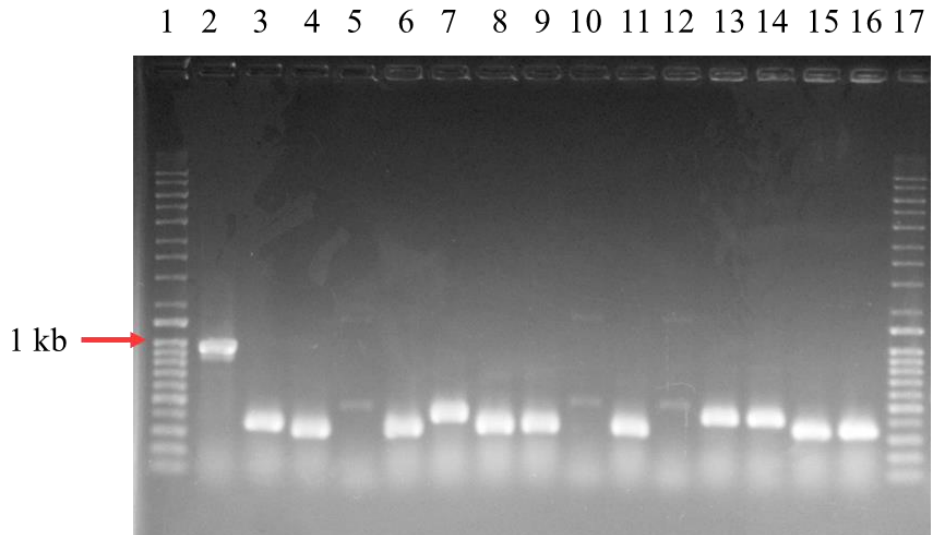


Figure 3.35. A 1% agarose gel of colony PCR screening of *E. coli* S17-1 cells transformed with the pKAGb2(-)*lafA2p* using primers pKAG-F and pKAG-R. **Lane 1 and 17:** Q-Step 4 DNA ladder. **Lane 2-16:** *E. coli* strains that were chloramphenicol resistant after transformation subjected to colony PCR. Expected band size (950bp) was obtained from screening the colony in lane 2.

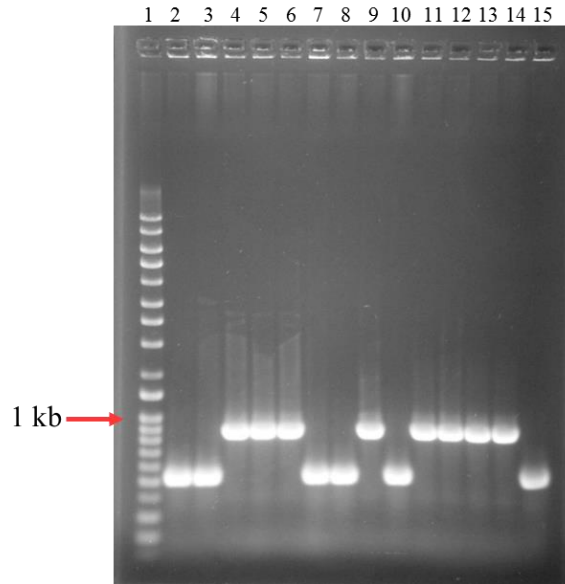


Figure 3.36. A 1% agarose gel of colony PCR screening of *E. coli* S17-1 cells transformed with the pKAGb2(-)*lafKp* using primers pKAG-F and pKAG-R. **Lane 1:** Q-Step 4 DNA ladder. **Lane 2-15:** *E. coli* strains that were chloramphenicol resistant after transformation subjected to colony PCR. Expected band size (820bp) was obtained from screening the colonies in lanes 4,5,6,9,11,12,13,and 14.

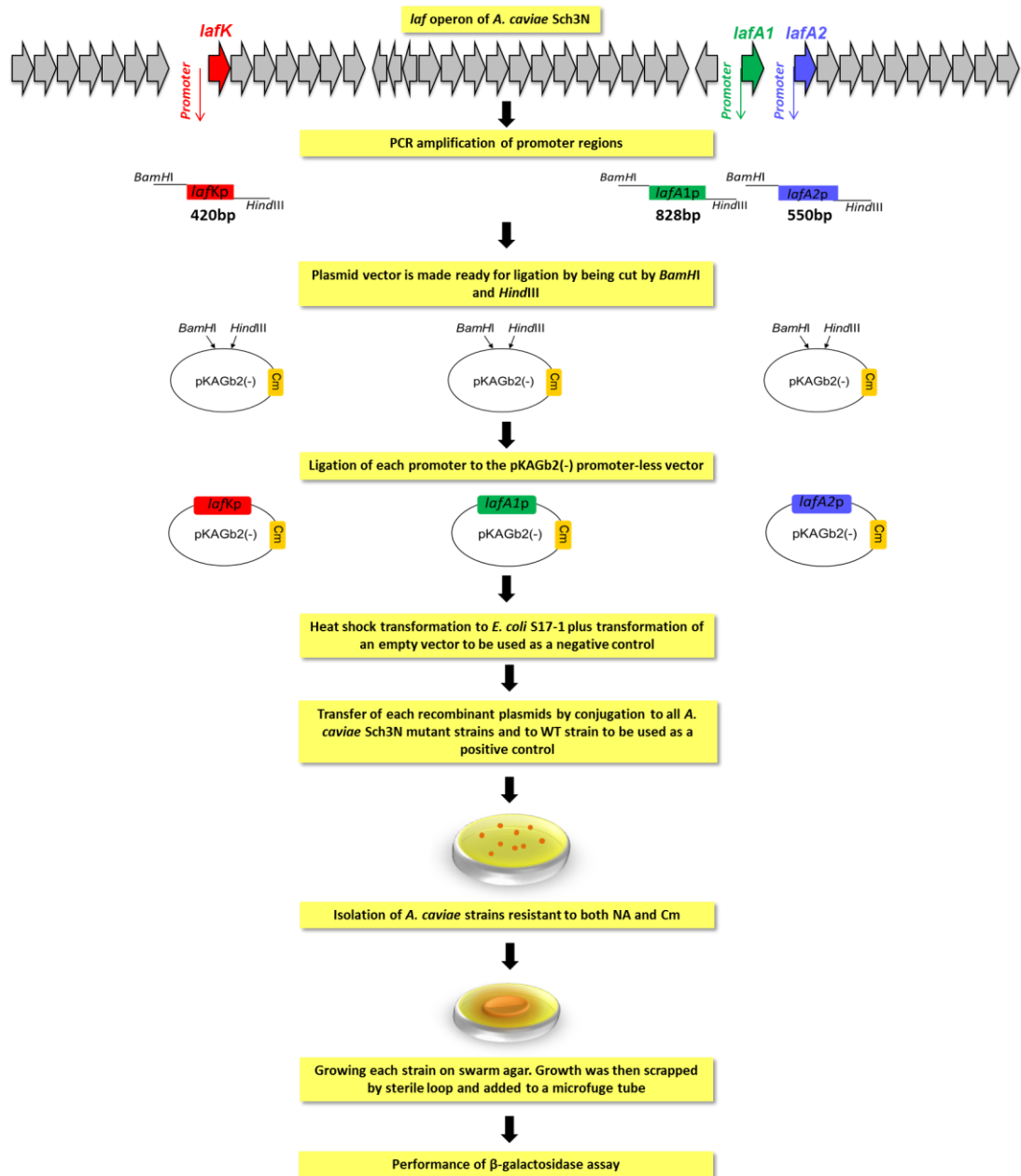


Figure 3.37. A schematic presentation showing the detailed steps used in this study to fuse the promoters of the three genes *lafK*, *lafA1*, and *lafA2* to the promoter-less vector pKAGb2(-). Activity of each of the fused promoters is then determined by performing a β -galactosidase assay.

3.3.3.2. β -galactosidase assay

The β -galactosidase assay was then carried out for all *A. caviae* mutants as well as for the wild type strain. The main objective of this study was to investigate the effect of mutations on the expression of the *A. caviae* Laf system, all mutants as well as the wild type strain were grown on swarm agar (to induce Laf genes expression). All *A. caviae* strains to be tested did swarm on the prepared agar. The obtained growth on swarm agar was scrapped off and its optical density adjusted to OD₆₀₀ of 0.5 to 0.7.

The activity of the promoter sequences of each of the three genes *lafA1*, *lafA2*, *lafK* in the presence of each mutation were quantitatively determined by adding the artificial β -galactosidase enzyme substrate ONPG to the reaction mixture. Principally, the β -galactosidase enzyme encoded by the *lacZ* gene will recognize ONPG and will split the molecule to two molecules, galactose and an *o*-nitrophenol compound which produces a yellow colour which can be measured by the spectrophotometer and thus the promoter activity can be determined according to the yellow colour intensity. A yellow colour was successfully obtained upon testing all mutants as well as the wild type strain. Yellow colour absorbance was measured and Miller units were calculated for all tested strains followed by statistical analysis of the obtained data. Figures 3.38, 3.39, and 3.40 show the activity of each of the three promoters in all *A. caviae* mutants as determined by the β -galactosidase assay.

Statistical analysis indicates the existence of a significant variation the activity of *lafA1* promoter among all mutants ($p < 0.05$). Examining the graph in figure 3.38 reveals a very high *lafA1* promoter activity in the three mutants MA1, MA2, and MA5. MA1 showed 4.5-fold increase in the activity of the *lafA1* promoter, while MA2 and MA5 each gave approximately a 6-fold increase in the activity of the *lafA1* promoter. Activity of *lafA1* promoter was 2-fold higher in MA10 than its activity in the wild type ($p = 0.01$). Except for MA7, all other mutant strains showed a slight increase in Miller units over the units obtained from testing the wild type, with Miller units ranging from just 2 units higher than the wild type (MA8) to 64 units higher (MA9, 1.7-fold higher). The mutant MA7 gave a Miller unit value of 65.24 which is less than the value of units obtained following testing of the wild type (87.44).

When *lafA2* promoter activity was analysed with β -galactosidase assay, however, results were different from those obtained when testing the activity of *lafA1* promoter (figure 3.39). Mutant strain MA10 showed a very high *lafA2* promoter activity (2289.61 Miller units) which was the highest among all the mutants and approximately 1.5-fold higher than the *lafA2* promoter activity measured in the wild type strain ($p=0.04$). The rest of the mutants showed a *lafA2p* activity which is significantly less than its activity in the wild type strain ($p<0.05$).

There was a significant variation in *lafK* promoter activity ($p<0.05$) when tested against in all mutant strains in comparison to its activity tested in the wild type strain (figure 3.40). Mutant strain MA10 showed approximately 1.5-fold increase in *lafKp* activity compared to its activity in the wild type strain ($p= 0.0005$). The *lafKp* activity in mutant strain MA12 was 10 Miller units higher than its activity in the wild type strain ($p= 0.02$). The activity of *lafKp* in the rest of the mutant strains was lower than its activity in the wild type strain. The lowest activity of *lafKp* was measured in the mutant MA13 with a Miller units value of only 16.54 compared to 42.53 Miller units measured when *lafKp* activity was tested in the wild type strain ($p= 0.0007$).

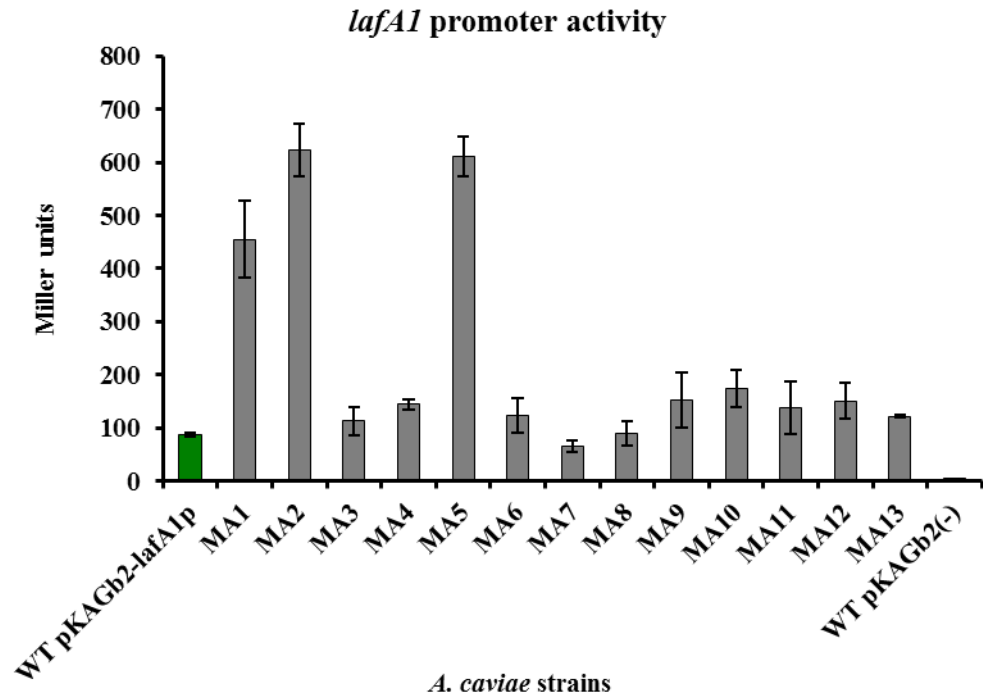


Figure 3.38. Analysis of *lafA1* promoter activity in *A. caviae* GGDEF-EAL mutants and WT grown on swarm agar using β -galactosidase assay, results expressed in Miller units. Test was done in triplicate. Bars represent mean values of the three readings. Error bars represent the standard deviation around the mean. **WT pKAGb2-*lafA1p***: positive control (green-coloured bar). **MA1**: *Azoto*, **MA2**: *AHA2484*, **MA3**: *AHA0383mshH*, **MA4**: *Coma*, **MA5**: *AHA1800*, **MA6**: *AHA4237*, **MA7**: *AHA0093*, **MA8**: *AHA0862*, **MA9**: *MorA*, **MA10**: *AHA3342*, **MA11**: *AHA3469*, **MA12**: *AHA2698*, **MA13**: *AHA2092*. **WT pKAGb2(-)**: empty vector (negative control). Results showed a significant variation ($p < 0.05$) using single factor ANOVA test.

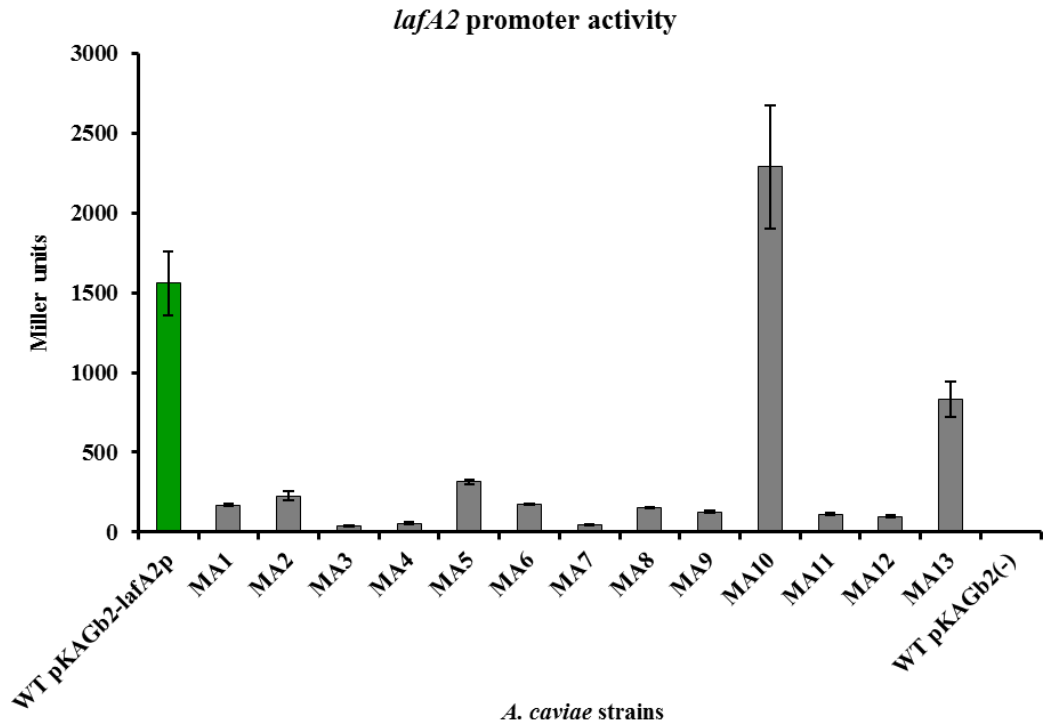


Figure 3.39. Analysis of *lafA2* promoter activity in *A. caviae* GGDEF-EAL mutants using β -galactosidase assay, results expressed in Miller units. Test was done in triplicate. Bars represent mean values of the three readings. Error bars represent the standard deviation around the mean. **WT pKAGb2-*lafA2p***: positive control (green-coloured bar). **MA1**: *Azoto*, **MA2**: *AHA2484*, **MA3**: *AHA0383mshH*, **MA4**: *Coma*, **MA5**: *AHA1800*, **MA6**: *AHA4237*, **MA7**: *AHA0093*, **MA8**: *AHA0862*, **MA9**: *MorA*, **MA10**: *AHA3342*, **MA11**: *AHA3469*, **MA12**: *AHA2698*, **MA13**: *AHA2092*. **WT pKAGb2(-)**: empty vector (negative control). Results showed a significant variation ($p < 0.05$) using single factor ANOVA test.

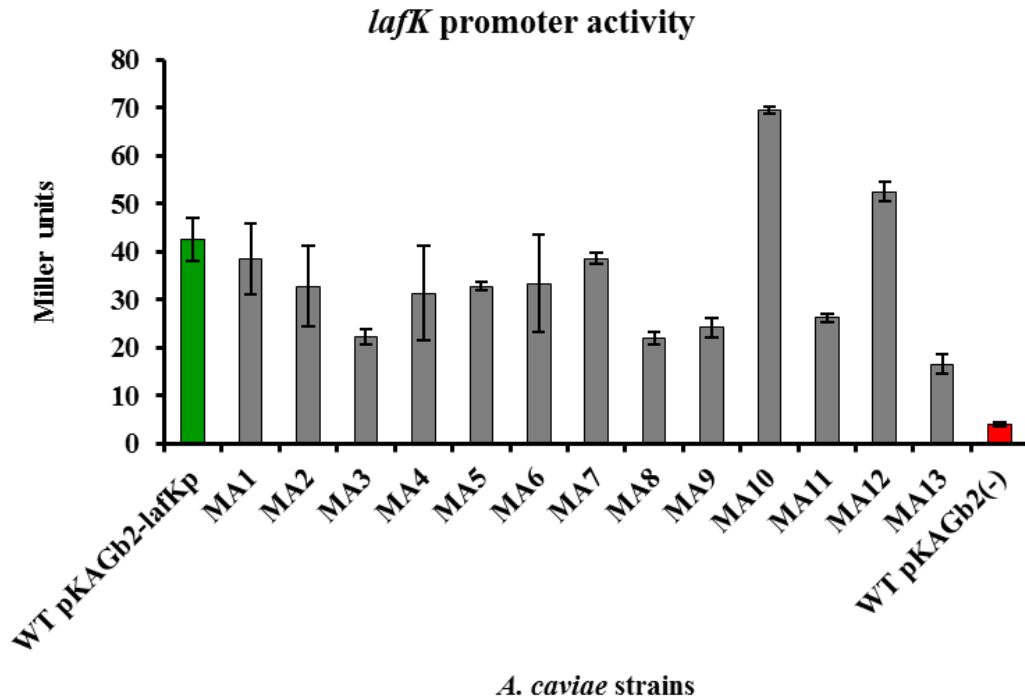


Figure 3.40. Analysis of *lafK* promoter activity in *A. caviae* GGDEF-EAL mutants using β -galactosidase assay, results expressed in Miller units. Test was done in triplicate, bars represent mean values of the three readings. Error bars represent the standard deviation around the mean. **WT pKAGb2-*lafKp***: positive control (green-coloured bar). **MA1**: *Azoto*, **MA2**: *AHA2484*, **MA3**: *AHA0383mshH*, **MA4**: *Coma*, **MA5**: *AHA1800*, **MA6**: *AHA4237*, **MA7**: *AHA0093*, **MA8**: *AHA0862*, **MA9**: *MorA*, **MA10**: *AHA3342*, **MA11**: *AHA3469*, **MA12**: *AHA2698*, **MA13**: *AHA2092*. **WT pKAGb2(-) [empty vector]**: negative control (red-coloured bar). Results showed a significant variation ($p < 0.05$) using single factor ANOVA test.

3.3.4. Complementation and over expression of the *A. caviae* genes *AHA2484*, *AHA3342*, and *AHA2698*

The three *A. caviae* GGDEF-EAL genes *AHA2484* (MA2), *AHA3342* (MA10), and *AHA2698* (MA12) were chosen to perform a complementation study in which the three genes were re-introduced in multi-copy number back into the three *A. caviae* mutant strains in which those three genes were knocked out. This was followed by determining the effect of re-introducing the genes on the ability of the three mutants to swim and swarm as well as on their ability to form a biofilm on borosilicate glass tubes and Congo Red agar. The same three genes were also overexpressed in the wildtype strain *A. caviae* Sch3N to observe any change in its lifestyle.

The reason these three genes were chosen to be complemented and overexpressed is because the mutant strain MA2 and MA12 both showed less ability to bind the Congo Red dye (figure 3.32), MA12 showed drastic reduction in biofilm formation on borosilicate glass tubes (figure 3.30), and because the activities of the *lafA2* and *lafK* promoters were very high when tested in the MA10 background in comparison to their activities tested against all other mutants as well as against the wild type strain (figures 3.39 and 3.40). The gene *AHA2484* is composed of 1662bp and encodes a protein composed of 553aa and has a molecular weight of 62230.594 Da. the gene *AHA3342* is composed of 1788bp and encodes a protein composed of 595aa and has a molecular weight of 66578.25 Da. The gene *AHA2698* is composed of 1926bp and encodes a protein composed of 641aa and has a molecular weight of 71,015.27 Da. The predicted domain architecture of the three GGDEF-EAL containing proteins is shown in figure 3.41.

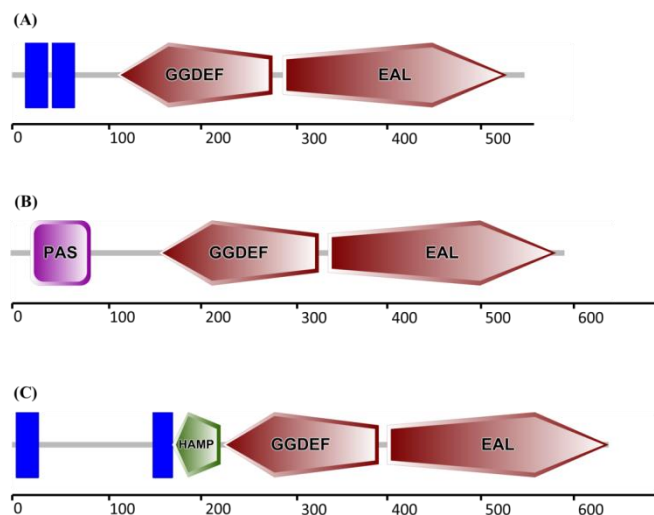


Figure 3.41. The predicted domain architecture of the three *A. caviae* Sch3N GGDEF-EAL containing proteins obtained using SMART online software (<http://smart.embl-heidelberg.de/>). (A) The protein *AHA2484* is composed of 553aa, it possesses two trans-membrane helix regions (one starts at position 15 and ends at position 37 while the second one starts at position 44 and ends at position 66), a GGDEF domains (starts at position 113 and ends at position 281), and an EAL domain (starts at position 292 and ends at position 534). (B) The protein *AHA3342* is composed of 595aa, it possesses a PAS domain (starts at position 21 and ends at position 86), a GGDEF domain (starts at position 159 and ends at position 331), and an EAL domain (starts at position 341 and ends at position 586). (C) The protein *AHA2698* is composed of 641aa, it possesses two trans-membrane helix regions (one starts at position 5 and ends at position 27 while the second one starts at position 152 and ends at position 171), a HAMP domain (starts at position 172 and ends at position 224), a GGDEF domain (starts at position 226 and ends at position 394), and an EAL domain (starts at position 403 and ends at position 641).

3.3.4.1. Construction of plasmids containing the *A. caviae* genes *AHA2484*, *AHA3342*, and *AHA2698* for complementation and overexpression

Oligonucleotide primers were specifically designed to flank 200bp upstream and downstream of the three genes. The primers contained restriction digestion linkers for later cloning of the three genes. The linkers were *Hind*III and *Xba*I for later digestion of *AHA2484* and *AHA3342* PCR amplicons, and *Eco*RI and *Xba*I for later digestion of the *AHA2698* PCR amplicons. The linkers will allow for the directional insertion into the broad-host range plasmid pBBR1MCS5 (Gm^R) previously digested once with *Hind*III and *Xba*I and another time with *Eco*RI and *Xba*I. PCR amplification was successful and the correct band sizes were obtained for the three genes. As a confirmatory step, DNA sequences of all amplified genes were determined, and were found to be correct. Restriction digestion was performed for the PCR amplicons of each gene (figure 3.42) and for the pBBR1MCS5 plasmid vector. Digestions of both inserts and plasmid vector were correct.

Ligation of each of the genes to the pBBR1MCS5 was carried out as previously described. Transformation into *E. coli* DH5 α was done by heat shock and transformed cells were plated on LB agar containing gentamicin. Successful isolation of Gm^R *E. coli* DH5 α colonies was accomplished and colonies were screened for the correct clone by colony PCR using the same custom designed primers used initially for their amplification. The colony PCR indicated successful cloning of each of the three genes (figures 3.43-45). Plasmids were extracted from the first colony in each cloning experiment and the DNA sequence of each insert was determined using the custom designed primers. DNA sequencing confirmed the successful cloning of each of the three genes.

3.3.4.2. Transfer of plasmids containing each of the genes *AHA2484*, *AHA3342*, and *AHA2698* to *A. caviae* wild type strain and *A. caviae* mutant strains MA2, MA10, and MA12 by conjugation

The plasmids were then transferred again by heat-shock to *E. coli* S17-1 to be transferred by conjugation to the *A. caviae* mutant strains MA2, MA10, and MA12 for complementation as well as to the wild type *A. caviae* strain for overexpression. Oxidase-positive colonies which were both nalidixic acid- and gentamicin-resistant were successfully isolated on LB agar containing the two antibiotics.

The three complemented *A. caviae* strains MA2pBBR1MCS5-*AHA2484*, MA10pBBR1MCS5-*AHA3342*, and MA12pBBR1MCS5-*AHA2698* were then tested using motility assay, biofilm assay using borosilicate glass tubes and Congo Red agar. The same phenotypic tests were also done for the *A. caviae* Sch3N strains containing each of the three plasmid constructs pBBR1MCS5-*AHA2484*, pBBR1MCS5-*AHA3342*, and pBBR1MCS5-*AHA2698*.

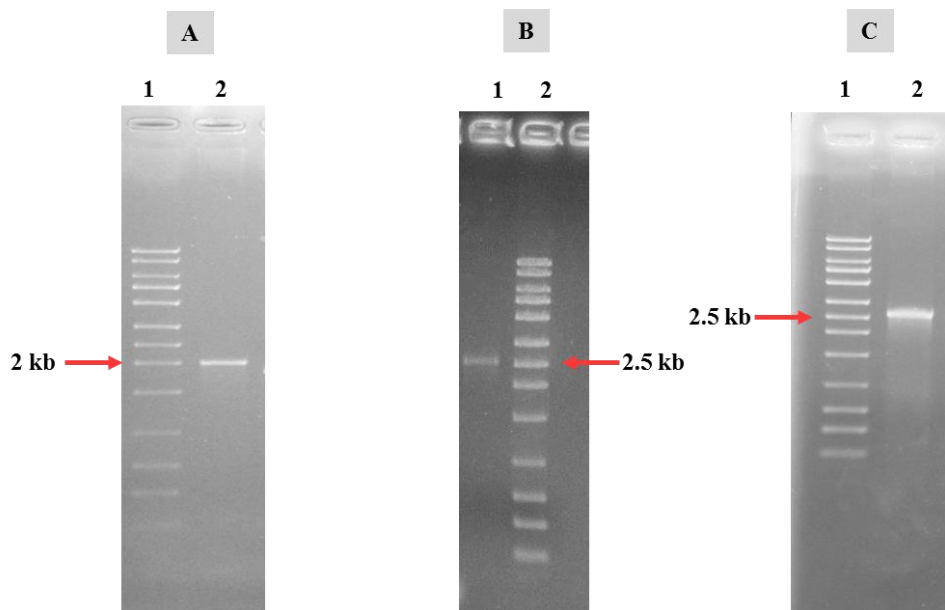


Figure 3.42. A 1% agarose gel showing restriction digestion of the PCR amplicons of the genes: (A) *AHA2484* (2010bp) digested with *Hind*III and *Xba*I, (B) *AHA3342* (2459bp) digested with *Hind*III and *Xba*I, and (C) *AHA2698* (2578bp) digested with *Eco*RI and *Xba*I. Ladders: Norgen Biotek DNA ladder.

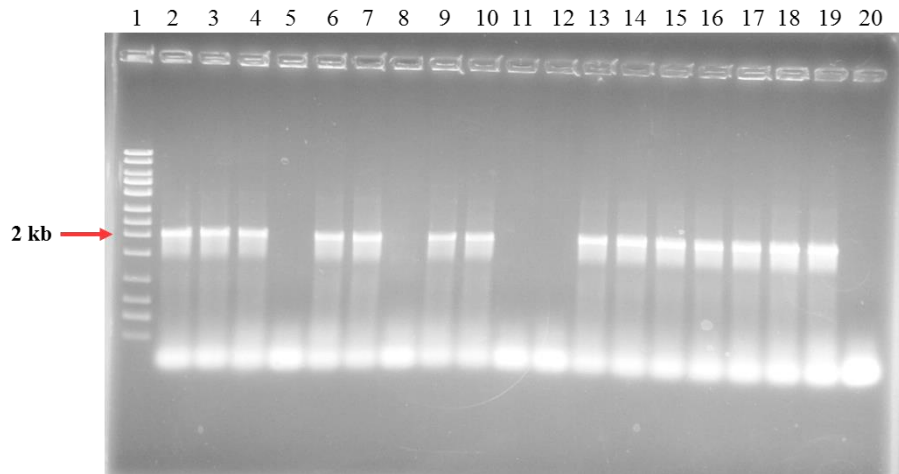


Figure 3.43. A 1% agarose gel showing colony PCR screening of *E. coli* DH5 α transformed with pBBR1MCS5-*AHA2484* using primers compAHA2484(2)-F and compAHA2484(2)-R. **Lane 1:** Norgen biotek DNA ladder. **Lane 2-20:** *E. coli* strains which were gentamicin resistant after transformation subjected to colony PCR. Expected band size (2010 bp) was obtained from screening colonies in lanes: 2, 3, 4, 6, 7, 9, 10, 13, 14, 15, 16, 17, 18, and 19.

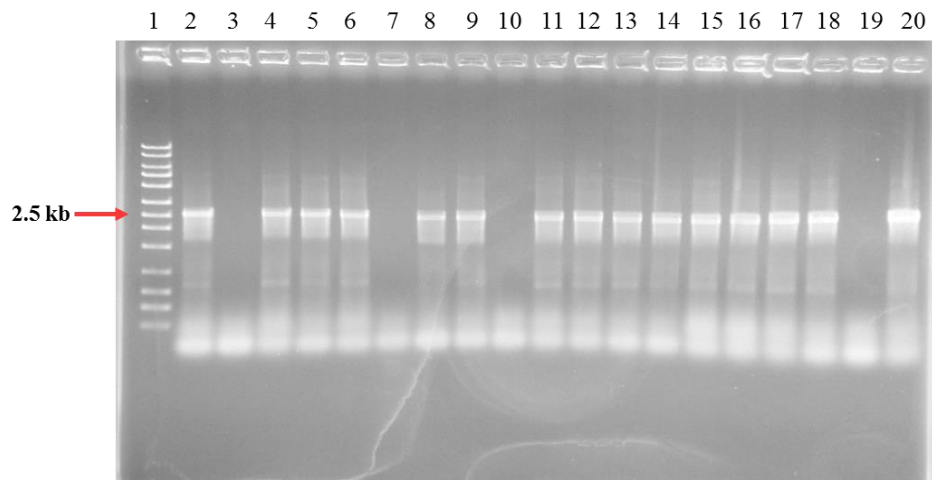


Figure 3.44. A 1% agarose gel showing colony PCR screening of *E. coli* DH5 α transformed with pBBR1MCS5-*AHA3342* using primers compAHA3342(10)-F and compAHA3342(10)-R. **Lane 1:** Norgen biotek DNA ladder. **Lane 2-20:** *E. coli* strains which were gentamicin resistant after transformation subjected to colony PCR. Expected band size (2459bp) was obtained from screening colonies in lanes: 2, 4, 5, 6, 8, 9, 11, 12, 13, 14, 15, 16, 17, 18, and 20.

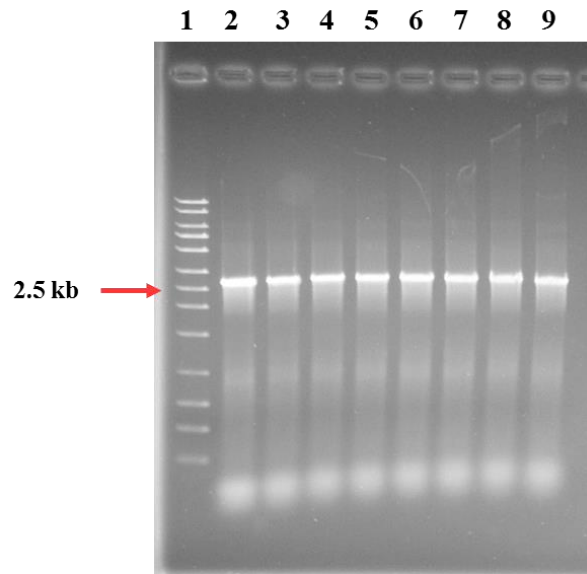


Figure 3.45. A 1% agarose gel showing colony PCR screening of *E. coli* DH5 α transformed with pBBR1MCS5-*AHA2698* using primers compAHA2698(12)-F and compAHA2698(12)-R. **Lane 1:** Norgen biotek DNA ladder. **Lane 2-9:** *E. coli* strains which were gentamicin resistant after transformation subjected to colony PCR. Expected band size (2578bp) was obtained from screening colonies in lanes: 2,3,4,5,6,7,8,and 9.

3.3.4.3. Phenotypic effects of complementation and overexpression of the *A. caviae* gene *AHA2484*

Neither overexpression of *AHA2484* in MA2 background nor its overexpression in the wild type background resulted in a noticeable effect on swimming motility (figure 3.46). Also, all strains overexpressing *AHA2484* were actively swarming. Swarming diameters ranged from 3.7cm to 4.7cm, from 3.2cm to 7.5cm, from 4.7 to 7.8cm, and from 3.2cm to 3.9cm for *A. caviae* Sch3N, MA2, MA2pBBR1MCS5-*AHA2484*, and for *A. caviae* pBBR1MCS5-*AHA2484*, respectively (figure 3.47). As shown in figure 3.32, generation of the mutant strain MA2 (*AHA2484*::pKNG101) resulted in the formation of smooth translucent colonies with a faint reddish-coloured centre on Congo Red agar. Complementation of *AHA2484* in MA2 and its overexpression in the wild type strain resulted in the formation of red-coloured rugose type of colonies as shown in figure 3.48. Finally, complementation of *AHA2484* did not result in a significant change in the formed biofilm on borosilicate glass tubes as both MA2 and MA2pBBR1MCS5-*AHA2484* biofilms were quantified to be 0.18 and 0.183, respectively ($p=0.910$). Overexpression of *AHA2484* in *A. caviae*

Sch3N also did not show any difference in biofilm density in comparison to the wild type strain ($p=0.932$) (figure 3.46).

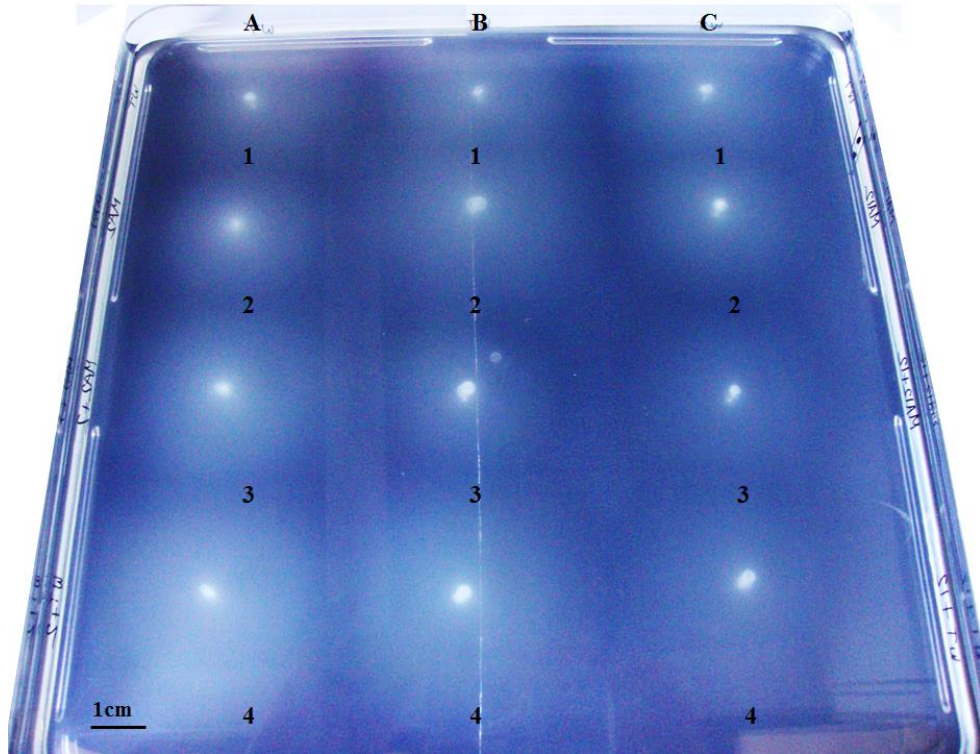


Figure 3.46. Swim agar plate (0.25% agar) showing the effect of complementation and overexpression of the *A. caviae* genes *AHA2484*, *AHA3342*, *AHA2698*. **(A-1)** *A. caviae* Sch3N (wild type). **(A-2)** Mutant strain MA2. **(A-3)** MA2 pBBR1MCS5-*AHA2484* (complementation). **(A-4)** *A. caviae* pBBR1MCS5-*AHA2484* (overexpression). **(B-1)** *A. caviae* Sch3N (wild type). **(B-2)** Mutant strain MA10. **(B-3)** MA10 pBBR1MCS5-*AHA3342* (complementation). **(B-4)** *A. caviae* pBBR1MCS5-*AHA3342* (overexpression). **(C-1)** *A. caviae* Sch3N (wild type). **(C-2)** Mutant strain MA12. **(C-3)** MA12 pBBR1MCS5-*AHA2698* (complementation). **(C-4)** *A. caviae* pBBR1MCS5-*AHA2698* (overexpression).

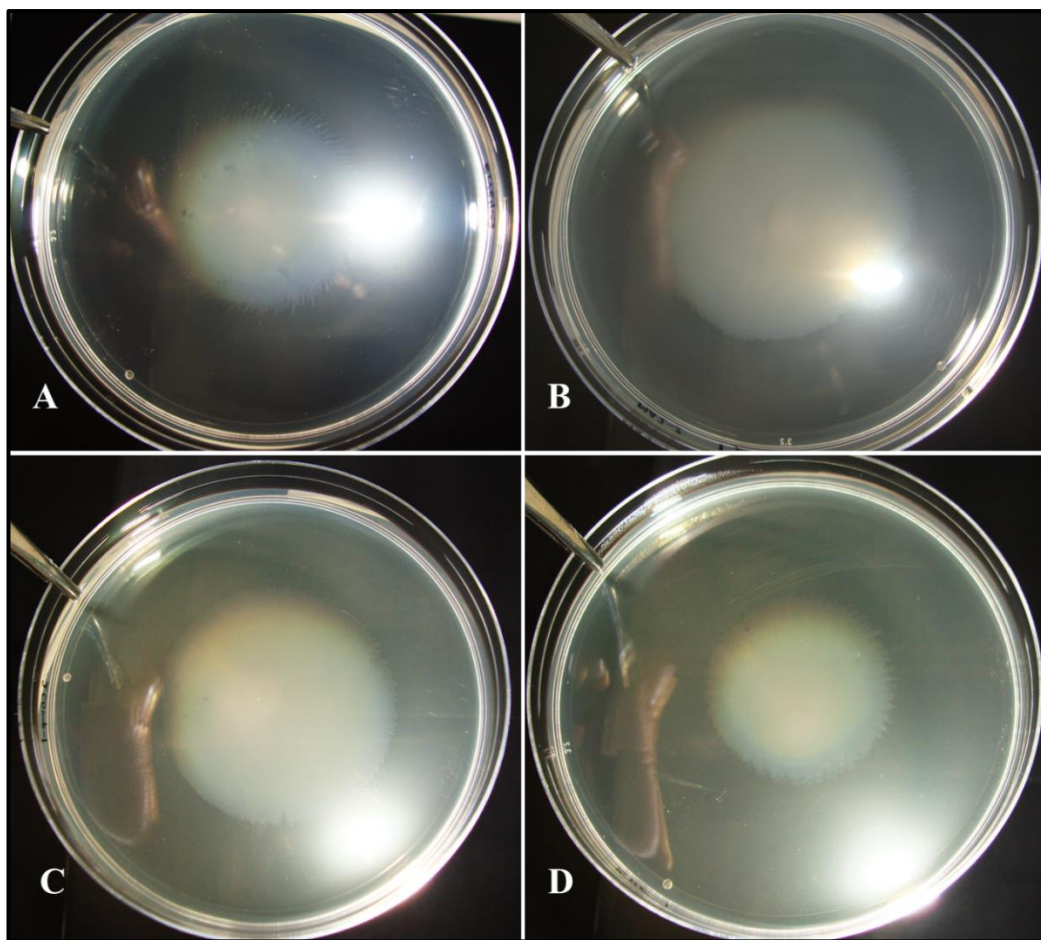


Figure 3.47. Swarm agar plates (0.6% Eiken agar) showing the effect of complementation and overexpression of the *A. caviae* gene *AHA2484*. **(A)** *A. caviae* Sch3N (wild type). **(B)** Mutant strain MA2 **(C)** MA2 pBBR1MCS5-*AHA2484* (complementation). **(D)** *A. caviae* pBBR1MCS5-*AHA2484* (overexpression). The pictures show all strains to be actively swarming.

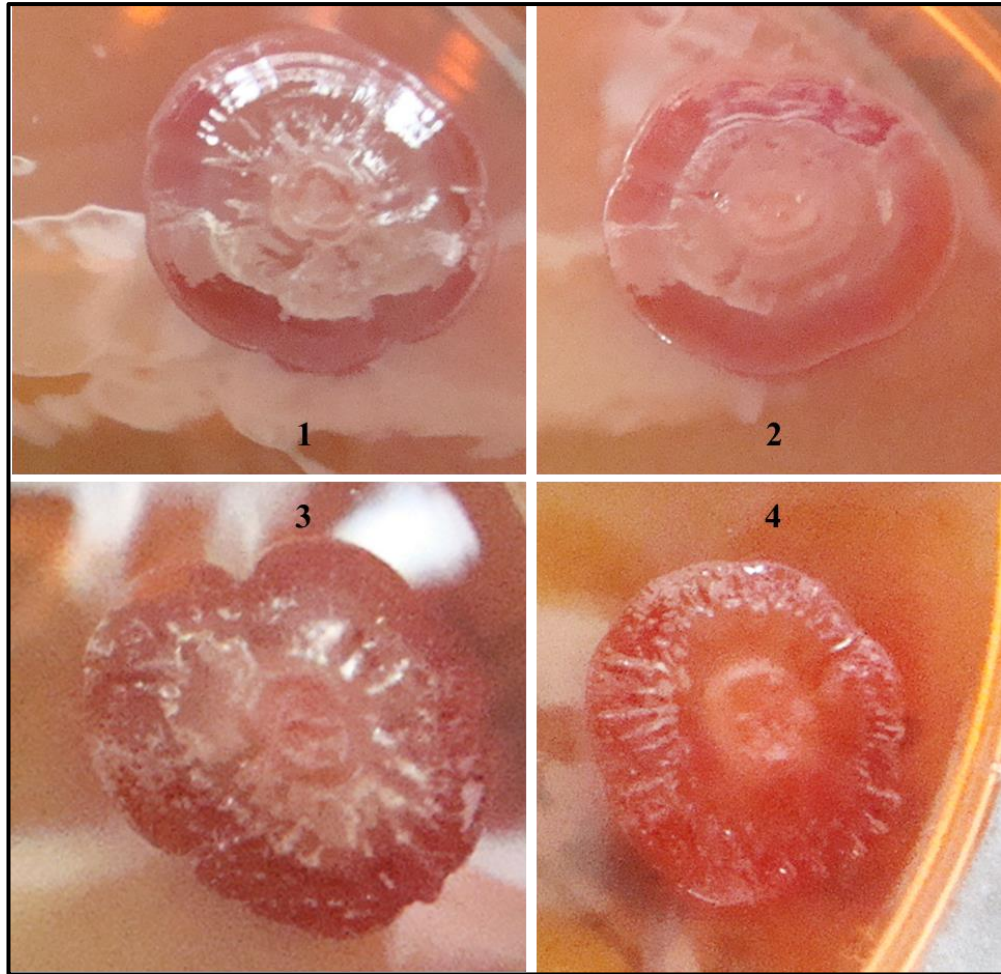


Figure 3.48. Colonies of *A. caviae* strains on Congo Red agar (0.025%) showing the results of complementation and overexpression of the *A. caviae* gene *AHA2484*. **(1)** *A. caviae* Sch3N (wild type). **(2)** Mutant strain MA2. **(3)** MA2 pBBR1MCS5-*AHA2484* (complementation). **(4)** *A. caviae* pBBR1MCS5-*AHA2484* (overexpression). Plates were incubated at 37°C for 24hrs followed by incubating them at room temperature for 5 days to allow for colour development. The pictures show that overexpression of *AHA2484* results in the formation of red-coloured rugose type of colonies.

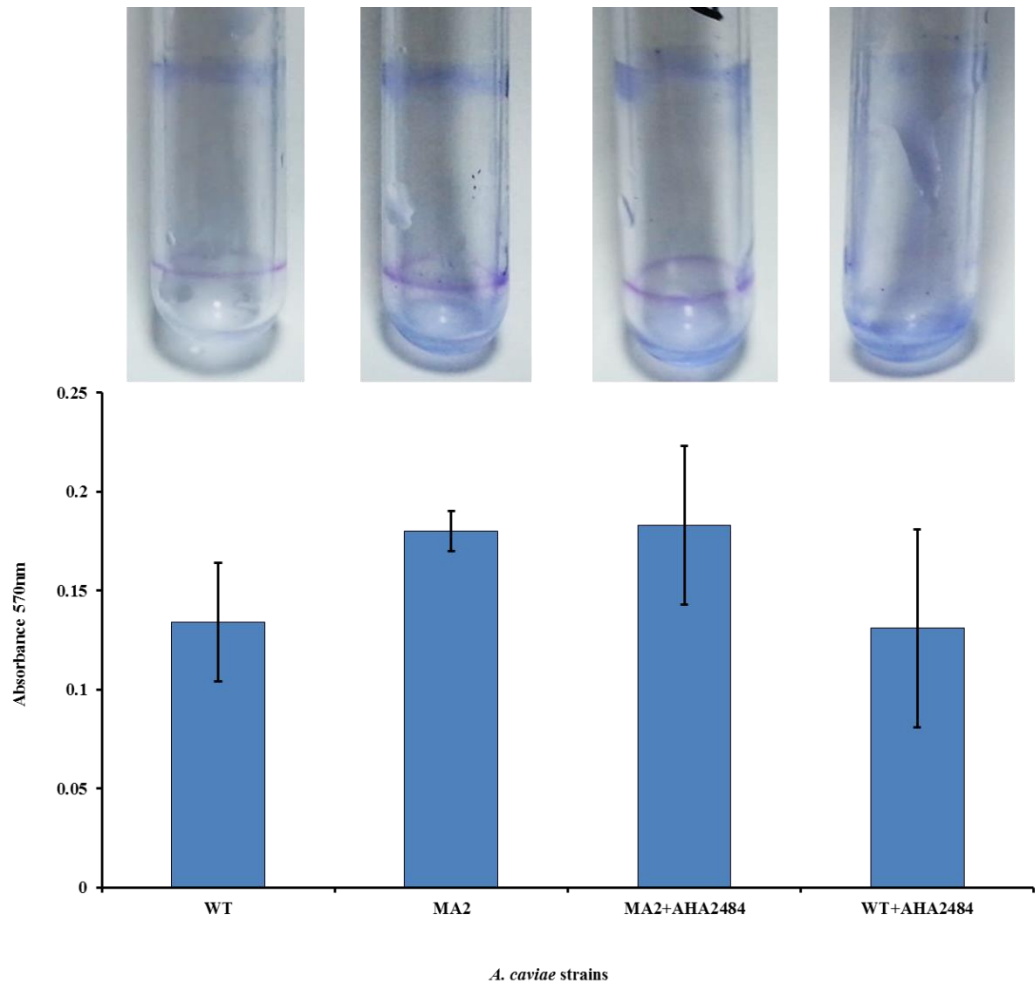


Figure 3.49. Biofilm assay results quantified. **WT:** *A. caviae* Sch3N. **MA2:** Mutant strain *A. caviae* *AHA2484::pKNG101*. **MA2+AHA2484:** MA2 pBBR1MCS5-*AHA2484* (complementation). **WT+AHA2484:** *A. caviae* Sch3N pBBR1MCS5-*AHA2484* (overexpression). Test was done in triplicate. Bars represent the mean values of the three readings. Error bars represent the standard deviation around the mean. Results showed no significant variation in biofilm density ($p>0.05$) using ANOVA-Single Factor test. Above each bar is the corresponding borosilicate glass tube picture containing the biofilm before being dissolved and quantified.

3.3.4.4. Phenotypic effects of complementation and overexpression of the gene *AHA3342*

Overexpression of *AHA3342* into both MA10 and *A. caviae* wild type backgrounds did not affect the ability of the tested strains to swim, as shown above in figure 3.46. Also, the ability of both MA10 and Sch3N to swarm was not affected with the overexpression of *AHA3342* (figure 3.50). The average swarm diameter was measured for *A. caviae* Sch3N (wild type), mutant strain MA10, MA10 pBBR1MCS5-*AHA3342*, and *A. caviae* pBBR1MCS5-*AHA3342* to be 4.3cm, 3.0cm, 2.7cm, and 4.9cm, respectively.

As indicated elsewhere in this chapter, MA10 formed similar colonies to those formed by the wild type on Congo Red agar which were translucent with a dark red centre. However, the complemented strain MA10pBBR1MCS5-*AHA3342* and the wild type strain overexpressing the gene *AHA3342* both produced colonies with rough margins as shown in figure 3.51.

The effects of complementation and overexpression of the gene *AHA3342* on the ability of *A. caviae* Sch3N to form a biofilm on borosilicate glass tubes have been tested (figure 3.52). The mutant strain MA10 showed a 1.8-fold increase in biofilm density compared to the density formed by the wild type strain ($p= 0.02$). When the knocked out gene *AHA3342* was then complemented by re-introducing it in multi-copy number in the MA10 mutant strain, the complemented strain showed a statistically non-significant reduction in biofilm density in comparison to the density formed by the wild type strain ($p= 0.121$). When the gene *AHA3342* was introduced into the wild type strain in a multi-copy number (overexpressed), a very slight (statistically non-significant) reduction occurred in biofilm density formed by the strain overexpressing *AHA3342* in comparison to the biofilm density formed by the wild type strain ($p= 0.520$).

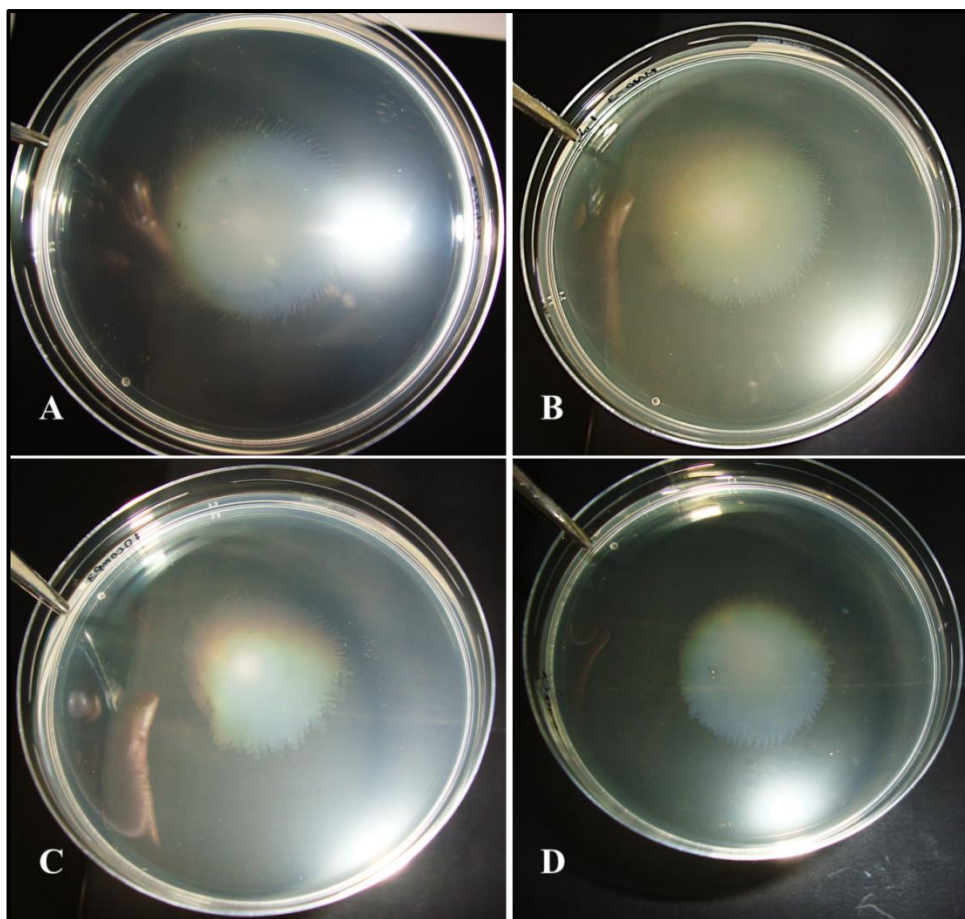


Figure 3.50. Swarm agar plates (0.6% Eiken agar) showing the effect of complementation and overexpression of the *A. caviae* gene *AHA3342*. **(A)** *A. caviae* Sch3N (wild type). **(B)** mutant strain MA10 **(C)** MA10 pBBR1MCS5-*AH3342* (complementation). **(D)** *A. caviae* pBBR1MCS5-*AHA3342* (overexpression). The pictures show all strains to be actively swarming.

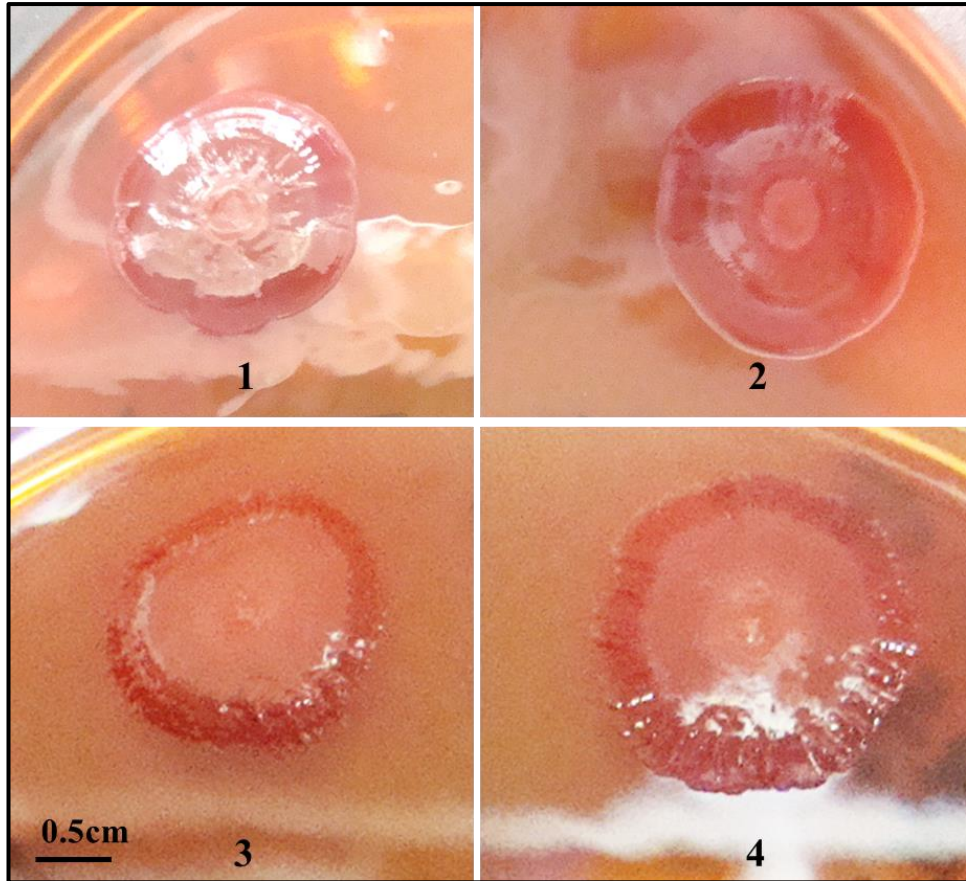


Figure 3.51. Congo red (0.025%) agar plate showing the effect of complementation and overexpression of the *A. caviae* gene *AHA3342*. (1) *A. caviae* Sch3N (wild type) (2) Mutant strain MA10. (3) MA10 pBBR1MCS5-*AHA3342* (complementation) (4) *A. caviae* pBBR1MCS5-*AHA3342* (overexpression). Plates were incubated at 37°C for 24hrs followed by incubating them at room temperature for 5 days to allow for colour development. The picture shows that overexpression of *AHA3342* results in colonies with rough margins.

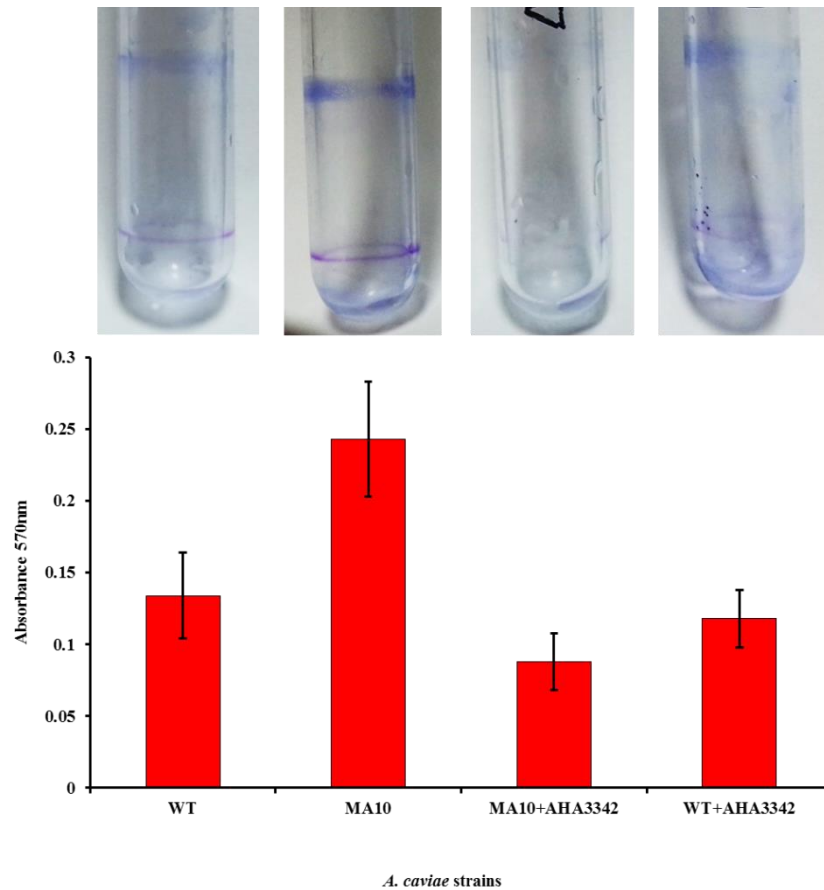


Figure 3.52. Biofilm assay results quantified. **WT:** *A. caviae* Sch3N. **MA10:** Mutant strain *A. caviae* *AHA3342::pKNG101*. **MA10+AHA3342:** MA10 pBBR1MCS5-*AHA3342* (complementation). **WT+AHA3342:** *A. caviae* Sch3N pBBR1MCS5-*AHA3342* (overexpression). Test was done in triplicate. Bars represent the mean values of the three readings. Error bars represent the standard deviation around the mean. Results showed significant variation ($p < 0.05$) in biofilm density using ANOVA-Single Factor test. Above each bar is the corresponding borosilicate glass tube picture containing the biofilm before being dissolved and quantified.

3.3.4.5. Phenotypic effects of complementation and overexpression of the gene *AHA2698*

The mutant strain MA12 was shown previously in this chapter to be actively swimming and swarming. Introducing the gene *AHA2698* in a multicopy number in either MA12 background or in *A. caviae* background did not result in any effect on swimming motility of the tested *A. caviae* strains (figure 3.46). However, introducing pBBR1MCS5-*AHA2698* into MA12 resulted in a big reduction in swarming motility with the average swarming diameter been measured to be 0.8cm (figure 3.53C). Also, introducing pBBR1MCS5-*AHA2698* into the wild type strain has resulted in a complete loss of swarming motility (figure 3.53D).

Growing the mutant strain MA12 on Congo Red agar previously resulted in the formation of translucent smooth colonies with a faint red-coloured centre. Complementation of the gene *AHA2698* resulted in the formation of red-coloured smooth colonies on Congo Red agar, and overexpression of the same gene in the wild type strain formed red-coloured colonies with slightly rough surface and smooth margins (figure 3.54).

When the ability of *A. caviae* mutants to form a biofilm was previously tested using borosilicate glass tubes, the mutant MA12 showed the least biofilm density ($p=0.0006$). Complementation of the gene *AHA2698* did not rescue the ability of MA12 to form a biofilm on borosilicate glass tubes (figure 3.55). Overexpression of the gene *AHA2698* in *A. caviae* Sch3N resulted in more than 50% reduction ($p=0.009$) in biofilm density when compared to the biofilm density formed by the wild type strain (figure 3.55). Table 3.1 summarizes the results obtained following mutation, complementation, and overexpression of the *A. caviae* genes *AHA2484*, *AHA3342*, and *AHA2698*.

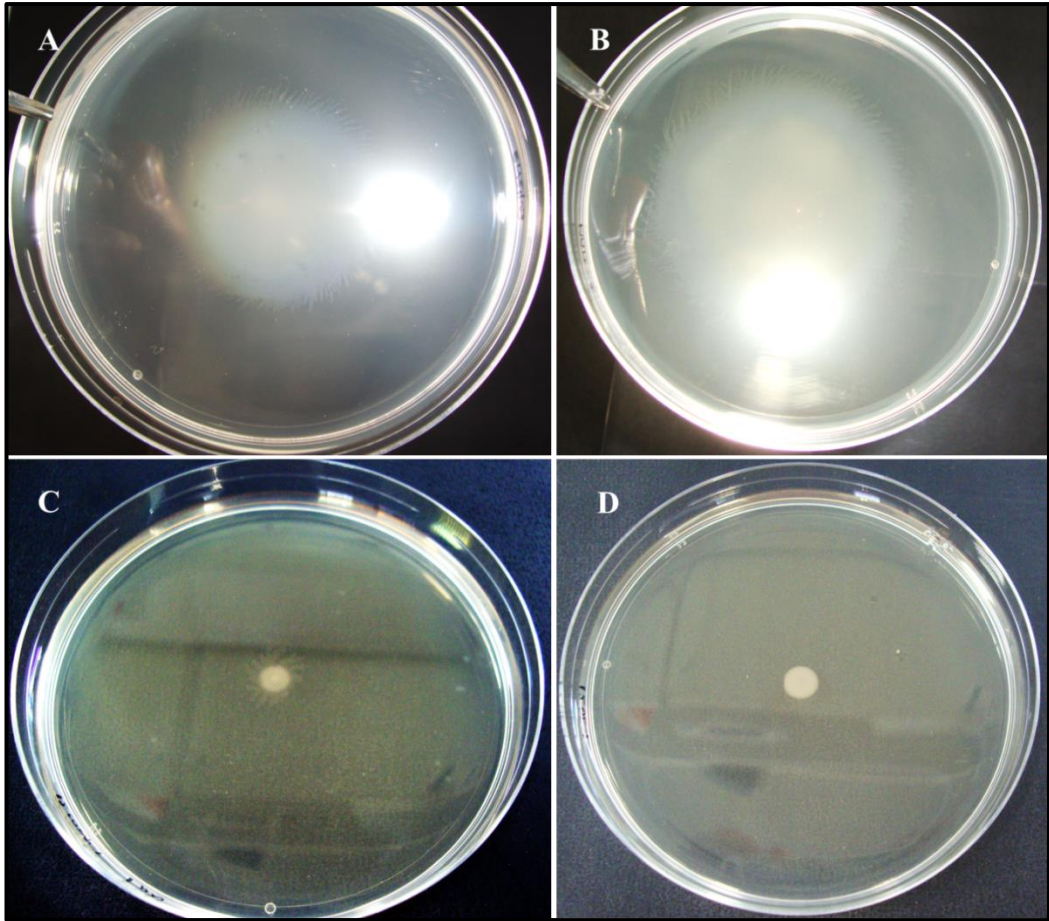


Figure 3.53. Swarm agar plates (0.6% Eiken agar) showing the effect of complementation and overexpression of the *A. caviae* gene *AHA2698*. **(A)** *A. caviae* Sch3N (wild type). **(B)** mutant strain MA12 **(C)** MA12 pBBR1MCS5-*AHA2698* (complementation). **(D)** *A. caviae* pBBR1MCS5-*AHA2698* (overexpression). The pictures show that the loss of the gene *AHA2698* has no effect on swarming motility **(B)**, but its presence in a multicopy number results in either a big reduction in swarming motility **(C)** or a complete loss of swarming motility **(D)** in *A. caviae* Sch3N.

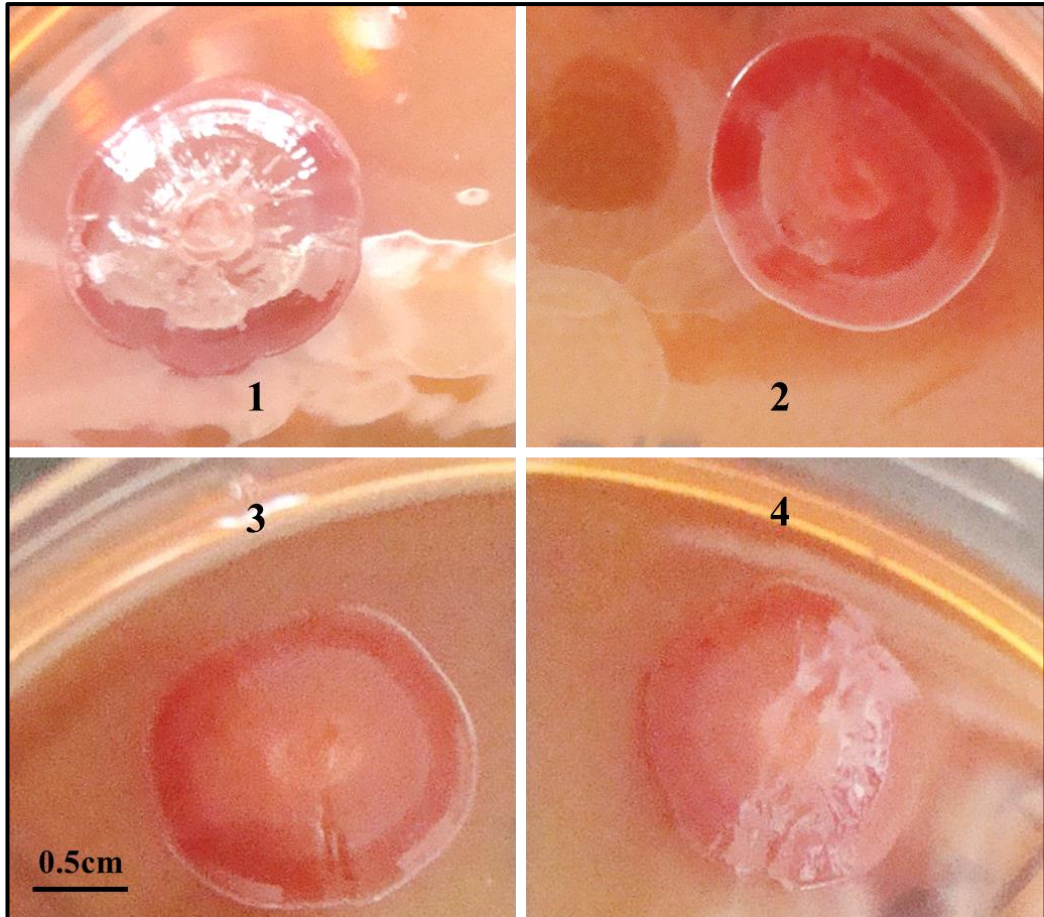


Figure 3.54. Congo Red (0.025%) agar plate showing the result of complementation and overexpression of the *A. caviae* gene *AHA2698*. **(1)** *A. caviae* Sch3N (wild type strain). **(2)** MA12 *AHA2698::pKNG101* **(3)** MA12 pBBR1MCS5-*AHA2698* (complementation). **(4)** *A. caviae* pBBR1MCS5-*AHA2698* (overexpression). Plates were incubated at 37°C for 24hrs followed by incubating them at room temperature for 5 days to allow for colour development. The pictures show that both mutating and complementing the gene *AHA2698* result in reddish-coloured smooth colonies. Overexpression of *AHA2698* in the wildtype strain results in slightly rough reddish colonies with smooth margins.

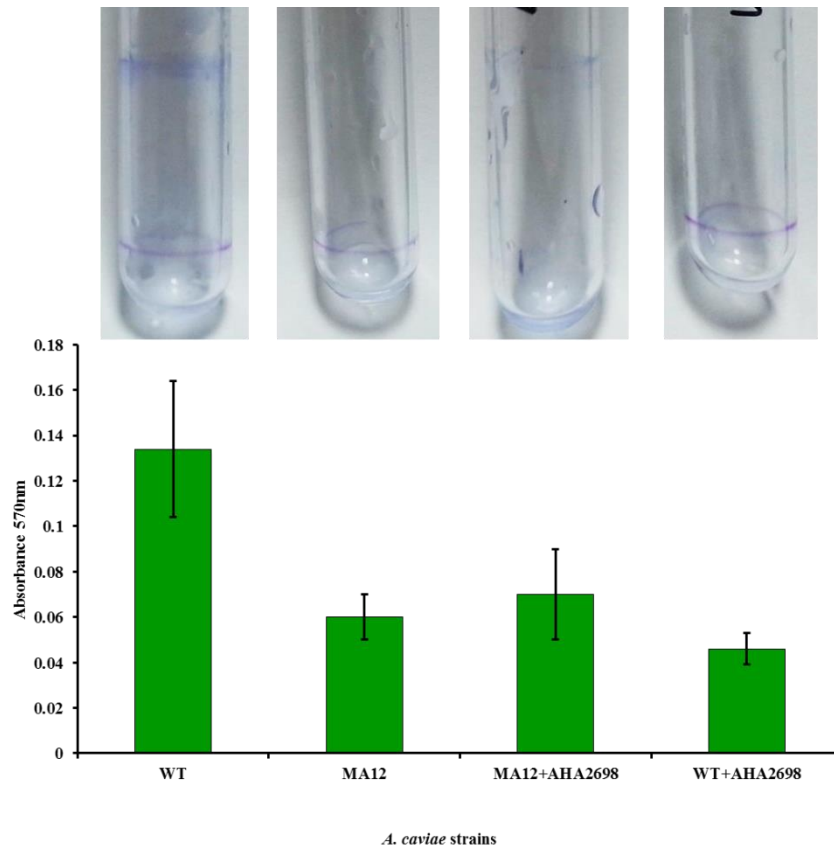


Figure 3.55. Biofilm assay results quantified. **WT:** *A. caviae* Sch3N. **MA12:** Mutant strain *A. caviae* *AHA2698*::pKNG101. **MA12+AHA2698:** MA12 pBBR1MCS5-*AHA2698* (complementation). **WT+AHA2698:** *A. caviae* Sch3N pBBR1MCS5-*AHA2698* (overexpression). Test was done in triplicate. Bars represent the mean values of the three readings. Error bars represent the standard deviation around the mean. Results showed significant variation in biofilm density ($p < 0.05$) using ANOVA-Single Factor test. Above each bar is the corresponding borosilicate glass tube picture containing the biofilm before being dissolved and quantified.

Table 3.1. Summary of the results obtained following mutation, complementation, and overexpression of the *A. caviae* genes *AHA2484*, *AHA3342*, and *AHA2698*.

Mutation:						
Mutated gene	<i>A. caviae</i> strain	Ability to swim	Ability to swarm	Biofilm on borosilicate glass	CR agar morphology	Ability to bind CR dye
<i>AHA2484</i>	MA2	+++	+++	++	translucent smooth colonies, faint red-coloured centre	+
<i>AHA3342</i>	MA10	+++	+++	+++	translucent colonies, undulated margins, dark red-coloured centre	+++
<i>AHA2698</i>	MA12	+++	+++	+	translucent smooth colonies, faint red-coloured centre	+
Complementation:						
Complemented gene	<i>A. caviae</i> strain	Ability to swim	Ability to swarm	Biofilm on borosilicate glass	CR agar morphology	Ability to bind CR dye
<i>AHA2484</i>	MA2	+++	+++	++	Red-coloured rugose type of colonies	+++
<i>AHA3342</i>	MA10	+++	+++	+	Reddish colonies with rough margins	+++
<i>AHA2698</i>	MA12	+++	+	+	Reddish smooth colonies	+++
Overexpression:						
Overexpressed gene	<i>A. caviae</i> strain	Ability to swim	Ability to swarm	Biofilm on borosilicate glass	CR agar morphology	Ability to bind CR dye
<i>AHA2484</i>	Sch3N (WT)	+++	+++	+	Red-coloured rugose type of colonies	+++
<i>AHA3342</i>	Sch3N (WT)	+++	+++	++	Reddish colonies with rough margins	+++
<i>AHA2698</i>	Sch3N (WT)	+++	-	+	Reddish colonies with slightly rough surface and smooth margins	+++

3.4. Discussion

In this chapter the thirteen genes in the *A. caviae* Sch3N genome were mutated. Subsequently, the effects of these mutations were monitored on the strains ability to form biofilms, swim or swarm. The effects on a number of lateral flagellar gene transcriptional fusions were also investigated.

3.4.1. Hypothesis testing

Before mutating the genes, a preliminary experiment was undertaken to determine whether the GGDEF-EAL domains play a direct role in the lifestyle of *Aeromonas*. This was done by attempting to separately overexpress three *Aeromonas* genes which encode a single GGDEF domain (*AHA1208*), a single EAL domain (*AHA0382*), and a dual GGDEF-EAL domain (*mshH*) in *A. caviae* Sch3N using a medium-copy number plasmid vector. This was followed by performing phenotypic tests to help determine the effects of such overexpression on *A. caviae* lifestyle.

3.4.1.1. Overexpression of *AHA1208*

When the GGDEF encoding gene *AHA1208* was introduced into *A. caviae* Sch3N the gene clearly enhanced the cell's ability to form a thick biofilm on the surface of the borosilicate glass tubes as seen by naked eye. Quantification of the formed biofilm by the strain *A. caviae* pBBR1MCS5-*AHA1208* gave an absorbance mean value which was just 0.039 higher than that obtained with the wild type strain. The difference, however, was statistically significant. In addition, when the *AHA1208* gene was overexpressed in *A. caviae* Sch3N it resulted in the formation of rugose colonies. This type of colonies has been described previously as being indicative of elevated levels of c-di-GMP (Nakhamchik *et al.*, 2008). Furthermore, when Rahman and colleagues have overexpressed the *Salmonella* protein AdrA (containing a GGDEF domain) into *A. veronii* the resulting colonies were reddish in colour (Rahman *et al.*, 2007). It seems that *AHA1208* overexpression resulted in an increase in biofilm production which itself resulted in more binding of the Congo Red dye.

The wild type strain produced translucent colonies with a dark red centre and with margins being sometimes (not always) slightly undulate and even slightly whitish. This colony morphology has been described previously for *Shigella* species and enteroinvasive strains of *E. coli* cultivated on CR agar only when incubated at 37°C for 18hrs (Qadri *et al.*, 1988). Qadri and colleagues have described such colonies as being

pigmented and the strains as being capable of binding the CR dye. Development of translucent colonies with a dark red centre has as well been described for *Salmonella* Typhimurium DT 98 grown on CR agar (Tiwari *et al.*, 2002). Such colony morphology of the studied *Salmonella* strain was reported as an indication of a strong binding of the Congo Red dye. Consequently, *A. caviae* Sch3N seem to have the ability to form a biofilm as indicated by the formation of a dark red centre, however, its biofilm was less than that formed by the *A. caviae* strain overexpressing AHA1208 and resulting in the rugose type of colony.

Genes homologous to the single domain encoding gene *AHA1208* of *A. caviae* Sch3N are known to be present in other *A. caviae* strains as well as in other *Aeromonas* species, these include: *A. caviae* Ae398, *A. media* WS, *A. hydrophila* ATCC7966, *A. salmonicida* A449, *A. aquariorum* AAK1, and the four strains of *A. veronii*: AER39, B565, AMC35, and AMC34 (personal communication from Dr. Shaw). The protein AHA1208 possesses the conserved residues GGDEF (in its A-site) and RGTD (in its I-site). Perhaps AHA1208 acts as a diguanylate cyclase which synthesizes c-di-GMP in *A. caviae* and plays a direct role in biofilm production by this species.

Kozlova and colleagues have overexpressed the GGDEF domain-encoding gene *AHA0701h* in both the wild type strain and different quorum sensing (QS) mutant strains during their study of the co-regulation between the QS system and the c-di-GMP signalling system in *A. hydrophila* SSU (Kozlova *et al.*, 2011). *AHA0701h* was chosen from many GGDEF domain-encoding genes in the genome of *A. hydrophila* due to its location downstream of the *luxS* gene. LuxS seems to be involved in the synthesis of a class of signalling molecules referred to as autoinducers-2 (AI-2) which are used by some bacteria during the phenomenon of quorum sensing (Vendeville *et al.*, 2005), and thus, it was chosen by Kozlova and co-workers to be investigated as it was a good candidate for investigating the co-regulation between the two systems. When the group overexpressed the gene *AHA0701h* in the wild type *A. hydrophila* SSU they observed a dramatic increase in biofilm production in comparison to the wild type strain containing the vector (positive regulation). Also, Kozlova research group have found that overproduction of the GGDEF domain encoding gene *AHA0701h* in *A. hydrophila* SSU results in a reduction in swimming motility of the tested strain (no swarming was tested). The results of Kozlova and colleague were similar to the results obtained by Rahman and colleagues who found the GGDEF domain-containing protein AdrA of

Salmonella Typhimurium to both enhance biofilm production and reduce swimming motility when overexpressed in *A. veronii* biovar *sobria* AEW43 (Rahman *et al.*, 2007). Similarly, we have found the overproduction of AHA1208 to enhance the ability of *A. caviae* to form a biofilm, however, over production of AHA1208 had no effect on the ability of *A. caviae* to swim or swarm.

Our results, are in agreement with the findings of Nakhamchik and co-workers (Nakhamchik *et al.*, 2008) who overproduced the *Vibrio vulnificus* GGDEF-containing protein DcpA (diguanylate cyclase protein A) in *V. vulnificus* and found the overexpression to have no effect on motility of the tested strain although it enhanced biofilm formation and the formation of the rugose morphotype. They attempted to explain why the high level of c-di-GMP generated by overexpression of DcpA had no effect on motility in *V. vulnificus* by providing three possible explanations. Firstly, it is possible that a specific total cytoplasmic concentration of c-di-GMP is needed to show an effect on motility rather than a random elevated concentration of the second messenger. Secondly, perhaps a specific local concentration of c-di-GMP was needed to show an effect on motility. Thirdly, perhaps motility in *V. vulnificus* is not controlled by c-di-GMP in the first place.

Although we have not measured the exact cellular concentration of c-di-GMP in the *A. caviae* strain overproducing AHA1208, bioinformatic analysis of the AHA1208 gene sequence revealed its predicted DGC activity. Nakhamchik and colleagues have not attempted to measure the cellular concentration of c-di-GMP in *V. vulnificus* overproducing the DcpA protein (Nakhamchik *et al.*, 2008). Before performing their study they, however, have performed bioinformatics analyses which revealed the domain architecture of DcpA protein to contain both a GAF domain and a GGDEF domain, a result which encouraged them to test its activity. The conserved domain analysis performed in our study for AHA1208 protein of *A. caviae* Sch3N revealed a degree of similarity to the protein PleD. The PleD protein is a GGDEF domain containing protein encoded in the genome of *Caulobacter crescentus* that functions as a response regulator (Hecht *et al.*, 1995). The PleD protein is involved in a signal transduction pathway which leads to the *C. crescentus* cells to stop swarming and starts the process of stalk formation (i.e., involved in cellular transition from motility to sessility).

3.4.1.2. Overexpression of *AHA0382*

We have chosen to study the *A. caviae* protein *AHA0382* because of its predicted phosphodiesterase activity due to its possession of a conserved EAL motif. Although cloning of the EAL domain encoding gene *AHA0382* was successful in *E. coli* cells, its transfer to *A. caviae* Sch3N by conjugation failed after several attempts. *A. caviae* Sch3N cells failed to grow on LB plates containing gentamicin while *E. coli* cells were actively growing on the same plates following their heat shock transformation with pBBR1MCS5-*AHA0382* and their incubation for 24hrs at 37°C. These results suggest that overexpression of *AHA0382* was actually toxic to the *A. caviae* cell and thus prevented us from performing phenotypic studies. As *AHA0382* is encoded within the genome of *A. caviae* but not encoded within the genome of *E. coli*, it seems that its toxic effect(s) are only observed on *A. caviae* cells. The toxicity of *AHA0382* to *A. caviae* Sch3N could be due to a role played by this protein in the replication of *A. caviae* cells (cell cycle progression) which led to the complete inhibition of growth upon its overexpression. Another possible explanation of the *AHA0382* toxicity is that it's possession of two trans-membrane helix regions (i.e., a membrane protein). Generally, the membrane proteins do control the entry and exit of substances across the cell membrane. Thus, overexpression of the membrane protein *AHA0382* in *A. caviae* might have caused a cellular toxicity due to the permeability of the *A. caviae* cell membrane being severely altered.

3.4.1.3. Overexpression of *MshH*

Overexpression of *MshH* in *A. caviae* Sch3N caused a reduction in the ability of the bacterium to form a biofilm on borosilicate glass tubes. Also, the colonies formed on Congo Red agar following overexpression of *MshH* were not showing a big difference from those formed by the wild type strain growing on the same medium (both had a dark red centre and translucent margins). The slightly dry undulated colonies of *A. caviae* pBBR1MCS-*mshH* were not of the rugose type which seems to be linked with the active biofilm production and predicted DGC activity. In addition, the *MshH* protein contains the non-conserved sequence AGQVF which indicates the lack of DGC activity. Although these facts support a possible phosphodiesterase activity for the *MshH* protein, the protein does not possess the three conserved residues necessary for an enzymatically active PDE and instead it contains the sequence ELL.

The *mshH* gene is conserved in the MSHA locus of several bacteria including *Aeromonas* spp. and *Vibrio* spp. (Hadi *et al.*, 2012). Originally, the MSHA locus was given for the locus present in certain strains of *V. cholerae* that encodes the genes for the production of a surface pilus referred to as mannose-sensitive haemagglutinin (MSHA) by these *V. cholerae* strains (Marsh *et al.*, 1999). Genetic characterization of the bundle-forming pilus (Bfp) locus in *A. veronii* bv. Sobria revealed a similarity to the MSHA locus of *V. cholerae* (Hadi *et al.*, 2012), and thus, the genes of both loci in both bacteria were given the same names. In *V. cholerae*, the MshH is also referred as an MSHA biogenesis protein (Marsh *et al.*, 1999). The role of the GGDEF-EAL encoding gene *mshH* in adherence to HEp-2 cells and biofilm formation was previously studied in our lab. Our group found that a mutation in the *mshH* gene did not cause any effect on the ability of *A. veronii* to form a biofilm when compared to the wild type strain (Hadi *et al.*, 2012). Hadi and colleagues, however, showed that the mutation in the *mshH* gene resulted in a 48% reduction in the mutant's ability to adhere to HEp-2 cells in comparison to the adherence ability of the wild type strain. Thus, it seems that *A. veronii* MshH protein plays a role in adherence and so it was chosen to test our hypothesis.

3.4.2. Mutations in *A. caviae* GGDEF-EAL encoding genes

In this study, the thirteen mutant strains were found to be able to actively swim and swarm on motility agar plates. This result suggests that c-di-GMP does not directly control the motility in *A. caviae*. The active motility of the mutant strains, however, does not rule out any indirect role played by the GGDEF-EAL proteins of *A. caviae* in the complex c-di-GMP network leading eventually in some kind of involvement in *A. caviae* lifestyle. In addition, perhaps the loss of one of the dual domain encoding genes is being compensated by the other GGDEF-EAL encoding genes.

Colonies of swarming *A. caviae* cells appeared in two forms. The first form is the uniform colonies with a serrated margin swarming on 0.7% Oxoid agar plates, the second form is the colonies with irregular margins appearing on 0.6% Eiken agar plates. Both types of colonies, however, represent active swarming and do not indicate any difference in between colonies. Thus, both types of agar are considered reliable to test for swarming of *A. caviae*. Kirov and colleagues have previously studied different swarm agar recipes and also have compared using media components from different manufacturers (Kirov *et al.*, 2002). They have concluded that different agar

concentrations have an effect on swarming motility and that the source of agar used for solidification also affected the swarming abilities of the studied *Aeromonas* species. They have reported Eiken agar to be very powerful and always supports swarming of *Aeromonas* while Oxoid agar occasionally causes failure of the bacteria to swarm. In our study, Eiken agar has always supported the swarming of *A. caviae* when the inoculated plates were incubated at room temperature. When Oxoid agar was used as a solidifying agent in our study, tween 80 was always used as a surfactant and the inoculated agar plates were always incubated in a humid box at 30°C to allow the bacteria to swarm.

The produced biofilms for all mutant strains were stronger after 24hrs of incubation but became weaker when the glass tubes were incubated for 48hrs. This observation is in agreement with the results obtained by Kirov and colleagues who determined the peak biofilm density for *A. caviae* to be obtained (most commonly) following 16 to 20hrs of incubation with a notably less density being obtained following incubation periods of more than 30hrs (Kirov *et al.*, 2004).

Testing the promoters activities of *lafA1*, *lafA2*, and *lafK* against *A. caviae* GGDEF-EAL mutants indicated that the mutations resulted in variability in the activity of these promoters. This indicates that perhaps all of the GGDEF-EAL-containing proteins in *A. caviae* Sch3N do play a role in the *laf* genes expression in the studied strain. The variation in activity between *lafA1* and *lafA2* is due possibly to their expression being controlled by different regulators as in the case with the expression of the polar flagellins *flaA* and *flaB* which have been found to be regulated by different factors (Wilhelms *et al.*, 2011).

3.4.2.1. Complementation and overexpression of AHA2484, AHA3342, and AHA2698.

Mutating the gene *AHA2484* resulted in the formation of smooth colonies with a faint-reddish centre on CR agar. Although the *A. caviae* protein AHA2484 is not predicted to have a diguanylate cyclase or phosphodiesterase activity due to its possession of the non-conserved residues SGADF and EIY, however, the protein might be involved in extracellular polysaccharide production as its overexpression caused the formation of the rugose type of colonies. When a *cpsA::lacZ* mutation was introduced in the CPS (capsular polysaccharide) locus of *V. parahaemolyticus* the mutation caused a

great reduction in the ability of the bacterium to express *cps* genes when the *cps::lacZ* expression was measured in Miller units (Boles *et al.*, 2002). More importantly, a change in *V. parahaemolyticus* colony morphology from rough (wild type strain) to a smooth type (*cps::lacZ* mutant) was observed. Although the colony morphology of *V. parahaemolyticus* in the indicated study might not be identical to the morphology of *A. caviae* Sch3N in our study, however, the principle of colony morphology conversion from a rough (or relatively rough) morphology to a smooth one is similar to our finding with MA2 and MA12. Production of extracellular polysaccharide is important for the development of bacterial biofilms.

The mutant strain MA12 (*AHA2698::pKNG101*) showed a drastic decrease in its ability to form a biofilm on borosilicate glass tubes in comparison to both the wild type stain and the rest of the mutants. Our bioinformatics analysis revealed that the protein AHA2698 does not contain the conserved residues necessary for diguanylate cyclase and phosphodiesterase activities. The protein contains the residues SATEY and ELF, and thus, it does not seem to be directly involved in the synthesis or breakdown of c-di-GMP. Perhaps *A. caviae* AHA2698 plays an indirect role in biofilm production. Complementing *AHA2698* did not rescue biofilm production on borosilicate glass tubes, however, it caused a great reduction in swarming motility (but not swimming). It seems that AHA2698 plays a role in controlling the synthesis or movement of lateral flagella because of its activity being only related to swarming and biofilm production both of which are mediated by lateral flagella. The protein AHA2698 is predicted to possess two trans-membrane helices as well as a HAMP domain. The HAMP domain is called so for its presence in histidine kinases, adenylyl cyclases, methyl-accepting chemotaxis proteins, and phosphatases (Parkinson, 2010). The HAMP domain is involved in signal transduction (Parkinson, 2010).

The *A. caviae* protein AHA3342 contains the residues GADEF and EAL as well as a conserved RxxD motif (RPGD). This protein was thus predicted to have a phosphodiesterase activity (which promotes more motility and less sessility). As described earlier, the complementation and overexpression studies did not show a strong support for the role of AHA3342 in reducing biofilm production. Perhaps the phosphodiesterase activity of this protein can be determined using different experimental conditions than those used in our study. The promoters of the genes *lafA2* and *lafK* showed a very high activity when measured in MA10 (*AHA3342::pKNG101*)

background. It is possible that *A. caviae* protein AHA3342 plays a role in the lateral flagellar genes expression in a c-di-GMP dependant or independent manner. The protein AHA3342 is also predicted to possess a PAS domain which is a sensory domain found in numerous signalling proteins. The PAS domain is known to be involved in signalling not only in bacteria but also in Eukaryotes and it has been described as being able to bind to a very large number of molecules (Henry *et al.*, 2011). The PAS domain is usually found linked to other effector domains and it is composed of around 100 amino acids (Henry *et al.*, 2011). The PAS domain has been suggested to be directly involved in the following three functions within the bacterial cell: (1) Perception of a variety of stimuli, (2) Transfer of the signal, and (3) Protein-protein interactions (Henry *et al.*, 2011).

3.4.3. Reliability and reproducibility of biofilm assay and growth on CR agar

Although biofilm assay using the borosilicate glass tubes is generally a reliable method and have allowed us in this study to obtain interesting findings, the results obtained by this test, however, can be influenced by different factors. A study performed by Bechet and Blondeau investigated the factors affecting the ability of *A. caviae* to form a biofilm on glass tubes has emphasized on the influence of the growth phase, inoculum size, agitation, incubation temperature, incubation duration, and growth medium used on the ability of *A. caviae* to form a biofilm on glass tubes (Bechet *et al.*, 2003). The same study indicated that acidification of the medium due to the utilization of glucose (which is a component of the BHI broth used in biofilm assay in this study) can as well affect biofilm formation. For example, when tested for the first time, a mutation in the gene *AHA3342* resulted in the formation of a biofilm on borosilicate tubes which was slightly less than that formed by the wild type. Testing MA10 (*AHA3342::pKNG101*) again during the complementation study resulted in the formation of a biofilm which was much larger than the one formed by wild type strain. This could be due to any of the experimental factors mentioned above or it could be due to another GGDEF-EAL containing protein compensating for the loss of AHA3342 in MA10.

During this study, in some experiments, the Congo Red agar test appeared more sensitive than the borosilicate glass tubes in detecting variations among the tested *A. caviae* strains. In other experimental settings, however, the test failed to produce the same morphotype. Although cultivation on CR agar seem to be a reliable method for

biofilm detection, the method has been reported to require careful control especially with regard to incubation temperature and freshness of the original cultures (Qadri *et al.*, 1988). Slight variations in these parameters in our study, especially incubation of CR plates at room temperature might have resulted in the formation of different colony morphotypes by the same strain.

Chapter 4

The effect of *pilZ* gene knockout on *A. caviae*

Sch3N lifestyle

Chapter 4: The effect of *pilZ* gene knockout on *A. caviae* Sch3N lifestyle

4.1. Introduction

Proteins containing the PilZ domain have been reported in the literature as being able to bind c-di-GMP. The PilZ domain was found to be part of the cellulose synthase enzyme in *Gluconoacetobacter xylinus* and was experimentally shown to bind c-di-GMP in this bacterium (Weinhouse *et al.*, 1997). The PilZ domain of the *E. coli* protein YcgR has been demonstrated to bind c-di-GMP and the YcgR protein has been suggested to be directly involved in controlling motility in *E. coli* (Ryjenkov *et al.*, 2006). Pratt and colleagues have detected five regions in the genome of *V. cholerae* which all encode PilZ domains and have named them *plzA*, *plzB*, *plzC*, *plzD*, and *plzE* (Pratt *et al.*, 2007). Extensive experimental testing of the five domains revealed that two of them, namely, PlzC and PlzD are able to specifically bind c-di-GMP. In addition, the researchers have found that sometimes the PilZ domains do not have to bind c-di-GMP to exert their functions. The domains might play a regulatory role that is c-di-GMP independent. For example, the group suggested PlzB and PlzC to be positive regulators of motility in *V. cholerae* regardless of the cellular level of c-di-GMP and also have suggested PlzD to be a negative regulator of motility in the same species. Finally, the protein PA4608 in *Pseudomonas aeruginosa* has been reported to be involved in cellular processes controlled by c-di-GMP. This protein was found to contain a PilZ domain and was experimentally confirmed to bind c-di-GMP (Ramelot *et al.*, 2007). The lateral flagellar operon of *A. caviae* encodes a PilZ domain containing protein. We suggest that this protein might be involved in regulating swarming motility in *A. caviae* and /or be a receptor for c-di-GMP.

The *A. caviae* PilZ domain investigated in this chapter is encoded in the *laf* operon, it is composed of 459bp open reading frame (GC content = 63.39%), it has an amino acid length of 152 and a predicted molecular weight of 16662.371 Da (Unpublished data). This chapter provides a description for the knockout of *A. caviae pilZ* gene followed by a demonstration of the effects of this mutation on the phenotype of *A. caviae* Sch3N. The chapter illustrates the effects of generating a mutation in *pilZ* gene on motility, biofilm formation, binding to Congo Red (CR), and lateral flagellin promoter activity. Also, the chapter provides evidence that the *pilZ* gene is actively transcribed during swarming motility of *A. caviae*.

4.2. Testing the expression of *pilZ* gene during swarming

During the annotation of the *A. caviae* Sch3 genome sequence, an open reading frame encoding a PilZ-like protein was detected. This gene appeared to be conserved in other aeromonads that had the lateral flagellar gene cluster as well as *Shewanella* species. The gene *pilZ* was located immediately downstream of the lateral flagellar motor protein encoding gene *lafU*. Therefore, we have attempted to test whether the genes *pilZ* and *lafU* are actually being actively expressed during swarming of *A. caviae* Sch3N by using reverse transcription polymerase chain reaction (RT-PCR).

Custom designed oligonucleotide primers that would specifically hybridize to an internal region within each of the two *A. caviae* genes *pilZ* and *lafU* were designed. Oligonucleotide primers to amplify the region between the two genes were as well specifically designed. As a positive control for the RT-PCR, oligonucleotide primers to amplify an internal region within the polar flagellin gene *flaA* of *A. caviae* Sch3N (as it is constitutively expressed) were as well custom designed (figure 4.1). All custom designed primers were first tested by performing an ordinary PCR using *A. caviae* genomic DNA. The PCR protocol was optimized and all tested primer pairs generated a clear band with the expected size following optimizing the PCR annealing temperature. The primers were then ready to be used in RT-PCR to amplify the same tested regions following generation of cDNA.

Before extracting the total RNA of *A. caviae* Sch3N to check for the expression of *pilZ* and *lafU*, there was a need to first induce the expression of the *laf* operon by allowing *A. caviae* cells to swarm on swarm agar plates, prepared as previously described. The growth from swarming *A. caviae* Sch3N was scrapped from the swarm agar surface using a sterile loop and then was collected in a sterile microfuge tube. The total RNA of the collected swarming *A. caviae* was then successfully extracted using the protocol described in chapter 2. The extracted RNA was then used in the RT-PCR to check for the active expression of *pilZ* and *lafU*. The genes *pilZ* and *lafU*, as well as the region between them, were found to be actively expressed during swarming motility of *A. caviae* Sch3N (figure 4.2). Also, the positive control, *flaA* gene, was found to be expressed. No band was detected on agarose gel for the no-RNA negative control sample used in the RT-PCR. The no-RNA negative control sample was included to detect false positive results appearing due to contamination of the reagents or lab tools used with genomic DNA. A complete illustration of all steps used to check for the

expression of *pilZ* and *lafU* genes by RT-PCR during swarming of *A. caviae* Sch3N is provided in figure 4.3.

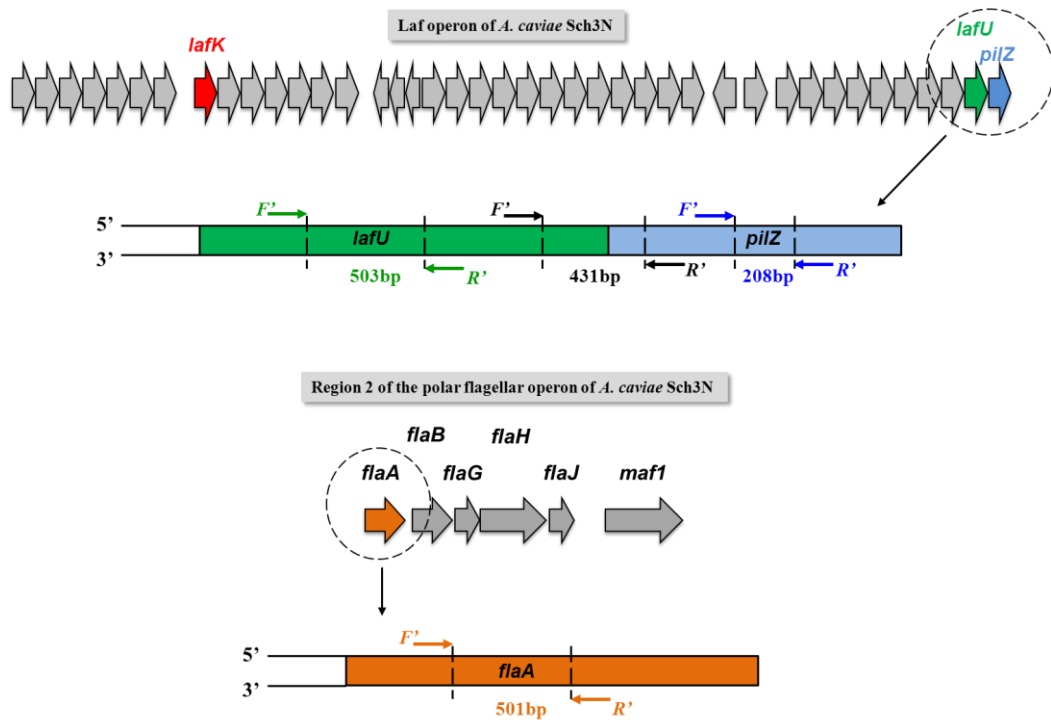


Figure 4.1. Sites of the custom designed oligonucleotide primers used to check for the expression of *pilZ* and *lafU* genes during swarming motility of *A. caviae* by RT-PCR. The *lafK* gene shown in red colour is the proposed master regulator of the lateral flagellar operon expression. The genes of *A. caviae* polar flagellum are encoded in 5 regions, only region 2 which contains *flaA* gene is shown in this figure.

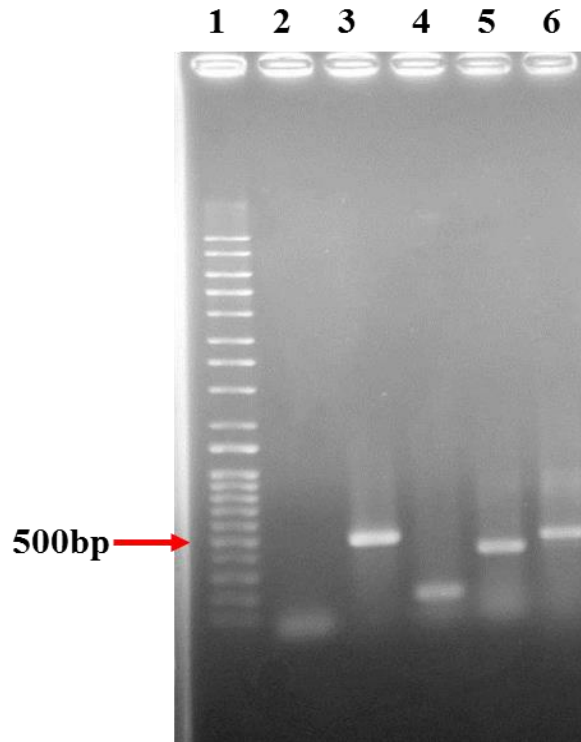


Figure 4.2. A 1% agarose gel showing the expression of the genes *pilZ* and *lafU* during the swarming of *A. caviae* using RT-PCR. **Lane 1:** Q-Step 4 DNA ladder. **Lane 2:** No RNA sample (negative control) using primers FlaA-MA-F and FlaA-MA-R. **Lane 3:** Internal region (501bp) within *flaA* gene (positive control) using primers FlaA-MA-F and FlaA-MA-R. **Lane 4:** internal region (208bp) within *pilZ* gene using primers intPilZ-F and intPilZ-R. **Lane 5:** the region shared between *pilZ* and *lafU* genes (431bp) using primers LafU-F and intPilZ-R. **Lane 6:** internal region (503bp) within *lafU* gene using primers LafU-MA-F and LafU-MA-R. The RT-PCR results suggest the active expression of both *pilZ* and *lafU* genes during swarming of *A. caviae* Sch3N.

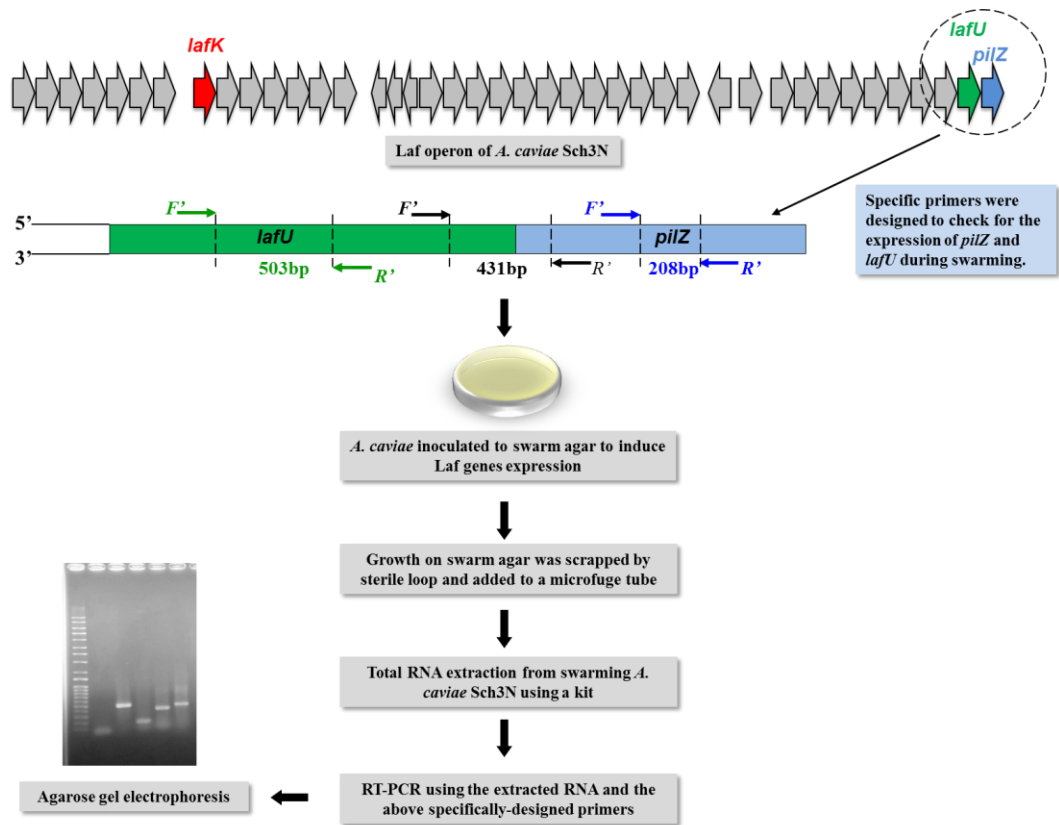


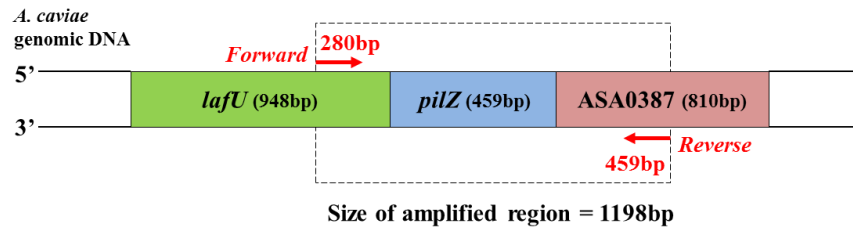
Figure 4.3. Schematic presentation of the procedure used to study the expression of *pilZ* and *lafU* during swarming of *A. caviae* Sch3N.

4.3. *pilZ* gene knockout

The *pilZ* gene was knocked out by insertion of a Km^R cassette. To do this, specific oligonucleotide primers were designed for PCR amplification of the gene. The forward primer was designed to hybridize to a DNA region which is 280bp upstream of *pilZ* gene (i.e., within the *lafU* gene) while the reverse primer was designed to bind a region which is 459bp downstream of the *pilZ* gene (i.e., within the gene *ASA0387*) as shown in figure 4.4. PCR amplification of *pilZ* using the custom designed primers was successful (figure 4.5).

The next step was to use the high copy number cloning vector pGEM-T-Easy (figure 4.6) to clone the amplified *pilZ* gene in *E. coli* DH5 α . The pGEM-T-Easy vector system I is provided by the manufacturer (Promega) as a linearized vector with a single T overhang at both ends. This feature allows perfect ligation to the PCR amplicons generated using the *Taq* DNA polymerase, used in this study, as it generates extra As. Ligation mixture was prepared as previously described in chapter 2. Figure 4.7 shows the ligation mixture containing the correct size of the recombinant plasmid pGEM-*pilZ* before being transferred by heat shock to *E. coli* DH5 α .

(A)



(B)

```

ACCCCTTTGCCGGTGACAACTACAGCAACTGGGAGCTCTCCTCCGATCGCGCCATGATGGCGAGGCGTGTC
CTGCTTGCTGGCGGCATGCCCCCGAGCGGGTGGGTTCAGGTGGTTCGCCATGTCGGATACCATGCTGGACAAC
ACCGCCGATCCCAAAGGCAGCCAGAACCGCCGCATCGAGTTGCTGGTGATGACGACCCAGGCGGAAAAGAGC
CTGGAGCAGCTGTTCAAGTGCCTAAACCAAGCCGCCACCCGGACAGCCAAGGATGCCGTTGCCCATGGAAC
CCCTGACGCCGATCTGCCCCCGTGACACCGTTCAAGGATCCAGGCGCAAACCTGCCGCGTGGTATCTCCA
TGACGGGACCACGCCCCGGAATCCAGAGTTGCGGCATCGCGGCCCGGCTCATGGTCTCCGGCCTGCTGTT
CGACAAGCGCATCGGACGGGCGGTGATCAAGGATATCGGACCGGGTGGGGTCGGTTTCTCGCCCCGCCCCG
TTTTACCTTGCCGATAACGTCAGCTGTCGTTGTCACCGCGGATCGTGTGCGGTGTCATATACCCATCG
CAGGGCCATAGGACAGTACCTCAGCTTCTACGGCGCGCATGGGTTCGATCCTGACTCGGTGGATCTCGCGCC
TGTTCTGAGCCACTGGCGCCACTGTTTCATGGCGCCAGCAGAGGGCGAGCCTGCTCCAATCCAGTGGATCC
GGCAACCGCTCAAGAGTGAAGCCTCCCCGCCCATGTCCAGTCCCCGTGCAGGCAGCAACAGCAGGGGATCG
TGCAGGCTTTCCAGGGACACGGCCCGCACCAGCTGCGGGCGTGTCTCTTGATGGCGCGGGGCAGGAGGGCC
TTGCTCCGCCATAACGATGGGGCAGTCACTCACCTCCCGGGGATCGGGCAATCGCCAGGCGGGATTCCAC
CGGCTTGCCTCGTTTCATGGCAACCCCCCGTTCCATGGCCCCACTCCAGCAATGAGCAGCCCCCGGCTGCCGC
CATACCCGATATTTTCTCCCGCTGCCAGGGCGGCAGGACAAAACCGTGTGCGCGCTCTGTCCAGCAAT
TGGGAGAGCGGAGGAAGCGCCACATAGAGGCGGTTTCGGTAGGCAATTGCAACTCCACACATTGGCT
GTCCCGCGTTGAGCACCGCCTTCACTCTTCCCTCTCCGCGT

```

Figure 4.4. Region of *A. caviae* genomic DNA containing the *pilZ* gene to be cloned and knocked out. (A) Organization of the region showing the size of *pilZ* gene and the sizes of genes upstream and downstream of *pilZ*, plus the exact location of the forward and reverse primers (red arrows) used for PCR amplification. (B) The DNA sequence of the PCR amplified region. **Green-coloured sequence:** Part of *lafU* gene (280bp). **Blue-coloured sequence:** *pilZ* gene (459bp) containing the *EcoRV* restriction site GATATC (highlighted in grey) used later for Km^R cassette insertion. **Red-coloured sequence:** Part of *ASA0387* gene (459bp). The sequence highlighted in yellow corresponds to the forward primer and the sequence highlighted in light blue corresponds to the reverse primer. The final size of the PCR amplified region containing the *pilZ* gene is 1198 bp.

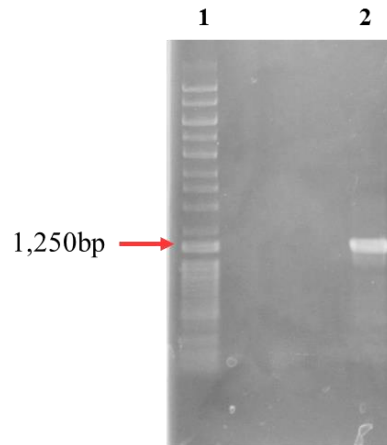


Figure 4.5. 0.8% agarose gel showing PCR amplification of *pilZ* gene using the custom designed primers PilZ-F and PilZ-R and genomic DNA of *A. caviae* Sch3N. (1) Q-Step 4 DNA ladder. (2) Amplified DNA region containing *lafU*, *pilZ*, and *ASA0387*(1198bp).

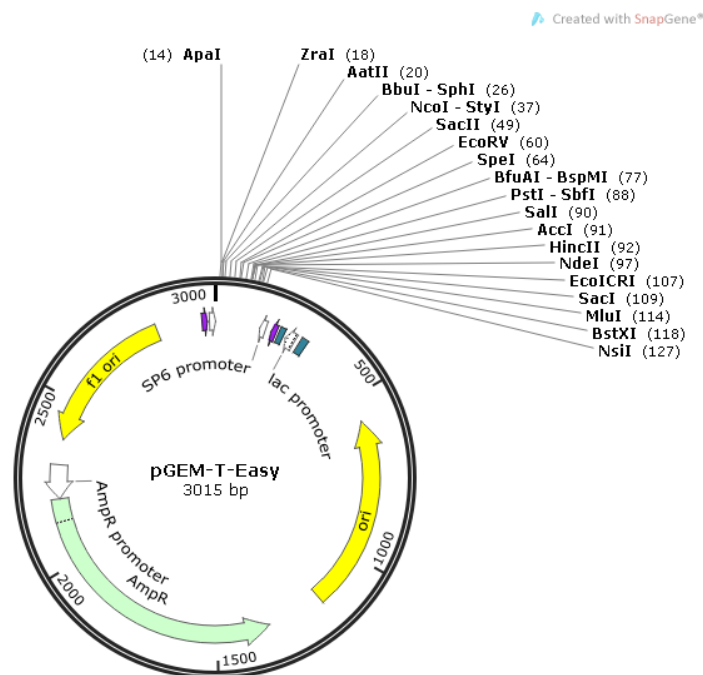


Figure 4.6. A map showing the main features of the high copy number plasmid vector pGEM-T-Easy vector (Promega) used in this study. The universal primers M13-F and M13-R flanking the polylinker region are shown as purple-coloured arrows. Other features shown are the SP6 promoter, *lac* promoter, the ampicillin resistance gene (*AmpR*). This map was generated using SnapGene Software.

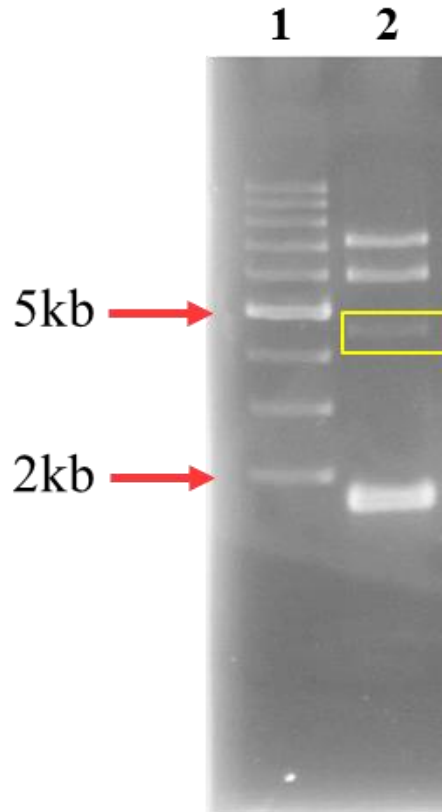


Figure 4.7. A 1% agarose gel showing the ligation mixture containing pGEM-T plasmid and PCR amplified *pilZ* gene. **Lane 1:** Supercoiled DNA ladder (Promega). **Lane 2:** Recombinant plasmid pGEM-*pilZ*, the yellow frame shows the band with correct size (4213bp) which indicates successful ligation. Lane 2 also shows *pilZ* PCR products (1198bp) and supercoiled non-recombinant plasmids (>5Kb). The ligation mixture was then transformed to *E. coli* DH5 α .

The ligation mixture was then transferred by heat shock to *E. coli* DH5 α as previously described. The transformed *E. coli* DH5 α cells were then plated on LB plates containing ampicillin plus IPTG and X-gal for blue/white screening. White colonies were successfully obtained which indicated successful cloning. Several white colonies were then screened for containing the recombinant plasmid pGEM-*pilZ* by PCR using the custom designed primers PilZ-F and PilZ-R. Colony PCR screening indicated a successful cloning of *A. caviae pilZ* gene in *E. coli* DH5 α (figure 4.8). The recombinant plasmid pGEM-*pilZ* was then extracted from colony number 2 and was subjected to DNA sequencing using the universal primers T7-F and SP6-R to confirm successful cloning of *pilZ* gene and to determine its orientation. DNA sequencing results confirmed the cloning of *A. caviae pilZ* gene in *E. coli* DH5 α . To obtain the Km cassette, the pUC4kixx plasmid was digested by *Sma*I restriction enzyme (which generates blunt ends) and the digested plasmid was then run on a 0.8% agarose gel followed by gel extraction of the 1.4Kb Km cassette using the gel extraction protocol described in chapter 2. The Km cassette was successfully extracted from the agarose gel. The recombinant plasmid pGEM-*pilZ* was then digested using the blunt-end generating restriction enzyme *Eco*RV and was then ligated to the previously extracted Km cassette using T4 DNA ligase, as previously described. The ligation mixture was then transformed by heat shock to *E. coli* DH5 α competent cells. The transformed cells were then plated on LB plates containing both ampicillin and kanamycin. Few ampicillin- and kanamycin-resistant colonies were successfully isolated after 24hrs of incubation at 37°C indicating successful construct creation (figure 4.9).

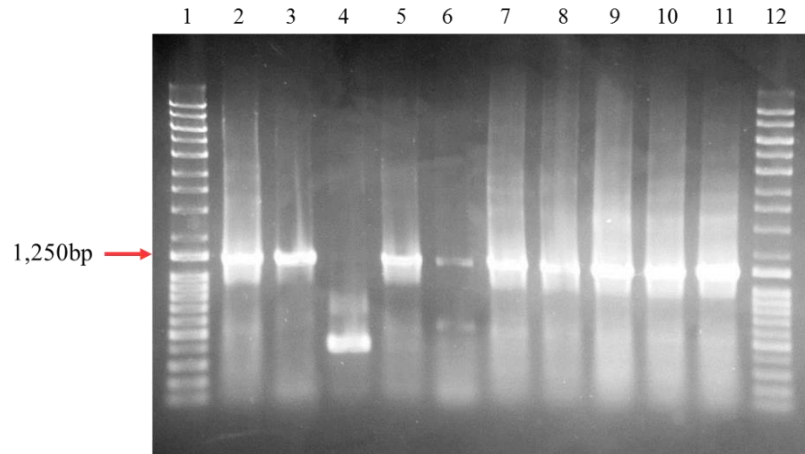


Figure 4.8 A. 1% agarose gel showing colony PCR screening of *E. coli* DH5 α transformed with pGEM-*pilZ* using primers PilZ-F and PilZ-R. **Lane 1 and 12:** Q-Step 4 DNA ladder. **Lane 2-11:** *E. coli* strains that were ampicillin resistant after transformation subjected to colony PCR. Expected band size (1198bp) was obtained from screening colonies in lanes 2,3,5,6,7,8,9,10, and 11. Successful cloning of *pilZ* was confirmed by DNA sequencing using universal primers T7-F and SP6-R following extraction of the recombinant plasmid from colony number 2.

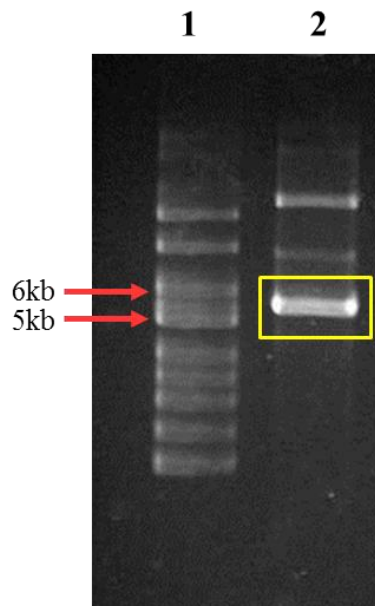


Figure 4.9. A 1% agarose gel showing the successful construction of pGEM-*pilZ*::Km. **Lane 1:** Supercoiled DNA ladder (NEB). **Lane 2:** pGEM-*pilZ*::Km (5613bp) extracted from ampicillin- and kanamycin-resistant *E. coli* DH5 α .

The next step was to allow a double cross over event to occur in order to create a permanent mutation in the *pilZ* gene in *A. caviae* genome. This was done by a series of steps which are explained in the following paragraphs.

The extracted recombinant plasmid pGEM-*pilZ*::Km was used as a template for a PCR reaction to amplify *pilZ*::Km (mutated gene) using the enzyme KOD polymerase. The KOD enzyme has a proof reading ability and generates blunt ended PCR products. PCR amplification of *pilZ*::Km by KOD resulted in the generation of multiple bands. The band which corresponds to *pilZ*::Km was gel extracted. Gel extraction of *pilZ*::Km was successful. The extracted *pilZ*::Km was then inserted into the suicide plasmid pKNG101 (streptomycin resistant) in order to accomplish the double cross over event. To perform this insertion, the plasmid pKNG101 was cut using *Sma*I restriction enzyme (which generates blunt ends). The *Sma*I digestion of pKNG101 was successful.

A ligation reaction was then carried out using the digested pKNG101 and the gel extracted *pilZ*::Km PCR amplicons. The ligation mixture was then transferred by heat shock to *E. coli* CC118 λ *pir* competent cells. The transformed *E. coli* CC118 λ *pir* cells were then plated on LB plates containing both streptomycin and kanamycin. Streptomycin- and kanamycin-resistant *E. coli* CC118 λ *pir* colonies (containing pKNG101*pilZ*::Km) were successfully isolated (figure 4.10). Successful insertion of *pilZ*::Km into pKNG101 plasmid was then confirmed by DNA sequencing using primers pKNG101-F and pKNG101-R.

The recombinant plasmid pKNG101-*pilZ*::Km was transferred from *E. coli* CC118 λ *pir* to *A. caviae* Sch3N by a triparental conjugation in the presence of the helper plasmid pRK2013 which helped in the mobilization of the recombinant plasmid. Principally, once the recombinant plasmid is introduced into the *A. caviae* cell a double cross over homologous recombination event is expected to happen between pKNG101-*pilZ*::Km and the *pilZ* gene in the *A. caviae* genome as shown in figure 4.11. This will result in the transfer of the Km cassette from the recombinant plasmid into the *A. caviae* *pilZ* gene leading to the permanent knock out of the *pilZ* gene in *A. caviae* Sch3N genome. The triparental mixture of cells indicated above was prepared followed by plating of the mixture on LB plates containing kanamycin and nalidixic acid. This resulted in the isolation of oxidase-positive nalidixic acid-resistant colonies that were also kanamycin-resistant. These colonies were then streaked on two sets of LB plates.

The first set contained the two antibiotics kanamycin and streptomycin and the second set contained both nalidixic acid and kanamycin. The reason for streaking the colonies on two different sets was to find an *A. caviae* colony which was resistant to both kanamycin and nalidixic acid but sensitive to streptomycin, and thus, indicating a successful double cross over event. Out of 150 colonies screened by the steps described above, two oxidase positive colonies were found to be resistant to both kanamycin and nalidixic acid but sensitive to streptomycin. One of these two colonies was chosen for further analysis and was named MA124.

Mutation of the *A. caviae pilZ* gene (which contains the Km^R cassette) was then confirmed by performing a PCR reaction to amplify the mutated gene and compare its size with that of the wild type *pilZ* gene. To perform this PCR reaction, the genomic DNA of MA124 and that of the wild type strain were extracted as described previously to be used as DNA templates, and the amplification was carried out using the primers PilZ-F and PilZ-R and *GoTaq* DNA polymerase (Promega). Agarose gel electrophoresis following this PCR reaction revealed the size of the amplified *pilZ* gene in MA124 (containing the Km cassette) to be of 2,598bp while the size of the same gene in the wild type strain to be of 1198bp (figure 4.12). As the amplified *pilZ* gene in MA124 was larger in size than the one from the wild type strain, this PCR result indicated a successful permanent knockout of the *A. caviae pilZ* gene in MA124. A schematic presentation of the detailed procedure used in this study to knockout *pilZ* in *A. caviae* Sch3N is shown in figure 4.13. The mutant strain MA124 was then further studied in an attempt to find out any role played by the PilZ domain in the lifestyle of *A. caviae* Sch3N.

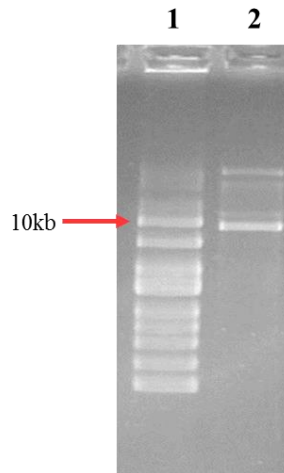


Figure 4.10. A 1% agarose gel showing the recombinant plasmid pKNG101-*pilZ*::km extracted from streptomycin- and kanamycin-resistant *E. coli* CC118 λ *pir* colony. **Lane 1:** Supercoiled DNA ladder (NEB). **Lane 2:** pKNG101-*pilZ*::km (9,584bp). This recombinant plasmid was then transferred by conjugation to *A. caviae* Sch3N for a double cross over event leading to permanent *pilZ* gene knockout in *A. caviae* Sch3N.

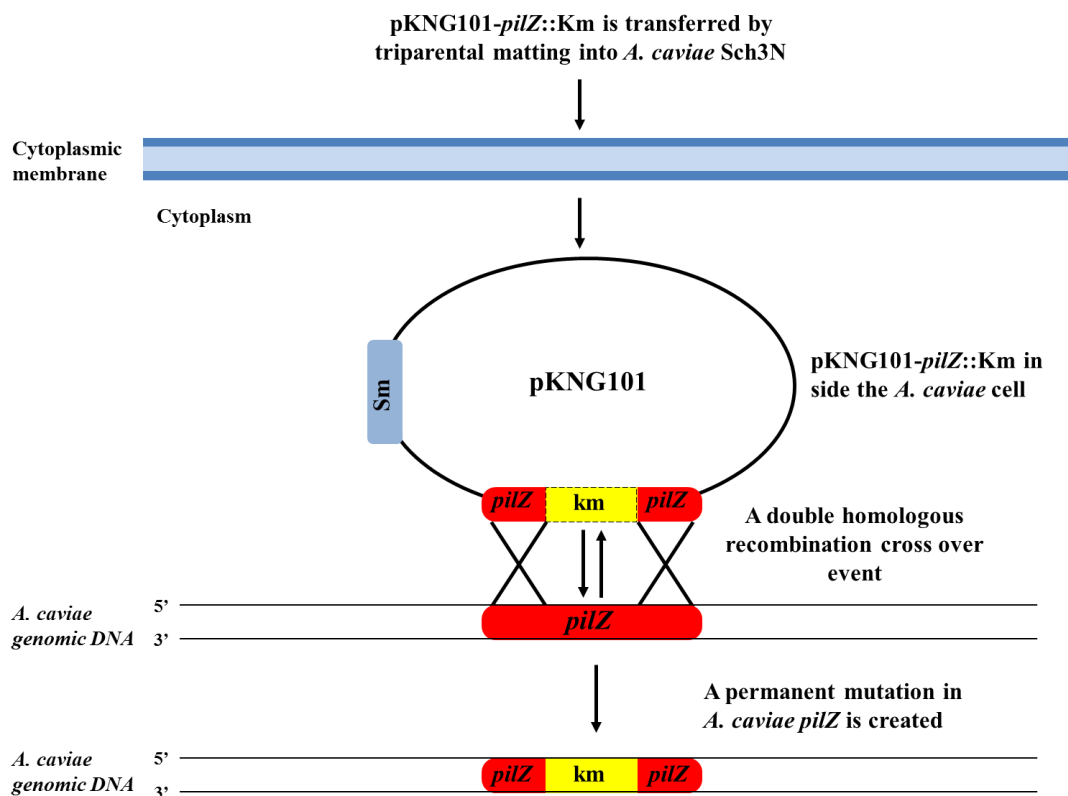


Figure 4.11. A schematic representation of the double cross over event which led to the transfer of the Km cassette from the recombinant plasmid pKNG101-*pilZ*::Km to the *A. caviae pilZ* and thus resulted in a permanent mutation in *A. caviae* Sch3N *pilZ* gene.

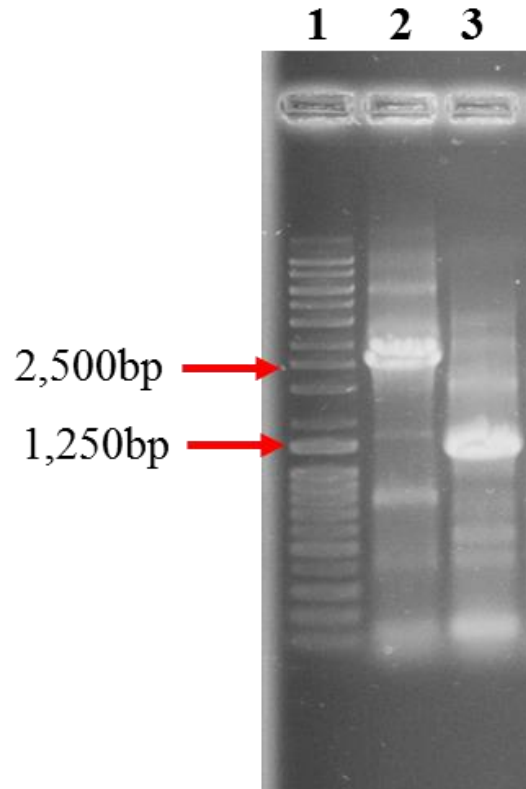


Figure 4.12. A 1% agarose gel showing the PCR amplification of the mutated *A. caviae* *pilZ* gene and the wild type *pilZ* gene from genomic DNA. **Lane 1:** Q-Step 4 DNA ladder. **Lane 2:** *pilZ::km* (2,598bp) in the genome of MA124. **Lane 3:** *pilZ* (1,198 bp) in the genome of *A. caviae* Sch3N (wild type strain).

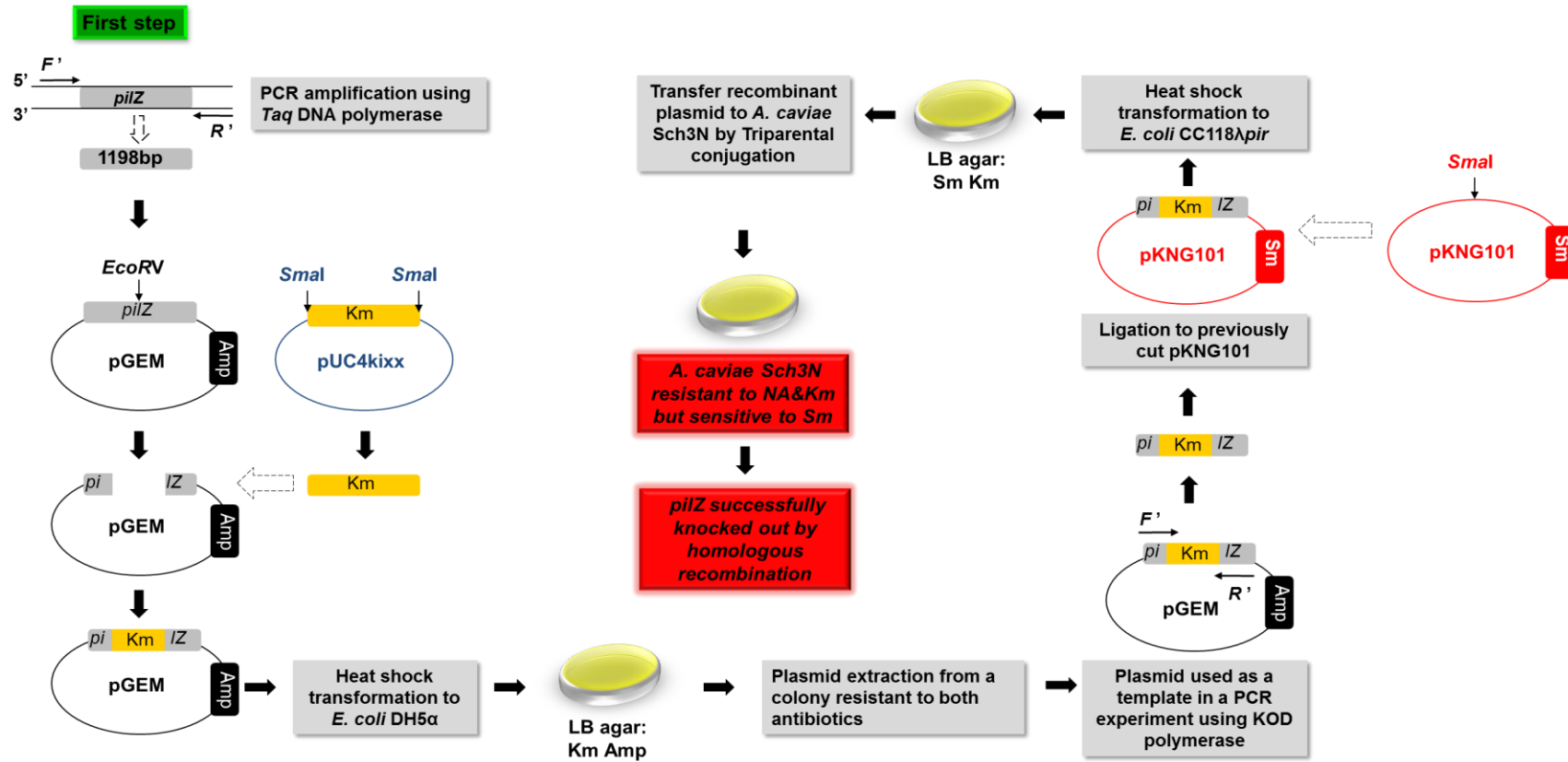


Figure 4.13. Schematic presentation of the complete procedure used in this study to knock out *pilZ* gene in *A. caviae* Sch3N. **Amp**: ampicillin, **Km**: kanamycin, **Sm**: streptomycin.

4.3.1. Phenotypic studies of MA124

The effects of the *pilZ* gene knockout on the ability of *A. caviae* Sch3N to swim, swarm, and form a biofilm were investigated in this chapter.

4.3.1.1. Motility assay

The ability of the strain MA124 to swim and swarm was tested using motility agar assay as previously described. The strain MA124 was found to be actively swimming and swarming on 0.25% and 0.8% agar plates, respectively. The migration rate of MA124 on both swim agar (figure 4.14) and swarm agar (figure 4.15) was similar to that of the wild type strain.

4.3.1.2. Biofilm assay

The effect of *pilZ* gene knock out on the ability of *A. caviae* Sch3N to form a biofilm on borosilicate glass tubes was tested (figure 4.16 and 4.17). The strain MA124 was found to be able to form a biofilm on borosilicate glass tubes. Visual inspection appeared to show a decrease in biofilm formation by the mutant, however, quantitative assays showed the density of the formed biofilm to be statistically insignificant when compared to the wild type ($p=0.264$). In addition, the amount of biofilm formed by both the wild type strain and the mutant strain MA124 after 48hrs of incubation in the glass tubes was less than the amount of biofilm formed by the same strains after 24hrs of incubation.

4.3.1.3. Growth on Congo Red agar

The effect of generating a mutation in *pilZ* gene on the ability of *A. caviae* to bind the Congo Red dye was tested using 0.025% Congo Red agar plates, as described in chapter two. The colony morphology of MA124 (*pilZ::Km*) on Congo Red agar was similar to the colony morphology formed on the same medium by the wild type strain (figure 4.18). Both strains formed translucent (i.e., light-coloured) colonies with a dark red centre and slightly undulated margins. As described elsewhere in this study, this colony morphology indicates the ability of the tested strain to bind the Congo Red dye due to its ability to form extracellular substances which are necessary for biofilm formation (e.g., polysaccharaides) and to which the dye becomes bound.



Figure 4.14. A swim (0.25%) agar plate showing the effect of *pilZ* gene mutation on the swimming ability of *A. caviae* following incubation at room temperature for 24hrs (1) Mutant strain MA124 (*pilZ::Km*) (2) *A. caviae* Sch3N (wild type strain). The picture shows a similar migration rate for both *A. caviae* strains on swim agar.

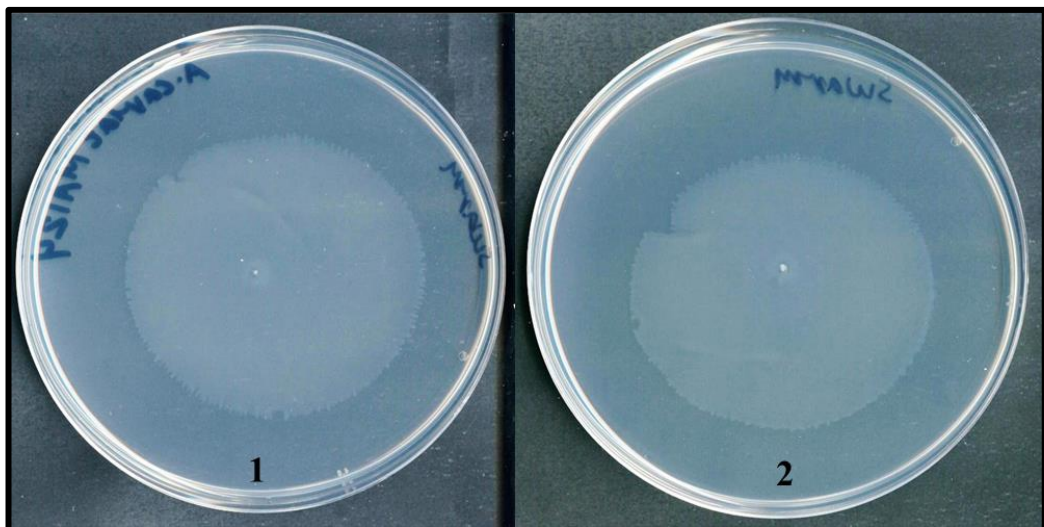


Figure 4.15. Two swarm (0.8%) agar plates showing the effect of *pilZ* gene mutation on the swarming ability of *A. caviae* following incubation at 30°C in a humid box for 48hrs. (1) Mutant strain MA124 (*pilZ::Km*) (2) *A. caviae* Sch3N (wild type strain). The pictures shows a similar migration rate for both *A. caviae* strains on swarm agar.

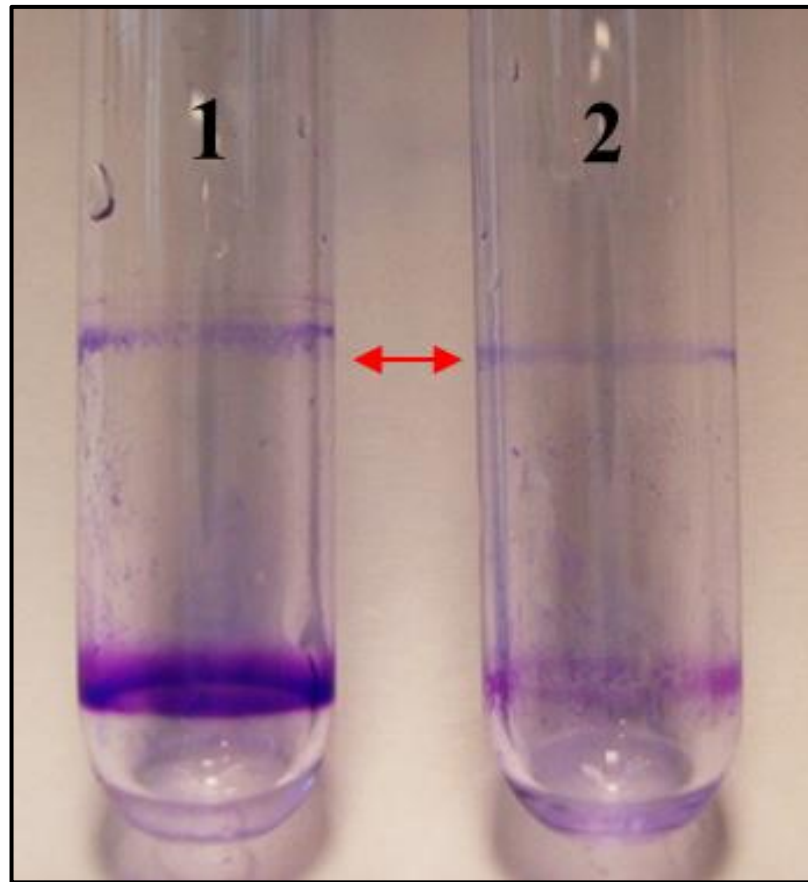


Figure 4.16. Biofilm assay using borosilicate glass tube to test the effect of introducing a mutation in *pilZ* gene on the ability of *A. caviae* to form a biofilm. **(1)** *A. caviae* Sch3N (wild type). **(2)** MA124 (*A. caviae pilZ::Km*). Tubes were incubated for 24hrs at 37°C. The pictures shows a slight reduction in the ability of MA124 to form a biofilm.

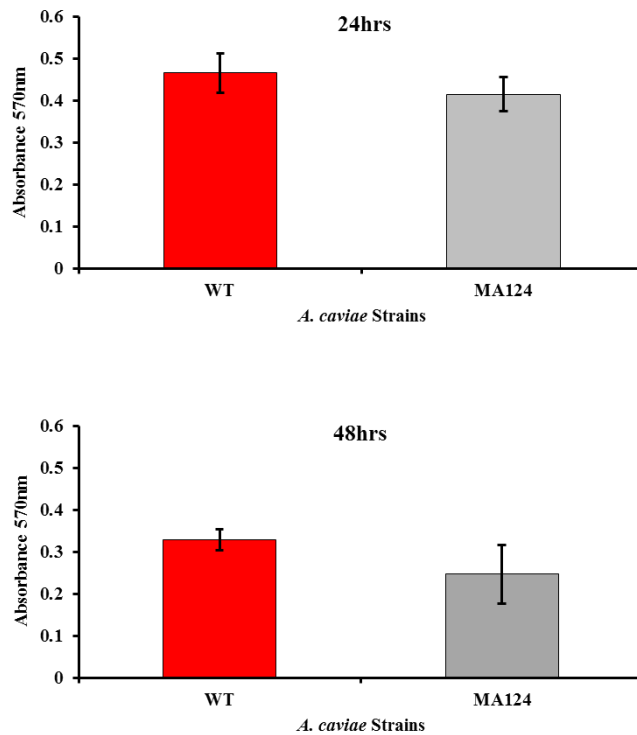


Figure 4.17. Biofilm assay quantified. The graphs show the effect of *pilZ* gene knockout on the ability of *A. caviae* to form a biofilm on borosilicate glass tubes following 24hrs and 48hrs of incubation at 37°C. **WT:** *A. caviae* Sch3N (wild type). **MA124:** *A. caviae* mutated strain *pilZ::Km*. Error bars represent the standard deviation around the mean. Statistical analysis indicated a non-significant variation ($p>0.05$) using the Student's t-Test.

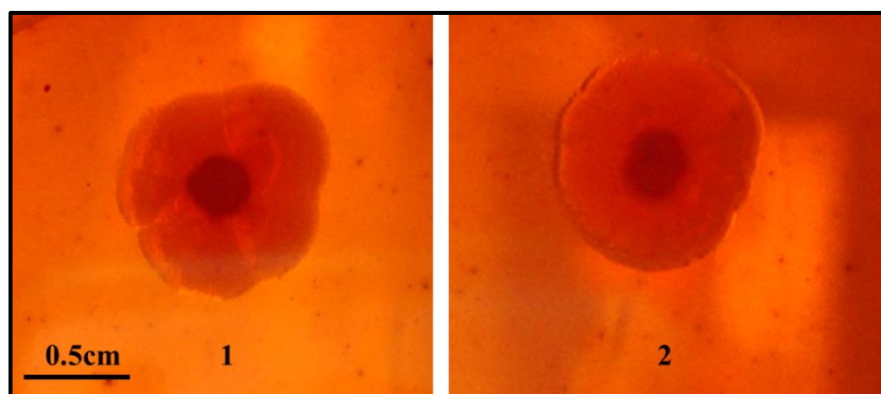


Figure 4.18. Colonies of *A. caviae* strains growing on Congo red (0.025%) agar plate to test the effect of *pilZ* gene knockout on the ability of *A. caviae* to bind the Congo red dye after 27hrs of incubation at room temperature. **(1)** *A. caviae* Sch3N (wild type). **(2)** Mutant strain MA124 (*A. caviae pilZ::Km*). Both strains formed colonies with a dark red centre which indicated the ability of both strains to bind the Congo Red dye.

4.3.2. Transcriptional fusions

To examine the effect of the *pilZ* gene knockout on the expression of the lateral flagellins LafA1 and LafA2 as well as on the expression of the LafK regulatory protein, the promoters of the genes encoding these three proteins were separately fused to the promoter-less plasmid vector pKAGb2(-) and were then introduced separately to MA124. As described previously, pKAGb2(-) contains the *lacZ* reporter gene which encodes the β -galactosidase enzyme which (by measuring its expression) is used to indicate the activity of the fused promoter.

The activity of the *lafA1* promoter was measured by β -galactosidase assay as shown in figure 4.19. The *lafA1* promoter activity in MA124 background was higher than its activity in the wild type background. Statistical analysis, however, revealed a non-significant variation in the *lafA1* promoter activity tested against the two backgrounds ($p=0.169$). The large error bar is probably due to differences in the rates of swarming on motility agar. The strain MA124pKAG-*lafA1*p was swarming at a faster rate on one swarm agar plate than the other resulting in two different migration zones which have probably resulted in the reported large error. The error, however, does not rule out the fact that there is an increase in *lafA1* promoter activity resulting from the mutation in *pilZ* gene.

The activity of *lafA2* promoter was measured by β -galactosidase assay as shown in figure 4.20. The *lafA2* promoter activity in MA124 background was around 50% less than its activity tested against the wild type background. In addition, this reduction in *lafA2* promoter activity was statistically significant ($p=0.002$).

The activity of *lafK* promoter was determined by β -galactosidase as shown in figure 4.21. There was no significant difference between the activity of *lafK* promoter against the wild type background and its activity against the MA124 background ($p=0.543$).

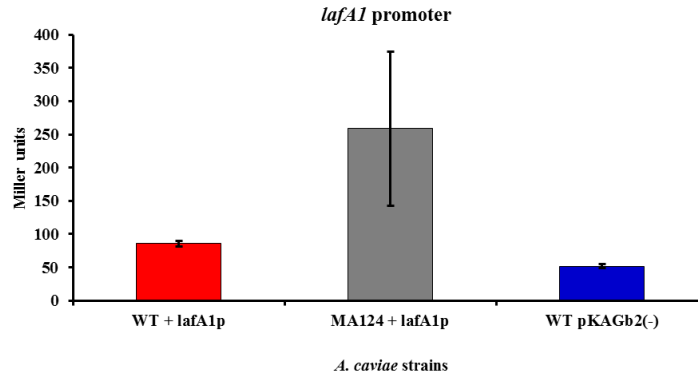


Figure 4.19. Analysis of *lafA1* promoter activity in *A. caviae pilZ* mutant and WT grown on swarm agar using β -galactosidase assay, results expressed in Miller units. Test was done in duplicate. Bars represent mean values of the two readings. Error bars represent the standard deviation around the mean. **Red-coloured bar:** positive control (*A. caviae* pKAGb2-*lafA1p*). **Grey-coloured bar:** MA124pKAGb2-*lafA1p*. **Blue-coloured bar:** negative control [*A. caviae* pKAGb2(-)]. Results showed a non-significant variation ($p > 0.05$) using single factor ANOVA test.

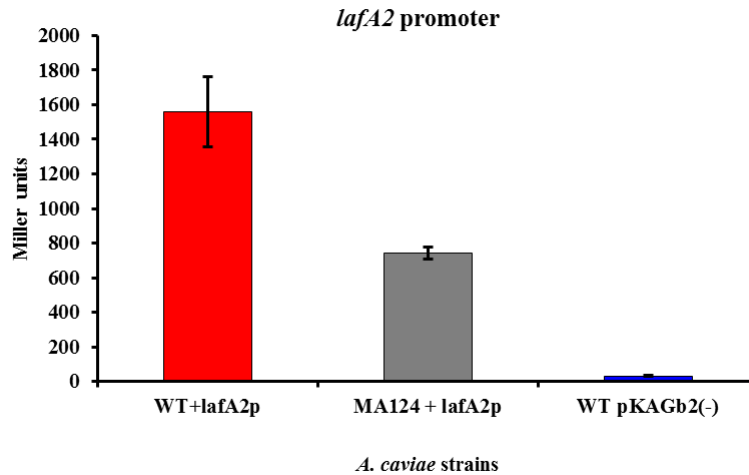


Figure 4.20. Analysis of *lafA2* promoter activity in *A. caviae pilZ* mutant and WT grown on swarm agar using β -galactosidase assay, results expressed in Miller units. Test was done in triplicate. Bars represent mean values of the three readings. Error bars represent the standard deviation around the mean. **Red-coloured bar:** positive control (*A. caviae* pKAGb2-*lafA2p*). **Grey-coloured bar:** MA124pKAGb2-*lafA2p*. **Blue-coloured bar:** negative control [*A. caviae* pKAGb2(-)]. Results showed a significant variation ($p < 0.05$) using single factor ANOVA test.

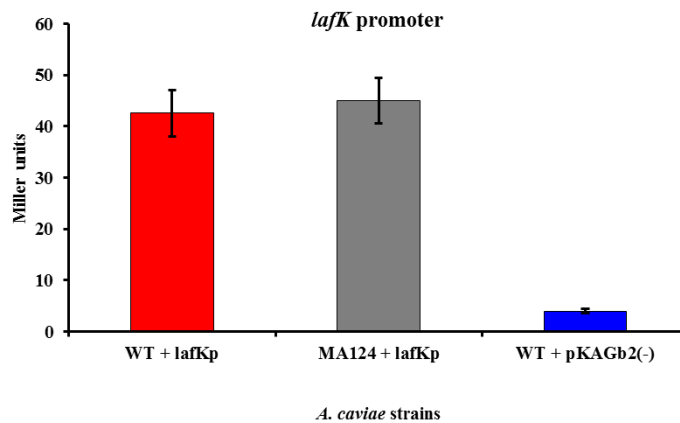


Figure 4.21. Analysis of *lafK* promoter activity in *A. caviae pilZ* mutant and WT grown on swarm agar using β -galactosidase assay, results expressed in Miller units. Test was done in triplicate. Bars represent mean values of the three readings. Error bars represent the standard deviation around the mean. **Red-coloured bar:** positive control (*A. caviae* pKAGb2-*lafKp*). **Grey-coloured bar:** MA124pKAGb2-*lafKp*. **Blue-coloured bar:** negative control [*A. caviae* pKAGb2(-)]. Statistical analysis of the *lafKp* activity in the wild type and MA124 backgrounds revealed a non-significant variation ($p>0.05$) using Student's t-Test.

4.4. Discussion

In this chapter we have attempted to investigate whether mutating the *A. caviae pilZ* gene would result in any effect on motility and biofilm formation, and whether the mutation would have an effect on the activity of the lateral flagellin promoters or the activity of the *lafK* promoter, the gene which is suggested to encode the master regulator of the *laf* operon in *A. caviae*.

4.4.1. PilZ expression during swarming of *A. caviae*

Our results suggested the active expression of *lafU* and *pilZ* during swarming motility of *A. caviae* Sch3N. The gene *lafU* is composed of 948bp (62.55% GC content). The LafU protein is composed of 315 amino acids, and it has a molecular weight of 35230.59 Da (*A. caviae* Sch3 unpublished data). Using SMART domain architecture prediction software indicated that LafU possesses a single trans-membrane region which starts at amino acid number 21 and ends at amino acid number 43. As explained in chapter 1, LafU is one of the two flagellar motor proteins in *A. caviae*. Subjecting the *A. caviae* LafU amino acid sequence to blastp online software (NCBI) to search the protein database for similar proteins allowed us to detect the putative

conserved domains shown in figure 4.22. Searching the database showed that our LafU protein is similar to LafU or MotB (LafU homolog in *V. parahaemolyticus*) in different bacterial species. In addition, upstream of *lafU* is the *A. caviae* motor protein LafT (homologous to MotA in *V. parahaemolyticus*).

It is known that the *E. coli* PilZ domain containing protein YcgR directly interacts with the motor proteins resulting principally in the disturbance of the interaction between the flagellar rotor and the stator and consequently resulting in the slow down of *E. coli* flagella (Armitage *et al.*, 2010). Some studies indicated that YcgR interacts with the stator protein MotA (LafT) (Boehm *et al.*, 2010), while others indicated its interaction to be actually with the two rotor proteins FliG and FliM (Paul *et al.*, 2010). Still further studies are needed to find out where exactly the interaction of PilZ protein does occur in *E. coli* flagella and whether there are other motor proteins involved in the interaction (Armitage *et al.*, 2010).

As indicated elsewhere in this study, the lateral flagellar system in *A. caviae* is required for both swarming motility and biofilm formation. We have not attempted to detect the expression of *lafT* (*motA*) by RT-PCR. The expression of the two *A. caviae* genes *lafU* (*motB*) and *pilZ* during swarming motility perhaps indicates the involvement of PilZ domain in protein-protein interaction which eventually leads to the slowing down of the rotation of *A. caviae* flagella when the environmental conditions stimulate sessility.

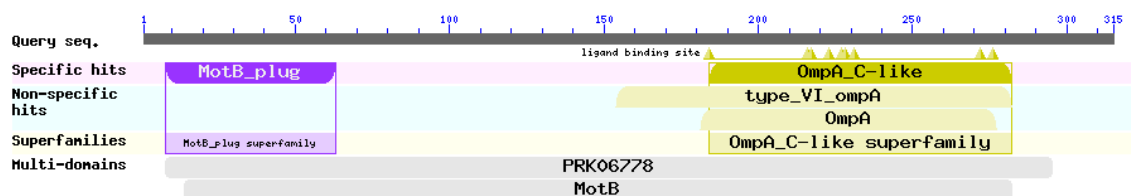


Figure 4.22. The putative conserved domains detected in *A. caviae* protein LafU using the NCBI blast tool. The detected domains include MotB (flagellar motor protein) and an outer-membrane protein A (OmpA)-like domain. The scale represents the amino acids sequence. Specific hits represent the statistically significant sequences that highly matched the sequence of LafU (high confidence). The non-specific hits represent the statistically less significant matches (less confidence). The multi-domains hits represent a detected similarity to one of several domains contained in multi-domain containing proteins.

4.4.2. Phenotypic effects of *A. caviae pilZ* gene knockout

4.4.2.1. Effects of *pilZ* gene knockout on *A. caviae* motility

It has been suggested that high c-di-GMP concentration (in the presence of its receptors) promotes a sessile lifestyle. Thus, deletion of a c-di-GMP receptor would result in a more motile lifestyle, unless there are other receptors or alternative mechanisms by which the second messenger exerts its functions. The PilZ domain has been strongly suggested to be a c-di-GMP receptor. In our study, deletion of the *A. caviae* PilZ domain located in the *laf* operon was expected to result in the studied *A. caviae* strain to be actively motile. Indeed, our results indicated that MA124 (*pilZ::Km*) was able to both swim and swarm and in a similar rate to that of the wild type strain. It would have been a good step to add to our study to test the motility of the wild type and the mutant strain MA124 following the introduction of a GGDEF domain which was previously tested for the DGC enzymatic activity (i.e., artificially raise the cellular level of c-di-GMP). This would theoretically result in a more sessile life style in the wild type strain but would have no effect on motility of MA124 (in which the *pilZ* gene was knocked out) unless other c-di-GMP receptors exist.

Our results are in agreement with the results of Pultz and colleagues who have studied the PilZ domain protein YcgR of *S. Typhimurium* and who have found the mutated strain $\Delta YcgR$ to be able to actively swim (Pultz *et al.*, 2012). They have attempted to determine the c-di-GMP binding affinity for the studied PilZ domain after which they have attempted to artificially raise the c-di-GMP concentration to reach the specific level needed by this domain to inhibit motility. When they have re-introduced the YcgR protein into the *S. Typhimurium* $\Delta ycgR$ and artificially raised the c-di-GMP concentration the strain lost its ability to swim and turned to a sessile lifestyle, which confirmed that the PilZ-containing YcgR protein was a c-di-GMP receptor in *S. Typhimurium*. We expect to have the same outcome on the motility of *A. caviae* if the binding affinity of *A. caviae* PilZ domain was known and if we complement the *A. caviae pilZ* gene in MA124 along with artificially raising the level of c-di-GMP within MA124 to the required effective concentration. Pratt and colleagues have attempted to study the effect of deleting the five PilZ domains encoding genes of *V. cholerae* on motility (Pratt *et al.*, 2007). Similar to our findings, they found the deletion of the two genes *plzC* and *plzD* to have no effect on motility of *V. cholerae*.

4.4.2.2. Effects of *pilZ* gene knockout on the ability of *A. caviae* to form a biofilm

Our results, unexpectedly, showed that *A. caviae* did not lose its ability to form a biofilm with the loss of PilZ domain. The mutant strain MA124 was even able to produce colonies on Congo Red agar which were similar to the colonies of the wild type, and thus, its ability to produce extracellular substances which might be necessary to form a biofilm was comparable to that of the wild type strain. We have not measured the level of c-di-GMP in MA124 during the experimental conditions used in the biofilm assay, however, it is obvious that the second messenger concentration was good enough in both the wild type strain and the *pilZ* mutant strain to cause biofilm formation. The growth of bacteria in a glass tube stimulated the synthesis of more c-di-GMP, as the synthesis of the molecule is usually in response to the signals sent from the surrounding environment. It seems, thus, that c-di-GMP in MA124 was able to bind to a downstream receptor other than PilZ and thus was able to form a biofilm, even though it was slightly less in density than the biofilm formed by the wild type strain. A good candidate to be an alternative c-di-GMP receptor is the riboswitch located upstream of *A. caviae lafK* gene. As mentioned in chapter 1 of this study, riboswitches are RNA domains which have been reported to function as receptors for c-di-GMP. More information about *A. caviae lafK* riboswitch is provided in Chapter 5 of this study. Another possibility is that *A. caviae* PilZ domain encoded in the *laf* operon of the bacterium does not bind c-di-GMP in the first place. A study to determine the binding affinity of *A. caviae* PilZ domain to c-di-GMP is thus warranted followed by another study to determine the effective c-di-GMP concentration required for *A. caviae* PilZ to show its function.

Our results are in agreement with those obtained by Pratt and colleagues who found the deletion of two of the five PilZ domain encoding genes in *V. cholerae*, namely *plzC* and *plzD*, to result in the formation of biofilms with a similar density to the one formed by the wild type strain (Pratt *et al.*, 2007). In an attempt to explain their results, the authors suggested the involvement of proteins other than PlzC and PlzD in the process of biofilm formation and that the exact mechanism by which c-di-GMP controls biofilm production is still not very well understood.

4.4.3. Effects of *A. caviae pilZ* gene knockout on the promoters activities of the genes *lafA1*, *lafA2*, and *lafK*

It seems from our results that deletion of the *pilZ* gene has a positive regulatory effect on the lateral flagellin LafA1 expression, however, it has a negative regulatory effect on the lateral flagellin LafA2 expression. There does not seem to be any regulatory effect of *pilZ* gene deletion on the expression of the regulatory protein LafK. Regulation of lateral flagella is complex and mutations may affect the homeostasis of its regulation. The lack of PilZ might have resulted in a higher concentration of c-di-GMP which has affected the expression of *lafA1* and *lafA2* by directly or indirectly affecting their regulators by an unknown mechanism.

Chapter 5

The role of *lafK* riboswitch as a c-di-GMP receptor

Chapter 5: The role of *lafK* riboswitch as a c-di-GMP receptor

5.1. Introduction

Riboswitches are conserved RNA domains present in the 5'-untranslated region of the mRNA of different genes (Ryan *et al.*, 2012). In the literature, there are different classes of riboswitches, among these are the c-di-GMP interacting riboswitches. There are two types of c-di-GMP riboswitches (type-I and type-II) (Ryan *et al.*, 2012) and they have been described as c-di-GMP effectors (Hengge, 2009). Riboswitches in general do exist in large numbers among bacteria and their main role seems to be the control of gene expression (Sondermann *et al.*, 2012). The control of gene expression by c-di-GMP riboswitches can occur at the transcriptional or translational levels (Ryan *et al.*, 2012). Thus, by binding to a riboswitch, c-di-GMP can modulate different cellular processes in bacteria especially those related to bacterial motility and its lifestyle in relation to the surrounding environment (Ryan *et al.*, 2012). It is due to the last fact that c-di-GMP interacting riboswitches are also referred to as the GEMM motif or GEMM element for the Genes for the Environment Membranes and Motility (Hengge, 2009). Riboswitches are generally composed of an aptamer, to which the ligand molecule binds, and an expression platform which due to the aptamer binding to a metabolite undergoes structural changes that result in either activation or repression of the expression of genes located downstream of the riboswitch (Ryan *et al.*, 2012).

The identification of riboswitches occurs mainly by bioinformatic analysis of the bacterial sequence (Sondermann *et al.*, 2012). In this study, computational analysis of the DNA sequence upstream of the *A. caviae* *lafK* gene allowed us to detect a c-di-GMP type I riboswitch. C-di-GMP type I riboswitches have been previously detected in *V. cholerae* (Sudarsan *et al.*, 2008). As mentioned elsewhere in this study, LafK is considered as the master regulator of the lateral flagellar genes expression in *V. parahaemolyticus* (Stewart *et al.*, 2003). Wilhelms and colleagues have recently attempted to determine the transcriptional hierarchy for *A. hydrophila* lateral flagella (Wilhelms *et al.*, 2013). During their study, they have noticed that different gene clusters were under the control of several promoters and that the transcription of many genes was LafK-independent. Wilhelms and co-workers have, thus, rejected the probability that LafK acts as the master regulator for the expression of the *laf* operon in *A. hydrophila*. The LafK protein of *A. hydrophila*, however, was found to be an essential protein for the synthesis of lateral flagella (Canals *et al.*, 2006a) and many of

the *A. hydrophila* lateral flagellar genes were determined to be sigma-54 and LafK-dependant (Wilhelms *et al.*, 2013).

In this chapter we present an *in silico* analysis of the region upstream of *lafK* gene of *A. caviae* Sch3N. An important finding in our computational analysis is the presence of a riboswitch upstream of *lafK* gene. We then have investigated the activity of the predicted *lafK* promoter in the presence and absence of the *lafK* riboswitch by deleting this riboswitch from the promoter region, fusing the promoter to a promoterless vector containing the *lacZ* reporter gene and performing a β -galactosidase assay. As the activity of the predicted *lafK* promoter was found to be different in the presence and absence of the *lafK* riboswitch, we have further tested the predicted *lafK* promoter activity following deletion of each of the two riboswitch hairpins (P1 and P2 loops) and also following creating a mutation within the stem of the P1 hairpin. The activity of the *lafK* promoter following this riboswitch dissection was determined by β -galactosidase assay. Also in this chapter, complementation of a *lafK* mutant strain previously created in our group (which has no ability to swarm) with a plasmid construct containing *A. caviae* *lafK* gene with its riboswitch deleted was done. The complemented strain was studied by motility assay. Finally, investigating whether overexpressing *lafK* Δ riboswitch in liquid medium would result in lateral flagellar genes expression in *A. caviae* was performed using western blot technique.

5.2. Bioinformatic analysis of *A. caviae* *lafK* gene

5.2.1. *A. caviae* *lafK* gene promoter location prediction using computational analysis

We have used an online software provided by the Berkeley Drosophila Genome Project to analyse the 418bp DNA sequence upstream of *A. caviae* *lafK* gene to predict the *lafK* promoter location. This was able to predict the location of the promoter as shown in figure 5.1. The predicted promoter gave a score of 0.97 and was found to start at position 48 and to end at position 93 of the analysed 418 nucleotides. The *lafK* promoter prediction position for *A. caviae* Sch3N exactly matched the experimentally derived promoter for *A. hydrophila* AH-3 (Wilhelms *et al.*, 2013).

5.2.2. Prediction of *lafK* GEMM riboswitch location and architecture

The Rfam online software was used to analyse the 418 nucleotides region upstream of *A. caviae* *lafK* gene for the existence of c-di-GMP riboswitches. The 418bp

DNA sequence upstream of *A. caviae* *lafK* gene was found to contain a single c-di-GMP type-I riboswitch which starts at position 194 and ends at position 281 (figure 5.2).

The architecture of the predicted *A. caviae* *lafK* GEMM riboswitch was modelled based on several published studies which have mainly focused on studying and predicting the architecture of the Vc2 GEMM riboswitch in *V. cholerae* (Weinberg *et al.*, 2007, Sudarsan *et al.*, 2008, Smith *et al.*, 2011b). Vc2 is one of the two *V. cholerae* GEMM RNA type I riboswitches which is composed of 110 nucleotides and is located upstream of a gene named *VC1722* which is homologous to *tfoX*, a gene encoding a regulatory protein involved in DNA uptake and competence of *V. cholerae* (Sudarsan *et al.*, 2008). A multiple sequence alignment between the DNA sequence of *A. caviae* *lafK* GEMM type I riboswitch and Vc2 has given a score of 54.92 and is shown in figure 5.3. The predicted architecture of *A. caviae* *lafK* GEMM type I riboswitch is shown in figures 5.4 and 5.5.

Our GEMM riboswitch is predicted to be composed of 71 nucleotides and its architecture is suggested to be composed of two domains or hairpins called P1 and P2. The first hairpin (P1) is believed to be the aptamer to which c-di-GMP binds and it is composed of two stems (paired bases). The first stem is composed of two base pairs and the other stem is composed of six base pairs and both stems are separated by an internal loop. The P1 hairpin is capped with a terminal loop which contains the common 5'-GAAA-3' tetraloop sequence. The P2 hairpin is proposed to be the expression platform of the *lafK* riboswitch. Like the P1 hairpin, the P2 hairpin is also composed of two stems, the first stem consists of 10 base pairs and the second one is composed of 5 base pairs. The two stems are separated by an internal loop which contains the 11-nucleotides tetraloop receptor sequence 5'-UCUAACAAUGA-3' (which is expected to interact with the 5'-GAAA-3' tetraloop sequence). The P2 hairpin is also capped with a terminal loop. Downstream of the P2 domain exists a Rho-independent transcription termination sequence which is expected to base-pair with itself and form another hairpin loop which interferes with the RNA polymerase resulting in transcription termination. Based on this suggested architecture of the *lafK* GEMM riboswitch, we have designed several transcriptional fusion experiments to study the potential role played by the riboswitch and by each of its two domains P1 and P2.

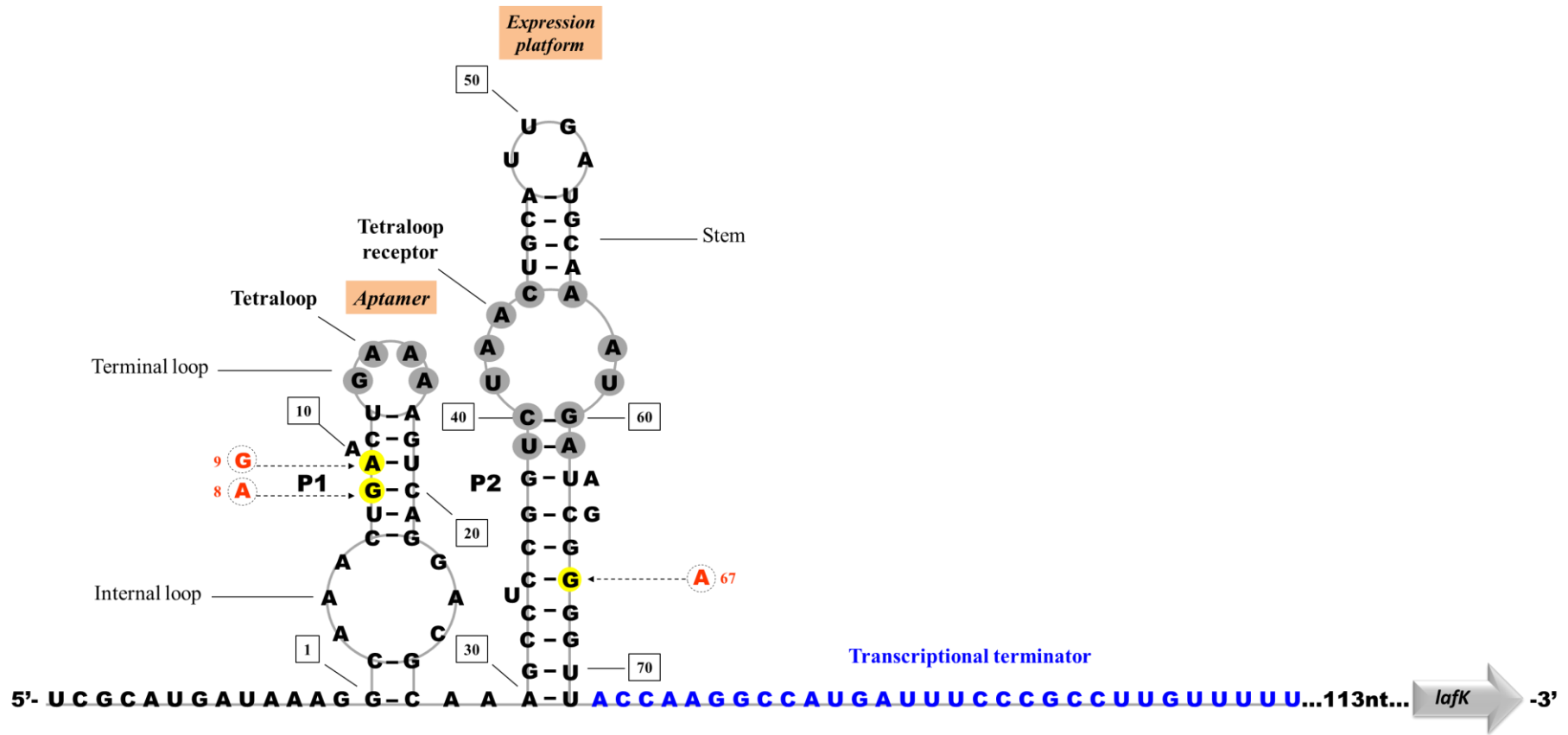


Figure 5.4 (previous page). RNA sequence and suggested architecture of the *A. caviae* *lafK* GEMM c-di-GMP type I riboswitch based on the published architecture of *V. cholerae* GEMM type I riboswitch Vc2 (Weinberg *et al.*, 2007, Sudarsan *et al.*, 2008). The riboswitch is composed of 71 nucleotides as numbered in the figure. The figure shows the sequence of P1 and P2 hairpins with their stems and both internal and terminal loops. A Rho-independent transcriptional terminator sequence is shown in blue colour. The tetraloop sequence (5'-GAAA-3') and the suggested 11-nucleotides tetraloop receptor sequence (5'-UCUAACAAUGA-3') are shown in grey dots. Mutations were introduced into the stems of P1 and P2 domains. Original nucleotides are shown in yellow dots while newly introduced nucleotides (mutations) are shown in red.

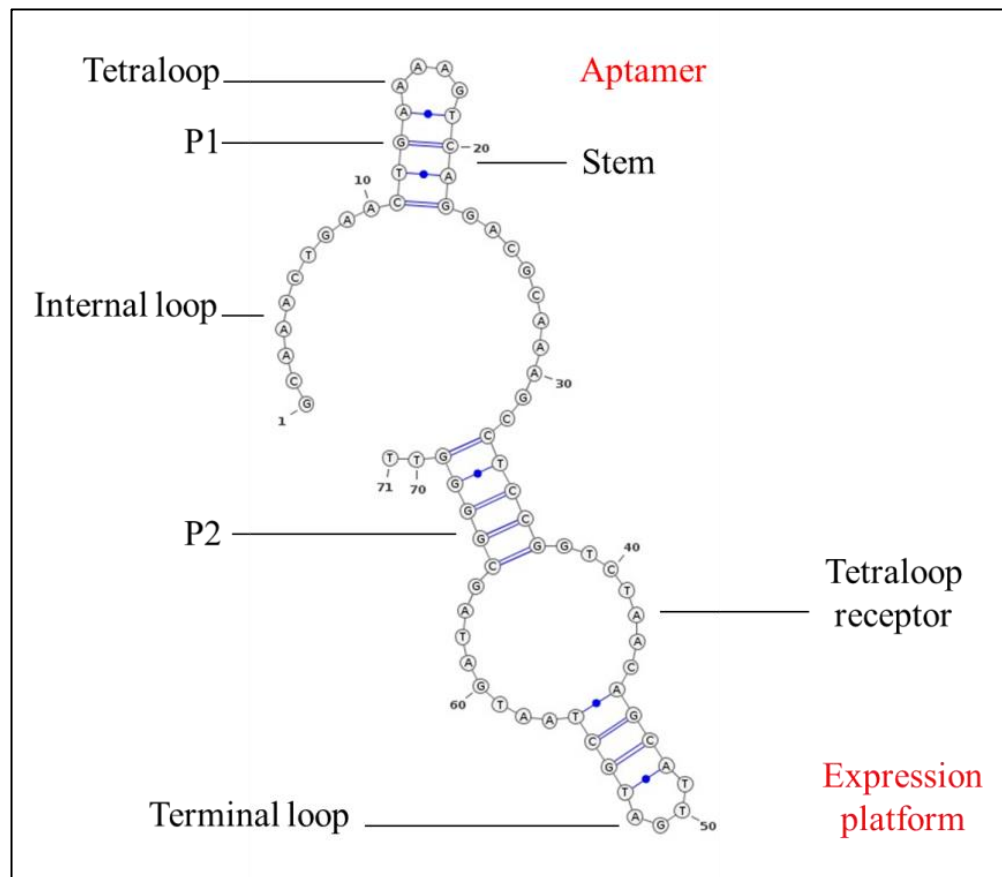


Figure 5.5. The secondary structure of the *A. caviae* *lafK* GEMM c-di-GMP type I riboswitch in dot-bracket notation. The numbers indicate the start and the end of the 71 nucleotides long riboswitch. The image was generated using CYLOFOLD online RNA secondary structure prediction software (<http://cylofold.abcc.ncifcrf.gov/>).

5.2.3. Computational analysis of *lafK* open reading frames and conserved domains

The *lafK* gene was analyzed for the existence of open reading frames (ORF). The analysis revealed the existence of a long open reading frame which starts at position 1 with the start codon ATG (Methionine) to position 1376 with stop codon TAA. Subjecting the amino acids sequence of the LafK protein to the blastp online tool (NCBI) showed that the 458aa composing the LafK protein include a REC domain, a CheY-like receiver domain, and a sigma-54 interaction domain (figure 5.6). Also, the bioinformatics analysis places the LafK protein in the AAA superfamily of proteins (for the ATPases Associated with a wide variety of cellular Activities). Altogether, and comparing our results to the literature we have designed the genetic structure shown in figure 5.7 and we have decided to proceed with our plans to study the *lafK* riboswitch using our bioinformatics data.

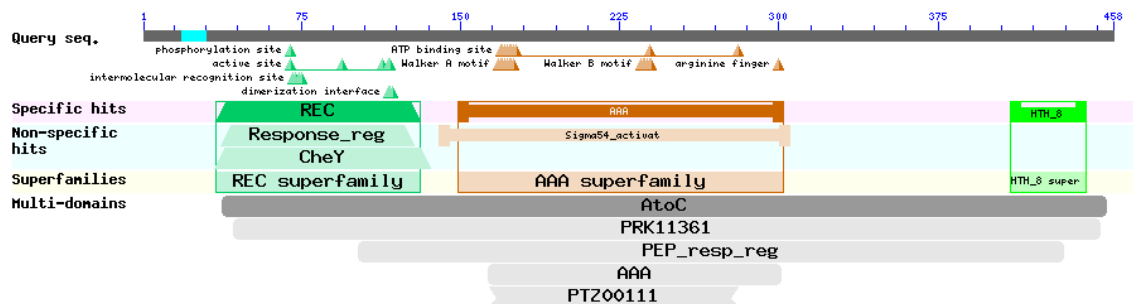


Figure 5.6. Putative conserved domains detected within *A. caviae* LafK protein using the NCBI blastp tool (<http://blast.ncbi.nlm.nih.gov/Blast.cgi>). The figure shows the detection of a REC domain, a CheY-like receiver domain, and a sigma-54 interaction domain. The analysis result places the LafK protein in the AAA superfamily of proteins (for the ATPases Associated with a wide variety of cellular Activities). The scale represents the number of amino acids.

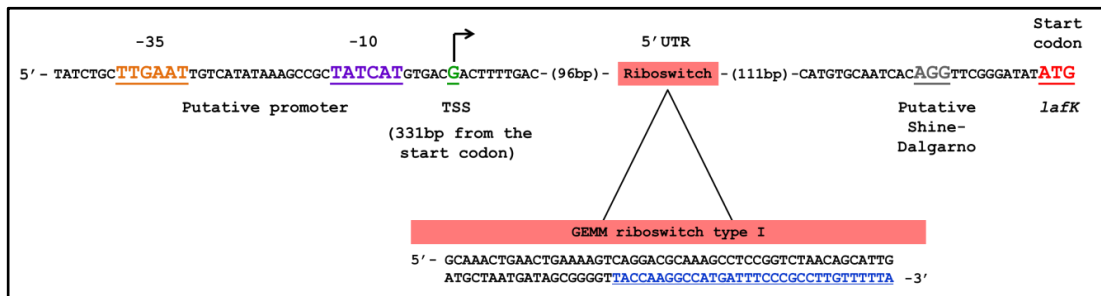


Figure 5.7. The predicted genetic structure of the region upstream of *A. caviae* *lafK* gene. The figure shows the -35 and -10 regions, the transcription start site (TSS), the GEMM c-di-GMP riboswitch type I located in the 5'UTR, a putative Shine-Dalgarno sequence, and the *lafK* start codon ATG. Analysis of the GEMM riboswitch type I indicates the presence of a Rho-independent transcription terminator sequence (underlined blue colour).

5.3. Effect of *A. caviae* *lafK* riboswitch deletion on lateral flagellar genes expression

5.3.1. *lafK* riboswitch deletion using the Spliced Overlap Extension (SOE) PCR technique

In order to evaluate the role of the riboswitch on *lafK* expression it was deleted. The riboswitch deletion was performed using the Spliced Overlap Extension (SOE) PCR technique and the level of the lateral flagellar gene expression was determined using the β -galactosidase assay as a measure of promoter activity. The SOE technique is a three-step PCR experiment. Four oligonucleotide primers were designed and were numbered 1 to 4. Principally, two of these primers (no.1 and 3) are considered external primers which should contain restriction digestion linkers for later cloning into the promoter probe vector pKAGb2(-), and two of them (no.2 and 4) are internal primers which do not have to contain any restriction digestion linkers but their 3' ends must overlap with each other so that any region between the overlapping ends will be deleted at the end of the SOE PCR experiment. Figure 5.8 contains a schematic presentation of the steps of SOE PCR used to delete *lafK* riboswitch.

The genomic DNA of *A. caviae* Sch3N was extracted as previously described, and the first PCR was performed using primers Ribodel1-F and Ribodel2-R plus the enzyme platinum *Pfx* DNA polymerase. The first PCR step was successful as the expected band size of 327bp was obtained (figure 5.9). The second PCR step was then performed using the same PCR reaction parameters but with the primers Ribodel4-F and Ribodel3-R. The second PCR step gave bands with a size of 179bp (figure 5.9). Finally, the third PCR reaction was performed using the amplification products of both the first and the second PCR reactions (mixed together) as a template to be amplified using the external primers Ribodel1-F and Ribodel3-R and the enzyme platinum *Pfx* DNA polymerase. The third step of the SOE PCR gave a single PCR product with the expected size of 506bp on agarose gel (figure 5.10). Successful deletion of the *lafK* c-di-GMP-I riboswitch was confirmed by DNA sequencing. The PCR amplicons were then ready to be cloned in the promoter-less *lacZ* vector pKAGb2(-) followed by performing a β -galactosidase assay to measure the expression of the *A. caviae* *lafK* gene in the absence of the riboswitch.

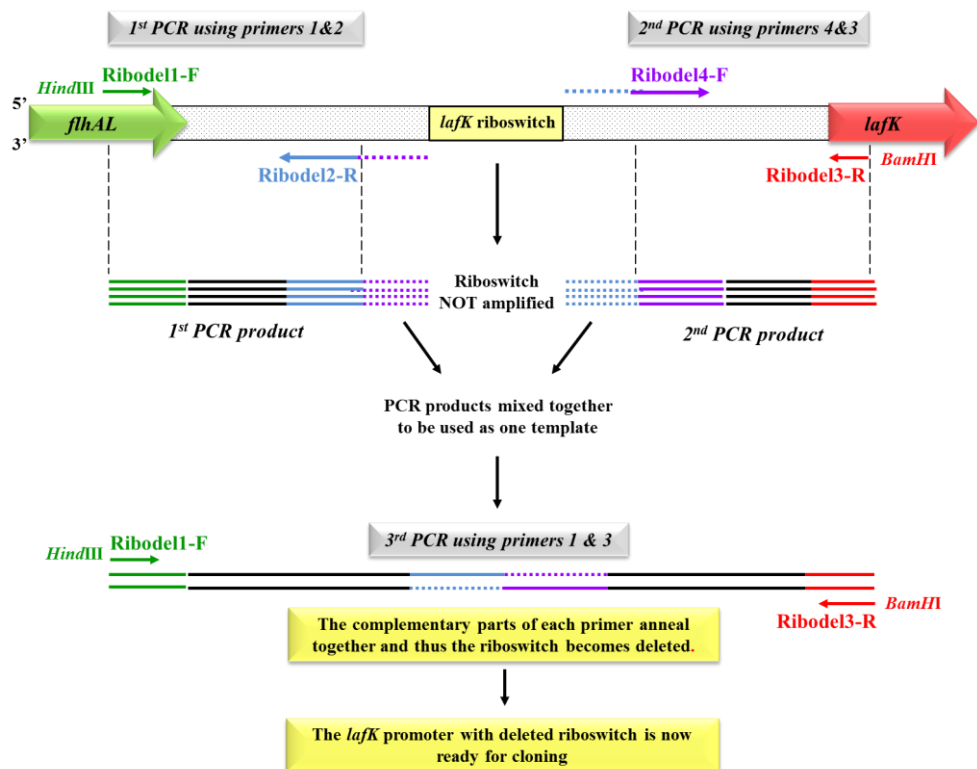


Figure 5.8. A schematic presentation of the Spliced Overlap Extension (SOE) PCR technique used in this study to delete the *lafK* riboswitch in *A. caviae* Sch3N.

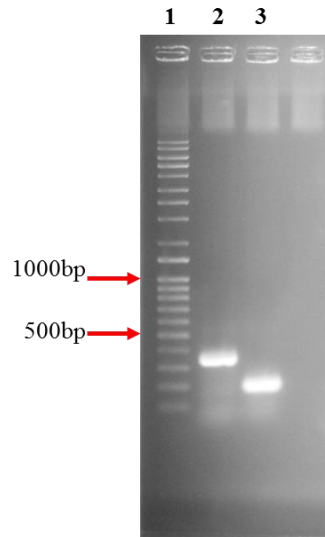


Figure 5.9. A 1% agarose gel showing the products of the first and the second PCR steps of the spliced overlap extension (SOE) PCR technique used to delete the *lafK* ribswitch of *A. caviae* Sch3N. **Lane 1:** Q-Step 4 DNA ladder. **Lane 2:** PCR product of the first PCR reaction (327bp) using primers Ribodel1-F and Ribodel2-R. **Lane 3:** PCR product of the second PCR reaction (179bp) using primers Ribodel4-F and Ribodel3-R. These products were then used as one template (mixed together) in the third PCR step during which they will overlap resulting in deletion of the DNA sequence between them and production of a single band.

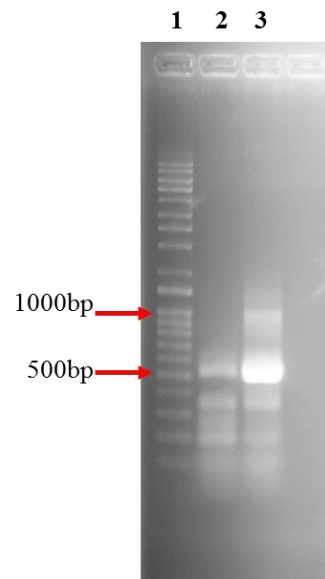


Figure 5.10. A 1% agarose gel showing the single PCR product of the third step of the Spliced Overlap Extension (SOE) PCR technique used to delete the *A. caviae* Sch3N *lafK* ribswitch. **Lane 1:** Q-Step 4 DNA ladder. **Lane 2 and 3:** Product of the third PCR reaction (done twice) using primers Ribodel1-F and Ribodel3-R. The amplicon size (506bp) was correct in both lanes. DNA sequencing of amplicons in lane 3 (showing the stronger signal) confirmed the successful deletion of the *lafK* ribswitch. The PCR products were then cloned in the promoter-less vector pKAGb2(-) and the effect of the ribswitch deletion on lateral flagellar genes expression was quantitatively determined by β -galactosidase assay.

5.3.2. Quantitative determination of the effect of *A. caviae* *lafK* riboswitch deletion on the lateral flagellar genes expression using β -galactosidase assay

5.3.2.1. Fusion of *lafKp* and *lafKp* Δ riboswitch to the promoter-less plasmid vector pKAGb2(-)

In order to study the effect of the *lafK* riboswitch deletion on the *A. caviae* lateral flagellar gene expression, a DNA region containing the wild type *lafK* promoter and the *lafKp* Δ riboswitch each were cloned separately into the promoter-less plasmid vector pKAGb2(-). This vector contains the reporter gene *lacZ* in order to perform the β -galactosidase assay to quantitatively determine the effect of riboswitch deletion on the expression of the *lacZ* gene and subsequently on the *laf* operon. The effect of riboswitch deletion on *lacZ* expression was studied in two backgrounds namely, *A. caviae* Sch3N and *E. coli* DH5 α .

The first step was to clone the *lafK* promoter (containing the riboswitch) in pKAGb2(-). Oligonucleotide primers LafKp-F and LafKp-R containing *Bam*HI and *Hind*III restriction digestion linkers were designed to amplify a 577bp DNA region upstream of *lafK* by PCR (figure 5.11). PCR amplification was performed and the sequence of the amplicons was confirmed by DNA sequencing. The obtained PCR products were then purified and digested with *Bam*HI and *Hind*III as previously described. This was followed by ligation to the promoter-less plasmid vector pKAGb2(-) which was previously digested with the same two restriction enzymes. The ligation mixture was then transferred by heat shock to *E. coli* DH5 α . The transformed *E. coli* DH5 α were then plated on LB plates containing chloramphenicol. *E. coli* DH5 α colonies resistant to chloramphenicol were successfully isolated. The chloramphenicol-resistant colonies were then screened by PCR for the presence of the recombinant plasmid using primers LafKp-F and LafKp-R. The colony PCR screening results indicated a successful cloning of the wildtype *lafK* promoter region containing the *lafK* riboswitch in *E. coli* DH5 α (figure 5.12).

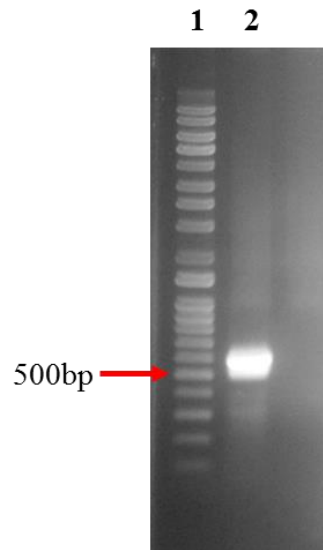


Figure 5.11. A 1% agarose gel showing PCR amplification of a 577bp DNA region upstream of *lafK* which contains a riboswitch. **Lane 1:** Q-Step 4 DNA ladder. **Lane 2:** PCR amplicons of *lafK* promoter region with *lafK* riboswitch (577bp) amplified using primers LafKp-F and LafKp-R.

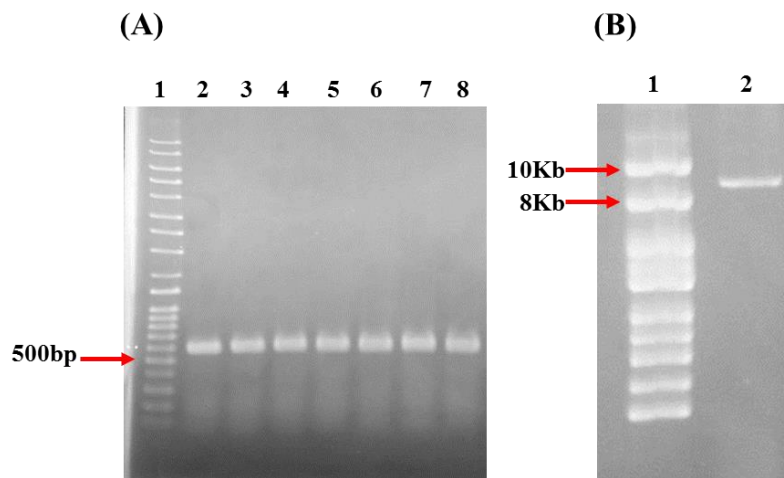


Figure 5.12. 1% agarose gels showing successful cloning of *lafK* promoter in *E. coli* DH5 α (A) PCR screening of seven chloramphenicol-resistant *E. coli* DH5 α colonies transformed with the recombinant plasmid pKAG-*lafKp*. (A-1): Q-Step 4 DNA ladder. (A2-8): PCR amplicons of the cloned 577bp DNA region amplified using the primers LafKp-F and LafKp-R. (B) Miniprep extraction of the recombinant plasmid pKAG-*lafKp* (B-1): Supercoiled DNA ladder (NEB). (B- 2): Recombinant pKAG-*lafKp* containing c-di-GMP-I riboswitch (9347 bp) extracted from a chloramphenicol-resistant *E. coli* DH5 α colony.

The recombinant plasmid containing the wild type *lafK* riboswitch was extracted from a chloramphenicol-resistant *E. coli* DH5 α colony and was then transformed by heat shock to *E. coli* S17-1 in order to transfer it by bacterial conjugation to *A. caviae* Sch3N. Bacterial conjugation was performed as previously described and oxidase-positive colonies which were resistant to both nalidixic acid and chloramphenicol were successfully isolated on LB agar. *E. coli* DH5 α and *A. caviae* Sch3N containing the recombinant plasmid which includes the wildtype riboswitch were then ready to be included as positive controls in the β -galactosidase assay to study the effect of riboswitch deletion on the expression of *A. caviae* *laf* operon. The next step was to ligate the *lafKp* Δ riboswitch to pKAGb2(-) followed by transferring the recombinant plasmid to *E. coli* DH5 α by heat shock and to *A. caviae* Sch3N by conjugation, exactly as done above with the wild type riboswitch.

The PCR products of the third PCR step of the (SOE) PCR *lafKp* Δ riboswitch were purified and then digested using *Bam*HI and *Hind*III restriction enzymes. This step was followed by their ligation to the promoter-less plasmid vector pKAGb2(-) previously cut with the same two restriction enzymes. The ligation mixture was then transferred by heat shock to *E. coli* DH5 α competent cells. Transformation was followed by plating of the cells on LB agar containing chloramphenicol. Several chloramphenicol-resistant *E. coli* DH5 α colonies were isolated on chloramphenicol-containing LB agar, and screened by PCR using the primers Ribodel1-F and Ribodel3-R. Colony PCR screening showed amplicons with the expected size of 506bp on an agarose gel which indicated a successful cloning of *lafKp* Δ riboswitch in *E. coli* DH5 α (figure 5.13). Cloning of *lafKp* Δ riboswitch was further confirmed by DNA sequencing which clearly showed the deletion of the 71bp region containing the riboswitch.

The recombinant plasmid was then extracted from one chloramphenicol-resistant *E. coli* DH5 α colony and was then transferred by heat shock to *E. coli* S17-1. The transformation was successful and one of the *E. coli* S17-1 colonies was then used to transfer the recombinant plasmid to *A. caviae* Sch3N by bacterial conjugation, as previously described. Conjugal transfer of pKAG-*lafKp* Δ riboswitch to *A. caviae* resulted in isolation of oxidase-positive colonies on LB agar containing both nalidixic acid and chloramphenicol.

The two bacterial species, namely, *E. coli* DH5 α and *A. caviae* Sch3N containing the recombinant plasmid pKAG-*lafKp* Δ riboswitch were then ready to carry out a β -galactosidase assay to quantitatively determine the effect of *lafK* riboswitch deletion on the expression of the *A. caviae* lateral flagellar genes. Figure 5.14 provides a schematic presentation of all steps of the promoter fusion experiment.

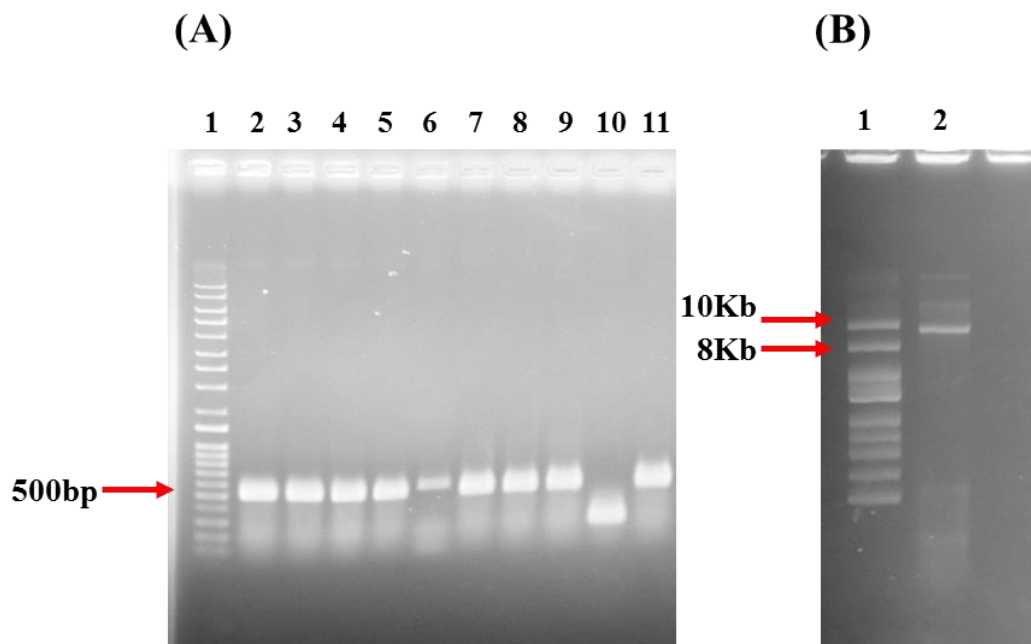


Figure 5.13. 1% agarose gels showing successful cloning of *lafKp* Δ riboswitch in *E. coli* DH5 α (A) PCR screening of ten chloramphenicol-resistant colonies of *E. coli* DH5 α cells transformed with pKAG-*lafKp* Δ riboswitch. (A, Lane 1): Q-Step 4 DNA ladder. (A, Lane 2-11): PCR amplicons obtained using primers Ribodel1-F and Ribodel3-R, correct band size is 506bp which was obtained in all colonies except number 10. (B) Miniprep extraction of pKAG-*lafKp* Δ riboswitch. (B, Lane 1): Supercoiled DNA ladder (NEB). (B, Lane 2): Recombinant plasmid pKAG-*lafKp* Δ riboswitch (9276bp) extracted from one chloramphenicol-resistant *E. coli* DH5 α colony.

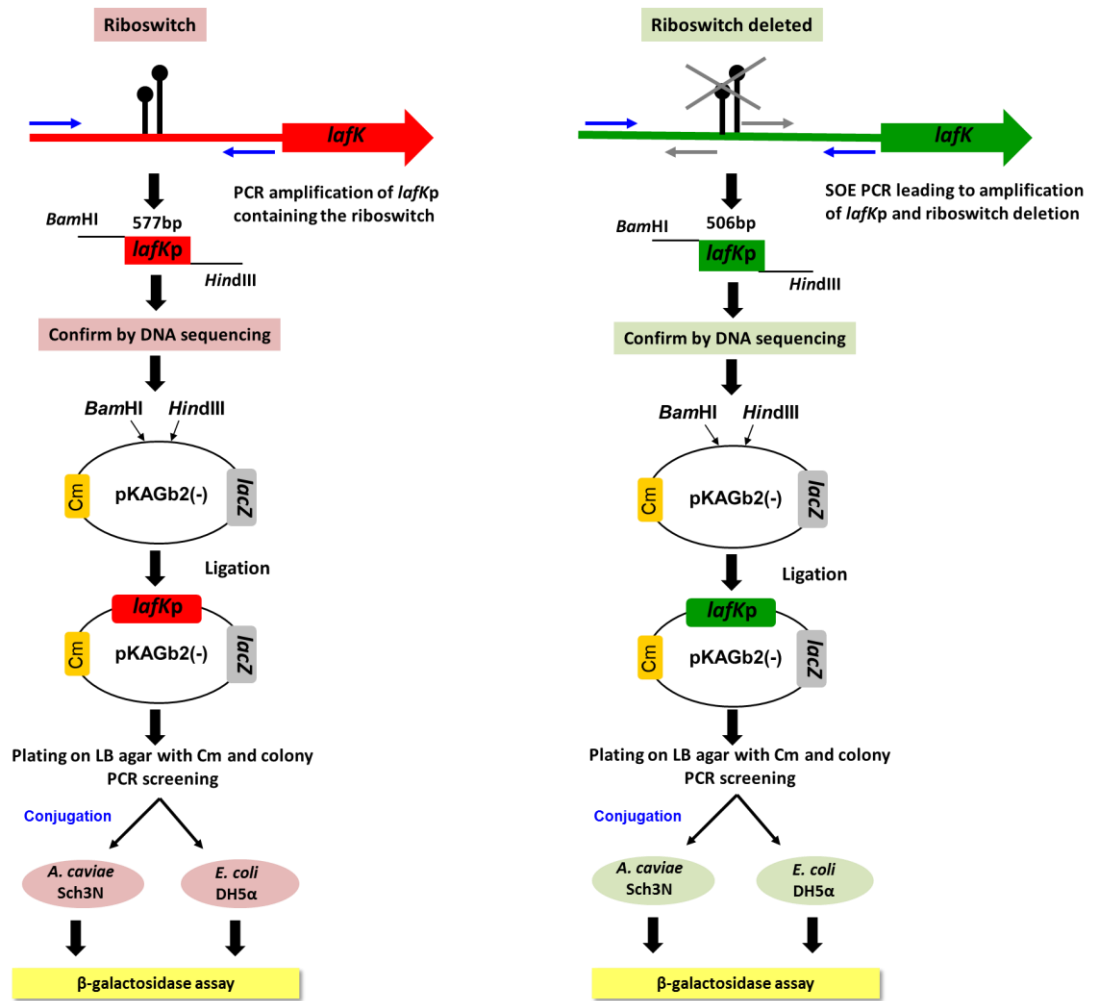


Figure 5.14. A schematic presentation of the procedure used to fuse the *lafK* promoter and the *lafKp*Δriboswitch to the promoterless vector pKAGb2(-) preceding the β-galactosidase assay which was used to investigate the effect of riboswitch deletion on the *lafK* gene expression.

5.3.2.2. β -Galactosidase assay results

β -Galactosidase assays were performed as previously described, and the effect of riboswitch deletion on *A. caviae* *lafK* gene expression in the two backgrounds *E. coli* DH5 α and *A. caviae* Sch3N was quantitatively determined as shown in figure 5.15. A dramatic increase in *lacZ* gene expression was observed in the absence of the *lafK* c-di-GMP type I riboswitch in both bacterial backgrounds. When the *lafK* promoter activity was tested in *A. caviae* background, the average number of Miller units for the wild type *lafK* promoter was determined to be 87.78 in comparison to 7410.13 Miller units measured for the *lafKp* Δ riboswitch (84-fold increase, $p=0.00002$). Also, the *lacZ* reporter gene expression in *E. coli* DH5 α background increased from an average value of 64.89 Miller units in the presence of the wild type *lafK* promoter (containing the riboswitch) to an average value of 16852.13 Miller units upon fusion of the *lafKp* Δ riboswitch (259-fold increase, $p=0.0000003$).

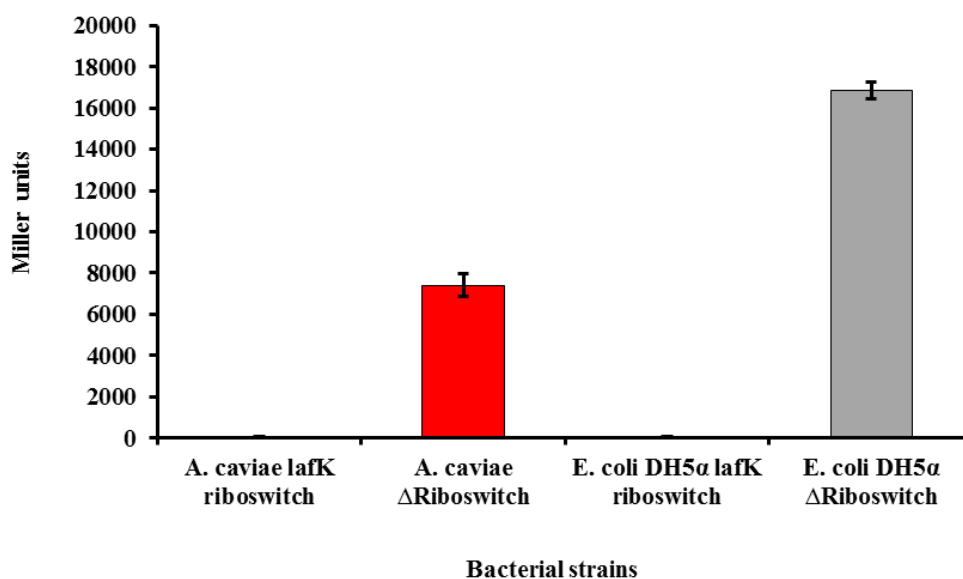


Figure 5.15. Analysis of *lafK* promoter activity in the presence and absence of the *lafK* c-di-GMP type I riboswitch in *A. caviae* (red colour) and *E. coli* DH5 α (grey colour) using β -galactosidase assay, results expressed in Miller units. The test was done in triplicate. Bars represent mean values of the three readings. Error bars represent the standard deviation around the mean. Results showed a significant variation ($p<0.05$) using single factor ANOVA test.

5.4. Effect of deleting the P1 and P2 hairpins of the *lafK* riboswitch on *A. caviae* lateral flagellar genes expression

5.4.1. P1 and P2 hairpins deletion using the Spliced Overlap Extension (SOE) PCR technique

The *lafK* c-di-GMP type I riboswitch in *A. caviae* Sch3N is composed for two loops, the P1 loop and the P2 loop. In order to find out which of these two loops is actually essential for the activity of the riboswitch, they were separately deleted from the *lafK* promoter followed by fusing the mutated promoter to the promoter-less vector pKAGb2(-). Deletion of the P1 and P2 loops was done using the Spliced Overlap Extension (SOE) PCR technique used previously to delete the *lafK* riboswitch. As described previously, oligonucleotide primers were designed to overlap in certain DNA regions resulting eventually in P1 and P2 deletions.

To delete the P1 region the primers Ribodel1-F and Ribodel5-P1-R were used for the first PCR step, and Ribodel3-R with Ribodel6-P1-F for the second PCR step (figure 5.16). The first PCR reaction yielded a product with a size of 327bp and the second PCR step yielded a product with 223bp (figure 5.17). The amplicons sizes obtained were as expected. The products from first and second PCR were then used as a template in the third step of the SOE-PCR which will result in the overlap of the two products and consequently the deletion of the P1 region. The primers used in the third PCR reaction were Ribodel1-F (containing a *Hind*III linker) and Ribodel3-R (containing a *Bam*HI linker). The third PCR step resulted in the expected product size (550bp) on an agarose gel (figure 5.18). The restriction digestion linkers were added to the primers for later cloning of the 550bp region in pKAGb2(-). To confirm the deletion of the 27 nucleotides corresponding to the P1 region, the amplicons of the third PCR step were subjected to DNA sequencing which confirmed the deletion of the P1 region of the *lafK* riboswitch. The mutated *lafK* promoter was then ready to be fused to the promoter less vector pKAGb2(-).

To delete the P2 region the primers Ribodel1-F and Ribodel7-P2-R were used for the first PCR step, and Ribodel3-R with Ribodel8-P2-F for the second PCR step (figure 5.19). The first PCR yielded products with a size of 356bp and the second PCR yielded products with a size of 179bp (figure 5.17). The sizes of the PCR amplicons were as expected.

As in the case with P1 deletion, the first and the second PCR products were used as a template for the third PCR reaction of the SOE-PCR technique. Amplification was performed using the primers Ribodel1-F (containing a *Hind*III linker) and Ribodel3-R(containing a *Bam*HI linker). The third PCR step was successful and the expected 535bp PCR products were obtained on an agarose gel (figure 5.18). The restriction digestion linkers were added to the primers for later ligation of the 535bp region to pKAGb2(-). To confirm the deletion of the 42 nucleotides corresponding to the P2 region, the amplicons of the third PCR step were subjected to DNA sequencing which confirmed the deletion of the 42 nucleotides corresponding to the P2 loop. The mutated *lafK* promoter region was then ready to be fused to the promoter less vector pKAGb2(-).

5.4.2. Quantitative determination of the effect of P1 and P2 hairpins deletion on the lateral flagellar genes expression using β -galactosidase assay

5.4.2.1. Fusion of *lafKp* Δ P1 and *lafKp* Δ P2 to the promoter-less plasmid vector pKAGb2(-)

PCR amplicons lacking the P1 and P2 regions were then separately purified and digested by the restriction enzymes *Hind*III and *Bam*HI. This was followed by separately ligating them to the promoter-less vector pKAGb2(-) previously cut with the same restriction enzymes. The ligation mixture containing pKAG-*lafKp* Δ P1 and the one containing the pKAG-*lafKp* Δ P2 were separately transformed to *E. coli* DH5 α by heat shock, after which *E. coli* cells were plated on LB agar containing chloramphenicol. Chloramphenicol-resistant *E. coli* colonies were isolated and were subjected to colony PCR screening to confirm cloning of *lafKp* Δ P1 and *lafKp* Δ P2. The colony PCR screening was carried out using the custom designed primers pKAG-F and pKAG-R which flank the polylinker region in pKAGb2(-). PCR screening of *E. coli* colonies indicated successful fusion of *lafKp* Δ P1 (figure 5.20) and *lafKp* Δ P2 (figure 5.21) to pKAGb2(-).

The recombinant plasmids were then extracted from *E. coli* DH5 α and were separately introduced by heat-shock to *E. coli* S17-1 which was then used to transfer the plasmids to *A. caviae* Sch3N by conjugation. Conjugal transfer of the recombinant plasmids to *A. caviae* Sch3N resulted in isolation of oxidase-positive colonies which were both nalidixic acid- and chloramphenicol- resistant on LB agar.

The resulting *A. caviae* strains were then used in a β -galactosidase assay to investigate the effects of P1 and P2 loops deletions on *lafK* promoter activity. Testing the *lafK* promoter activity following the deletion of P1 and P2 by β -galactosidase assay in *E. coli* DH5 α background was also done for comparison. An overview of the procedure used to delete the two loops and to clone the mutated riboswitch is shown in figure 5.22.

5.4.2.2. β -Galactosidase assay results

Quantitative analyses of the effects of P1 and P2 deletions on the activity of *lafK* promoter were determined using β -galactosidase assay. The activity of *lafK* promoter was measured in two backgrounds: *A. caviae* Sch3N and *E. coli* DH5 α , (figure 5.23).

Analysis of *lafK* promoter activity in the *A. caviae* background following deletion of P1 and P2 loops indicated that these deletions caused an alteration in *lafK* promoter activity. As mentioned earlier in this chapter, deletion of *lafK* riboswitch resulted in enhancement of *lafK* promoter activity in comparison to when it is present. This fact was again confirmed here, as shown in figure 5.23. The average value of Miller units was 4515.49 when *lafKp* Δ riboswitch was tested in comparison to an average value of 70.75 Miller units obtained when testing the activity of the wild type *lafK* promoter (containing the riboswitch). This result indicated a 63-fold increase in the activity of *lafK* promoter following riboswitch deletion. Deletion of P1 and P2 resulted in further enhancement of *lafK* promoter activity, as the activity obtained in these two settings exceeded the Miller units obtained with *lafKp* Δ riboswitch. In comparison to the activity of the wildtype promoter (average 70.75 Miller units), P1 deletion caused 155-fold increase in *lafK* promoter activity (average 11008.86 Miller units). This increase in activity was 2.4-fold (59% more than) the activity of *lafKp* Δ riboswitch (average 4515.49 Miller units) and was found to be statistically significant ($p < 0.05$). Deletion of P2 loop resulted in 112-fold increase in activity (average 7980.23 Miller units) compared to the wild type promoter (average 70.75 Miller units). This value of promoter activity was 1.7-fold (43.5% more than) the activity of *lafKp* Δ riboswitch (average 4515.49 Miller units) and it was found to be statistically significant ($p < 0.05$). The activity of *lafKp* Δ P2 was, however, 3028 Miller units less than the activity of *lafKp* Δ P1 ($p = 0.00002$).

Similar to when tested in the *A. caviae* background, testing *lafKp* Δ riboswitch activity in the *E. coli* DH5 α background showed a dramatic increase (231-fold) in activity (average 12413.64 Miller units) compared to the wildtype riboswitch (average 53.58 Miller units). However, testing the activity of *lafK* promoter in the *E. coli* DH5 α background following deletion of P1 and P2 domains gave different results than when tested in the *A. caviae* background. In comparison to the activity of the wild type *lafK* promoter (average 53.58 Miller units), deletion of P1 resulted in 181-fold increase in activity (average 9741.75 Miller units), which was 21.6% less than the activity of *lafKp* Δ riboswitch (average 12413.64 Miller units), $p=0.057$. Deletion of P2 domain resulted in 165-fold increase in *lafK* promoter activity (average 8885.92 Miller units) in comparison to its activity in the presence of the wildtype riboswitch (average 53.58 Miller units). The activity of *lafKp* Δ P2 was, however, 28.5% less than the activity of *lafKp* Δ riboswitch (average 12413.64 Miller units), with the reduction being statistically significant ($p=0.019$). Finally, when comparing the *lafK* promoter activity in the setting of P1 deletion (average 9741.75 Miller units) to its activity in the setting of P2 deletion (average 8885.92 Miller units) we did not find a statistically significant difference, $p=0.214$.

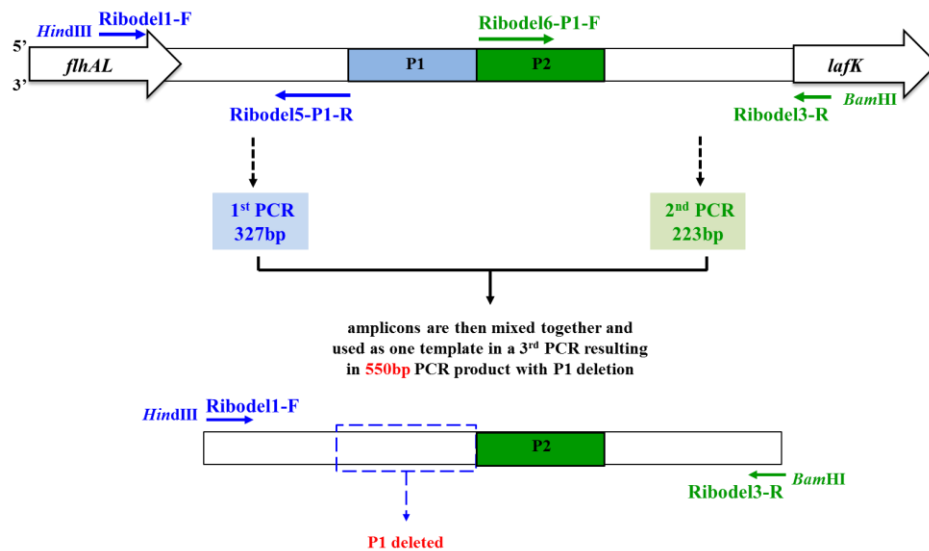


Figure 5.16. A schematic presentation showing the position of each of the four primers used in SOE-PCR to delete the P1 region of the *lafK* riboswitch.

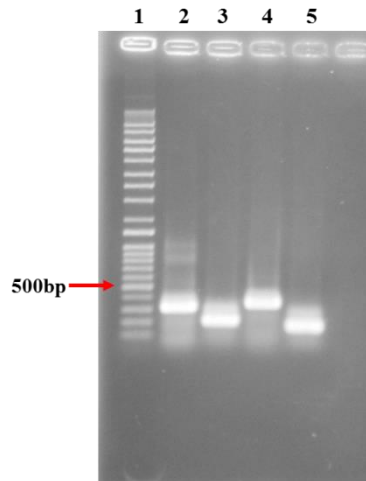


Figure 5.17. A 1% agarose gel showing amplicons of the first and second PCR steps of the three step SOE-PCR technique used to delete the P1 and P2 loops of the *A. caviae* *lafK* riboswitch. **Lane 1:** Q-Step 4 DNA ladder. **Lane 2:** amplicons of the first PCR step to delete P1 loop using primers Ribodel1-F and Ribodel5-P1-R, band size 327 bp. **Lane 3:** amplicons of the second PCR step to delete P1 loop using primers Ribodel3-R with Ribodel6-P1-F, band size 223 bp. **Lane 4:** amplicons of the first PCR step to delete P2 loop using primers Ribodel1-F and Ribodel7-P2-R, band size 356 bp. **Lane 5:** amplicons of the second PCR step to delete P2 loop using primers Ribodel3-R and Ribodel8-P2-F, band size 179 bp. These amplicons were used later as template in the third PCR reaction to obtain amplicons with deleted P1 and P2 loops.

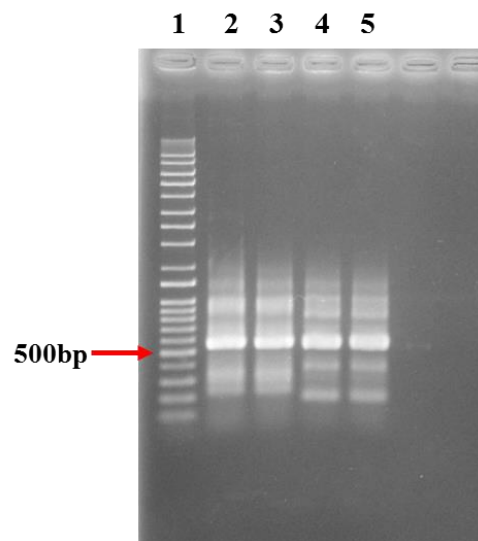


Figure 5.18. A 1% agarose showing amplicons of the third PCR step of the SOE-PCR technique used to delete P1 or P2 loops of the *A. caviae* *lafK* riboswitch. **Lane 1:** Q-Step 4 DNA ladder. **Lanes 2 and 3:** PCR amplicons (550 bp) generated using primers Ribodel1-F and Ribodel3-R and resulting in deletion of the P1 region (done twice). **Lanes 4 and 5:** PCR amplicons (535 bp) generated using primers Ribodel1-F and Ribodel3-R and resulting in deletion of the P2 region (done twice).

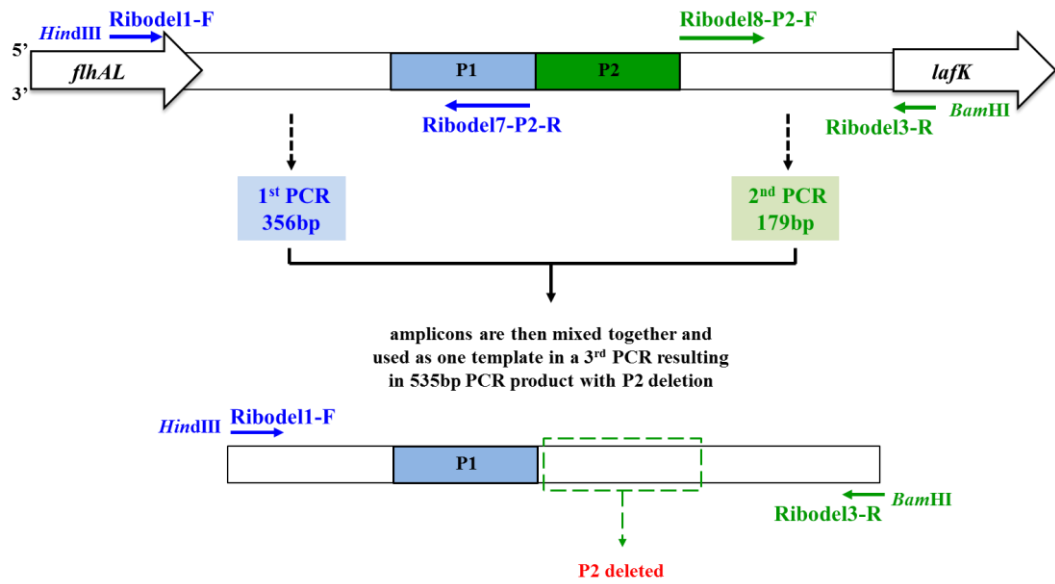


Figure 5.19. A schematic presentation showing the position of each of the four primers used in SOE-PCR to delete the P2 region of the *lafK* riboswitch.

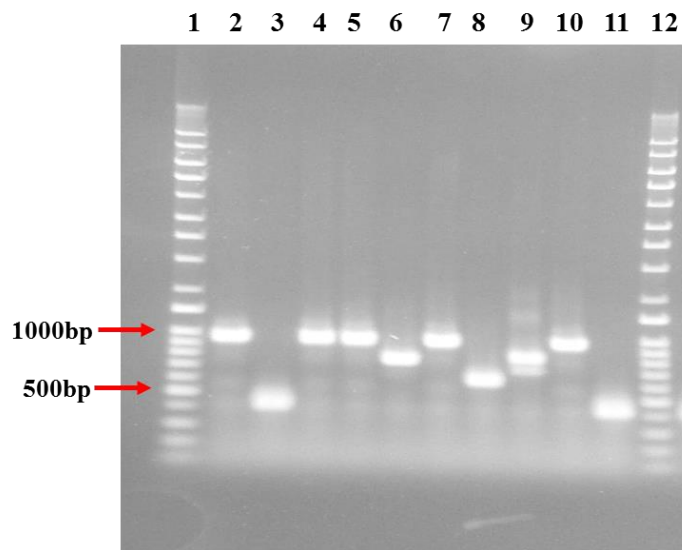


Figure 5.20. A 1% agarose gel showing colony PCR screening of *E. coli* DH5 α cells transformed with pKAG-*lafK* Δ P1 using primers pKAG-F and pKAG-R. **Lane 1 and 12:** Q-Step 4 DNA ladder. **Lane 2-11:** *E. coli* strains that were chloramphenicol resistant after transformation subjected to colony PCR. Expected band size (950 bp) was obtained from screening colonies in lanes 2, 4, 5, 7 and 10.

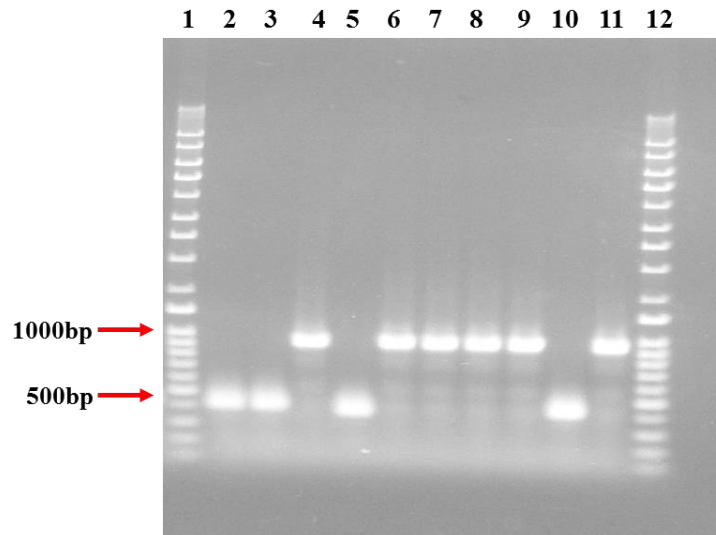


Figure 5.21. A 1% agarose gel showing colony PCR screening of *E. coli* DH5 α cells transformed with pKAG-*lafK* Δ P2 using primers pKAG-F and pKAG-R. **Lane 1 and 12:** Q-Step 4 DNA ladder. **Lane 2-11:** *E. coli* strains that were chloramphenicol resistant after transformation subjected to colony PCR. Expected band size (935 bp) was obtained from screening colonies in lanes 4, 6, 7, 8, 9 and 11.

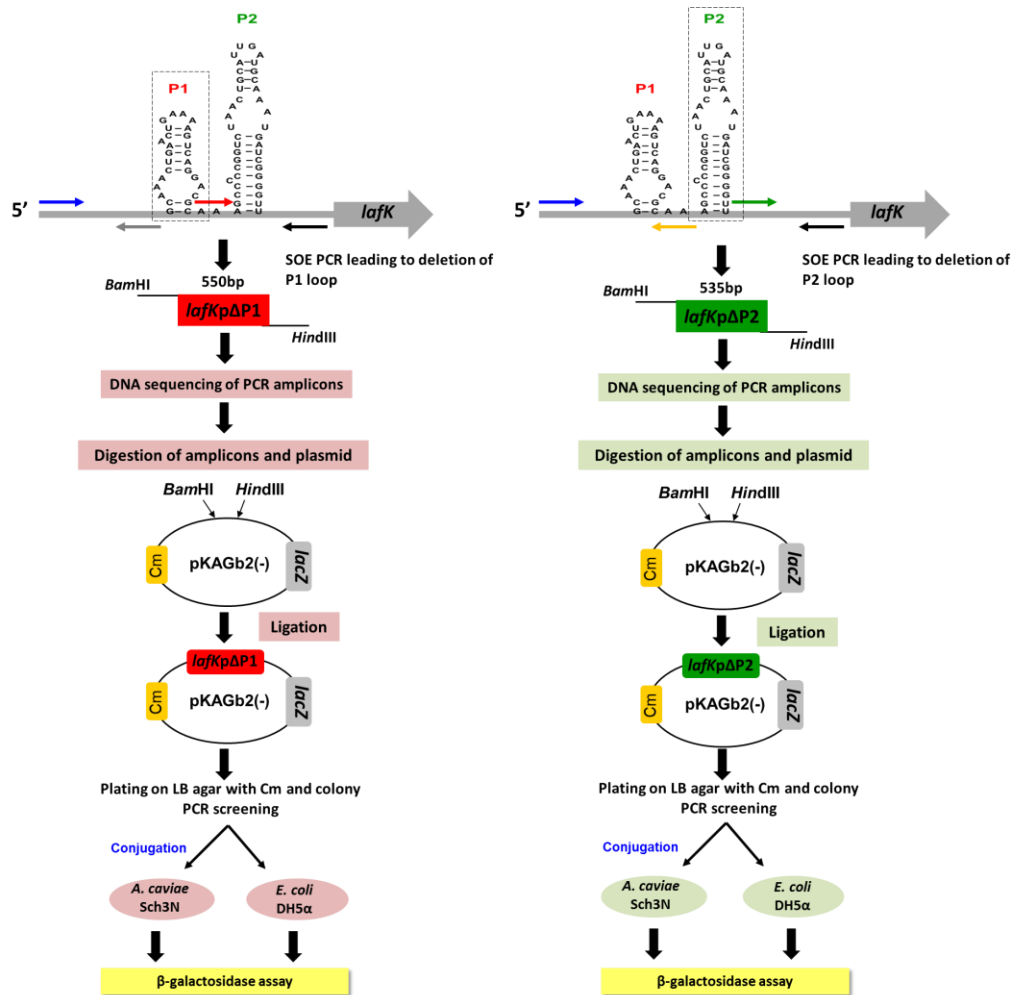


Figure 5.22. An overview of the procedure used to separately delete P1 and P2 loops of *lafK* riboswitch followed by cloning the mutated promoter region in the promoter-less vector pKAGb2(-). The recombinant plasmids were then introduced separately to *A. caviae* Sch3N and *E. coli* DH5 α which were then used to perform a β -galactosidase assay to investigate the effects of P1 and P2 deletions on the *lafK* promoter activity.

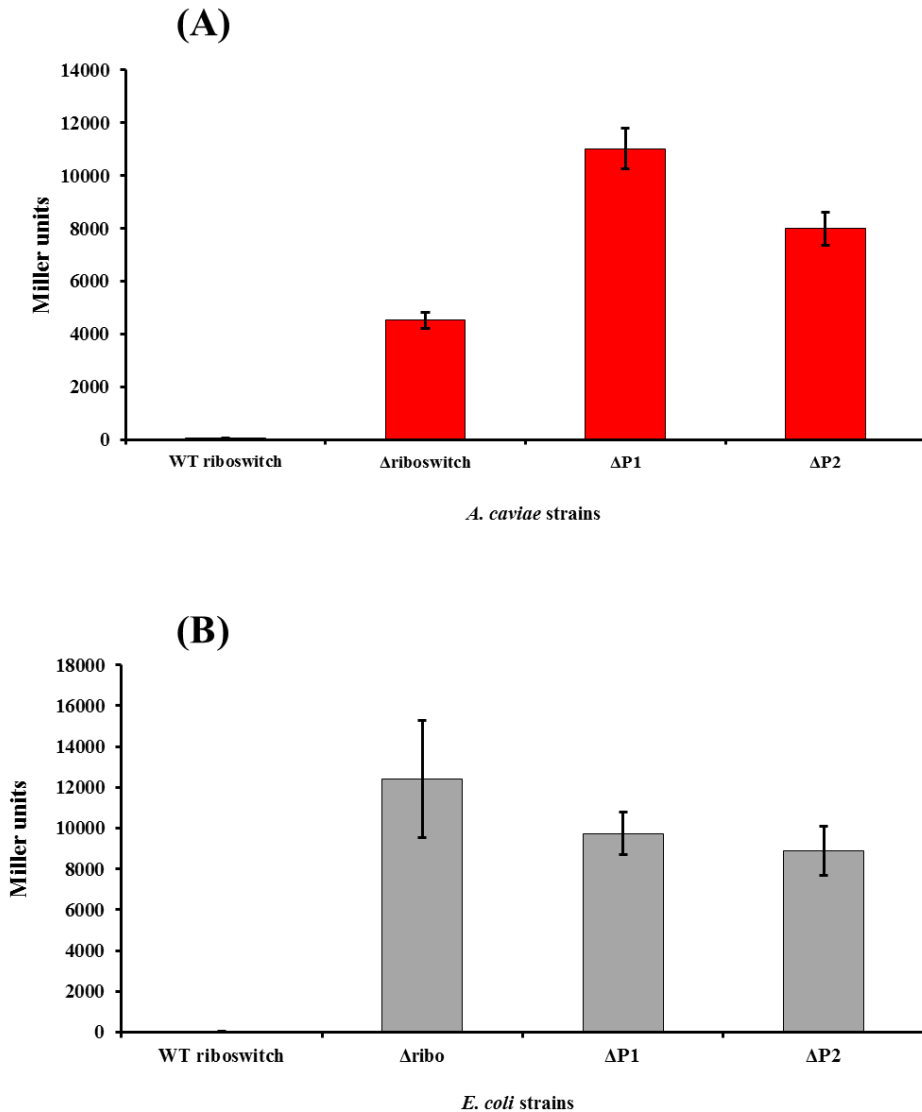


Figure 5.23. Analysis of *lafK* promoter activity in the presence and absence of the c-di-GMP type I riboswitch and following the deletion of P1 and P2 loops of the riboswitch in *A. caviae* Sch3N **(A)** and in *E. coli* DH5 α **(B)** using β -galactosidase assay, results expressed in Miller units. Test was done in triplicate. Bars represent mean values of the three readings. Error bars represent the standard deviation around the mean. Results showed a significant variation ($p < 0.05$) using single factor ANOVA test.

5.5. Effect of creating mutations within the stems of the P1 and P2 hairpins on the *A. caviae* lateral flagellar genes expression

5.5.1. Creating mutations within the stems of P1 and P2 loops using the Spliced Overlap Extension (SOE) PCR technique

We have attempted to create two mutations in the stem of each of the two loops of the *lafK* riboswitch which would lead to structural disturbance of the loops and consequently their function. This would help us to determine whether the two loops or any one of them is essential for the riboswitch function. Two nucleotides within the stem of P1 loop were attempted to be changed by Spliced Overlap Extension (SOE) PCR technique, namely the nucleotide number eight (guanine to adenine) and nucleotide number nine (adenine to guanine) as shown in figure 5.4. In addition, nucleotide number 35 in the stem of P2 loop was attempted to be changed from guanine to adenine by the same technique (figure 5.4). Figures 5.24 and 5.25 show the positions of the primers used in each of the two experiments and also the changed nucleotides.

To change the two nucleotides in P1 stem, the primers Ribodel1-F and Ribodel-P1AG-R were used for the first PCR and primers Ribodel-P1AG-F with Ribodel3-R for the second PCR. The first PCR step resulted in products with a size of 350bp and the second PCR step resulted amplicons with a size of 250bp (figure 5.26). The obtained sizes were as expected. The third PCR step was then carried out using the products of the first and the second PCRs as a single template with the primers Ribodel1-F (containing *Hind*III linker) and Ribodel3-R (containing *Bam*HI linker). The third PCR step was successful, as the expected amplicon size of 600bp was obtained (figure 5.27). The amplicons of the third PCR step were subjected to DNA sequencing to confirm that the nucleotide number eight was changed from guanine to adenine and that nucleotide number nine was changed from adenine to guanine. The DNA sequencing results confirmed the indicated nucleotide changes.

To change the nucleotide number 35 in the stem of P2 loop of *lafK* riboswitch from guanine to adenine by SOE-PCR technique, two new overlapping oligonucleotide primers, namely Ribodel-P2A-F and Ribodel-P2A-R were designed. The primer Ribodel-P2A-F was designed to contain a single base (adenine) that is different from its corresponding wild type base (guanine). The primer Ribodel-P2A-R was designed to contain a thymidine base that is different from its corresponding wild type base

(cytosine). The first PCR step using primers Ribodel1-F and Ribodel-P2A-R yielded amplicons with a size of 400bp, and amplification using primers Ribodel-P2A-F and Ribodel3-R in the second PCR step yielded products of 208bp, as shown in figure 5.28. The amplicons sizes yielded by the first and the second PCR steps of the SOE-PCR were as expected. A third PCR step was then performed using the amplicons of the first and the second PCR steps as a single template. The primers used in the third PCR step were Ribodel1-F (containing *Hind*III linker) and Ribodel3-R (containing *Bam*HI linker). The third PCR was successful as the reaction yielded amplicons of a size of 608bp on agarose gel (figure 5.27). The amplicons were subjected to DNA sequencing which has confirmed the nucleotide change. The 608bp amplification product was then ready to be fused into the promoterless vector pKAGb2(-).

5.5.2. Quantitative determination of the effect of creating a mutation within the stem of P1 domain on the *A. caviae* lateral flagellar genes expression using the β -galactosidase assay

5.5.2.1. Fusion of *lafKp* with a mutation in the stem of P1 domain to the promoterless plasmid vector pKAGb2(-)

The amplicons generated by SOE-PCR which contain the *lafK* riboswitch with its P1 stem been mutated (600bp) and those in which the P2 stem been mutated (608bp) were separately purified and digested with *Bam*HI and *Hind*III. They were then ligated to the previously cut pKAGb2(-). Each of the two ligation mixtures was then transformed by heat shock to *E. coli* DH5 α . The transformed *E. coli* cells were then plated on chloramphenicol-containing LB agar plates. Chloramphenicol-resistant *E. coli* cells transformed with pKAG-*lafKp*P1AG were isolated and colony PCR screening using primers pKAG-F and pKAG-R resulted in amplicons with a size of 1000bp which confirmed the cloning of *lafK* promoter containing the disturbed P1 loop in *E. coli* DH5 α (figure 5.29). Transformation of *E. coli* DH5 α competent cells with the ligation mixture of pKAG-*lafKp*P2A, however, failed after several attempts with no growth obtained on LB plates containing chloramphenicol inspite of the control plates giving good results. The fact that there was not even a single *E. coli* DH5 α colony growing on LB plates with chloramphenicol following transformation with pKAG-*lafKp*P2A seems to indicate an inhibitory effect of the introduced mutation which might have prevented the *E. coli* cells from growing. It was decided to limit our study to investigate the effect of the mutations introduced into the stem of P1 loop on the activity of *lafK* promoter.

The recombinant plasmid pKAG-*lafK*pP1AG was extracted from *E. coli* DH5 α and was transformed by heat shock to *E. coli* S-17-1 which was then used for the conjugal transfer of the recombinant plasmid to *A. caviae* Sch3N. The mating mixture was cultured on LB agar containing both chloramphenicol and nalidixic acid. Oxidase-positive colonies were isolated indicating successful transfer of pKAG-*lafK*pP1AG to *A. caviae* Sch3N. *A. caviae* pKAG-*lafK*pP1AG and *E. coli* pKAG-*lafK*pP1AG were then used to perform a β -galactosidase assay.

5.5.2.2. β -Galactosidase assay results

To investigate the effect of the nucleotide changes made in the stem of the P1 domain of the *lafK* riboswitch, the plasmid construct pKAG-*lafK*pP1AG was subjected to β -galactosidase assay in the two backgrounds *A. caviae* Sch3N and *E. coli* DH5 α . The results of the assay are shown in figure 5.30. Tested in *A. caviae*, the nucleotide changes in P1 resulted in an average value of 2559.1 Miller units in comparison to an average value of 70.75 Miller units obtained upon testing the wild type riboswitch, $p < 0.05$. This is a 36-fold increase in *lafK* promoter activity resulting from changing the two indicated nucleotides in P1 domain. Tested in *E. coli* DH5 α , pKAG-*lafK*pP1AG gave an average value of 5167.59 Miller units in comparison to an average value of 53.58 Miller units obtained when testing the activity of the wild type promoter (pKAG-*lafK*p), $p = 0.000003$. This is a 96-fold increase in *lafK* promoter activity resulting from changing two nucleotides in the stem of P1 hairpin. These results indicate that the nucleotides number 8 (guanosine) and number 9 (adenine) in the stem of the P1 hairpin are important for the activity of the *lafK* riboswitch.

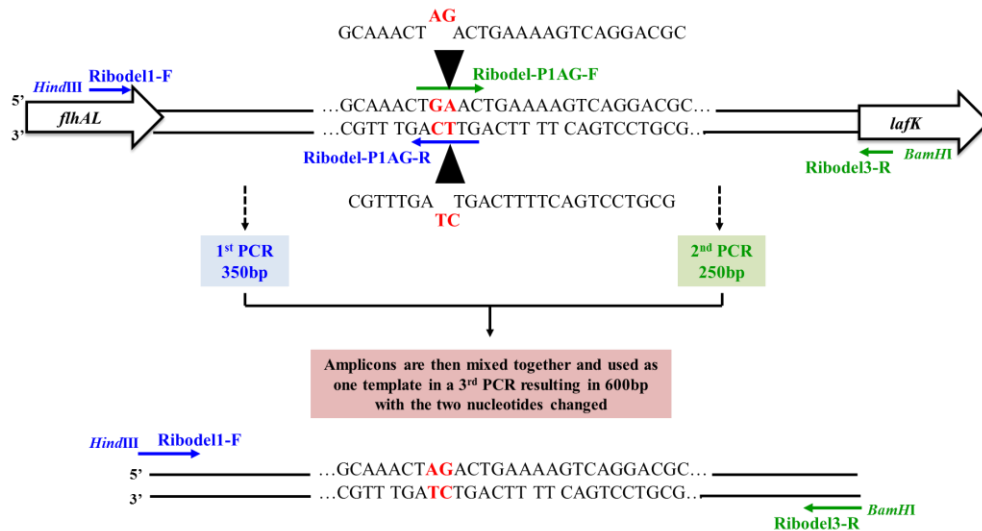


Figure 5.24. A schematic presentation showing the positions of the primers Ribodel-P1AG-F and Ribodel-P1AG-R used to change two nucleotides in the stem of P1 loop of *lafK* riboswitch by Spliced Overlap Extension (SOE)-PCR technique. The guanine in position number eight was changed to adenine and the adenine in position number nine was changed to guanine. The changes in the stem were performed to create a structural disturbance in the P1 loop in an attempt to determine the effect of this alteration on the activity of *lafK* riboswitch.

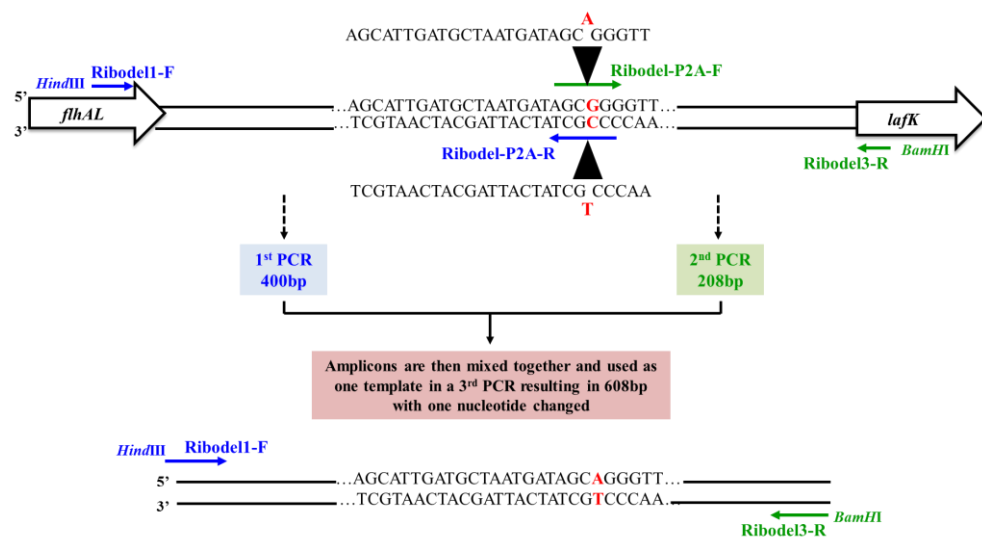


Figure 5.25. A schematic presentation showing the positions of the primers Ribodel-P2A-F and Ribodel-P2A-R used to change one nucleotide in the stem of P2 loop of *lafK* riboswitch by Spliced Overlap Extension (SOE)-PCR technique. The guanine in position number 35 was changed to adenine. This mutation was attempted to create a structural disturbance in the P2 loop in order to determine the effect of this alteration on the activity of *lafK* riboswitch.

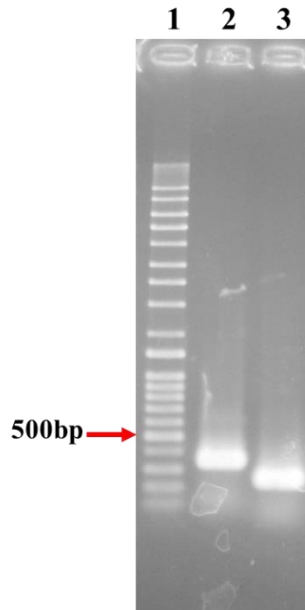


Figure 5.26. A 1% agarose gel showing the first and the second PCR steps of the three step SOE-PCR used to create mutations within the stem of P1 loop of *lafK* riboswitch. **Lane 1:** Q-Step 4 DNA ladder. **Lane 2:** Amplification using primers Ribodel1-F and Ribodel-P1AG-R (350bp). **Lane 3:** Amplification using primers Ribodel-P1AG-F and Ribodel3-R (250bp). These PCR products will then overlap in the third PCR step of the SOE-PCR technique leading to changing of two nucleotides in the stem of P1 loop.

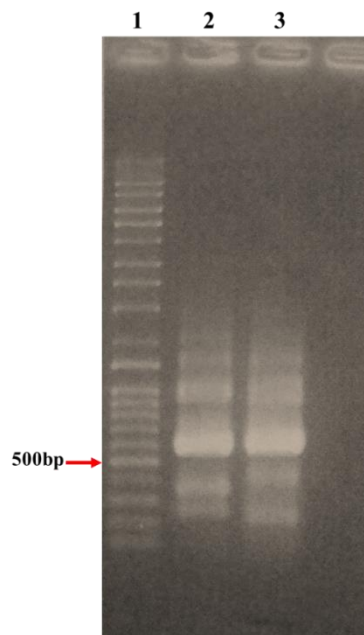


Figure 5.27. A 1% agarose showing amplicons of the third PCR step of the SOE-PCR technique used to create mutations within the stems of P1 and P2 loops of the *A. caviae* *lafK* riboswitch. **Lane 1:** Q-Step 4 DNA ladder. **Lane 2:** PCR amplicons (600bp) generated using primers Ribodel1-F and Ribodel3-R and resulting in two nucleotides changed within the stem of P1 loop. **Lane 3:** PCR amplicons (608bp) generated using primers Ribodel1-F and Ribodel3-R and resulting in a single nucleotide change within the stem of the P2 loop.

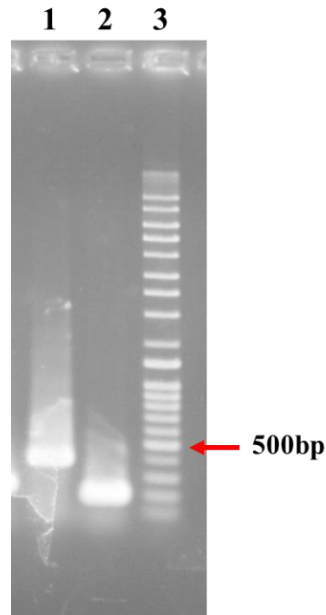


Figure 5.28. A 1% agarose gel showing the first and the second PCR steps of the three step SOE-PCR used to create a mutation within the stem of the P2 loop of *lafK* riboswitch. **Lane 1:** Amplification using primers Ribodel1-F and Ribodel-P2A-R (400bp). **Lane 2:** Amplification using primers Ribodel-P2A-F and Ribodel3-R (208bp). **Lane 3:** Q-Step 4 DNA ladder. These PCR products will then overlap in the third PCR step of the SOE-PCR technique leading to a change in one nucleotide in the stem of P2 loop.

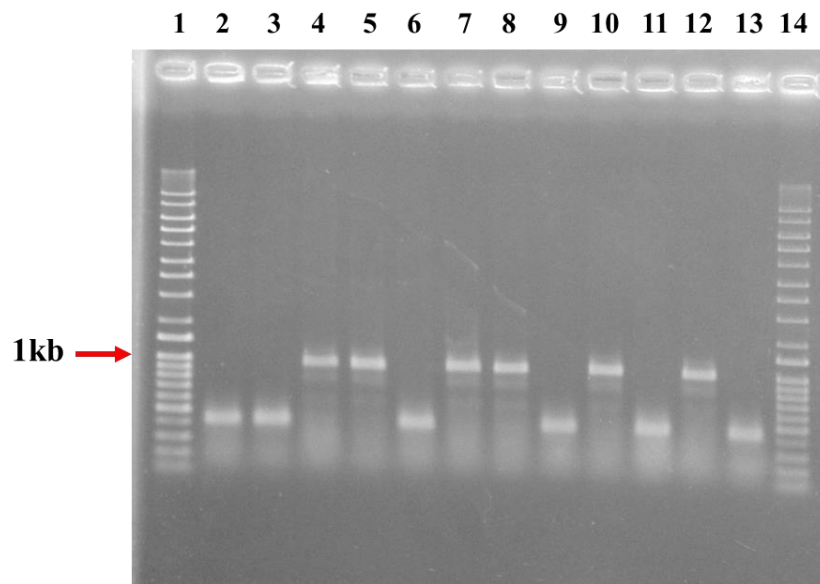


Figure 5.29. A 1% agarose gel showing colony PCR screening of *E. coli* DH5 α cells transformed with pKAG-*lafK*pP1AG using primers pKAG-F and pKAG-R. **Lane 1 and 14:** Q-Step 4 DNA ladder. **Lane 2-13:** *E. coli* strains that were chloramphenicol resistant after transformation subjected to colony PCR. Expected band size (1000bp) was obtained from screening colonies in lanes 4, 5, 7, 8, 10 and 12.

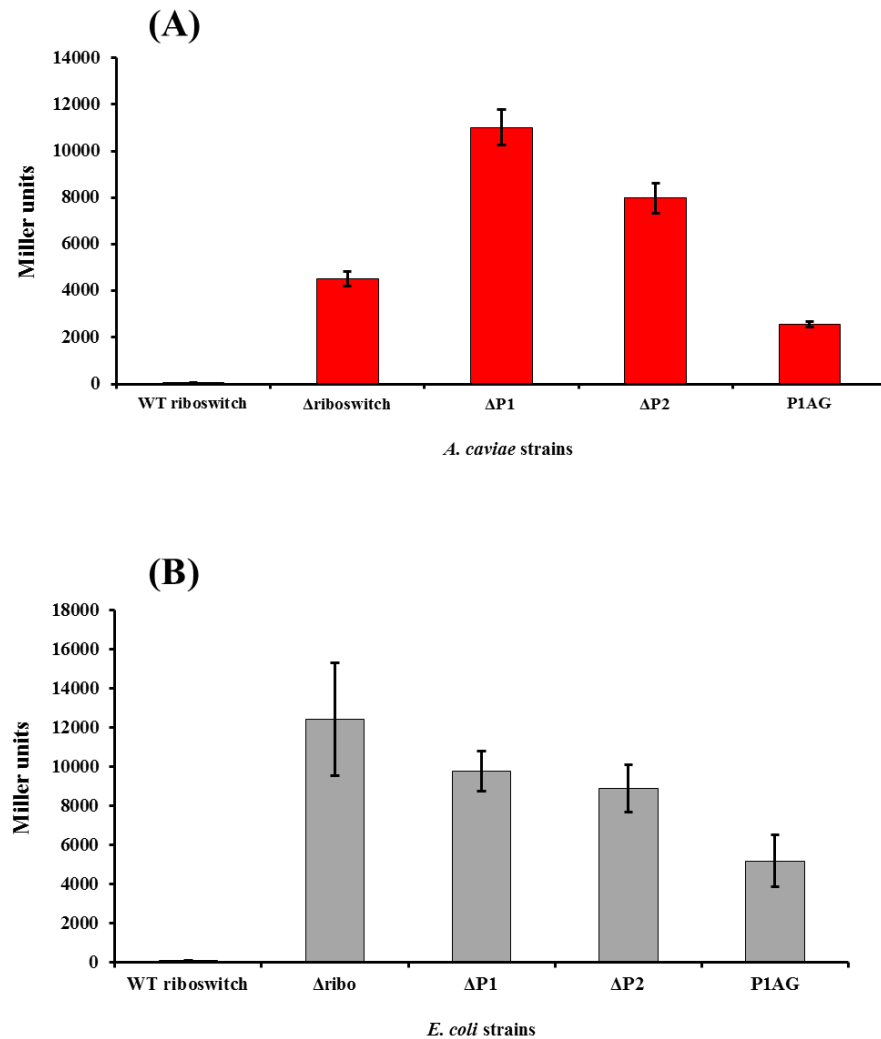


Figure 5.30. Analysis of *lafK* promoter activity using β -galactosidase assay following the change of two nucleotides in the stem of the P1 loop of the *lafK* riboswitch. The graph shows other strains for comparison. **(A)** Activity in *A. caviae* Sch3N background. **(B)** Activity in *E. coli* DH5 α background. Results expressed in Miller units. **WT:** *A. caviae* Sch3N. **Δ Ribo:** pKAG-*lafK*p Δ riboswitch. **Δ P1:** pKAG-*lafK*p Δ P1 loop. **Δ P2:** pKAG-*lafK*p Δ P2 loop. **Δ P1AG:** pKAG-*lafK*pP1AG (two nucleotides changed). Test was done in triplicate from a liquid culture. Bars represent mean values of the three readings. Error bars represent the standard deviation around the mean. Results showed a significant variation ($p < 0.05$) using single factor ANOVA test.

5.6. Complementation of *lafK* gene with *lafK*Δriboswitch

Our group has previously knocked out the *A. caviae* *lafK* gene by insertion of a kanamycin cassette with the generated mutant strain *A. caviae* *lafK*::Km designated CM100. This mutation was shown to cause a defect in the ability of *A. caviae* to swarm. As deletion of the riboswitch appears to cause a large increase in transcription of *lafK*, in this study we have attempted to complement this mutation by introducing the *lafK* gene into CM100 but after the deletion of the c-di-GMP-I riboswitch. This complementation experiment was expected to rescue swarming motility in CM100 and also possibly to result in CM100 pBBR1MCS5- *lafK*Δriboswitch to produce lateral flagella in liquid medium.

5.6.1. Deletion of *lafK* riboswitch and introducing *lafK*Δriboswitch into CM100

To fulfil the above objective, we have used the three step spliced overlap extension (SOE) PCR technique to amplify the *lafK* gene and delete the *lafK* riboswitch. Four custom designed oligonucleotide primers were used to perform this deletion along with using the *A. caviae* genomic DNA as a template. The location of each of these primers is shown in the schematic presentation in figure 5.31. The first PCR step was done by using primers Ribodel1-F and Ribodel2-R which resulted in the production of amplicons with the size of 327bp (figure 5.32). The second PCR step was performed using the primers Ribodel4-F and ribodel3fliEL-R which have resulted in the production of 1569bp amplicons (figure 5.32). The products of the first and the second PCR steps were then mixed together and were used as one DNA template to perform the third PCR step of the SOE-PCR technique. The two primers Ribodel1-F and Ribodel3fliEL-R were used to perform the third PCR step. This PCR step was expected to result in the deletion of the c-di-GMP-I riboswitch as a result of the previous first and second PCR amplicons (used here as one template) being overlapped. The third PCR step was considered successful as a single band appeared on agarose gel with the expected size of 1896bp (figure 5.33). The DNA sequence of the 1896bp PCR amplicons was then determined to confirm the deletion of *lafK* riboswitch. DNA sequencing confirmed the deletion of the riboswitch upstream of *A. caviae* *lafK* gene. The *lafK*Δriboswitch was then ready to be cloned into the broad-host range vector pBBR1MCS-5 to complement *lafK*::Km in CM100.

To proceed with cloning, the 1896bp PCR amplicons were purified and double digested with *Hind*III and *Bam*HI. The digested products were then ligated to the plasmid pBBR1MCS5 (Gm^R) which was previously cut with the same restriction enzymes. The ligation mixture was then transformed by heat shock to *E. coli* DH5 α competent cells. The transformed *E. coli* cells were then plated on LB agar containing gentamicin and the plates were incubated at 37°C for 24hrs. Colonies of gentamicin-resistant *E. coli* DH5 α cells were successfully isolated. The colonies were then subjected to colony PCR screening using the primers Ribodel1-F and Ribodel3fliEL-R to confirm insertion of *lafK* Δ riboswitch into pBBR1MCS5. Colony PCR screening confirmed the insertion of *lafK* Δ riboswitch into pBBR1MCS5 (figure 5.34).

The plasmid construct pBBR1MCS5-*lafK* Δ riboswitch was then extracted from *E. coli* DH5 α and was then transformed to *E. coli* S17-1 by heat shock. The transformed *E. coli* S17-1 cells were then used for the conjugal transfer of pBBR1MCS5-*lafK* Δ riboswitch to *A. caviae* *lafK*::Km (CM100). The conjugation mixture was then plated on LB plates containing both nalidixic acid and gentamicin. Oxidase-positive colonies resistant to both nalidixic acid and gentamicin were isolated on LB agar plates which indicated the successful transfer of pBBR1MCS5-*lafK* Δ riboswitch to CM100. The complemented strain CM100 pBBR1MCS5-*lafK* Δ riboswitch was then ready to be tested by motility assay and western blot.

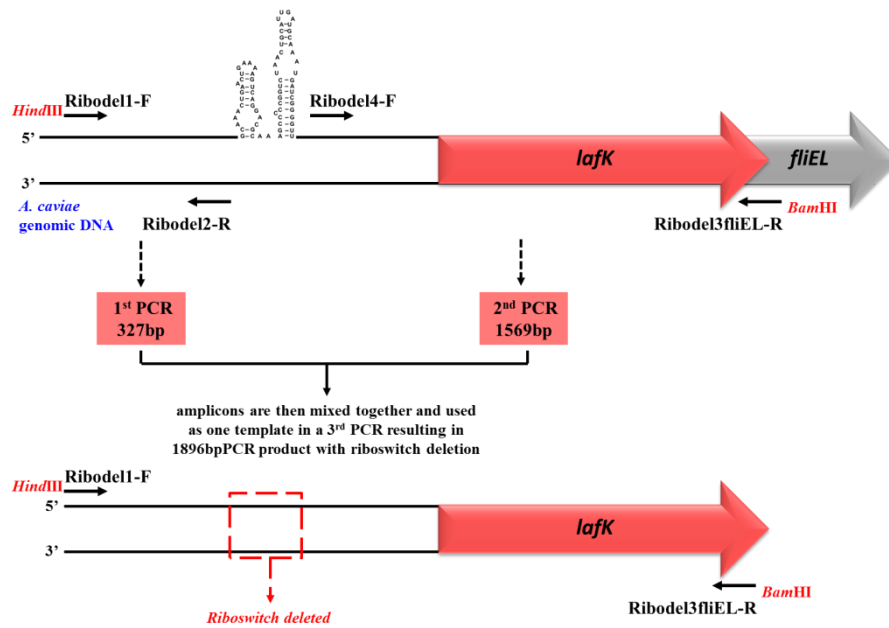


Figure 5.31. Position of the four custom designed oligonucleotide primers used to amplify the whole *A. caviae* *lafK* gene and the deletion of the riboswitch by Spliced Overlap Extension (SOE) PCR technique. The primers ribodel2-R and Ribodel4-F do contain overlapping sequences at their 5' ends for when they overlap the riboswitch becomes deleted. Primer Ribodel1-F includes a *Hind*III restriction digestion linker and primer Ribodel3fliEL-R includes a *Bam*HI restriction digestion linker. Both linkers are shown in red colour and were added to the primers for later cloning of *lafK* Δ ribo in pBBR1MCS5 to be overexpressed in *A. caviae* *lafK*::Km background.

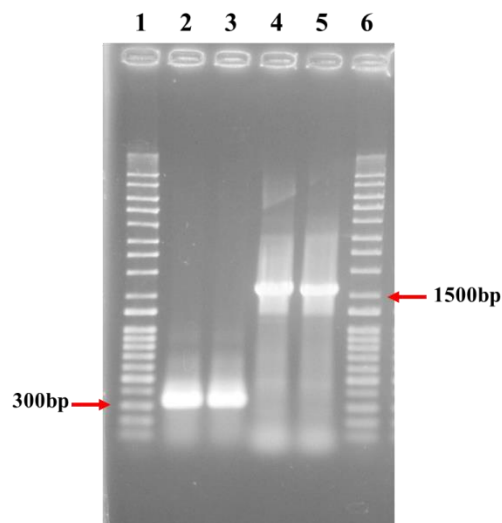


Figure 5.32. A 1% agarose gel showing the first and the second PCR steps of the three step SOE-PCR used to both amplify the *A.caviae* *lafK* gene and to delete the *lafK* riboswitch. **Lane 1 and 6:** Q-Step 4 DNA ladder. **Lane 2 and 3:** Amplification (done twice) using primers Ribodel1-F and Ribodel2-R (327bp). **Lane 4 and 5:** Amplification using primers Ribodel4-F and Ribodel3fliEL-R (1569bp). These PCR products will then overlap in the third PCR step of the SOE-PCR technique leading to amplification of the whole *lafK* gene of *A. caviae* plus the deletion of the riboswitch upstream of the *lafK* gene.

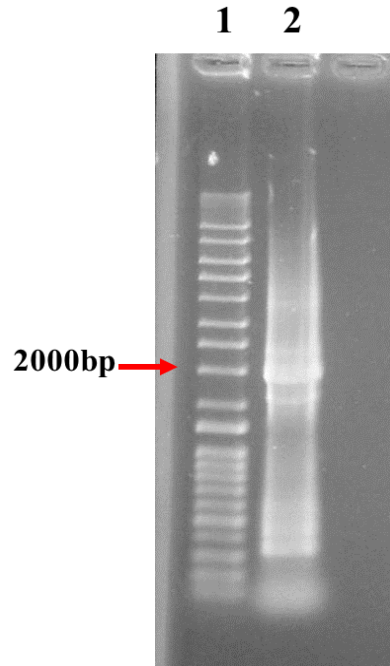


Figure 5.33. A 1% agarose showing amplicons of the third PCR step of the SOE-PCR technique used to amplify the whole *A. caviae* *lafK* gene and delete the riboswitch located upstream of *lafK* gene. **Lane 1:** Q-Step 4 DNA ladder. **Lane 2:** PCR amplicons (1896bp) generated using primers Ribodel1-F and Ribodel3fliEL-R and resulting in *lafK* riboswitch being deleted.

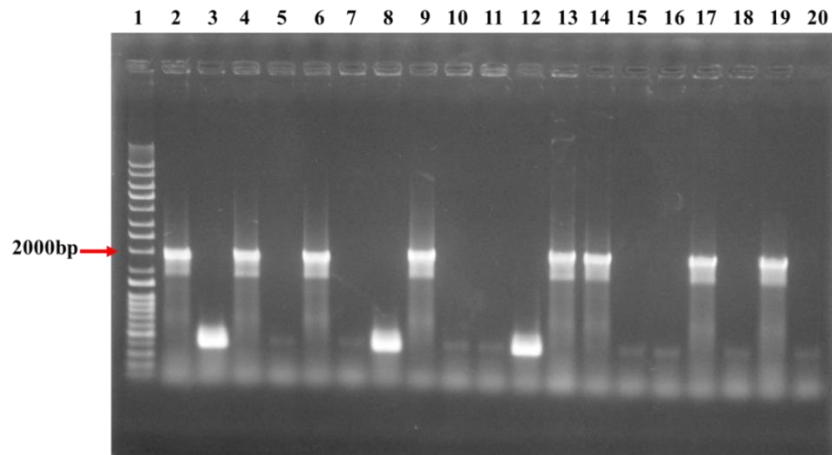


Figure 5.34. A 1% agarose gel showing colony PCR screening of *E. coli* DH5 α cells transformed with pBBR1MCS5-*lafK* Δ riboswitch using primers Ribodel1-F and Ribodel3fliEL-R. **Lane 1:** Q-Step 4 DNA ladder. **Lane 2-20:** *E. coli* strains that were gentamycin resistant after transformation subjected to colony PCR. Expected band size (1896bp) was obtained from screening colonies in lanes 2, 4, 6, 9, 13, 14, 17, and 19.

5.6.2. Testing the complemented strain using the motility assay

The strain CM100 pBBR1MCS5-*lafK*Δ*ribo* was tested for its ability to both swarm figure (5.35) and swim (figure 5.36). As shown in the figures, the strain CM100 was not able to swarm and was as well deficient in swimming as its swim zone diameter ranged from 0.9cm to 1.5cm. Both swarming and swimming types of motility were rescued by introduction of pBBR1MCS5-*lafK*Δ*ribo* into the mutant strain CM100.

The average swarm diameter for the complemented strain was 1.62cm in comparison to that for the wild type strain which was equal to 3.94cm. The average swim diameter for the complemented strain was measured to be 2.6cm while the average swim diameter of the wild type strain was measured to be 4.86cm.

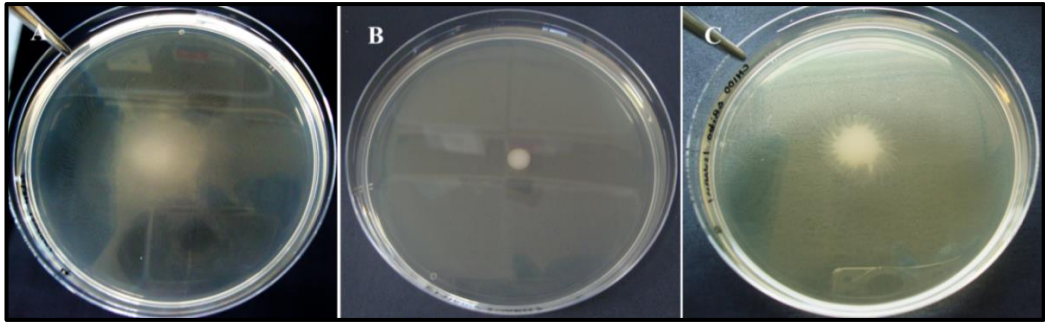


Figure 5.35. Testing the ability of CM100 pBBR1MCS5-*lafK*ΔRibo to swarm on 0.6% Eiken agar after 24hrs of incubation at room temperature. **(A)** *A. caviae* Sch3N (wild type). **(B)** CM100. **(C)** CM100 pBBR1MCS5-*lafK*ΔRibo. The test shows that swarming motility was rescued in CM100 following introducing pBBR1MCS5-*lafK*ΔRibo.

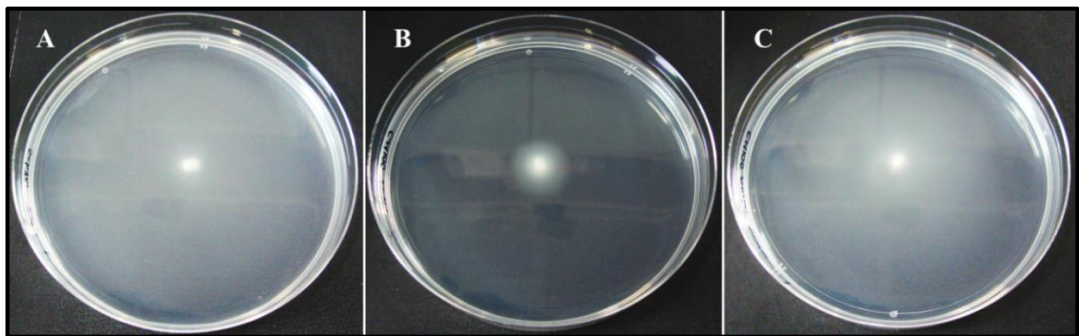


Figure 5.36. Testing the ability of CM100 pBBR1MCS5-*lafK*ΔRibo to swim on 0.25% agar after 24hrs of incubation at room temperature. **(A)** *A. caviae* Sch3N (wild type). **(B)** CM100. **(C)** CM100 pBBR1MCS5-*lafK*ΔRibo. The test shows that swimming motility was rescued in CM100 following introducing pBBR1MCS5-*lafK*ΔRibo.

5.6.3. Testing the ability of the complemented strain to produce the lateral flagellin protein when grown in liquid medium

After finding that *lafK* riboswitch has an inhibitory effect on the expression of the lateral flagella in *A. caviae* and that its deletion causes an active expression of the lateral flagella of this bacterium, we wanted to investigate whether deletion of the riboswitch will cause a constitutive expression of the lateral flagella not only during swarming but also during swimming (i.e., in liquid medium). Finding this will confirm the direct and crucial role played by the *lafK* riboswitch in controlling *A. caviae* lateral flagella genes expression. To do this we have decided to perform a western blot technique which will allow us to specifically detect the polar flagellin protein and the lateral flagellin protein of *A. caviae* using specific antibodies. Detection of either the polar flagellin or the lateral flagellin in the western blot will indicate which type of flagella is being expressed by the tested *A. caviae* strain under the experimental settings used in our study.

To perform a western blot CM100 pBBR1MCS5-*lafK*Δribo was grown in both BHI broth (swimming state) and on swarm agar. The positive control *A. caviae* Sch3N (wild type) and the negative control CM100 (mutant strain) were also grown in both BHI broth and on swarm agar to be included in the western blot experiment for comparison. Each of the three tested strains was inoculated to three BHI broth tubes and three swarm agar plates. The broth cultures were incubated at 37°C for 24hrs with shaking. The swarm agar plates were incubated at room temperature for 24hrs. The swimming and swarming bacteria were then subjected to western blot analysis which gave the results shown in figure 5.37.

Preliminary western blot experiments showed that during swimming of the wild type strain *A. caviae* Sch3N there was an expression of the polar flagellin protein which is needed for the formation of the single polar flagellum used by the bacterium for swimming. Also, in the wild type strain, there was a weak expression of the lateral flagellin protein appearing as a faint band.

During swimming of the mutant strain CM100 only the polar flagellin protein was expressed by the bacterium and there was no expression of the lateral flagellin protein due to the absence of the regulatory protein, LafK. However, when the latter strain was complemented with *lafK*Δribo, the complemented strain was able to express

the lateral flagellin protein during swimming, with the bands appearing in the western blot picture to be as dark as the bands corresponding to the polar flagellin protein constitutively expressed by the same strain.

During swarming motility of the wild type strain (which requires the formation of lateral flagella), there was an expression of the polar flagellin protein, a result which is expected as the single polar flagellum is known to be constitutively expressed in *Aeromonas*, and there was also a strong expression of the lateral flagellin protein needed for the formation of the lateral flagella. As the lateral flagella are produced by the cell in large numbers, the lateral flagellin protein is also needed in large numbers and so its corresponding band appeared in the picture to be thicker and darker than the band corresponding to the polar flagellin protein formed by the wild type strain.

No lateral flagellin protein was expressed by the mutant strain CM100 but there was an expression of the polar flagellin protein. Finally, the complemented strain CM100 pBBR1MCS5-*lafK*Δribo was not only able to express the polar flagellin protein but was also able to express the lateral flagellin protein. In the western blot, the bands corresponding to the lateral flagellin protein formed by the complemented strain appeared as dark as the bands of the same protein formed by the wild type strain.

All together, the results of the western blot technique indicated that deletion of *lafK* riboswitch has resulted in a possible constitutive expression of the lateral flagellin protein during both swarming and swimming of *A. caviae* Sch3N.

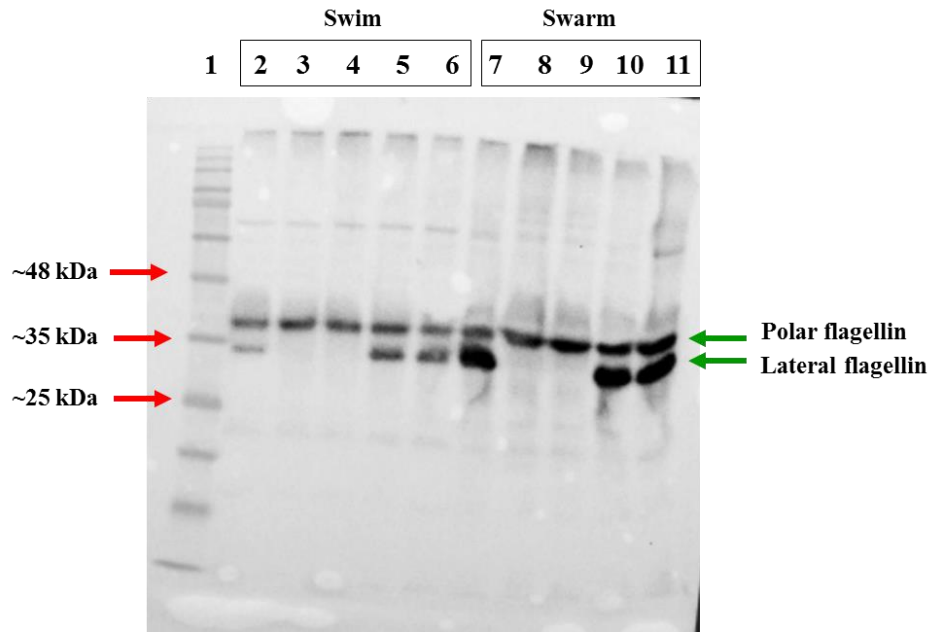


Figure 5.37. Western blot showing specific detection of polar and lateral flagellin proteins expressed following complementing *lafK* gene in CM100 with pBBR1MCS5-*lafK* Δ ribo during both swarming and swimming. Whole cell bacterial proteins were separated by 12% SDS-PAGE then blotted onto nitrocellulose membrane. The polar and lateral flagellins were detected with rabbit anti-polar and anti-lateral flagellin antibodies. (1) BLUeye Prestained Protein Ladder (Tris-Glycine 4~20%). (2) *A. caviae* Sch3N (wild type). (3) CM100. (4) CM100 (duplicate). (5) CM100 pBBR1MCS5-*lafK* Δ ribo. (6) CM100 pBBR1MCS5-*lafK* Δ ribo (duplicate). (7) *A. caviae* Sch3N (wild type). (8) CM100. (9) CM100 (duplicate). (10) CM100 pBBR1MCS5-*lafK* Δ ribo. (11) CM100 pBBR1MCS5-*lafK* Δ ribo (duplicate). The picture shows the active expression of the lateral flagellin protein during both swarming and swimming of CM100 pBBR1MCS5-*lafK* Δ ribo.

5.7. Discussion

In this chapter we have provided important information about *Aeromonas lafK* c-di-GMP-I riboswitch which seem to indicate its function of being a modulator which senses the high or low levels of c-di-GMP and controls the expression of the *laf* genes accordingly. Our data also suggest that LafK could be the major regulator of the transcription of lateral flagella genes in *A. caviae*.

Our *in silico* analysis of the DNA region upstream of *lafK* gene identified a sigma-70 consensus sequence. This is in agreement with the computational analysis results obtained by Wilhelms and colleagues for the region upstream of *lafK* gene of *A. caviae* Sch3N (the same strain used in our study) which showed the existence of a sigma-70 sequence located 331 nucleotides upstream of the start codon of *lafK* gene (Wilhelms *et al.*, 2013). In addition, the same group of researchers have performed a 5'RACE analysis for the same region in *A. hydrophila* AH-3 by which they have detected a sigma-70 promoter sequence located 335 nucleotides upstream of *lafK* start codon (Wilhelms *et al.*, 2013). Although performed using the DNA of *A. hydrophila* AH-3, the 5'RACE results of Wilhelms and colleagues strongly supports our *in silico* results as the species belongs to the same genus and the difference in promoter location was not big (only 4 nucleotides).

Weinberg and co-workers have performed an extensive study on bacterial structured RNAs (Weinberg *et al.*, 2007). In their study, they have explained that riboswitches are examples of *cis*-regulatory elements which are predicted to have their “5'-regulatory configuration” when they are found in the 5'UTR of a gene, precisely, located downstream of the transcription start site (TSS). This fact supports our proposed genetic structure of the region upstream of *lafK* gene as the TSS was predicted to be upstream of the riboswitch by 105 nucleotides. In addition, during their extensive sequence analyses Weinberg and co-workers found the GEMM motif to be widespread in bacteria and to have the 5'-regulatory configuration in the majority of studied bacterial sequences with the motif being very common in the order *Vibrionales*. The last fact has encouraged us to compare the sequence of *A. caviae lafK* GEMM type I riboswitch with the sequence of the well studied *V. cholerae* Vc2 GEMM type I riboswitch.

We have predicted the architecture of the *lafK* riboswitch to have P1 and P2 hairpins. This architecture is similar to the one described for *V. cholerae* type I GEMM motif Vc2 (Weinberg *et al.*, 2007, Sudarsan *et al.*, 2008). Studying the GEMM motif of more than 300 bacterial species revealed that P1 is highly conserved in both sequence and structure and that the two hairpins (P1 and P2) are usually linked by three adenine residues (AAA) (Weinberg *et al.*, 2007). In our *lafK* GEMM riboswitch model, the two hairpins are also linked by AAA.

A regulatory RNA needs to be folded in order to be active and the tertiary interactions are known to stabilize such folding (Fiore *et al.*, 2013). Folding of riboswitches to tertiary structures allows them to selectively bind to c-di-GMP (Smith *et al.*, 2011b). An example of the tertiary interactions is the tetraloop-receptor interactions which was extensively reviewed by Fiore and colleagues (Fiore *et al.*, 2013). Our *lafK* GEMM riboswitch contained the tetraloop sequence GAAA which we have suggested an 11 nucleotide sequence in the P2 loop to be considered as its receptor sequence for the tertiary interaction and stabilization of the *lafK* riboswitch. The tetraloop sequence GAAA is the most common sequence of what is referred to as GNRA tetraloop, where, N is any nucleotide and R is either G or A (Fiore *et al.*, 2013). The GNRA tetraloops are very widespread, are mostly found capping a hairpin with a conserved length (e.g., P1), and are well known to strongly interact with a conserved eleven nucleotide receptor (Fiore *et al.*, 2013), hence our suggested tetraloop receptor to be composed of eleven nucleotides. The GAAA-receptor tertiary interaction has been identified in riboswitches and this interaction (which occurs by hydrogen bonding) is known to be highly specific and very stable (Fiore *et al.*, 2013). The stable interaction occurs when the tetraloop becomes docked into the receptor groove (Fiore *et al.*, 2013).

Weinberg and colleagues have explained the mechanisms by which riboswitches regulate the transcription of genes under their control. One of the discussed mechanisms was the existence of a Rho-independent terminator sequence which ends with several uracil bases (Weinberg *et al.*, 2007). In our model of *lafK* riboswitch there are 30 nucleotides located immediately downstream of the riboswitch which we suggest to be considered as a Rho-independent terminator sequence as the last 5 bases of this sequence were uracil bases. Weinberg and co-workers suggested the terminator sequence to fold forming a stem or a hairpin which prevents gene expression whenever this was needed by the cell.

Sudarsan and colleagues have studied the binding of c-di-GMP to *V. cholerae* GEMM type I Vc2 riboswitch using in-line probing (Sudarsan *et al.*, 2008). They have proved that c-di-GMP is the ligand for the Vc2 aptamer and that the nucleotides at the base of the P1 and P2 hairpins undergo structural modulation which is important for binding of the second messenger. Furthermore, Smith and colleagues have studied the interaction between Vc2 riboswitch and the c-di-GMP and have provided a crystal structure for such binding and predicted a second architecture for the Vc2 riboswitch after binding to c-di-GMP (Smith *et al.*, 2011b). Based on the indicated study of Smith and colleagues, we have predicted the *lafK* GEMM riboswitch type I to form the structure shown in figure 5.38 following binding to c-di-GMP.

Altogether, our transcriptional fusion results suggested that the wildtype *lafK* c-di-GMP-I riboswitch has an inhibitory effect on the transcription of the lateral flagella genes in *A. caviae*, i.e., an “off” switch. Our conclusion was further confirmed by the Western blot analysis results which have shown that the absence of the riboswitch (the “off” switch) resulted in the production of *A. caviae* lateral flagella not only during swarming but also during swimming. It should be noticed, however, that these were the results of preliminary experiments which need to be further confirmed in the future.

Another transcriptional fusion followed by performance of a β -galactosidase assay is recommended to be done in the future by interested researchers to further confirm the role played by the *lafK* GEMM motif as an off switch. The *lafK* wildtype promoter (containing the GEMM riboswitch) and the same promoter lacking the riboswitch can separately be fused to pKAGb2(-). Each of the recombinant plasmids containing the *lacZ* reporter gene can then separately be introduced into *A. caviae*. This is followed by separately introducing other recombinant plasmids, one of which contains a GGDEF domain and the other contains an EAL domain into the same *A. caviae* strain containing the first pKAGb2(-) recombinant plasmid. The activity of *lafK* promoter with and without the riboswitch can then be tested during high and low levels of c-di-GMP during both swimming and swarming of *A. caviae*. It is recommended to insert the GGDEF and EAL domains into inducible plasmids (e.g., induced by arabinose or IPTG) to allow more control/titration on the cellular level of c-di-GMP. This experiment is expected to give the results shown in figure 5.39 which supports our suggestion of *lafK* riboswitch to be c-di-GMP receptor.

Both the aptamer (the P1 domain) and the expression platform (P2 domain) of the riboswitch seem to be involved in inhibition of *laf* genes expression in *A. caviae*, according to our findings. This is evident from the high expression of the *lacZ* reporter gene in the β -galactosidase assay following deletion of either of the two loops. Also, the structure of the P1 stem of *lafK* riboswitch seems to be important for its function as changing two nucleotides within the P1 base-pair structure has also disturbed the *lafK* riboswitch from performing its ordinary function in *A. caviae*.

Opposite to the activity of the *A. caviae* wild type *lafK* riboswitch tested in our study, the wild type Vc2 riboswitch in *V. cholerae* showed a very high expression when tested by Sudarsan and co-workers using β -galactosidase assay, which suggests that Vc2 acts as an “ON switch” in *V. cholerae* (Sudarsan *et al.*, 2008). In addition, changing two nucleotides in the P1 base-paired region of the Vc2 caused a disruption of the P1 structure which showed a dramatic decrease in the Vc2 riboswitch activity when measured by β -galactosidase assay indicating that P1 is important for the “ON” activity of the Vc2 riboswitch.

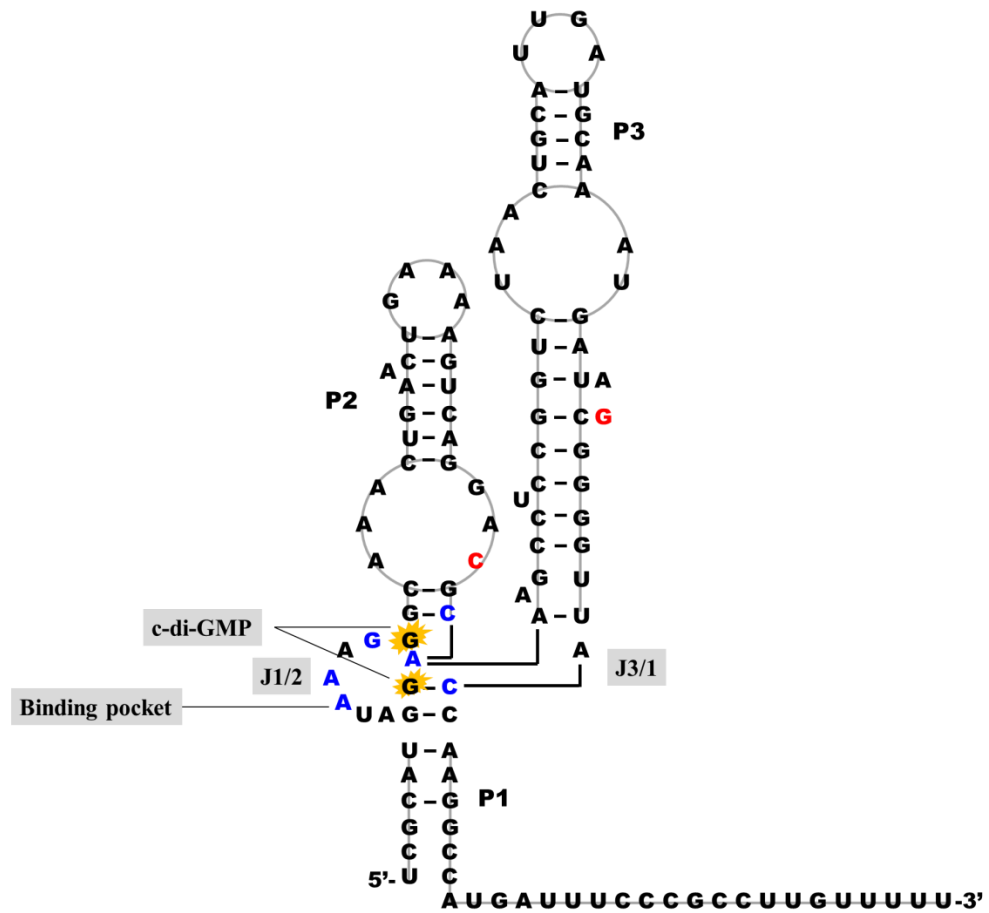


Figure 5.38. Predicted architecture of *A. caviae lafK* GEMM riboswitch type I after binding to c-di-GMP based on the study of Smith and colleagues on *V. cholerae* Vc2 riboswitch (Smith *et al.*, 2011b). Nucleotides shown in red (C and G) are universally conserved nucleotides involved in bridging P2 and P3 hairpins and are required for c-di-GMP binding. C-di-GMP (shown in yellow stars) binds to the pocket which exists in the junction between P1, P2, and P3. Bases shown in blue colour are those expected to recognize and directly interact with c-di-GMP. J letter is for the word junction.

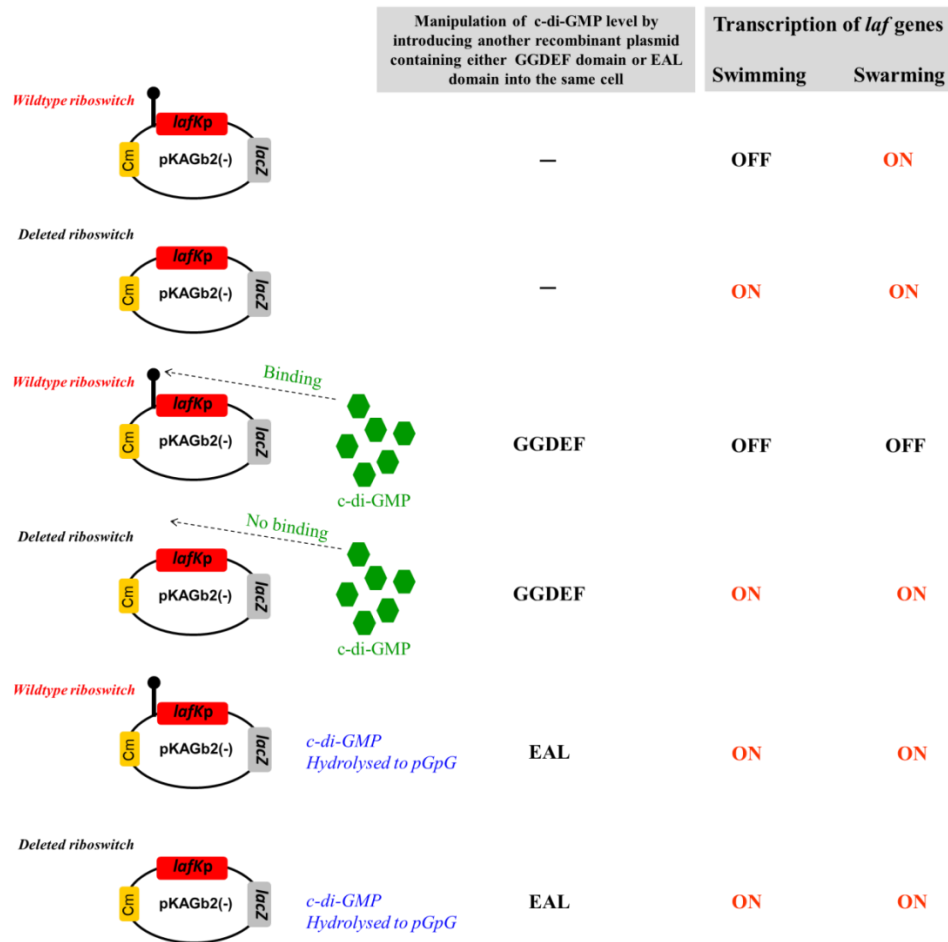


Figure 5.39. The proposed results for a recommended promoter fusion experiment which can further confirm the role played by the *lafK* riboswitch as a c-di-GMP receptor directly involved in *A. caviae* *laf* genes expression. The proposed experiment depends on the introduction of two recombinant plasmids one of them carrying the promoter under investigation and the other carrying a protein with either a diguanylate cyclase activity or a phosphodiesterase activity to artificially increase and decrease the cellular level of c-di-GMP.

Our results suggested a role played by the riboswitch in the transcription of the *laf* genes. A recent study, however, done by Wilhelms and colleagues have provided evidence that the lateral flagella genes in *A. hydrophila* AH-3 are actively transcribed not only on solid and in semi solid media but also in liquid media (Wilhelms *et al.*, 2013). They have performed β -galactosidase assays to measure the activity of the promoters of the three *A. hydrophila* AH-3 genes *lafK* (regulatory protein), *lafA* (lateral flagellin protein), and also *lafB* (flagella capping protein HAP-2) when the bacteria were grown on solid and semi-solid media as well as in liquid media. The activities of all three promoters were found to be the same. Also, they have found the same three genes to be actively transcribed during an RT-PCR reaction which they have described its results as being surface/viscosity independent.

Wilhelms and co-workers, however, have shown that although the lateral flagella genes of *A. hydrophila* AH-3 were transcribed in liquid they were not translated (Wilhelms *et al.*, 2013). To prove this fact they have grown *A. hydrophila* AH-3 cells on solid media and in semi-solid and liquid media. They then have performed a Western blot analysis using whole cells and supernatants (before and after shearing) to detect the production of the lateral flagella in all three media using lateral flagellin-specific antibodies. No interaction of the antibodies was detected with any of the *A. hydrophila* samples grown in liquid, which means that the lateral flagella, under their tested conditions, were not produced even though their genes were transcribed.

We have performed transcriptional fusions and our results suggested an inhibitory role of the riboswitch in *laf* genes transcription. Considering the results of Wilhelms and colleagues mentioned above that the *laf* genes in *A. hydrophila* are constitutively transcribed in liquid media and also on solid media gives less value for our finding that the *lafK* riboswitch acts as an “off” switch which stops lateral flagella genes from being transcribed. However, considering the numerical values obtained in our study using the β -galactosidase assay strongly supports our hypothesis that the *lafK* riboswitch has a relative inhibitory role on *laf* genes transcription. The Miller units obtained from measuring the *lacZ* gene transcription in the presence of the wild type riboswitch were just 87.78 units in comparison to a value of 7410.13 units in the absence of the riboswitch. We can thus give a value of (+1) to the level of *laf* genes transcription in the presence of the wild type *lafK* promoter containing the riboswitch and give a (+5) to the level of *laf* genes transcription in the absence of the *lafK*

riboswitch. In other words, the transcription of the *laf* genes in *A. caviae* is greatly enhanced in the absence of the riboswitch.

Both our Western blot analysis results as well as those of Wilhelms and co-workers (Wilhelms *et al.*, 2013) clearly show (using polar flagellin-specific antibodies) the constitutive production of the single polar flagellum in both liquid and solid media by both *A. caviae* (our study) and *A. hydrophila* AH-3 (Wilhelms and colleagues study). Wilhelms and colleagues showed in their Western analysis (using lateral flagellin-specific antibodies) that lateral flagella production (i.e., translation) was completely absent when the wild type *A. hydrophila* AH-3 was grown in liquid. Our Western analysis, however, showed a small amount of lateral flagella (appearing as a faint band on the blot) to be produced by the wild type strain *A. caviae* Sch3N when it was grown in a liquid medium. The intensity of this band in our blot was, however, much weaker than when the wild type was grown on swarm agar, i.e., the production of lateral flagella on solid agar was much stronger. This small amount of lateral flagella produced by *A. caviae* during swimming under the experimental conditions used in our study could be due to a surrounding signal received by the bacteria which have caused it to start the production of lateral flagella (induction). For example, the cells might have started to form a biofilm on the surface of the tube they were grown in shortly before starting the Western blot analysis (during the preparation for the experiment). Biofilm production on surfaces requires production of lateral flagella.

Chapter 6

Final Conclusions

Chapter 6: Final conclusions

The c-di-GMP molecule is known to control many cellular processes in bacteria, however, the mechanisms by which it does this control are still largely unknown. The basic components of the c-di-GMP pathway is the enzymes responsible for its turnover, receptors or modulators which sense its cellular level and mediate the transfer of its signal, and finally the different targets which receive the signal. C-di-GMP has been suggested to control important cellular processes in bacteria, particularly, virulence genes expression, cell cycle progression, and the switch between motility and sessility. Mesophilic *Aeromonas* species are known to possess two different flagellar systems, a single polar flagellum (constitutively expressed) and many peritrichous lateral flagella only expressed when the *Aeromonas* cells move as a group over surfaces (swarm). It is very well known that bacteria in biofilms (sessile lifestyle) are more resistant to antibiotics and immune cells. In addition, bacteria colonize the human intestine by forming a biofilm. Lateral flagella of *Aeromonas* species are known to be a crucial requirement for biofilm formation and bacteria need to move first as a group (swarm) in order for them to effectively colonize a human tissue prior to being sessile and form a biofilm. We thus believe that the lateral flagella in mesophilic *Aeromonas* species are ideal targets for c-di-GMP and that this molecule does control the switch between motility and sessility in mesophilic *Aeromonas* species.

In this study, we have investigated the role played by the thirteen GGDEF-EAL domains containing proteins encoded in *A. caviae* genome in the turnover of c-di-GMP. We also have mutated a gene which encodes a protein which contains one of the well studied c-di-GMP receptors, the *pilZ* domain, and finally, we have investigated the role played by an RNA domain as a c-di-GMP receptor. Our target was the lateral flagella in *A. caviae*. Our study thus investigated different possible components for a single c-di-GMP pathway (which is part of the complex c-di-GMP network) within *A. caviae* Sch3N.

We were able to suggest that overexpression of *A. caviae* proteins containing the conserved residues GGDEF (for example AHA1208) can enhance biofilm production (i.e., promote a sessile lifestyle) and thus these proteins might be enzymatically active diguanylate cyclases which synthesize c-di-GMP. We also were able to suggest that *A. caviae* GGDEF-EAL proteins which contain non-conserved residues can still be involved in determining the lifestyle of *A. caviae*. For example,

AHA2484 was suggested to be involved in extracellular polysaccharide production which is important for the development of bacterial biofilms. Another example of *A. caviae* proteins containing non-conserved residues is the protein AHA2698 which, when overexpressed, caused a great reduction in swarming motility and thus was suggested to play a role in controlling the synthesis or movement of lateral flagella. All GGDEF-EAL-containing proteins in *A. caviae* are suggested to be involved in the expression of the lateral flagellar genes. Mutating the *A. caviae* GGDEF-EAL-encoding genes affected the activities of three important promoters in the *A. caviae* lateral flagellar operon, namely, *lafA1p*, *lafA2p*, and *lafKp*.

Our *in silico* analysis results suggest that the promoter of the *lafK* gene is sigma-70-dependent and that it contains a c-di-GMP type I riboswitch. Also, we have determined that the gene *pilZ* was actively transcribed during swarming motility of *A. caviae* Sch3N. The fact that *pilZ A. caviae* mutant is able to form a biofilm suggests that PilZ domain in *A. caviae* either does not function as a c-di-GMP receptor or its deletion is compensated by *lafK* riboswitch.

We have predicted the architecture of *A. caviae* *lafK* GEMM riboswitch type I to be composed of P1 and P2 hairpins. The deletion of the *lafK* c-di-GMP type I riboswitch (both hairpins) in our study has resulted in a dramatic increase in *lacZ* reporter gene expression. This allowed us to conclude that the riboswitch acts as an “OFF switch” preventing or attenuating *lafK* gene expression when the cell is not in need of the lateral flagella. We suggest the mechanism of action for the *lafK* riboswitch to be a Rho-independent transcription termination mechanism. Separate deletion of P1 or P2 also resulted in enhancement of *lacZ* reporter gene expression, which indicates that each of the two hairpins is important for the activity of the *lafK* c-di-GMP type I riboswitch. We believe that the hairpin P1 is the aptamer to which c-di-GMP binds and that the hairpin P2 is the expression platform of the *lafK* riboswitch. Changing two nucleotides in the stem of the P1 hairpin (the aptamer) resulted in *lafK* promoter activity to be greatly increased (loss of riboswitch inhibitory action). Disturbing the aptamer structure might have resulted in improper folding of the expression platform and thus have affected the riboswitch activity. Our results suggest that the nucleotides number 8 (guanosine) and number 9 (adenine) in the stem of the P1 hairpin are important for maintaining a specific structure for P1 hairpin which is necessary for the activity of the *lafK* riboswitch.

Overexpressing *lafK* gene following deletion of its riboswitch in Δ *lafK* background (a strain which is unable to swarm) not only rescued swarming motility but also resulted in a constitutive expression of the lateral flagellin protein in liquid cultures during swimming. These findings indicate that *lafK* c-di-GMP type I riboswitch has a direct and crucial role in controlling *A. caviae* lateral flagellar genes expression.

Appendix

Primers used in this study

Appendix: Primers used in this study

I- Primers used to mutate GGDEF-EAL-encoding genes (custom designed)

Primer name	Primer sequence (5'-3')	Linkers	Gene name	Amplicon size
Azoto-F Azoto-R	GCGGATCCTCAACCTGCCCATCGCGCTG GCGGATCCCCCATCACCAGGGAGGCGA	GC-clamp (bold) <i>Bam</i> HI restriction site (underlined)	<i>Azoto</i>	350bp
AHA2484-MA-F AHA2484-MA-R	GCGCGGATCCCCGAATTGCATAATCAGGCG GCGCGGATCCCGGATCACCATCTGGGTCA	GC-clamp (bold) <i>Bam</i> HI restriction site (underlined)	<i>AHA2484</i>	739bp
AHA0383mshH-F AHA0383mshH-R	GCGGATCCGCGAGCAGCAAGGGAACGGT GCGGATCCTGGTACTGCGCGCAACTGG	GC-clamp (bold) <i>Bam</i> HI restriction site (underlined)	<i>AHA0383mshH</i>	370bp
Coma-MA-F Coma-MA-R	GCGCGGATCCCTGGCGTTGTCTTCATCG GCGCGGATCCCACGGCGCTGGTTTCGAG	GC-clamp (bold) <i>Bam</i> HI restriction site (underlined)	<i>Coma</i>	827bp
AHA1800-F AHA1800-R	GCGGATCCGCTGGAGCATCGCCACCTGG GCGGATCCCACCTCCCCATCTGGGCCA	GC-clamp (bold) <i>Bam</i> HI restriction site (underlined)	<i>AHA1800</i>	772 bp
AHA4237-F AHA4237-R	GCGGATCCACACACTCTGCCCTCTGCAACAT GCGGATCCTCGAGTTGCTGTGCGCACCT	GC-clamp (bold) <i>Bam</i> HI restriction site (underlined)	<i>AHA4237</i>	745bp
AHA0093-MA-F AHA0093-MA-R	GCGGATCCGGTGTGGAACAAGCGCAAG GCGGATCCGGTCTGGAACCTCCAGGGT	GC-clamp (bold) <i>Bam</i> HI restriction site (underlined)	<i>AHA0093</i>	958bp
AHA0862-F AHA0862-R	GCGGATCCTATACGGGCAACGACGCGCG GCGGATCCGGCCGTCTCGTTGAGCAGGG	GC-clamp (bold) <i>Bam</i> HI restriction site (underlined)	<i>AHA0862</i>	627bp
MorA-F MorA-R	GCGGATCCGGCTGTCTGCGGTGGCCTTT GCGGATCCTGAGCAGATCCCCGCCTCC	GC-clamp (bold) <i>Bam</i> HI restriction site (underlined)	<i>MorA</i>	795bp
AHA3342 -F AHA3342 -R	GCGGATCCGAGGGGTTGCAACGCAGGCT GCGGATCCTGCCGAAGTCGTCGATGGCG	GC-clamp (bold) <i>Bam</i> HI restriction site (underlined)	<i>AHA3342</i>	691bp
AHA3469-F AHA3469-R	GCGGATCCTCGGCATCGCCCATGGCAAG GCGGATCCGGATCGCGGAACCTGCAGGGG	GC-clamp (bold) <i>Bam</i> HI restriction site (underlined)	<i>AHA3469</i>	442bp
AHA2698-F AHA2698-R	GCGGATCCGTCGGCCACCCTGGACAAGC GCGGATCCACAGCGCACCGCTTCTCCC	GC-clamp (bold) <i>Bam</i> HI restriction site (underlined)	<i>AHA2698</i>	664bp
AHA2092-F AHA2092-R	GCGGATCCGCGGTGACGCGTTACACCCA GCGGATCCGCCGGTTCGGGCAACGAAGA	GC-clamp (bold) <i>Bam</i> HI restriction site (underlined)	<i>AHA2092</i>	735bp

II- Primers used for complementing GGDEF-EAL encoding genes (custom designed)

Primer name	Primer sequence (5'-3')	Linkers	Amplified gene	Amplicon size
CompAHA2484(2)-F	GCAAGCTTGGTGTCTACGGGTTCTAGCA	GC-clamp (bold)	<i>AHA2484</i>	2010bp
CompAHA2484(2)-R	GCTCTAGAGCGGACGACGAGCTCAATGC	<i>HindIII</i> restriction site (italic) <u>XbaI</u> restriction site (underlined)		
CompAHA3342(10)-F	GCAAGCTTAGATAGCGGGCATGTTGGCC	GC-clamp (bold)	<i>AHA3342</i>	2459bp
CompAHA3342(10)-R	GCTCTAGACAGACCATCCTCATACCACT	<i>HindIII</i> restriction site (italic) <u>XbaI</u> restriction site (underlined)		
CompAHA2698(12)-F	GCGAATTCAACCAGATGCGTTTCATCGA	GC-clamp (bold)	<i>AHA2698</i>	2578bp
CompAHA2698(12)-R	GCTCTAGATGTACAGGGTTGAGTCTCTT	<i>EcoRI</i> restriction site (italic) <u>XbaI</u> restriction site (underlined)		

III- Primers used to overexpress GGDEF-EAL encoding genes (custom designed)

Primer name	Primer sequence (5'-3')	Linkers	Amplified gene	Amplicon size
AHA1208-F	GCCTCGAGCATATGGCACGCCACTCGCT	GC-clamp (bold)	<i>AHA1208</i>	1219bp
AHA1208-R	GCTCTAGACTCTACTACGGTGAACAGGT	<i>XhoI</i> restriction site (italic) <u>XbaI</u> restriction site (underlined)		
AHA0382-F	GCCTCGAGTCAGGTGTGTAGCCATATCC	GC-clamp (bold)	<i>AHA0382</i>	1833bp
AHA0382-R	GCTCTAGAGGCAGTGGTTCTCATCTCGG	<i>XhoI</i> restriction site (italic) <u>XbaI</u> restriction site (underlined)		

IV- Primers used for *lafA1*, *lafA2*, and *lafK* promoters fusions (custom designed)

Primer name	Primer sequence (5'-3')	Linkers	Amplified region	Amplicon size
pARL23-LafA1p-F pARL23-LafA1p-R1	GCAAGCTTCCGAATCGCCACGGGGATAT <u>GCGGATCCGCC</u>CAGCATCTTGTTGGTGT	GC-clamp (bold) <i>HindIII</i> restriction site (italic) <i>Bam</i> HI restriction site (underlined)	<i>lafA1</i> promoter	828bp
lafA2p-F lafA2p-R	GCGCAAGCTTGTCTGGAGCACACCGTCAAC GCGCGGATCCCGTTGCGCATGCCGACCTTC	GC-clamp (bold) <i>HindIII</i> restriction site (italic) <i>Bam</i> HI restriction site (underlined)	<i>lafA2</i> promoter	550bp
lafKp-F lafKp-R	GCAAGCTTCGAAGTCATCGGGACTCTGGGCTGA GCGGATCCCTAGATAAATCAGAAAACAT	GC-clamp (bold) <i>HindIII</i> restriction site (italic) <i>Bam</i> HI restriction site (underlined)	<i>lafK</i> promoter	420bp

V- Primers used to knockout pilZ gene (custom designed)

Primer name	Primer sequence 5'-3'	Region	Size of amplicon
PilZ-F	ACCCCCTTTGCCGGTGACAA	280 bp upstream of <i>pilZ</i> (within <i>lafU</i>) and 459 bp downstream of <i>pilZ</i> (within ASA0387)	1198bp
PilZ-R	ACGCGGGAGAGGGAAGAGTA		

VI- Primers used in RT-PCR (custom designed)

Primer name	Primer sequence (5'-3')	Amplified region	Amplicon size
intPilZ-F intPilZ-R	TGGTATCTCCATGACGGGAC CCAGCACGATCCGCGGTGACAA	Internal region within <i>pilZ</i>	208bp
LafU-F intPilZ-R	GATACCATGCTGGACAACACC CCAGCACGATCCGCGGTGACAA	A shared region between <i>lafU</i> gene (154bp) and <i>pilZ</i> gene (277bp)	431bp
LafU-MA-F LafU-MA-R	CCGACTTCACCCTGGCCATG CATCAGCAGATGGCGGAAATAG	Internal region within <i>lafU</i>	503bp
FlaA-MA-F FlaA-MA-R	GCAACGCCAACGACGGCAT GCTTGCTATCTACGACTTCC	Internal region within <i>flaA</i>	501bp

VII- Primers used for *lafK* riboswitch deletion, dissection and complementation (custom designed)

Primer name	Primer sequence (5'-3')	Linkers	Amplicon size	Purpose
Ribodel1-F	GCGCAAGCTT ATGCCCCAGCTCAGAC	GC-clamp (bold)	327bp	<i>lafK</i> Riboswitch deletion to examine <i>lafK</i> promoter activity
Ribodel2-R	TCATGGCCTTGGTCTTTATCATGCGACGACCC	<i>Hind</i> III restriction site (underlined)		
Ribodel4-F	GTCGCATGATAAAGACCAAGGCCATGATTTCC	GC-clamp (bold)	179bp	<i>lafK</i> Riboswitch deletion to examine <i>lafK</i> promoter activity
Ribodel3-R	GCGCGGATCC TATTGAATTTTCCTTGCTAGATAAATCAGAAAAC	<i>Bam</i> HI restriction site (underlined)		
Ribodel1-F	GCGCAAGCTT ATGCCCCAGCTCAGAC	GC-clamp (bold)	327bp	Deletion of P1 loop of <i>lafK</i> riboswitch
Ribodel5-P1-R	GACCGGAGGCTTTCTTTATCATGCGACGACCC	<i>Hind</i> III restriction site (underlined)		
Ribodel6-P1-F	GTCGCATGATAAAGAAAGCCTCCGGTCTAACAGC	GC-clamp (bold)	223bp	Deletion of P1 loop of <i>lafK</i> riboswitch
Ribodel3-R	GCGCGGATCC TATTGAATTTTCCTTGCTAGATAAATCAGAAAAC	<i>Bam</i> HI restriction site (underlined)		
Ribodel1-F	GCGCAAGCTT ATGCCCCAGCTCAGAC	GC-clamp (bold)	356bp	Deletion of P2 loop of <i>lafK</i> riboswitch
Ribodel7-P2-R	TCATGGCCTTGGTTTGCGTCCTGACTTTTCAG	<i>Hind</i> III restriction site (underlined)		
Ribodel8-P2-F	AAGTCAGGACGCAAACCAAGGCCATGATTTCC	GC-clamp (bold)	179bp	Deletion of P2 loop of <i>lafK</i> riboswitch
Ribodel3-R	GCGCGGATCC TATTGAATTTTCCTTGCTAGATAAATCAGAAAAC	<i>Bam</i> HI restriction site (underlined)		

To be continued next page

VII- Primers used for *lafK* riboswitch deletion, dissection and complementation (custom designed) - continued

Primer name	Primer sequence (5'-3')	Linkers	Amplicon size	Purpose
Ribodel1-F P1AG-R	GCGCAAGCTT ATGCCCCAGCTCAGAC GCGTCCTGACTTTTCAGTCTAGTTTGC	GC-clamp (bold) <i>HindIII</i> restriction site (underlined)	350bp	To change an adenine to guanine and a guanine to adenine
P1AG-F Ribodel3-R	GCAAAGTAGACTGAAAAGTCAGGACGC GCGCGGATCC TATTGAATTTTCCTTGCTAGATAAATCAGAAAAC	GC-clamp (bold) <i>BamHI</i> restriction site (underlined)	250bp	To change an adenine to guanine and a guanine to adenine
Ribodel1-F P2A-R	GCGCAAGCTT ATGCCCCAGCTCAGAC AACCCCTGCTATCATTAGCATCAATGCT	GC-clamp (bold) <i>HindIII</i> restriction site (underlined)	400bp	To change a guanine to adenine
P2A-F Ribodel3-R	AGCATTGATGCTAATGATAGCAGGGTT GCGCGGATCC TATTGAATTTTCCTTGCTAGATAAATCAGAAAAC	GC-clamp (bold) <i>BamHI</i> restriction site (underlined)	208bp	To change a guanine to adenine
Ribodel1-F Ribodel2-R	GCGCAAGCTT ATGCCCCAGCTCAGAC TCATGGCCTTGGTCTTTATCATGCGACGACCC	GC-clamp (bold) <i>HindIII</i> restriction site (underlined)	327bp	<i>lafK</i> Riboswitch deletion to overexpress <i>lafK</i> gene
Ribodel4-F Ribodel3fliEL-R	GTCGCATGATAAAGACCAAGGCCATGATTTCC GCGCGGATCC CTCGCTGCATTTCTGCATCTGCT	GC-clamp (bold) <i>BamHI</i> restriction site (underlined)	1569bp	<i>lafK</i> Riboswitch deletion to overexpress <i>lafK</i> gene

VIII- Primers used for DNA sequencing and clone screening

Primer name	Primer sequence (5'-3')	Purpose
T7-F*	TAATACGACTCACTATAGGG	To sequence genes inserted into pGEM-T-Easy
SP6-R*	TATTTAGGTGACACTATAG	
pKNG101-F**	CTGCATCAACTTAAC GTAAAAAC	For sequencing and clone screening of inserts
pKNG101-R**	ACATGAGAATTCCCCTGGATTTC	
pKAGb2-F**	TGCACCCAACTGATCTTCAG	For sequencing and clone screening of inserts
pKAGb2-R**	TTTCCCAGTCACGACGTTGT	

*Universal primers provided by the core facility in the University of Sheffield

**Custom designed

References

References

- Abbott, S.L., Cheung, W.K. and Janda, J.M. (2003). The genus *Aeromonas*: biochemical characteristics, atypical reactions, and phenotypic identification schemes. *J Clin Microbiol* **41**, 2348-2357.
- Alm, R.A., Boder, A.J., Free, P.D. and Mattick, J.S. (1996). Identification of a novel gene, pilZ, essential for type 4 fimbrial biogenesis in *Pseudomonas aeruginosa*. *J Bacteriol* **178**, 46-53.
- Altarriba, M., Merino, S., Gavin, R., Canals, R., Rabaan, A., Shaw, J.G. and Tomas, J.M. (2003). A polar flagella operon (flg) of *Aeromonas hydrophila* contains genes required for lateral flagella expression. *Microb Pathog* **34**, 249-259.
- Amikam, D. and Galperin, M.Y. (2006). PilZ domain is part of the bacterial c-di-GMP binding protein. *Bioinformatics* **22**, 3-6.
- Armitage, J.P. and Berry, R.M. (2010). Time for bacteria to slow down. *Cell* **141**, 24-26.
- Bae, S.O., Sugano, Y., Ohi, K. and Shoda, M. (2004). Features of bacterial cellulose synthesis in a mutant generated by disruption of the diguanylate cyclase 1 gene of *Acetobacter xylinum* BPR 2001. *Appl Microbiol Biotechnol* **65**, 315-322.
- Baraquet, C. and Harwood, C.S. (2013). Cyclic diguanosine monophosphate represses bacterial flagella synthesis by interacting with the Walker A motif of the enhancer-binding protein FleQ. *Proc Natl Acad Sci U S A* **110**, 18478-18483.
- Baraquet, C., Murakami, K., Parsek, M.R. and Harwood, C.S. (2012). The FleQ protein from *Pseudomonas aeruginosa* functions as both a repressor and an activator to control gene expression from the *pel* operon promoter in response to c-di-GMP. *Nucleic Acids Res* **40**, 7207-7218.
- Barends, T.R., Hartmann, E., Griese, J.J., Beitlich, T., Kirienko, N.V., Ryjenkov, D.A., *et al.* (2009). Structure and mechanism of a bacterial light-regulated cyclic nucleotide phosphodiesterase. *Nature* **459**, 1015-1018.
- Batey, R.T. (2006). Structures of regulatory elements in mRNAs. *Curr Opin Struct Biol* **16**, 299-306.
- Beaz-Hidalgo, R. and Figueras, M.J. (2013). *Aeromonas* spp. whole genomes and virulence factors implicated in fish disease. *J Fish Dis* **36**, 371-388.
- Bechet, M. and Blondeau, R. (2003). Factors associated with the adherence and biofilm formation by *Aeromonas caviae* on glass surfaces. *J Appl Microbiol* **94**, 1072-1078.
- Bernheimer, A.W. and Avigad, L.S. (1974). Partial characterization of aerolysin, a lytic exotoxin from *Aeromonas hydrophila*. *Infect Immun* **9**, 1016-1021.
- Bharati, B.K., Sharma, I.M., Kasetty, S., Kumar, M., Mukherjee, R. and Chatterji, D. (2012). A full-length bifunctional protein involved in c-di-GMP turnover is required for long-term survival under nutrient starvation in *Mycobacterium smegmatis*. *Microbiology* **158**, 1415-1427.
- Blocker, A., Komoriya, K. and Aizawa, S. (2003). Type III secretion systems and bacterial flagella: insights into their function from structural similarities. *Proc Natl Acad Sci U S A* **100**, 3027-3030.
- Boehm, A., Kaiser, M., Li, H., Spangler, C., Kasper, C.A., Ackermann, M., *et al.* (2010). Second messenger-mediated adjustment of bacterial swimming velocity. *Cell* **141**, 107-116.
- Boles, B.R. and McCarter, L.L. (2002). *Vibrio parahaemolyticus* *scrABC*, a novel operon affecting swarming and capsular polysaccharide regulation. *J Bacteriol* **184**, 5946-5954.
- Breaker, R.R. (2008). Complex riboswitches. *Science* **319**, 1795-1797.

References

- Bucker, R., Krug, S.M., Rosenthal, R., Gunzel, D., Fromm, A., Zeitz, M., *et al.* (2011). Aerolysin from *Aeromonas hydrophila* perturbs tight junction integrity and cell lesion repair in intestinal epithelial HT-29/B6 cells. *J Infect Dis* **204**, 1283-1292.
- Buckley, J.T. and Howard, S.P. (1999). The cytotoxic enterotoxin of *Aeromonas hydrophila* is aerolysin. *Infect Immun* **67**, 466-467.
- Burr, S.E., Stuber, K., Wahli, T. and Frey, J. (2002). Evidence for a type III secretion system in *Aeromonas salmonicida* subsp. *salmonicida*. *J Bacteriol* **184**, 5966-5970.
- Canals, R., Altarriba, M., Vilches, S., Horsburgh, G., Shaw, J.G., Tomás, J.M. and Merino, S. (2006a). Analysis of the lateral flagellar gene system of *Aeromonas hydrophila* AH-3. *J Bacteriol* **188**, 852-862.
- Canals, R., Ramirez, S., Vilches, S., Horsburgh, G., Shaw, J.G., Tomas, J.M. and Merino, S. (2006b). Polar flagellum biogenesis in *Aeromonas hydrophila*. *J Bacteriol* **188**, 542-555.
- Cao, Z., Livoti, E., Losi, A. and Gartner, W. (2010). A blue light-inducible phosphodiesterase activity in the cyanobacterium *Synechococcus elongatus*. *Photochem Photobiol* **86**, 606-611.
- Ceylan, E., Berktaş, M. and Agaoglu, Z. (2009). The occurrence and antibiotic resistance of motile *Aeromonas* in livestock. *Trop Anim Health Prod* **41**, 199-204.
- Chacon, M.R., Soler, L., Groisman, E.A., Guarro, J. and Figueras, M.J. (2004). Type III secretion system genes in clinical *Aeromonas* isolates. *J Clin Microbiol* **42**, 1285-1287.
- Chan, C., Paul, R., Samoray, D., Amiot, N.C., Giese, B., Jenal, U. and Schirmer, T. (2004). Structural basis of activity and allosteric control of diguanylate cyclase. *Proc Natl Acad Sci U S A* **101**, 17084-17089.
- Chopra, A.K., Peterson, J.W., Xu, X.J., Coppenhaver, D.H. and Houston, C.W. (1996). Molecular and biochemical characterization of a heat-labile cytotoxic enterotoxin from *Aeromonas hydrophila*. *Microb Pathog* **21**, 357-377.
- Chopra, A.K., Pham, R. and Houston, C.W. (1994). Cloning and expression of putative cytotoxic enterotoxin-encoding genes from *Aeromonas hydrophila*. *Gene* **139**, 87-91.
- Christen, M., Christen, B., Allan, M.G., Folcher, M., Jenö, P., Grzesiek, S. and Jenal, U. (2007). DgrA is a member of a new family of cyclic diguanosine monophosphate receptors and controls flagellar motor function in *Caulobacter crescentus*. *Proc Natl Acad Sci U S A* **104**, 4112-4117.
- Christen, M., Christen, B., Folcher, M., Schauerte, A. and Jenal, U. (2005). Identification and characterization of a cyclic di-GMP-specific phosphodiesterase and its allosteric control by GTP. *J Biol Chem* **280**, 30829-30837.
- Chuang, H.C., Ho, Y.H., Lay, C.J., Wang, L.S., Tsai, Y.S. and Tsai, C.C. (2011). Different clinical characteristics among *Aeromonas hydrophila*, *Aeromonas veronii* biovar *sobria* and *Aeromonas caviae* monomicrobial bacteremia. *J Korean Med Sci* **26**, 1415-1420.
- Colwell, R.R., MacDonell, M.T. and De Ley, J. (1986). Proposal to Recognize the Family *Aeromonadaceae* fam. nov. *Int. J. Syst. Bacteriol.* **36**, 473-477.
- Dasgupta, N., Arora, S.K. and Ramphal, R. (2000). fleN, a gene that regulates flagellar number in *Pseudomonas aeruginosa*. *J Bacteriol* **182**, 357-364.
- Dasgupta, N., Ferrell, E.P., Kanack, K.J., West, S.E. and Ramphal, R. (2002). fleQ, the gene encoding the major flagellar regulator of *Pseudomonas aeruginosa*, is sigma70 dependent and is downregulated by Vfr, a homolog of *Escherichia coli* cyclic AMP receptor protein. *J Bacteriol* **184**, 5240-5250.
- Dasgupta, N. and Ramphal, R. (2001). Interaction of the antiactivator FleN with the transcriptional activator FleQ regulates flagellar number in *Pseudomonas aeruginosa*. *J Bacteriol* **183**, 6636-6644.

References

- De, N., Navarro, M.V., Raghavan, R.V. and Sondermann, H. (2009). Determinants for the activation and autoinhibition of the diguanylate cyclase response regulator W_{spR}. *J Mol Biol* **393**, 619-633.
- De, N., Pirruccello, M., Krasteva, P.V., Bae, N., Raghavan, R.V. and Sondermann, H. (2008). Phosphorylation-independent regulation of the diguanylate cyclase W_{spR}. *PLoS Biol* **6**, e67.
- Duerig, A., Abel, S., Folcher, M., Nicollier, M., Schwede, T., Amiot, N., *et al.* (2009). Second messenger-mediated spatiotemporal control of protein degradation regulates bacterial cell cycle progression. *Genes Dev* **23**, 93-104.
- Fadl, A.A., Galindo, C.L., Sha, J., Erova, T.E., Houston, C.W., Olano, J.P. and Chopra, A.K. (2006). Deletion of the genes encoding the type III secretion system and cytotoxic enterotoxin alters host responses to *Aeromonas hydrophila* infection. *Microb Pathog* **40**, 198-210.
- Fazli, M., O'Connell, A., Nilsson, M., Niehaus, K., Dow, J.M., Givskov, M., *et al.* (2011). The CRP/FNR family protein Bcam1349 is a c-di-GMP effector that regulates biofilm formation in the respiratory pathogen *Burkholderia cenocepacia*. *Mol Microbiol* **82**, 327-341.
- Ferguson, M.R., Xu, X.J., Houston, C.W., Peterson, J.W., Coppenhaver, D.H., Popov, V.L. and Chopra, A.K. (1997). Hyperproduction, purification, and mechanism of action of the cytotoxic enterotoxin produced by *Aeromonas hydrophila*. *Infect Immun* **65**, 4299-4308.
- Ferreira, R.B., Antunes, L.C., Greenberg, E.P. and McCarter, L.L. (2008). *Vibrio parahaemolyticus* ScrC modulates cyclic dimeric GMP regulation of gene expression relevant to growth on surfaces. *J Bacteriol* **190**, 851-860.
- Figueira, V., Vaz-Moreira, I., Silva, M. and Manaia, C.M. (2011). Diversity and antibiotic resistance of *Aeromonas* spp. in drinking and waste water treatment plants. *Water Res* **45**, 5599-5611.
- Figurski, D.H. and Helinski, D.R. (1979). Replication of an origin-containing derivative of plasmid RK2 dependent on a plasmid function provided in trans. *Proc Natl Acad Sci U S A* **76**, 1648-1652.
- Fiore, J.L. and Nesbitt, D.J. (2013). An RNA folding motif: GNRA tetraloop-receptor interactions. *Q Rev Biophys* **46**, 223-264.
- French, C.E., Bell, J.M. and Ward, F.B. (2008). Diversity and distribution of hemerythrin-like proteins in prokaryotes. *FEMS Microbiol Lett* **279**, 131-145.
- Furukawa, K., Gu, H., Sudarsan, N., Hayakawa, Y., Hyodo, M. and Breaker, R.R. (2012). Identification of ligand analogues that control c-di-GMP riboswitches. *ACS Chem Biol* **7**, 1436-1443.
- Gavín, R., Rabaan, A.A., Merino, S., Tomás, J.M., Gryllos, I. and Shaw, J.G. (2002). Lateral flagella of *Aeromonas* species are essential for epithelial cell adherence and biofilm formation. *Mol Microbiol* **43**, 383-397.
- Ghengehesh, K.S., Abeid, S.S., Jaber, M.M. and Ben-Taher, S.A. (1999). Isolation and haemolytic activity of *Aeromonas* species from domestic dogs and cats. *Comp Immunol Microbiol Infect Dis* **22**, 175-179.
- Giardina, G., Paiardini, A., Fernicola, S., Franceschini, S., Rinaldo, S., Stelitano, V. and Cutruzzola, F. (2013). Investigating the allosteric regulation of YfiN from *Pseudomonas aeruginosa*: clues from the structure of the catalytic domain. *PLoS One* **8**, e81324.
- Goñi-Urriza, M., Pineau, L., Capdepu, M., Roques, C., Caumette, P. and Quentin, C. (2000). Antimicrobial resistance of mesophilic *Aeromonas* spp. isolated from two European rivers. *J Antimicrob Chemother* **46**, 297-301.
- Guzzo, C.R., Salinas, R.K., Andrade, M.O. and Farah, C.S. (2009). PILZ protein structure and interactions with PILB and the FIMX EAL domain: implications for control of type IV pilus biogenesis. *J Mol Biol* **393**, 848-866.

References

- Hadi, N., Yang, Q., Barnett, T.C., Tabei, S.M., Kirov, S.M. and Shaw, J.G. (2012). Bundle-forming pilus locus of *Aeromonas veronii* bv. Sobria. *Infect Immun* **80**, 1351-1360.
- Hall, P. and Krieg, N. (1983). Swarming of *Azospirillum brasilense* on solid media. *Can J Microbiol* **29**, 1592-1594.
- Hanahan, D. (1983). Studies on transformation of *Escherichia coli* with plasmids. *J Mol Biol* **166**, 557-580.
- Hasegawa, K., Masuda, S. and Ono, T.A. (2006). Light induced structural changes of a full-length protein and its BLUF domain in YcgF(Blrp), a blue-light sensing protein that uses FAD (BLUF). *Biochemistry* **45**, 3785-3793.
- Hecht, G.B. and Newton, A. (1995). Identification of a novel response regulator required for the swarmer-to-stalked-cell transition in *Caulobacter crescentus*. *J Bacteriol* **177**, 6223-6229.
- Hengge, R. (2009). Principles of c-di-GMP signalling in bacteria. *Nat Rev Microbiol* **7**, 263-273.
- Henry, J.T. and Crosson, S. (2011). Ligand-binding PAS domains in a genomic, cellular, and structural context. *Annu Rev Microbiol* **65**, 261-286.
- Herrero, M., de Lorenzo, V. and Timmis, K.N. (1990). Transposon vectors containing non-antibiotic resistance selection markers for cloning and stable chromosomal insertion of foreign genes in gram-negative bacteria. *J Bacteriol* **172**, 6557-6567.
- Hickman, J.W. and Harwood, C.S. (2008). Identification of FleQ from *Pseudomonas aeruginosa* as a c-di-GMP-responsive transcription factor. *Mol Microbiol* **69**, 376-389.
- Hickman, J.W., Tifrea, D.F. and Harwood, C.S. (2005). A chemosensory system that regulates biofilm formation through modulation of cyclic diguanylate levels. *Proc Natl Acad Sci U S A* **102**, 14422-14427.
- Hobley, L., Fung, R.K., Lambert, C., Harris, M.A., Dabhi, J.M., King, S.S., et al. (2012). Discrete cyclic di-GMP-dependent control of bacterial predation versus axenic growth in *Bdellovibrio bacteriovorus*. *PLoS Pathog* **8**, e1002493.
- Huizinga, H., Esch, G. and Hazen, T. (1979). Histopathology of red-sore disease (*Aeromonas hydrophila*) in naturally and experimentally infected largemouth bass *Micropterus salmoides* (Lacepede). *Journal of Fish Diseases* **2**, 263-277.
- Hurley, J.H. (2003). GAF domains: cyclic nucleotides come full circle. *Sci STKE* **2003**, Pe1.
- Huys, G., Pearson, M., Kampfer, P., Denys, R., Cnockaert, M., Inglis, V. and Swings, J. (2003). *Aeromonas hydrophila* subsp. ranae subsp. nov., isolated from septicemic farmed frogs in Thailand. *Int J Syst Evol Microbiol* **53**, 885-891.
- Hänninen, M.L., Salmi, S., Mattila, L., Taipalinen, R. and Siitonen, A. (1995). Association of *Aeromonas* spp. with travellers' diarrhoea in Finland. *J Med Microbiol* **42**, 26-31.
- Inoue, K., Kosako, Y., Suzuki, K. and Shimada, T. (1991). Peritrichous flagellation in *Plesiomonas shigelloides* strains. *Jpn J Med Sci Biol* **44**, 141-146.
- Jalal, K.C., Faizul, H.N., Naim, M.A., John, B.A. and Kamaruzzaman, B.Y. (2012). Studies on water quality and pathogenic bacteria in coastal water Langkawi, Malaysia. *J Environ Biol* **33**, 831-835.
- Janda, J.M. and Abbott, S.L. (2010). The genus *Aeromonas*: taxonomy, pathogenicity, and infection. *Clin Microbiol Rev* **23**, 35-73.
- Janda, J.M. and Duffey, P.S. (1988). Mesophilic aeromonads in human disease: current taxonomy, laboratory identification, and infectious disease spectrum. *Rev Infect Dis* **10**, 980-997.

References

- Kampfer, P., Christmann, C., Swings, J. and Huys, G. (1999). In vitro susceptibilities of *Aeromonas* genomic species to 69 antimicrobial agents. *Syst Appl Microbiol* **22**, 662-669.
- Kaniga, K., Delor, I. and Cornelis, G.R. (1991). A wide-host-range suicide vector for improving reverse genetics in gram-negative bacteria: inactivation of the blaA gene of *Yersinia enterocolitica*. *Gene* **109**, 137-141.
- Kawagishi, I., Maekawa, Y., Atsumi, T., Homma, M. and Imae, Y. (1995). Isolation of the polar and lateral flagellum-defective mutants in *Vibrio alginolyticus* and identification of their flagellar driving energy sources. *J Bacteriol* **177**, 5158-5160.
- Kazmierczak, B.I., Lebron, M.B. and Murray, T.S. (2006). Analysis of FimX, a phosphodiesterase that governs twitching motility in *Pseudomonas aeruginosa*. *Mol Microbiol* **60**, 1026-1043.
- Kearns, D.B. (2010). A field guide to bacterial swarming motility. *Nat Rev Microbiol* **8**, 634-644.
- Khajanchi, B.K., Fadl, A.A., Borchardt, M.A., Berg, R.L., Horneman, A.J., Stemper, M.E., et al. (2010). Distribution of virulence factors and molecular fingerprinting of *Aeromonas* species isolates from water and clinical samples: suggestive evidence of water-to-human transmission. *Appl Environ Microbiol* **76**, 2313-2325.
- Khajanchi, B.K., Sha, J., Kozlova, E.V., Erova, T.E., Suarez, G., Sierra, J.C., et al. (2009). N-acylhomoserine lactones involved in quorum sensing control the type VI secretion system, biofilm formation, protease production, and in vivo virulence in a clinical isolate of *Aeromonas hydrophila*. *Microbiology* **155**, 3518-3531.
- Kim, Y.K. and McCarter, L.L. (2004). Cross-regulation in *Vibrio parahaemolyticus*: compensatory activation of polar flagellar genes by the lateral flagellar regulator LafK. *J Bacteriol* **186**, 4014-4018.
- Kim, Y.K. and McCarter, L.L. (2007). ScrG, a GGDEF-EAL protein, participates in regulating swarming and sticking in *Vibrio parahaemolyticus*. *J Bacteriol* **189**, 4094-4107.
- Kimura, M., Araoka, H. and Yoneyama, A. (2013). *Aeromonas caviae* is the most frequent pathogen amongst cases of *Aeromonas* bacteremia in Japan. *Scand J Infect Dis* **45**, 304-309.
- Kirov, S.M., Barnett, T.C., Pepe, C.M., Strom, M.S. and Albert, M.J. (2000). Investigation of the role of type IV *Aeromonas* pilus (Tap) in the pathogenesis of *Aeromonas* gastrointestinal infection. *Infect Immun* **68**, 4040-4048.
- Kirov, S.M., Castrisios, M. and Shaw, J.G. (2004). *Aeromonas* flagella (polar and lateral) are enterocyte adhesins that contribute to biofilm formation on surfaces. *Infect Immun* **72**, 1939-1945.
- Kirov, S.M., Tassell, B.C., Semmler, A.B., O'Donovan, L.A., Rabaan, A.A. and Shaw, J.G. (2002). Lateral flagella and swarming motility in *Aeromonas* species. *J Bacteriol* **184**, 547-555.
- Ko, J., Ryu, K.S., Kim, H., Shin, J.S., Lee, J.O., Cheong, C. and Choi, B.S. (2010). Structure of PP4397 reveals the molecular basis for different c-di-GMP binding modes by Pilz domain proteins. *J Mol Biol* **398**, 97-110.
- Kokare, C., Chakraborty, S., Khopade, A. and Mahadik, K. (2009). Biofilm: Importance and applications. *Indian Journal of Biotechnology* **8**, 159-168.
- Kotloff, K.L., Nataro, J.P., Blackwelder, W.C., Nasrin, D., Farag, T.H., Panchalingam, S., et al. (2013). Burden and aetiology of diarrhoeal disease in infants and young children in developing countries (the Global Enteric Multicenter Study, GEMS): a prospective, case-control study. *Lancet*.
- Kovach, M., Elzer, P., Hill, D., Robertson, G., Farris, M., Roop, R.n. and Peterson, K. (1995). Four new derivatives of the broad-host-range cloning vector pBBR1MCS, carrying different antibiotic resistance cassettes. *Gene* **166**, 175-176.

References

- Kovach, M.E., Phillips, R.W., Elzer, P.H., Roop, R.M., 2nd and Peterson, K.M. (1994). pBBR1MCS: a broad-host-range cloning vector. *Biotechniques* **16**, 800-802.
- Kozlova, E.V., Khajanchi, B.K., Popov, V.L., Wen, J. and Chopra, A.K. (2012). Impact of QseBC system in c-di-GMP-dependent quorum sensing regulatory network in a clinical isolate SSU of *Aeromonas hydrophila*. *Microb Pathog* **53**, 115-124.
- Kozlova, E.V., Khajanchi, B.K., Sha, J. and Chopra, A.K. (2011). Quorum sensing and c-di-GMP-dependent alterations in gene transcripts and virulence-associated phenotypes in a clinical isolate of *Aeromonas hydrophila*. *Microb Pathog* **50**, 213-223.
- Kozlova, E.V., Popov, V.L., Sha, J., Foltz, S.M., Erova, T.E., Agar, S.L., *et al.* (2008). Mutation in the S-ribosylhomocysteinase (*luxS*) gene involved in quorum sensing affects biofilm formation and virulence in a clinical isolate of *Aeromonas hydrophila*. *Microb Pathog* **45**, 343-354.
- Kraemer, S. (2004). Iron oxide dissolution and solubility in the presence of siderophores. *Aquat. Sci.* **66**, 3-18.
- Krasteva, P.V., Fong, J.C., Shikuma, N.J., Beyhan, S., Navarro, M.V., Yildiz, F.H. and Sondermann, H. (2010). *Vibrio cholerae* VpsT regulates matrix production and motility by directly sensing cyclic di-GMP. *Science* **327**, 866-868.
- Krejci, E., Andelova, A., Porazilova, I. and Sedlacek, I. (2006). [*Aeromonas* spp. as the causative agent of acute diarrhoea in children under 1 year of age]. *Epidemiol Mikrobiol Imunol* **55**, 92-98.
- Kupfer, M., Kuhnert, P., Korczak, B.M., Peduzzi, R. and Demarta, A. (2006). Genetic relationships of *Aeromonas* strains inferred from 16S rRNA, *gyrB* and *rpoB* gene sequences. *Int J Syst Evol Microbiol* **56**, 2743-2751.
- Lacey, M., Agasing, A., Lowry, R. and Green, J. (2013). Identification of the YfgF MASE1 domain as a modulator of bacterial responses to aspartate. *Open Biol* **3**, 130046.
- Lamy, B., Kodjo, A., and Laurent, F. (2009). Prospective nationwide study of *Aeromonas* infections in France. *J Clin Microbiol* **47**, 1234-1237.
- Lango, Z., Borsodi, A.K. and Micsinai, A. (2002). Comparative studies on *Aeromonas* strains isolated from Lakes Balaton (Hungary) and Ferto/Neusiedlersee (Hungary). *Acta Microbiol Immunol Hung* **49**, 37-45.
- Latchman, D.S. (1997). Transcription factors: an overview. *Int J Biochem Cell Biol* **29**, 1305-1312.
- Leduc, J.L. and Roberts, G.P. (2009). Cyclic di-GMP allosterically inhibits the CRP-like protein (Clp) of *Xanthomonas axonopodis* pv. citri. *J Bacteriol* **191**, 7121-7122.
- Lee, E.R., Baker, J.L., Weinberg, Z., Sudarsan, N. and Breaker, R.R. (2010). An allosteric self-splicing ribozyme triggered by a bacterial second messenger. *Science* **329**, 845-848.
- Lee, V.T., Matewish, J.M., Kessler, J.L., Hyodo, M., Hayakawa, Y. and Lory, S. (2007). A cyclic-di-GMP receptor required for bacterial exopolysaccharide production. *Mol Microbiol* **65**, 1474-1484.
- Levet-Paulo, M., Lazzaroni, J.C., Gilbert, C., Atlan, D., Doublet, P. and Vianney, A. (2011). The atypical two-component sensor kinase Lpl0330 from *Legionella pneumophila* controls the bifunctional diguanylate cyclase-phosphodiesterase Lpl0329 to modulate bis-(3'-5')-cyclic dimeric GMP synthesis. *J Biol Chem* **286**, 31136-31144.
- Li, G., Miller, A., Bull, H. and Howard, S.P. (2011a). Assembly of the type II secretion system: identification of ExeA residues critical for peptidoglycan binding and secretin multimerization. *J Bacteriol* **193**, 197-204.

References

- Li, T.N., Chin, K.H., Fung, K.M., Yang, M.T., Wang, A.H. and Chou, S.H. (2011b). A novel tetrameric PilZ domain structure from xanthomonads. *PLoS One* **6**, e22036.
- Li, T.N., Chin, K.H., Liu, J.H., Wang, A.H. and Chou, S.H. (2009). XC1028 from *Xanthomonas campestris* adopts a PilZ domain-like structure without a c-di-GMP switch. *Proteins* **75**, 282-288.
- Lim, B., Beyhan, S. and Yildiz, F.H. (2007). Regulation of *Vibrio* polysaccharide synthesis and virulence factor production by CdgC, a GGDEF-EAL domain protein, in *Vibrio cholerae*. *J Bacteriol* **189**, 717-729.
- Lindsay, D. and von Holy, A. (2006). Bacterial biofilms within the clinical setting: what healthcare professionals should know. *J Hosp Infect* **64**, 313-325.
- Lovering, A.L., Capeness, M.J., Lambert, C., Hopley, L. and Sockett, R.E. (2011). The structure of an unconventional HD-GYP protein from *Bdellovibrio* reveals the roles of conserved residues in this class of cyclic-di-GMP phosphodiesterases. *MBio* **2**.
- Malone, J.G., Williams, R., Christen, M., Jenal, U., Spiers, A.J. and Rainey, P.B. (2007). The structure-function relationship of WspR, a *Pseudomonas fluorescens* response regulator with a GGDEF output domain. *Microbiology* **153**, 980-994.
- Marsh, J.W. and Taylor, R.K. (1999). Genetic and transcriptional analyses of the *Vibrio cholerae* mannose-sensitive hemagglutinin type 4 pilus gene locus. *J Bacteriol* **181**, 1110-1117.
- Martinez, M.J., Simon-Pujol, D., Congregado, F., Merino, S., Rubires, X. and Tomas, J.M. (1995). The presence of capsular polysaccharide in mesophilic *Aeromonas hydrophila* serotypes O:11 and O:34. *FEMS Microbiol Lett* **128**, 69-73.
- Martino, M.E., Fasolato, L., Montemurro, F., Rosteghin, M., Manfrin, A., Patarnello, T., *et al.* (2011). Determination of microbial diversity of *Aeromonas* strains on the basis of multilocus sequence typing, phenotype, and presence of putative virulence genes. *Appl Environ Microbiol* **77**, 4986-5000.
- Mason, C. (2013) Investigation of the Modulation Mechanisms of the *Aeromonas caviae* LafK and PilZ Proteins and their Role in Swarming Motility. In *Molecular Biology and Biotechnology*. University of Sheffield.
- McCarter, L., Hilmen, M. and Silverman, M. (1988). Flagellar dynamometer controls swarmer cell differentiation of *V. parahaemolyticus*. *Cell* **54**, 345-351.
- McClain, J., Rollo, D.R., Rushing, B.G. and Bauer, C.E. (2002). *Rhodospirillum centenum* utilizes separate motor and switch components to control lateral and polar flagellum rotation. *J Bacteriol* **184**, 2429-2438.
- McMahon, M.A. and Wilson, I.G. (2001). The occurrence of enteric pathogens and *Aeromonas* species in organic vegetables. *Int J Food Microbiol* **70**, 155-162.
- Merighi, M., Lee, V.T., Hyodo, M., Hayakawa, Y. and Lory, S. (2007). The second messenger bis-(3'-5')-cyclic-GMP and its PilZ domain-containing receptor Alg44 are required for alginate biosynthesis in *Pseudomonas aeruginosa*. *Mol Microbiol* **65**, 876-895.
- Merino, S., Shaw, J.G. and Tomas, J.M. (2006). Bacterial lateral flagella: an inducible flagella system. *FEMS Microbiol Lett* **263**, 127-135.
- Miller, M.B. and Bassler, B.L. (2001). Quorum sensing in bacteria. *Annu Rev Microbiol* **55**, 165-199.
- Moro, E.M., Weiss, R.D., Friedrich, R.S., de Vargas, A.C., Weiss, L.H. and Nunes, M.P. (1999). *Aeromonas hydrophila* isolated from cases of bovine seminal vesiculitis in south Brazil. *J Vet Diagn Invest* **11**, 189-191.
- Mougel, C. and Zhulin, I.B. (2001). CHASE: an extracellular sensing domain common to transmembrane receptors from prokaryotes, lower eukaryotes and plants. *Trends Biochem Sci* **26**, 582-584.

References

- Nakhamchik, A., Wilde, C. and Rowe-Magnus, D.A. (2008). Cyclic-di-GMP regulates extracellular polysaccharide production, biofilm formation, and rugose colony development by *Vibrio vulnificus*. *Appl Environ Microbiol* **74**, 4199-4209.
- Namdari, H. and Bottone, E.J. (1990). Microbiologic and clinical evidence supporting the role of *Aeromonas caviae* as a pediatric enteric pathogen. *J Clin Microbiol* **28**, 837-840.
- Nayduch, D., Noblet, G.P. and Stutzenberger, F.J. (2002). Vector potential of houseflies for the bacterium *Aeromonas caviae*. *Med Vet Entomol* **16**, 193-198.
- Nhung, P.H., Hata, H., Ohkusu, K., Noda, M., Shah, M.M., Goto, K. and Ezaki, T. (2007). Use of the novel phylogenetic marker *dnaJ* and DNA-DNA hybridization to clarify interrelationships within the genus *Aeromonas*. *Int J Syst Evol Microbiol* **57**, 1232-1237.
- Nikolskaya, A.N., Mulikidjanian, A.Y., Beech, I.B. and Galperin, M.Y. (2003). MASE1 and MASE2: two novel integral membrane sensory domains. *J Mol Microbiol Biotechnol* **5**, 11-16.
- O'Rourke, J., Lee, A. and Fox, J.G. (1992). An ultrastructural study of *Helicobacter mustelae* and evidence of a specific association with gastric mucosa. *J Med Microbiol* **36**, 420-427.
- Parker, J.L., Day-Williams, M.J., Tomas, J.M., Stafford, G.P. and Shaw, J.G. (2012). Identification of a putative glycosyltransferase responsible for the transfer of pseudaminic acid onto the polar flagellin of *Aeromonas caviae* Sch3N. *Microbiologyopen* **1**, 149-160.
- Parkinson, J.S. (2010). Signaling mechanisms of HAMP domains in chemoreceptors and sensor kinases. *Annu Rev Microbiol* **64**, 101-122.
- Paul, K., Nieto, V., Carlquist, W.C., Blair, D.F. and Harshey, R.M. (2010). The c-di-GMP binding protein YcgR controls flagellar motor direction and speed to affect chemotaxis by a "backstop brake" mechanism. *Mol Cell* **38**, 128-139.
- Paul, R., Weiser, S., Amiot, N.C., Chan, C., Schirmer, T., Giese, B. and Jenal, U. (2004). Cell cycle-dependent dynamic localization of a bacterial response regulator with a novel di-guanylate cyclase output domain. *Genes Dev* **18**, 715-727.
- Pavan, M.E., Abbott, S.L., Zorzopulos, J. and Janda, J.M. (2000). *Aeromonas salmonicida* subsp. *pectinolytica* subsp. nov., a new pectinase-positive subspecies isolated from a heavily polluted river. *Int J Syst Evol Microbiol* **50**, 1119-1124.
- Petters, T., Zhang, X., Nesper, J., Treuner-Lange, A., Gomez-Santos, N., Hoppert, M., *et al.* (2012). The orphan histidine protein kinase SgmT is a c-di-GMP receptor and regulates composition of the extracellular matrix together with the orphan DNA binding response regulator DigR in *Myxococcus xanthus*. *Mol Microbiol* **84**, 147-165.
- Pierce, R.L., Daley, C.A., Gates, C.E. and Wohlgemuth, K. (1973). *Aeromonas hydrophila* septicemia in a dog. *J Am Vet Med Assoc* **162**, 469.
- Popoff, M.Y., Coynault, C., Kiredjian, M. and Lemelin, M. (1981). Polynucleotide sequence relatedness among motile *Aeromonas* species. **5**, 109-114.
- Pratt, J.T., Tamayo, R., Tischler, A.D. and Camilli, A. (2007). PilZ domain proteins bind cyclic diguanylate and regulate diverse processes in *Vibrio cholerae*. *J Biol Chem* **282**, 12860-12870.
- Pukatzki, S., McAuley, S.B. and Miyata, S.T. (2009). The type VI secretion system: translocation of effectors and effector-domains. *Curr Opin Microbiol* **12**, 11-17.
- Pultz, I.S., Christen, M., Kulasekara, H.D., Kennard, A., Kulasekara, B. and Miller, S.I. (2012). The response threshold of *Salmonella* PilZ domain proteins is determined by their binding affinities for c-di-GMP. *Mol Microbiol* **86**, 1424-1440.

References

- Qadri, F., Hossain, S.A., Ciznar, I., Haider, K., Ljungh, A., Wadstrom, T. and Sack, D.A. (1988). Congo red binding and salt aggregation as indicators of virulence in *Shigella* species. *J Clin Microbiol* **26**, 1343-1348.
- Rabaan, A.A., Gryllos, I., Tomás, J.M. and Shaw, J.G. (2001). Motility and the polar flagellum are required for *Aeromonas caviae* adherence to HEp-2 cells. *Infect Immun* **69**, 4257-4267.
- Rahman, M., Simm, R., Kader, A., Basseres, E., Römling, U. and Möllby, R. (2007). The role of c-di-GMP signaling in an *Aeromonas veronii* biovar *sobria* strain. *FEMS Microbiol Lett* **273**, 172-179.
- Ramelot, T.A., Yee, A., Cort, J.R., Semesi, A., Arrowsmith, C.H. and Kennedy, M.A. (2007). NMR structure and binding studies confirm that PA4608 from *Pseudomonas aeruginosa* is a PilZ domain and a c-di-GMP binding protein. *Proteins* **66**, 266-271.
- Ramos, H.C., Rumbo, M. and Sirard, J.C. (2004). Bacterial flagellins: mediators of pathogenicity and host immune responses in mucosa. *Trends Microbiol* **12**, 509-517.
- Rao, F., Yang, Y., Qi, Y. and Liang, Z.X. (2008). Catalytic mechanism of cyclic di-GMP-specific phosphodiesterase: a study of the EAL domain-containing RocR from *Pseudomonas aeruginosa*. *J Bacteriol* **190**, 3622-3631.
- Ren, C.P., Beatson, S.A., Parkhill, J. and Pallen, M.J. (2005). The Flag-2 locus, an ancestral gene cluster, is potentially associated with a novel flagellar system from *Escherichia coli*. *J Bacteriol* **187**, 1430-1440.
- Ritchings, B.W., Almira, E.C., Lory, S. and Ramphal, R. (1995). Cloning and phenotypic characterization of fleS and fleR, new response regulators of *Pseudomonas aeruginosa* which regulate motility and adhesion to mucin. *Infect Immun* **63**, 4868-4876.
- Roger, F., Lamy, B., Jumas-Bilak, E., Kodjo, A. and Marchandin, H. (2012). Ribosomal multi-operon diversity: an original perspective on the genus *Aeromonas*. *PLoS One* **7**, e46268.
- Romling, U., Galperin, M.Y. and Gomelsky, M. (2013). Cyclic di-GMP: the first 25 years of a universal bacterial second messenger. *Microbiol Mol Biol Rev* **77**, 1-52.
- Ross, P., Weinhouse, H., Aloni, Y., Michaeli, D., Weinberger-Ohana, P., Mayer, R., *et al.* (1987). Regulation of cellulose synthesis in *Acetobacter xylinum* by cyclic diguanylic acid. *Nature* **325**, 279-281.
- Ryan, R.P. and Dow, J.M. (2010). Intermolecular interactions between HD-GYP and GGDEF domain proteins mediate virulence-related signal transduction in *Xanthomonas campestris*. *Virulence* **1**, 404-408.
- Ryan, R.P., Fouhy, Y., Lucey, J.F., Crossman, L.C., Spiro, S., He, Y.W., *et al.* (2006). Cell-cell signaling in *Xanthomonas campestris* involves an HD-GYP domain protein that functions in cyclic di-GMP turnover. *Proc Natl Acad Sci U S A* **103**, 6712-6717.
- Ryan, R.P., Lucey, J., O'Donovan, K., McCarthy, Y., Yang, L., Tolker-Nielsen, T. and Dow, J.M. (2009). HD-GYP domain proteins regulate biofilm formation and virulence in *Pseudomonas aeruginosa*. *Environ Microbiol* **11**, 1126-1136.
- Ryan, R.P., Tolker-Nielsen, T. and Dow, J.M. (2012). When the PilZ don't work: effectors for cyclic di-GMP action in bacteria. *Trends Microbiol* **20**, 235-242.
- Ryjenkov, D.A., Simm, R., Romling, U. and Gomelsky, M. (2006). The PilZ domain is a receptor for the second messenger c-di-GMP: the PilZ domain protein YcgR controls motility in enterobacteria. *J Biol Chem* **281**, 30310-30314.
- Ryjenkov, D.A., Tarutina, M., Moskvina, O.V. and Gomelsky, M. (2005). Cyclic diguanylate is a ubiquitous signaling molecule in bacteria: insights into biochemistry of the GGDEF protein domain. *J Bacteriol* **187**, 1792-1798.

References

- Safari, M., Amache, R., Esmaeilshirazifard, E. and Keshavarz, T. (2014). Microbial metabolism of quorum-sensing molecules acyl-homoserine lactones, gamma-heptalactone and other lactones. *Appl Microbiol Biotechnol* **98**, 3401-3412.
- Sarimehmetoglu, B. and Kuplulu, O. (2001). Isolation and identification of motile *Aeromonas* species from chicken. *Dtsch Tierarztl Wochenschr* **108**, 465-467.
- Sasakura, Y., Hirata, S., Sugiyama, S., Suzuki, S., Taguchi, S., Watanabe, M., *et al.* (2002). Characterization of a direct oxygen sensor heme protein from *Escherichia coli*. Effects of the heme redox states and mutations at the heme-binding site on catalysis and structure. *J Biol Chem* **277**, 23821-23827.
- Schirmer, T. and Jenal, U. (2009). Structural and mechanistic determinants of c-di-GMP signalling. *Nat Rev Microbiol* **7**, 724-735.
- Schmidt, A.J., Ryjenkov, D.A. and Gomelsky, M. (2005). The ubiquitous protein domain EAL is a cyclic diguanylate-specific phosphodiesterase: enzymatically active and inactive EAL domains. *J Bacteriol* **187**, 4774-4781.
- Schoenhofen, I.C., Li, G., Strozen, T.G. and Howard, S.P. (2005). Purification and characterization of the N-terminal domain of ExeA: a novel ATPase involved in the type II secretion pathway of *Aeromonas hydrophila*. *J Bacteriol* **187**, 6370-6378.
- Scoaris, D., Bizerra, F., Yamada-Ogatta, S., Filho, B., Ueda-Nakamura, T., Nakamura, C. and Dias Filho, B. (2008). The occurrence of *Aeromonas* spp. in the Bottled Mineral Water, Well water and Tap water from the Municipal Supplies. *Brazilian Archives of Biology and Technology* **51**, 1049-1055.
- Senderovich, Y., Ken-Dror, S., Vainblat, I., Blau, D., Izhaki, I. and Halpern, M. (2012). A molecular study on the prevalence and virulence potential of *Aeromonas* spp. recovered from patients suffering from diarrhea in Israel. *PLoS One* **7**, e30070.
- Sepe, A., Barbieri, P., Peduzzi, R. and Demarta, A. (2008). Evaluation of recA sequencing for the classification of *Aeromonas* strains at the genotype level. *Lett Appl Microbiol* **46**, 439-444.
- Seshadri, R., Joseph, S.W., Chopra, A.K., Sha, J., Shaw, J., Graf, J., *et al.* (2006). Genome sequence of *Aeromonas hydrophila* ATCC 7966T: jack of all trades. *J Bacteriol* **188**, 8272-8282.
- Sha, J., Rosenzweig, J.A., Kozlova, E.V., Wang, S., Erova, T.E., Kirtley, M.L., *et al.* (2013). Evaluation of the roles played by Hcp and VgrG type 6 secretion system effectors in *Aeromonas hydrophila* SSU pathogenesis. *Microbiology* **159**, 1120-1135.
- Shimada, T., Sakazaki, R. and Suzuki, K. (1985). Peritrichous flagella in mesophilic strains of *Aeromonas*. *Jpn J Med Sci Biol* **38**, 141-145.
- Shin, J.S., Ryu, K.S., Ko, J., Lee, A. and Choi, B.S. (2011). Structural characterization reveals that a PilZ domain protein undergoes substantial conformational change upon binding to cyclic dimeric guanosine monophosphate. *Protein Sci* **20**, 270-277.
- Shinoda, S. and Okamoto, K. (1977). Formation and function of *Vibrio parahaemolyticus* lateral flagella. *J Bacteriol* **129**, 1266-1271.
- Sierra, J.C., Suarez, G., Sha, J., Baze, W.B., Foltz, S.M. and Chopra, A.K. (2010). Unraveling the mechanism of action of a new type III secretion system effector AexU from *Aeromonas hydrophila*. *Microb Pathog* **49**, 122-134.
- Simon, R., Priefer, U. and Puhler, A. (1983). A broad host range mobilization system for in vivo genetic engineering: transposon mutagenesis in Gram-negative bacteria. *Biotechnology* **1**, 784-791.
- Smith, K.D., Shanahan, C.A., Moore, E.L., Simon, A.C. and Strobel, S.A. (2011a). Structural basis of differential ligand recognition by two classes of bis-(3'-5')-cyclic dimeric guanosine monophosphate-binding riboswitches. *Proc Natl Acad Sci U S A* **108**, 7757-7762.

References

- Smith, K.D. and Strobel, S.A. (2011b). Interactions of the c-di-GMP riboswitch with its second messenger ligand. *Biochem Soc Trans* **39**, 647-651.
- Soler, L., Yanez, M.A., Chacon, M.R., Aguilera-Arreola, M.G., Catalan, V., Figueras, M.J. and Martinez-Murcia, A.J. (2004). Phylogenetic analysis of the genus *Aeromonas* based on two housekeeping genes. *Int J Syst Evol Microbiol* **54**, 1511-1519.
- Sondermann, H., Shikuma, N.J. and Yildiz, F.H. (2012). You've come a long way: c-di-GMP signaling. *Curr Opin Microbiol* **15**, 140-146.
- Stelitano, V., Giardina, G., Paiardini, A., Castiglione, N., Cutruzzola, F. and Rinaldo, S. (2013). C-di-GMP hydrolysis by *Pseudomonas aeruginosa* HD-GYP phosphodiesterases: analysis of the reaction mechanism and novel roles for pGpG. *PLoS One* **8**, e74920.
- Stewart, B.J., Enos-Berlage, J.L. and McCarter, L.L. (1997). The lonS gene regulates swarmer cell differentiation of *Vibrio parahaemolyticus*. *J Bacteriol* **179**, 107-114.
- Stewart, B.J. and McCarter, L.L. (2003). Lateral flagellar gene system of *Vibrio parahaemolyticus*. *J Bacteriol* **185**, 4508-4518.
- Strozen, T.G., Stanley, H., Gu, Y., Boyd, J., Bagdasarian, M., Sandkvist, M. and Howard, S.P. (2011). Involvement of the GspAB complex in assembly of the type II secretion system secretin of *Aeromonas* and *Vibrio* species. *J Bacteriol* **193**, 2322-2331.
- Suarez, G., Sierra, J.C., Erova, T.E., Sha, J., Horneman, A.J. and Chopra, A.K. (2010a). A type VI secretion system effector protein, VgrG1, from *Aeromonas hydrophila* that induces host cell toxicity by ADP ribosylation of actin. *J Bacteriol* **192**, 155-168.
- Suarez, G., Sierra, J.C., Kirtley, M.L. and Chopra, A.K. (2010b). Role of Hcp, a type 6 secretion system effector, of *Aeromonas hydrophila* in modulating activation of host immune cells. *Microbiology* **156**, 3678-3688.
- Suarez, G., Sierra, J.C., Sha, J., Wang, S., Erova, T.E., Fadl, A.A., *et al.* (2008). Molecular characterization of a functional type VI secretion system from a clinical isolate of *Aeromonas hydrophila*. *Microb Pathog* **44**, 344-361.
- Sudarsan, N., Lee, E.R., Weinberg, Z., Moy, R.H., Kim, J.N., Link, K.H. and Breaker, R.R. (2008). Riboswitches in eubacteria sense the second messenger cyclic di-GMP. *Science* **321**, 411-413.
- Suzuki, K., Babitzke, P., Kushner, S.R. and Romeo, T. (2006). Identification of a novel regulatory protein (CsrD) that targets the global regulatory RNAs CsrB and CsrC for degradation by RNase E. *Genes Dev* **20**, 2605-2617.
- Tal, R., Wong, H.C., Calhoun, R., Gelfand, D., Fear, A.L., Volman, G., *et al.* (1998). Three cdg operons control cellular turnover of cyclic di-GMP in *Acetobacter xylinum*: genetic organization and occurrence of conserved domains in isoenzymes. *J Bacteriol* **180**, 4416-4425.
- Tamayo, R., Pratt, J.T. and Camilli, A. (2007). Roles of cyclic diguanylate in the regulation of bacterial pathogenesis. *Annu Rev Microbiol* **61**, 131-148.
- Tao, F., He, Y.W., Wu, D.H., Swarup, S. and Zhang, L.H. (2010). The cyclic nucleotide monophosphate domain of *Xanthomonas campestris* global regulator Clp defines a new class of cyclic di-GMP effectors. *J Bacteriol* **192**, 1020-1029.
- Tarutina, M., Ryjenkov, D.A. and Gomelsky, M. (2006). An unorthodox bacteriophytochrome from *Rhodobacter sphaeroides* involved in turnover of the second messenger c-di-GMP. *J Biol Chem* **281**, 34751-34758.

References

- Tchigvintsev, A., Xu, X., Singer, A., Chang, C., Brown, G., Proudfoot, M., *et al.* (2010). Structural insight into the mechanism of c-di-GMP hydrolysis by EAL domain phosphodiesterases. *J Mol Biol* **402**, 524-538.
- Thomas, M. Unpublished pKAGb2(-). The University of Sheffield.
- Tiwari, R.P., Deol, K., Rishi, P. and Grewal, J.S. (2002). Factors affecting haemolysin production and congo red binding in *Salmonella enterica* serovar Typhimurium DT 98. *J Med Microbiol* **51**, 503-509.
- Tomas, J.M. (2012). The main *Aeromonas* pathogenic factors. *ISRN Microbiol* **2012**, 256261.
- Tseng, T.T., Tyler, B.M. and Setubal, J.C. (2009). Protein secretion systems in bacterial-host associations, and their description in the Gene Ontology. *BMC Microbiol* **9 Suppl 1**, S2.
- Tuckerman, J.R., Gonzalez, G. and Gilles-Gonzalez, M.A. (2011). Cyclic di-GMP activation of polynucleotide phosphorylase signal-dependent RNA processing. *J Mol Biol* **407**, 633-639.
- Vaseeharan, B., Ramasamy, P., Murugan, T. and Chen, J.C. (2005). In vitro susceptibility of antibiotics against *Vibrio* spp. and *Aeromonas* spp. isolated from *Penaeus monodon* hatcheries and ponds. *Int J Antimicrob Agents* **26**, 285-291.
- Vendeville, A., Winzer, K., Heurlier, K., Tang, C.M. and Hardie, K.R. (2005). Making 'sense' of metabolism: autoinducer-2, LuxS and pathogenic bacteria. *Nat Rev Microbiol* **3**, 383-396.
- Verstraeten, N., Braeken, K., Debkumari, B., Fauvart, M., Fransaeer, J., Vermant, J. and Michiels, J. (2008). Living on a surface: swarming and biofilm formation. *Trends Microbiol* **16**, 496-506.
- Vila, J., Ruiz, J., Gallardo, F., Vargas, M., Soler, L., Figueras, M.J. and Gascon, J. (2003). *Aeromonas* spp. and traveler's diarrhea: clinical features and antimicrobial resistance. *Emerg Infect Dis* **9**, 552-555.
- Vilches, S., Jimenez, N., Tomas, J.M. and Merino, S. (2009). *Aeromonas hydrophila* AH-3 type III secretion system expression and regulatory network. *Appl Environ Microbiol* **75**, 6382-6392.
- Vilches, S., Urgell, C., Merino, S., Chacon, M.R., Soler, L., Castro-Escarpulli, G., *et al.* (2004). Complete type III secretion system of a mesophilic *Aeromonas hydrophila* strain. *Appl Environ Microbiol* **70**, 6914-6919.
- Vilches, S., Wilhelms, M., Yu, H.B., Leung, K.Y., Tomas, J.M. and Merino, S. (2008). *Aeromonas hydrophila* AH-3 AexT is an ADP-ribosylating toxin secreted through the type III secretion system. *Microb Pathog* **44**, 1-12.
- von Graevenitz, A. (2007). The role of *Aeromonas* in diarrhea: a review. *Infection* **35**, 59-64.
- Wang, Z., Larocque, S., Vinogradov, E., Brisson, J.R., Dacanay, A., Greenwell, M., *et al.* (2004). Structural studies of the capsular polysaccharide and lipopolysaccharide O-antigen of *Aeromonas salmonicida* strain 80204-1 produced under in vitro and in vivo growth conditions. *Eur J Biochem* **271**, 4507-4516.
- Wassmann, P., Chan, C., Paul, R., Beck, A., Heerklotz, H., Jenal, U. and Schirmer, T. (2007). Structure of BeF3- modified response regulator PleD: implications for diguanylate cyclase activation, catalysis, and feedback inhibition. *Structure* **15**, 915-927.
- Weinberg, Z., Barrick, J.E., Yao, Z., Roth, A., Kim, J.N., Gore, J., *et al.* (2007). Identification of 22 candidate structured RNAs in bacteria using the CMfinder comparative genomics pipeline. *Nucleic Acids Res* **35**, 4809-4819.
- Weinhouse, H., Sapir, S., Amikam, D., Shilo, Y., Volman, G., Ohana, P. and Benziman, M. (1997). c-di-GMP-binding protein, a new factor regulating cellulose synthesis in *Acetobacter xylinum*. *FEBS Lett* **416**, 207-211.

References

- Whitney, J.C., Colvin, K.M., Marmont, L.S., Robinson, H., Parsek, M.R. and Howell, P.L. (2012). Structure of the cytoplasmic region of PelD, a degenerate diguanylate cyclase receptor that regulates exopolysaccharide production in *Pseudomonas aeruginosa*. *J Biol Chem* **287**, 23582-23593.
- Wigren, E., Liang, Z.X. and Romling, U. (2014). Finally! The structural secrets of a HD-GYP phosphodiesterase revealed. *Mol Microbiol* **91**, 1-5.
- Wilhelms, M., Gonzalez, V., Tomas, J.M. and Merino, S. (2013). *Aeromonas hydrophila* lateral flagellar gene transcriptional hierarchy. *J Bacteriol* **195**, 1436-1445.
- Wilhelms, M., Molero, R., Shaw, J.G., Tomas, J.M. and Merino, S. (2011). Transcriptional hierarchy of *Aeromonas hydrophila* polar-flagellum genes. *J Bacteriol* **193**, 5179-5190.
- Wilksch, J.J., Yang, J., Clements, A., Gabbe, J.L., Short, K.R., Cao, H., *et al.* (2011). MrkH, a novel c-di-GMP-dependent transcriptional activator, controls *Klebsiella pneumoniae* biofilm formation by regulating type 3 fimbriae expression. *PLoS Pathog* **7**, e1002204.
- Yang, C.Y., Chin, K.H., Chuah, M.L., Liang, Z.X., Wang, A.H. and Chou, S.H. (2011). The structure and inhibition of a GGDEF diguanylate cyclase complexed with (c-di-GMP)₂ at the active site. *Acta Crystallogr D Biol Crystallogr* **67**, 997-1008.
- Yu, H.B., Kaur, R., Lim, S., Wang, X.H. and Leung, K.Y. (2007). Characterization of extracellular proteins produced by *Aeromonas hydrophila* AH-1. *Proteomics* **7**, 436-449.
- Yáñez, M.A., Catalán, V., Apráiz, D., Figueras, M.J. and Martínez-Murcia, A.J. (2003). Phylogenetic analysis of members of the genus *Aeromonas* based on *gyrB* gene sequences. *Int J Syst Evol Microbiol* **53**, 875-883.
- Zgair, A.K. (2012). *Escherichia coli* flagellin stimulates pro-inflammatory immune response. *World J Microbiol Biotechnol* **28**, 2139-2146.
- Zhang, Y.L., Arakawa, E. and Leung, K.Y. (2002). Novel *Aeromonas hydrophila* PPD134/91 genes involved in O-antigen and capsule biosynthesis. *Infect Immun* **70**, 2326-2335.
- Zhang, Y.L., Lau, Y.L., Arakawa, E. and Leung, K.Y. (2003). Detection and genetic analysis of group II capsules in *Aeromonas hydrophila*. *Microbiology* **149**, 1051-1060.